

This guide demonstrates how to identify and describe key features of porphyry deposits. Topics emphasizing field observations related to porphyry deposits include a) identification of habits (textures or modes of occurrence) that aid in the concise description and recording of geology, alteration and ore mineralization, b) theoretical features of alteration and mineral deposition, c) essential aspects of deposit emplacement and d) major deposit models of porphyry deposits that include exploration vectors to ore location.

This guide will help:

- **geologists and experienced prospectors** wanting to upgrade or learn new exploration field skills, especially those involved in evaluating porphyry deposits or porphyry deposit prospects,
- **exploration managers** looking to train groups of field geologists to a higher level of expertise in exploration methodology and pattern recognition of vectors to ore zones,
- **geologists and managers** needing advanced and consistent coordination and efficient field exploration, and
- **executives or investors** involved in exploration ventures who need an overview of how best to understand, conduct and enhance field exploration.

Front cover is a photo of reverse circulation drilling in 2008 at the Don Luis porphyry-greisen tungsten prospect, central Sonora, Mexico.

PORPHYRY DEPOSITS

KEY FEATURES & MAJOR MODELS

How to Map & Log

COLIN I. GODWIN

Any part of this book may be reproduced, stored, or transmitted in any form by any means—graphic, electronic, or mechanical—without permission in writing from Colin I. Godwin. However, he would appreciate recording of, and receiving acknowledgement of, its use.

Preliminary editing by Nicole Barlow & Moretta Shuert, Purple Rock Inc., Victoria, BC, Canada, was supported by the Mineral Deposit Research Unit, Department of Earth, Ocean and Atmospheric Sciences, The University of British Columbia, BC, Canada.

Cover images by Colin I. Godwin.

Includes bibliographic references.

Portable document format (PDF) was made in Canada in 2023.

Recommended citation:

Godwin, C. I. (2023): Porphyry Deposits: Key Features & Major Models—How to Map & Log. Self published in Portable Document Format (PDF) by Colin I. Godwin, Port Moody, British Columbia, Canada: 166 p.

PORPHYRY DEPOSITS: KEY FEATURES & MAJOR MODELS

How to Map & Log

COLIN I. GODWIN

CONTENTS

INTRODUCTION.....	12
DEFINITIONS AND KEY FEATURES	16
TABLE 1. Economic features common to porphyry deposits.....	17
Definitions of porphyry and greisen.	19
Definition of pre- syn- or post-mineral and intermineral.	19
Definitions of alteration, hydrothermal, hypogene, ore shell, pyrite halo and supergene.....	20
Definitions of porphyry deposit, greisen porphyry deposit and gold porphyry deposit.	20
Definitions of breccia, breccia pipes, hydrothermal breccia, collapse breccia, fault breccia, pseudobreccia or crackle breccia, and sedimentary breccias and conglomerate.....	21
BASIC TYPES AND OVERVIEW PHOTOS.....	23
Figure 1. Looking north to Patton Hill at the Casino calcalkaline copper-gold-molybdenum porphyry deposit in central Yukon, Canada.....	24
Figure 2. Aerial view of the Endako porphyry molybdenum mine in central British Columbia, Canada.	25
Figure 3. Aerial view of the Copper Mountain alkaline porphyry copper-gold mine in south-central British Columbia, Canada.....	26
Figure 4. Don Luis tungsten-silver greisen-porphyry prospect in Sonora, Mexico.....	27
Figure 5. The Creston pit at the La Colorada gold-silver porphyry mine in Sonora, Mexico.	28
HABITS OF MINERALIZATION AND ALTERATION	29
Common Alteration Habits in Porphyry Deposits.....	29
Figure 6. Spatial relationships among vein, selvage, envelope, pervasive and disseminated habits of alteration.	30
TABLE 2. Habit of alteration.....	31
Breccia: Breccia Clasts and Breccia Matrix Habits	34
Disseminated Habit.....	34
Figure 7. Breccia, breccia clasts, breccia matrix, and ‘pseudobreccia’ or ‘crackle breccia’.....	35

Figure 8. Disseminated habit.	36
Envelope Habit.....	36
Flooded Habit.....	36
Figure 9. Drill core illustrating envelope habit.....	37
Figure 10. Veins and envelopes, locally with malachite from weathering.	38
Index Fossil Gusano Habit.....	38
Origin of gusano habit: a theory.	38
Figure 11. Flooded habit.	39
Porphyritic Habit.....	39
Figure 12. Gusano habit an index fossil for potential porphyry deposits at depth.	40
Figure 13. Examples of ‘productive’ or ‘wet’ syn-ore porphyry.	41
Selvedge Habit.....	41
Figure 14. Selvedge of quartz in contact with the wallrock, but within and the outer part of the vein.....	42
Sheeted Vein Habit.....	43
Figure 15. Outcrop illustrating sheeted veins.....	43
Stockwork Vein Habit.....	43
Figure 16. Stockwork quartz veins.	44
<i>Index Fossils: Unidirectional Solidification Texture (UST) or Habit in Brain Rock, Quartz Blobs and Quartz Breccias</i>	44
Figure 17. Unidirectional solidification banding in brain rock (index fossil).....	45
Story about brain rock with unidirectional solidification texture.....	45
Figure 18. Brain rock with unidirectional solidification bands in contact with earlier, surrounding feldspar-quartz porphyry at the Don Luis greisen prospect in Sonora, Mexico.	46
Figure 19. a) Massive magmatic quartz blob and b) associated quartz breccia at Don Luis greisen-porphyry prospect in Sonora, Mexico.....	47
Explaining UST banding in brain rock.....	47
<i>Index Fossil: Shatter Cleavage Related to Breccia</i>	48
Figure 20. Index fossil shatter cleavage from the Casino porphyry copper-gold deposit in central Yukon, Canada.	49
Story about shatter cleavage, an index fossil.	49
Figure 21. Shatter cleavage a) adjacent to the Braden pipe, El Teniente, central Chile, and b) at Galore Creek, British Columbia, Canada.	50
Habits Occurring in Multiple Ways or Events.....	50
Figure 22. Example of two veins of probable different ages.	51

REGIONAL SETTING, GROUND PREPARATION AND INTERMINERAL HISTORY	52
Definition of hornfels.....	53
Figure 23. The regional setting, ground preparation and intrusion and intermineral history of porphyry mineralization.....	54
TABLE 3. Features of regional setting, ground preparation and intrusion and intermineral history of porphyry mineralization in Figure 23.	55
PLUTON ASSOCIATIONS	57
Origin of S-, A- and I-type granitic rocks.	57
Origin of alkaline plutons	57
TABLE 4. Different types of porphyry deposits related to granitic associations.....	58
GENERALIZED MORPHOLOGY AND DESCRIPTION OF HYDROTHERMAL BRECCIAS.....	60
Story of conglomerate versus breccia at Casino, central Yukon, Canada.....	61
Figure 24. Generalized morphology of a breccia pipe in cross-section.	61
TABLE 5. Explanation of numbered features in Figure 24 on the morphology of hydrothermal breccias.	62
Figure 25. Hydrothermal cobble breccia from the Casino deposit in the Yukon, Canada.....	63
Figure 26. Hydrothermal breccia from Island Copper porphyry deposit, northern Vancouver Island, British Columbia, Canada.....	63
Figure 27. Hydrothermal breccia from the Granisle porphyry deposit, central British Columbia, Canada.	64
ORIGINS OF HYDROTHERMAL BRECCIA AND RELATIONSHIPS WITH PORPHYRITIC ROCKS	65
Figure 28. Marginal hydrothermal breccia at the Island Copper Mine, northern Vancouver Island, British Columbia, Canada.....	66
Figure 29. Relationships between porphyritic rocks and breccia bodies.	67
Discussion on Disequilibrium Porphyry and Breccia Formation	67
Brecciation from Abrupt Pressure Drop at Yellowstone Park, Wyoming, United States	68
SIGNIFICANCE AND CHARACTERISTICS OF MAGMATIC DYKES AND MAGMATIC BRECCIAS	69
Tourmalinite Dykes and Breccia.....	69
Definition of tourmalinite.	70
Opinion about the magmatic origin of tourmalinite breccia at Los Bronces, central-eastern Chile.	70
Story of tourmalinite balls at Syenite Mountain, west-central Yukon, Canada.....	70
Figure 30. Model for magmatic tourmalinite (tourmaline- quartz) dykes and breccia.	72
Figure 31. Magmatic tourmalinite (quartz-tourmaline) dykelets.	73
Figure 32. Tourmalinite breccia from the main breccia pipe at Sierra Gorda, northern Chile.....	74

Figure 33. Tourmalinite (quartz-tourmaline) breccia in the Braden breccia pipe at the El Teniente underground porphyry copper mine in central Chile.	74
Opinion on the mechanism of breccia emplacement.....	75
Opinion on the magmatic origin of magnetite–apatite dykes and magnetite–apatite breccia.	75
Definitions: Distinguishing a dyke from a vein.....	75
Magnetite-Apatite Dykes and Breccias.....	75
Figure 34. Model for magnetite-apatite type magmatic breccia and dykes.....	76
Figure 35. Magnetite-apatite magmatic breccia.....	77
Opinion on the significance of magnetite-apatite dykes and breccia in alkaline porphyry deposits.	77
CHEMISTRY AND PHASE RELATIONSHIPS AMONG HYPOGENE ALTERATION MINERALS.....	79
Equation 1 is the reaction between K-feldspar and muscovite (or sericite).	79
Equation 2 describes the reaction at the phase boundary between muscovite and kaolinite.	79
Figure 36. Phase diagram of temperature (°C) versus $m_{\text{KCl}}/m_{\text{HCl}}$ showing major alteration minerals in the porphyry environment.....	80
INFILTRATION-DIFFUSION MODEL FOR ALL SCALES OF HYPOGENE ALTERATION ZONING	81
Figure 37. Zoning patterns in porphyry deposits follow reactions of fluids passing through fractured rock by infiltration and diffusion.....	82
SUMMARY OF ALTERATION FACIES FOR HYPOGENE ZONING	84
TABLE 6. Mineral zoning of alteration facies from core to the periphery in calcalkaline (copper, molybdenum and gold), alkaline (copper and gold) and greisen (tin and tungsten and gold porphyry deposits).....	85
Figure 38. Examples in drillcore of pervasive a) potassic and phyllic and b) smectitic hydrothermal alteration.....	88
MODELS FOR QUARTZ-BEARING, CALCALKALINE PORPHYRY DEPOSITS RELATED TO GRANITIC BATHOLITHS	89
Figure 39. View of the Valley Copper mine from near the Alwyn mine, in the Highland Valley of south-central British Columbia, Canada.	91
Figure 40. Alwyn dyke(?) overview.....	92
Figure 41. Alwyn dyke(?) contact and mineralized float.	93
CLASSIC HYPOGENE ALTERATION MODELS FOR QUARTZ-BEARING, CALCALKALINE BATHOLITH- OR STOCK-RELATED COPPER-MOLYBDENUM PORPHYRY DEPOSITS	94
Figure 42. The classic Lowell and Guilbert calcalkaline porphyry deposit hypogene alteration model.	95
Figure 43. Andean epithermal top and porphyry bottom model.....	96
MODEL FOR QUARTZ-POOR, ALKALINE-DIORITE BATHOLITH-RELATED PORPHYRY DEPOSITS.....	98

Figure 44. Alteration model for batholith-related, quartz-poor alkaline-diorite porphyry deposits.	99
Comment on quartz-poor, alkaline-diorite granitic batholith- and stock-related porphyry deposits	100
MODEL FOR QUARTZ- AND MUSCOVITE-RICH STOCK- AND CUPOLA-RELATED GREISEN PORPHYRY DEPOSITS.....	101
Figure 45. Alteration model for greisen porphyry deposits.....	102
Figure 46. Geology of the West Zone of the Don Luis tungsten-silver greisen-porphyry deposit in Sonora, Mexico.	103
Figure 47. Surface-weathered greisen and fresh greisen in drill core.....	104
COMMENTS ON GOLD-SILVER PORPHYRY DEPOSITS	105
APPLICATION OF HYPOGENE ALTERATION STUDIES IN PORPHYRY DEPOSITS	106
SUPERGENE ALTERATION AND ENRICHMENT IN PORPHYRY DEPOSITS.....	107
Introduction	107
Chemistry of Supergene Leaching and Enrichment.....	107
Figure 48. Eh–pH diagram showing relationships among hypogene, supergene oxide and supergene sulfide minerals.....	108
Micron-thick coatings of chalcocite on pyrite.....	109
Supergene Silicate Alteration.....	109
Supergene Capping	109
Definitions of autogenetic gossan and epigenetic, transported, or exotic gossan.	110
Figure 49. Autogenetic limonite in capping in a) hydrothermal breccia, and b) in thin section from phyllic alteration in a pyrite halo.	111
TABLE 7. Calculation of minimum hypogene grade from jarosite and goethite percentages in capping generated by a single enrichment cycle.....	112
Story of grade reconstruction from capping limonite.	113
Supergene Copper Enrichment.....	113
Story about oxide-copper recovery at Mina Quetena, Atacama Desert, northern Chile.....	114
Figure 50. Supergene oxide mineralization with superimposed capping.....	114
Figure 51. Supergene oxide mineralization superimposed on supergene sulfide and hypogene mineralization.	115
Figure 52. General model for supergene alteration of hypogene mineralization in porphyry deposits.....	116
Figure 53. Cross section of the El Abra porphyry copper deposit, Chile, showing influence of faulting and hypogene mineralization on enrichment zones.	117
Supergene Copper Enrichment Cycles.....	117

Figure 54. Single and two cycle supergene copper enrichment from hypogene porphyry.....	119
Figure 55. Supergene capping and ore zones at the Toquepala porphyry deposit, southern Peru.	120
Exotic Copper Deposits	120
Figure 56. Exotic copper mineralization.	121
SUMMARY AND CONCLUSIONS ON PORPHYRY DEPOSITS	122
General Summary	122
Geology Summary.....	122
Hydrothermal Alteration Summary	123
Supergene Alteration and Enrichment Summary	123
Conclusions Regarding Porphyry Deposit Models	123
REFERENCES.....	125
ACKNOWLEDGMENTS.....	131
APPENDIX A: SUMMARY OF COMMON CODES, LOGGING TECHNIQUES AND DIAMOND DRILL LOGGING FORMATS USED IN DESCRIBING PORPHYRY DEPOSITS.....	132
Introduction	132
Codes that Facilitate Descriptions in Mapping and Logging of Porphyry Deposits	132
Four-Letter Rock Codes.....	132
TABLE A1: Rock names (4-letters capitalized).....	132
Three- and One-Letter or One-Number Codes	132
TABLE A2: General descriptive terms (1-number or 1- and 3-letters capitalized).....	133
Two Letter Mineral Codes.....	133
TABLE A3: Mineral names (2-letters capitalized).....	133
Logging Techniques for Describing Diamond Drillholes in Porphyry Deposits	133
Formats for Describing Diamond Drillholes, Trenches, and Outcrops in Porphyry Deposits	136
Figure A1. Logging format heading for pages 1 and 2 for logging drill core from a porphyry deposit.	138
Figure A2. Example of a logging template, page 1, for a diamond drill log, trench, or outcrop in a porphyry deposit environment.....	139
Figure A3. Example of a logging template of continuing page 2, for a diamond drill log, trench, or outcrop in a porphyry deposit environment.	140
TABLE A4. Explanation of logging formats related to porphyry deposits.....	141
Conclusions	142
APPENDIX B: COORDINATES OF DEPOSITS MENTIONED IN THE TEXT	143

Deposits or Deposit Areas Mentioned in the Text.....	143
Satellite Images.....	143
TABLE B1: Location of deposits mentioned in the text.....	143
APPENDIX C. PROBLEM SET RELATED TO THE GEOLOGY AND ALTERATION OF PORPHYRY DEPOSITS	145
C1. General Questions on Alteration Mineralogy in Porphyry Deposits	145
Question GEN01 [11]: Potassic ore mineral alteration.....	145
Question GEN02 [8]: Phyllic ore-mineral alteration.	145
Question GEN03 [8]: Propylitic ore-mineral alteration.	145
Question GEN04 [11]: Potassic alteration.	146
Question GEN05 [11]: Phyllic mineral alteration.....	146
Question GEN06 [11]: Advanced argillic mineral alteration.....	146
Question GEN07 [11] Intermediate argillic mineral alteration.....	147
Question GEN08 [11]: Propylitic mineral alteration.	147
Question GEN09 [12]: Supergene capping alteration.....	147
GEN10 [16]: Supergene oxide enrichment alteration.....	148
Question GEN11 [16]: Supergene sulfide enrichment alteration.....	148
C2. General Questions on Rocks and Mineralogy in Porphyry Deposits	148
Question GEN12 [14]: Rock descriptions.....	148
Figure C1. Rock with 3 mm diameter disk for scale.....	149
Question GEN13 [11]: Rock description.....	150
Figure C2. Rock with 3 mm diameter disk for scale.....	150
Question GEN14 [14]: Rock description.....	151
Figure C3. Rock thin section with 2 mm diameter central grain.	151
Question GEN15 [8]: Rock description.....	152
Figure C4. Example of an important habit.	152
Question GEN16 [14]: Rock description.....	153
Figure C5. Altered rock.....	153
Question GEN17 [14]: Rock description.....	154
Figure C6. Altered rock.....	154
C3. PROBLEM SET FOR THE INTERPRETATION OF GEOLOGY AND HYPOGENE ALTERATION FROM MAPS.....	155
Island Copper porphyry deposit, Vancouver Island, British Columbia, Canada.	155
Figure C7. Geological map of the open pit for the Island Copper porphyry mine, Vancouver Island, British Columbia, Canada.....	155

Question ICU01 [4]: Rock descriptions.	156
Question ICU02 [5]: Breccia description.	156
Question ICU03 [12]: Porphyry questions.	156
Question ICU04 [4]: Volcanic rock questions.....	156
Figure C8. Alteration map for the Island Copper porphyry deposit, Vancouver Island, British Columbia, Canada.	157
Question ICU05 [21].....	157
Question ICU06 [2]: Gold associations.....	158
Question ICU07 [3]: Tonnage question.....	158
Berg porphyry deposit, central British Columbia, Canada.....	159
Figure C9. Geology map of the Berg porphyry deposit, central British Columbia, Canada.	159
Question BER01 [7]: Significant regional geology.....	160
C4. PROBLEM SET FOR SUPERGENE ENRICHMENT IN PORPHYRY DEPOSITS	161
Figure C10. Supergene alteration at the Butte Porphyry Deposit (the richest hill on earth), Montana, USA.	161
Question SUP01 [12]: Capping and enrichment questions.....	161
Question SUP02 [2]: Supergene cycles.	162
Mark Summary for Questions C1 to C4	163
TABLE C1. Mark summary.	163
Your mark.....	164
ABOUT THE AUTHOR.....	165

INTRODUCTION

In this part, you will learn:

- a framework for studying porphyry deposits,
- where to get comprehensive reference material, and
- the significance of hypogene versus supergene environments.

This guide is an extension of the introductory guide, *Porphyry and Epithermal Deposits: Mineralization, Alteration and Logging* (Godwin, 2020), published by the Mineral Deposit Research Unit (MDRU) at the Department of Earth, Ocean and Atmospheric Sciences, The University of British Columbia, and the Mineral Deposit Division of the Geological Association of Canada. It is available from The Geological Association of Canada, at https://gac.ca/product-category/new_releases/ (regular price is \$70.00, discounted to \$38.50 for Members of the GAC). Before reading this guide, it would be helpful to be familiar with the basics presented in the above introductory guide—particularly the material in the appendices.

Porphyry Deposits: Key Features and Models focuses on key geology features and alteration common to porphyry deposits that can be identified in the field without expensive, sophisticated instruments. The emphasis is on practical, field-oriented exploration methodology that facilitates the location of ore.

Therefore, a framework is provided to learn about generalized models. These models detail spatial features common to porphyry deposits and supporting mineralogical, chemical, and physical details. Appendix A (from Godwin, 2020) facilitates descriptions by providing a) shorthand, readable codes for minerals, rocks and descriptive comments that allows rapid, accurate and consistent descriptions of geological/alteration features and b) logging methodologies and templates for describing diamond drill cores in a digitally compatible way. These codes and logging procedures are tried-and-true approaches that enhance the ability to communicate quickly, clearly, and descriptively in a way that facilitates ongoing digital manipulation, interpretation, and identification of vectors to ore locations.

A cautionary comment on models: “All models are wrong, some are useful” (Box, 1979). However, identifying features worth looking for is a crucial quality of models. If you are not focused on looking for specific features while in the field, they are more challenging to discover/observe. In addition, observations alone mean little unless interpreted within the larger framework provided by models—hopefully, models with guides to likely ore locations. Improvement of the presented geological models is expected as new deposit details become available and understood.

Resources with extensive, detailed, and voluminous compilations of the geology and alteration of porphyry deposits—required references for the serious porphyry explorationist—include:

- Carter, L.C., Williamson, B.J., Tapster, S.R., Costa, C., Grime, G.W., and Rollinson, G.K. (2021): Crystal mush dykes as conduits for mineralising fluids in the Yerington porphyry copper district, Nevada; *Commun Earth Environ* v. 2, no. 59. <https://doi.org/10.1038/s43247-021-00128-4>.
- Dilles, J.H. and Camus, F., editors (2001): A special issue devoted to porphyry copper deposits of northern Chile; *Economic Geology*, v. 96, p. 233–420.
- Hedenquist, J.W., Harris, M. and Camus, F., editors (2012): Geology and genesis of major copper deposits and districts of the world: a tribute to Richard H. Sillitoe; *Society of Economic Geologists, Inc., Special Publication Number 16*, 618 p.

- Hollister, V.F. (1978): Geology of the porphyry copper deposits of the western hemisphere; Society of Mining Engineers of The American Institute of Mining, Metallurgical, and Petroleum Engineers, Inc., 219 p.
- Reid, M.H. (1997): Hydrothermal alteration and its relationship to ore fluid composition; *in* H.L. Barnes (ed.), *Geochemistry of Hydrothermal Ore Deposits*, Third Edition, p. 303–365.
- Schroeter, T.G., editor (1995): *Porphyry deposits of the northwestern cordillera of North America*; Canadian Institute of Mining, Metallurgy and Petroleum, Special Volume 46, 888 p.
- Singer, Donald A, V.I. Berger, and B.C. Moring, 2008: *Porphyry Copper Deposits of the World: Database and Grade and Tonnage Models*, 2008. U.S. Geological Survey, Open-File Report 2008-1155, version 1.0.
- Sharman, E.R., J.R. Lang and J.B. Chapman, editors (2021): *Porphyry deposits of the Northwestern Cordillera of North America: a 25-year update*; Canadian Institute of Mining, Metallurgy and Petroleum, Special Volume 57.
- Sutherland Brown, A., editor (1976a): *Porphyry deposits of the Canadian Cordillera*; Canadian Institute of Mining and Metallurgy, Special Volume 15, 510 p.
- Titley, S.R., editor (1982): *Advances in geology of the porphyry copper deposits, southwestern North America*; The University of Arizona Press, 560 p.
- Titley, S.R. and Hicks, C.L., editors (1966): *Geology of the porphyry copper deposits, southwestern North America*; The University of Arizona Press, 287 p.

Key individual papers are published often, but some of note include:

- Beane, R.E. and Titley, S.R. (1981): Porphyry copper deposits, part II, hydrothermal alteration and mineralization; *in* B.J. Skinner (ed.), *Economic Geology Anniversary Volume 1905–1980*, p. 235–269.
- Burnham, C.W. (1979): Magma and hydrothermal fluids at the magmatic stage; *in* H.L. Barnes (ed.), *Geochemistry of Hydrothermal Ore Deposits*, 2nd Edition, Miley Interscience, New York, p. 71–136.
- Candela, P.A. and Piccoli, P.M. (2005): Magmatic processes in the development of porphyry-type ore systems; *in* M.D. Hannington (ed.), *Economic Geology, One Hundredth Anniversary Volume, 1905-2005*, p. 25–38.
- Černý, P., Blevin, P.L., Cuney, M. and London, D. (2005): Granite-related ore deposits; *in* M.D. Hannington (ed.), *Economic Geology, One Hundredth Anniversary Volume, 1905-2005*, p. 337–370.
- Chiaradia, M. (2020): Gold endowments of porphyry deposits controlled by precipitation efficiency; *Nature Communications*, v. 11, Article number 248. <https://www.nature.com/articles/s41467-019-14113-1.pdf>, <https://doi.org/10.1038/s41467-019-14113-1>
- Cox, D.P. (1986): Descriptive model of porphyry copper; *in* *Mineral Deposit Models*, US Geological Survey, Bulletin 1693, p. 76–79.
- Gustafson, L.B. and Hunt, J.B. (1975): The porphyry copper deposit at El Salvador, Chile; *Economic Geology*, v. 70, p. 857–912.
- Hedenquist, J.W. and Lowenstern, J.B. (1994): The role of magmas in the formation of hydrothermal ore deposits; *Nature*, v. 370, p. 519–527.
- Kirkham, R.V. and Dunne, K.P.E. (2000): World distribution of porphyry, porphyry-associated skarn, and bulk-tonnage epithermal deposits and occurrences; *Geological Survey of Canada, Open File 3792a*, 26 p.
- Kirwin, D.J. (2005): Unidirectional solidification textures associated with intrusion-related Mongolian mineral deposits; *in* R. Seltmann, O. Gerel and D.J. Kirwin (eds.), *Geodynamics and Metallogeny of Mongolia with a Special Emphasis on Copper and Gold Deposits; SEG-IAGOD Field Trip, 14–16 August 2005, 8th Biennial SGA Meeting, IAGOD Guidebook Series 11: CERCAMS/NHM London*, p. 63–84.
- Lowell, J.D. and Guilbert, J.M. (1970): Lateral and vertical alteration-mineralization zoning in porphyry copper deposits; *Economic Geology*, vol. 65, p. 373–408.

- Noble, D.C., Vidale, C.E., Miranda, M., Amaya, W. and McCormack, J.K. (2010): Ovoidal- and mottled-textured rock and associated silica veinlets and their formation by high-temperature outgassing of subjacent magmas; *in* R. Steininger and B. Pennell (eds.), *Great Basin Evolution and Metallogeny, Volume II*, p. 795–811.
- Rose, A.W. and Burt, D.M. (1979): Chapter 5, hydrothermal alteration; *in* H.L. Barnes (ed.), *Geochemistry of Hydrothermal Ore Deposits, Second Edition*, p. 173–235.
- Seedorff, E., Dilles, J.H., Proffett, J.M. Jr., Einaudi, M.T., Zurcher, L., Stavast, W.J.A., Johnson, D.A. and Barton, M.D. (2005): Porphyry deposits: characteristics and origin of hypogene features; *in* M.D. Hannington (ed.), *Economic Geology, One Hundredth Anniversary Volume, 1905-2005*, p. 251–298.
- Sillitoe, R.H. (1973): The tops and bottoms of porphyry deposits; *Economic Geology*, v. 68, p. 700–815.
- Sillitoe, R.H., Halls, C. and Grant, J.N. (1975): Porphyry tin deposits in Bolivia; *Economic Geology*, v. 70, p. 913–927.
- Sillitoe, R.H., 1997: Characteristics and controls of the largest porphyry copper-gold and epithermal gold deposits in the circum-Pacific region. *Australian Journal of Earth Sciences*, Vol. 44, p. 373-388.
- Sinclair, W.D. (2007): Porphyry deposits; *in* W.D. Goodfellow (ed.), *Mineral Deposits of Canada: A Synthesis of Major Deposit-Types, District Metallogeny, the Evolution of Geological Provinces, and Exploration Methods*; Geological Association of Canada, Mineral Deposits Division, Special Publication No. 5, p. 223–243.
- Singer, D.A, Berger, V.I. and Moring, B.C. (2008): Porphyry copper deposits of the world: database and grade and tonnage models, 2008; United States Geological Survey, Open-File Report 2008-1155, version 1.0.
- Thompson, A.J.B. and Thompson, J.F.H., editors (2015): Atlas of alteration: a field and petrographic guide to hydrothermal alteration minerals; *in* K.P.E. Dunne (Mineral Deposit Division series editor), Geological Association of Canada, 119 p.
- Titley, S.R. and Beane, R.E. (1981): Porphyry copper deposits, part I, geologic setting, petrology, and tectogenesis; *in* B.J. Skinner (ed.), *Economic Geology Anniversary Volume 1905–1980*, p. 214–234.
- White, W.H., Bookstrom, A.A., Kamilli, R.J., Ganster, M.W., Smith, R.P., Ranta, D.E. and Steininger, R.C. (1981): Character and origin of Climax-type molybdenum deposits; *in* B.J. Skinner (ed.), *Economic Geology Anniversary Volume 1905–1980*, p. 270–316.

Minerals likely to be encountered in the field are determined by whether they are found in the hypogene or supergene environments. Specifically, hypogene sulfide minerals are not common at the surface due to surface weathering and other supergene processes. Consequently, identifying secondary minerals becomes essential to the recognition of original hypogene mineralization. Water-table related supergene enrichment of copper grades is critical because supergene enriched sulfide and oxide minerals can be valuable; however, they often require specific recovery methods. Detailed mineral descriptions are in Godwin, 2020. Essential minerals, and their codes, related to porphyry deposits, are in Appendix A.

Supergene and hypogene minerals are variably found in field surface exposures. Hypogene sulfide minerals are not common at the surface due to surface weathering and other supergene processes. Consequently, the identification of secondary minerals associated with supergene mineralization becomes essential to interpreting precursor hypogene mineralization. Water-table-related supergene enrichment of grades is also vital because supergene-enriched sulfide and oxide minerals can be valuable; however, they often require specific recovery methods.

This guide highlights features relevant to describing and understanding the geology and alteration of porphyry deposits. The sequence of topics in the following text is

1. Definitions and key features emphasizing their tectonic setting and associated plutonic, porphyritic and breccia rocks,
2. Basic types and overview photos,
3. Habits of mineralization and alteration,
4. Structural and ground preparation related to emplacement,
5. A chemical phase diagram and an infiltration-diffusion model to explain hypogene zoning,
6. Idealized models of hypogene alteration facies and zoning for different deposit types with an emphasis on ore location and
7. Supergene alteration, where copper is removed and enrichment, where copper is added to underlying hypogene or pre-existing enriched mineralization.

Be sure you understand from this part that:

- ➔ **this guide is field-oriented,**
- ➔ **there is abundant, detailed literature about porphyry deposits,**
- ➔ **both hypogene alteration and supergene alteration/enrichment are described and**
- ➔ **alteration zoning can predict ore location.**

DEFINITIONS AND KEY FEATURES

In this section, you will learn:

- the definition of a porphyry deposit,
- about common host rocks,
- about size, grade, and other standard features, and
- definitions of some key features.

The definition of a porphyry deposit in 1960, when the author was an undergraduate, was a deposit that can be mined with a steam shovel. The implication, of course, is that porphyry deposits are large, and large-scale open-pit mining allows for recovery of relatively low grades of, most commonly, copper and molybdenum. Thus, porphyry deposits are large, low-grade deposits of, mainly, copper or molybdenum. Values from gold and silver can be important as by-products in sulfide concentrates, but this varies from deposit to deposit. These deposits, equidimensional in plan view, are most commonly mined by open-pit methods to depths of about 400 m; however, bulk underground mining is increasing. Porphyry deposits are frequently, but not always, marked by extensive rusty zones 500 m or more in diameter (e.g., Figure 1). These rusty-red ‘thumbprint’ alteration zones, composed mainly of limonite after pyrite (plus other oxidized sulfides), can be evident in the field and apparent on colour photographs and interpreted satellite imagery.

Host rocks for porphyry deposits are porphyry, breccia, granitic, and less often, volcanic. Deposits appear to be genetically related to porphyritic rocks, as the name suggests. Breccias also seem to be linked genetically to both the deposits and porphyry. Ore-mineralization occurs mainly as sulfides in veins and as disseminations imposed on highly fractured rock. Where porphyry deposits form in apical cupolas of stocks, alteration and mineralization can concentrate along fractures caused by the intrusion of the stocks.

In special situations, especially in porphyry molybdenum deposits, brain rock with unidirectional solidification texture in brain rock of stocks indicates potential ore mineralization—if only because of its occurrence at the large Henderson and Climax porphyry molybdenum mines in Colorado, United States, and at the giant Oyu Tolgoi porphyry copper-gold mine in the South Gobi region of Mongolia. Porphyry deposits found in differentiated batholiths (such as Valley Copper in the Guichon Creek batholith, Highland Valley, British Columbia, Canada, and Afton in the Iron Mask batholith, Kamloops, British Columbia, Canada) arguably are related to late, metal-rich, hydrous accumulation resulting from progressive precipitation of dominantly anhydrous minerals in earlier precipitated batholithic rocks.

The size and grade of porphyry deposits are typically at least 20 million tonnes with hypogene copper grades from 0.2 to 1.0%. Supergene enrichment can increase copper grades to several percent. Supergene enrichment can occur in non-glaciated areas (e.g., at Casino in Yukon, Canada [Figure 1]; porphyry deposits in Arizona, United States, and Chile and Peru. In a 1976 review of porphyry deposits in the Canadian Cordillera, Sutherland Brown, and Cathro (1976) found that, at that time, porphyry deposits in British Columbia, Canada, ranged from about 45 to 900 million tonnes with copper grades from 0.2 to 1.0% and total contained copper metal from 182,000 to 2,900,000 tonnes. A summary of economic features common to porphyry deposits is presented in TABLE 1.

TABLE 1. Economic features common to porphyry deposits

CuEq = copper equivalent (e.g., value of copper plus molybdenum in terms of copper value). The table was compiled mainly from the extensive, detailed, and voluminous compilations cited above.

Feature	Amount and area	Valuable hypogene minerals	Valuable supergene minerals
Surface and depth	Surface: generally greater than 500 m in diameter, and commonly at least 400 m in depth.	Hypogene minerals are found at the surface in glaciated terrains but are rare in areas that are supergene altered.	Supergene copper oxide minerals are sometimes recoverable. Supergene copper sulfides are generally recoverable.
Tonnage overall	Commonly 100–500 million tonnes. ≥300 million tonnes usually are ‘world class’.	Tonnage of ore is generally limited to the tonnage of the volume with a grade greater than a specified economic cut-off. For example, “The resource at the No-Name-Deposit is estimated at 125 million tonnes averaging 0.31% copper with a 0.2% copper cut-off.	It is included in the column to the left.
Copper grade	0.5– 3% CuEq. Better grades are the result of supergene enrichment, but these rich supergene zones are increasingly mined out.	Main minerals are chalcopyrite, bornite and molybdenite. Also relevant is the comment on ‘cut-off’ in the description for tonnage.	Chalcocite, covellite, chrysocolla, cuprite, chalcantite, antlerite and brochantite.
Molybdenum	≤1% MoS ₂ = 0.899% MoO ₃ = 0.599% Mo.	Molybdenite	Ferrimolybdate and powellite in capping is not recovered.

Gold and silver	≤0.5 g/t each; generally, they are by-products.	Silver, gold and electrum. Commonly associated with magnetite, hematite and molybdenite.	Some oxidized cappings have recoverable gold and silver by heap leaching.
Tin and tungsten	≤0.5% Sn = 0.64% SnO ₂ and/or 0.5% WO ₃ = 0.397% W.	Cassiterite, stannite, wolframite and scheelite.	
Pyrite	Pyrite is common in all deposits.	Pyrite generally is not economic and can promote acid generation problems. Locally pyrite is used to generate acid for leaching.	
Nepheline	Nepheline is locally abundant in nepheline syenite associated with alkaline porphyry deposits.	Nepheline, if free of iron impurities (e.g., biotite), might be valuable for glass manufacturing; it is not currently recovered.	
Mica and clay	≤10% might occur in some tailings.	Muscovite and other micas are not currently recovered but could be a valuable plastic additive.	Clay has unknown potential as a by-product in porphyry deposits; it is locally a source of pottery clay in supergene-altered greisen.
Gross value	Commonly billions of dollars.	Sum of the values for contained bornite, chalcopyrite and molybdenite, plus gold and silver and/or tin and tungsten credits.	Main minerals are chalcocite, chrysocolla, chalcantite, cuprite, antlerite and brochantite.

TABLE 1 illustrates that porphyry deposits are large, mineralized bodies of rock. These bodies were initially fractured so hydrothermal fluids could flow through and mineralize the rock. Because most of the fluid is magmatic in origin, these fluids were hot (250° to 650°C), and metals were transported in the fluid mainly as chloride complexes. New alteration minerals were formed as the fluids reacted with the rocks they passed through. As a result, compositions in the outward and upward moving fluids also changed. Systematic changes in moving fluid composition and in temperature result in zoning, within which there are predictable locations for ore mineralization. Consequently, zone mapping in the field by a geologist, with reference to porphyry deposit models, is crucial in exploration leading to mine discovery.

Definitions specifically related to porphyry deposits are in the insert that follows. Defined are a) *Definitions of porphyry and greisen*, b) *Definition of pre- syn- or post mineral and intermineral*, c) *Definitions of alteration, hydrothermal, hypogene, ore shell, pyrite halo and supergene* and d) *Definitions of porphyry deposit, greisen porphyry deposit and gold porphyry deposit*.

Definitions related to breccias are also in the following insert. Defined are *Definitions of breccia, breccia pipes, hydrothermal breccia, collapse breccia, fault breccia, pseudobreccia or crackle breccia, and sedimentary breccias and conglomerate*.

Definitions of porphyry and greisen.

Porphyry describes any igneous rock where conspicuous phenocrysts (larger crystals) are set in a finer-grained to glassy matrix or groundmass. Porphyry names are commonly modified to describe prominent phenocrysts, for example, quartz porphyry, feldspar porphyry and quartz-feldspar-biotite porphyry. Some porphyritic rocks explode into breccias and exude hydrothermal fluids that lead to ore mineralization and alteration. These hydrous, 'wet' or 'productive' porphyries are likely to be more ore productive than 'dry' porphyries. Pyrometasmatic deposits with skarn-mineral assemblages can be spatially related to porphyry deposits, where carbonate rocks occur peripherally to porphyry deposits.

Greisen consists essentially of quartz and muscovite without feldspar or biotite and resembles classic phyllic alteration facies. Where greisen is generated by S- or A-type granites, commonly associated minerals are fluorite, tourmaline, topaz, cassiterite and wolframite. Greisen, widely found within cupolas of stocks, forms massive bodies by altering pre-existing granitic rock and/or by the consolidation of a hydrous, terminal differentiation granitic phase in cupolas. Greisen veins cut rocks in granitic cupolas and extend into adjacent country-rock. Metal zoning and silicate zoning are common in both veins and massive bodies.

Definition of pre- syn- or post-mineral and intermineral.

Pre- syn- or post-mineral refers to the timing of intrusion of stocks, dykes and breccias. Syn-mineral implies a genetic link to ore mineralization. The classification is key to the recognition of the most significant events related to ore deposit formation.

Intermineral is the same as syn-mineral about intrusions of stocks, dykes and breccias. It can also be used to describe fracturing that occurs synchronously with mineralization. Thus, intermineral and syn-mineral are both used to define key intrusive events related to ore deposit formation.

Definitions of alteration, hydrothermal, hypogene, ore shell, pyrite halo and supergene.

Alteration means a *change* in mineralogy (sulfides, silicates, carbonates, etc.), fracturing and/or hornfelsing. Mapping all these features is key to locating likely ore zones within porphyry deposits.

Hydrothermal is derived from *hydro* = water and *thermal* = heat; therefore, *hydrothermal* simply means *hot water*. Heat transfer and transfer of dissolved components causing mineralization and alteration are major features of a *hydrothermal* system.

Hypogene is derived from *hypo* = under and *gene* = origin; therefore, *hypogene* = origin from below. Hypogene mineralization is primary mineralization formed at depth before modification by supergene processes.

Ore shell is a toroidal zone of economically valuable mineralization (high grades mainly of copper and/or molybdenum) surrounding the barren core of a porphyry deposit. It generally spans the contact of deposit-central potassic alteration marked by secondary K-feldspar and biotite (phlogopite) with the outwardly adjacent phyllic alteration dominated by quartz and muscovite (sericite). The ore shell is marked by high chalcopyrite/pyrite ratios, and by molybdenite, bornite and magnetite and specularite becoming more abundant toward and within the potassic portion of the shell. The ore shell is often expressed as moderate chargeability anomalies by an induced polarization (IP) geophysical survey; however, these anomalies are less intense than those related to the pyrite halo.

Pyrite halo is a toroidal zone outside of the ore shell in porphyry deposits. It occurs in the outer part of the phyllic alteration zone, and is marked by abundant quartz, muscovite (sericite), pyrite and high pyrite to chalcopyrite ratios. Grade of copper is usually too low to be economically valuable. The pyrite halo is often detected by high chargeability anomalies in induced polarization (IP) geophysical surveys. These high chargeability anomalies commonly are drilled before the lesser anomalies associated with the ore shell—with discouraging results. As a result, an IP geophysical survey to a facetious geologist is an ‘iron pyrite’ survey.

Supergene is derived from *super* = above and *gene* = origin; therefore, *supergene* = origin from above, or superimposed secondary mineralization formed relatively near the surface as opposed to deep hypogene processes. Thus, supergene alteration is related to surface conditions (e.g., temperature and rain), original mineralogy, permeability, and fluctuations in the water-table that defines a boundary between overlying oxidizing and underlying reducing conditions. *Subdivisions of supergene* alteration zones in porphyry deposits, working downwards, are a) *weathered* (referring to surface changes), b) *capping*, and c) *supergene enrichment* (commonly divisible into an overlying *supergene oxide* and an underlying *supergene sulfide*).

Definitions of porphyry deposit, greisen porphyry deposit and gold porphyry deposit.

Porphyry deposits are large (≥ 20 million tonnes), low-grade deposits of copper and/or molybdenum, tungsten and tin, and gold and silver, which, as the name suggests, are commonly associated with porphyritic rocks. A rusty surface thumbprint typically marks these deposits. The primary mineralization source is hydrothermal fluids exsolved from intrusive plutons. Systematic zoning of silicate, sulfide and carbonate alteration minerals and their mode or habit of occurrence commonly provide vectors to the location of orebodies. Some tungsten–tin±molybdenum±silver/gold greisen deposits are large enough to be included in the porphyry deposit category. Values from gold (generally < 0.5 g/t) and silver can be

important as by-products in sulfide concentrates. However, some deposits that contain only gold and silver can also be included as porphyry deposits. Porphyry deposits can represent deep underlying sources for epithermal deposits that might include Carlin-type deposits. Porphyry deposits are equidimensional in plan view and extend to variable depths. They are commonly mined by open-pit methods to depths of about 400 m. Underground bulk mining is becoming increasingly common as near-surface resources are mined out.

Greisen porphyry deposits (Elliott et al., 1995; cf. Sinclair, 1996) are bodies of quartz-muscovite phyllic alteration or greisen that are more than 20 million tonnes in size. Greisen porphyry deposits commonly have varying amounts of topaz, lepidolite, tourmaline, fluorite, and beryl. Economic potential is mainly in tin as cassiterite and/or lesser stannite, tungsten as wolframite and/or lesser scheelite and molybdenum as molybdenite; silver and gold can be associated. Greisen occurs near upper contacts of cupolas to highly evolved, rare-metal-enriched plutonic rocks commonly of the S or A types (see insert *Origin of S-, A- and I-type granitic rocks*) resulting in lithophile signatures in which uranium, thorium, rare earth elements and phosphates can be significant. Vein and disseminated mineralization in greisen has complex spherical zoning that varies vertically and horizontally, with the most economically significant mineralization located in core zones.

Gold porphyry deposits are bulk gold and silver deposits greater than 20 million tonnes in size. Gold and silver occur in calcalkaline granitic plutons and surrounding sediments associated with alteration typical of porphyry deposits (quartz veins with highly saline fluid inclusions, potassic and phyllic alteration, etc.). They might underly and form Carlin-type gold-silver deposits in carbonate/shale terrane.

Definitions of breccia, breccia pipes, hydrothermal breccia, collapse breccia, fault breccia, pseudobreccia or crackle breccia, and sedimentary breccias and conglomerate.

Breccia in the porphyry deposit environment (aside from sedimentary breccia, below) is a coarse-grained clastic rock composed of rotated and/or inflated clasts or fragments that are typically angular or rounded, held together by a relatively fine-grained matrix (cf. Sawkins and Sillitoe, 1985). Breccia can be named after the matrix composition, for example, tourmalinite *breccia* (tourmaline-quartz matrix) or *magnetite breccia* (magnetite-apatite matrix). Alternative qualifiers refer to process of formation, such as *hydrothermal breccia* (formed by rupturing due to hydrothermal explosion), *collapse breccia* (from stoping triggered by the corrosive action of hydrothermal fluids or by magma withdrawal), *magmatic breccia* (formed by rupture related to the intrusion of a magma melt or crystal mush with variable hydrous component) or *fault breccia*, (fragmentation results from frictional breaking and/or rock bursting in dilatant fractures). Detailed descriptions of breccia clasts and breccia matrix are essential, especially if either or both are mineralized/altered. Maximum fragment size, modal fragment size and *open* (matrix-supported) or *closed* (fragment-supported) framework, can be related emplacement energy. As a rule of thumb, if the percentage of fragments on a planar surface is less than 50%, the breccia is likely *open*, or matrix supported. Breccia and porphyry commonly are genetically related.

Breccia pipes, also referred to as diatremes or chimneys, are masses of breccia with an irregular cylindrical shape that intrude and crosscut earlier rocks. Diatreme (Doubrée, 1891) means 'through the hole' and implies emplacement by a drilling process that used the explosive energy of gas-charged magmas (cf. Bryant, 1968, and Bryner, 1968). Most breccia pipes are formed by an explosive mechanism accompanied by gas fluxing and fluidization (Reynolds, 1954; Richard and Courtright, 1958; Carr, 1960), rock bursting,

stope cave filling (Locke 1926; Gates, 1959; Perry, 1961; Norton and Cathles, 1973) and rounding of fragments by attrition due to movement during emplacement (Clark, 1990). Shatter cleavage is an index fossil for breccia because it occurs close to, or adjacent to, some breccias (see insert Story on index fossil shatter cleavage and Godwin, 1973, 1975 and 1976).

Hydrothermal breccia is formed by rupturing due to hydrothermal explosion and subsequent emplacement (cf. Burnham, 1985).

Collapse breccia is formed by volume reduction by processes such as magma withdrawal (cf. Perry, 1961), and dissolution by hydrothermal-related processes.

Fault breccia is formed by rupture due to faulting. Fragmentation is primarily a result of frictional breaking and/or rock bursting into dilatant zones.

Pseudobreccia or crackle breccia are commonly used terms but should be avoided. Pseudobreccia or crackle breccia describes a rock with a fragmental appearance due to alteration and/or veining in or around closely spaced fractures. However, there is no fragment rotation or fragment inflation by the intrusion of a matrix. Better names for 'pseudobreccia' or 'crackle breccia' would be 'altered crackle zone' or 'altered fracture zone' because the demonstration of fragment rotation and fragment dilation (inflation) by an intruded matrix, is essential to the definition of a breccia.

Sedimentary breccias and conglomerates are distinct from, but sometimes confused with, hydrothermal breccias of specific interest in porphyry and epithermal deposits. These two types can often be distinguished by careful examination of the matrix and fragments; specifically, mineralized/altered matrix or fragments indicates a hydrothermal origin (see insert *Story on conglomerate versus breccia at Casino, central Yukon, Canada*).

Late- or end-stage magmatic differentiation often can be related to economic mineralization and alteration of porphyry deposits. Bowen's (1956) reaction series provides a simple model for why potassic minerals (e.g., K-feldspar and biotite) and sodic minerals (e.g., albite) form late. In addition to the framework provided by Bowen's reaction series, most minerals in granitic rocks are anhydrous, poor in metals and do not entrain atoms of odd size or charge. Later magmatic differentiates tend to become more hydrous and increasingly enriched in potassium, sodium, fluorine, chlorine, metals (e.g., copper and molybdenum, and sometimes iron) and some elements of odd size or charge (e.g., boron, sulfur and phosphorous). Thus, end-stage phases form immiscible and hydrous tourmalinite (silica, boron, fluorine and metals) and magnetite-apatite (iron, phosphorous, fluorine and metals) magmas. The fluids are also exsolved from the magma to become hydrothermal mineralizers, resulting in the deposition of veins and disseminations of sulfide and oxide mineralization (e.g., chalcopyrite, bornite, pyrite, magnetite, cassiterite, wolframite and molybdenite) associated with porphyry deposits.

Be sure you know from this section the:

- ➔ definitions for main deposit features,
- ➔ general characteristics of size and grade,
- ➔ common host rock associations, and
- ➔ specifics about breccias.

BASIC TYPES AND OVERVIEW PHOTOS

In this section you will:

- learn a fundamental twofold division of porphyry deposits, and
- see overview photos for different porphyry deposits.

Porphyry deposits can generally be related to two types of intrusive rocks. Those that are:

1. Hosted mainly within genetically related batholiths that are either a) quartz-bearing, calcalkaline, or b) quartz-poor, alkaline and/or dioritic.
2. Hosted in, or related mainly to, granitic dykes and/or to apices and cupolas of granitic stocks.
3. Some porphyry deposits are hosted in volcanic and/or sedimentary rocks, but these generally are spatially related to the intrusive categories above.

Sutherland Brown (1976a) divided porphyry deposits in British Columbia, Canada, into three types: plutonic, phallic, and volcanic. The plutonic type is equivalent to the granitic-batholith type described here. The phallic type is the same as the granitic dyke or stock and cupola type. The volcanic type describes granitic dyke or stock-cupola type deposits where the significant mineralization is within volcanic rocks surrounding and/or underlain by dykes, and/or stock and cupola.

Overview photos in Figures 1 to 5 provide an overview of the large size and appearance of porphyry deposits of different types. These, as related to the general types above, are:

- Figure 1. Calcalkaline granitic stock: *Casino calcalkaline porphyry copper-molybdenum-gold deposit* in central Yukon, Canada,
- Figure 2. Quartz-rich calcalkaline granitic batholith: *Endako molybdenum porphyry mine* in central British Columbia, Canada,
- Figure 3. Quartz-poor alkaline and dioritic batholith: *Copper Mountain alkaline-diorite copper-gold porphyry deposit mine* near Princeton, south-central British Columbia, Canada,
- Figure 4. Calcalkaline granitic cupola: *Don Luis tungsten-silver greisen-porphyry prospect* in Sonora, Mexico, and
- Figure 5. Calcalkaline granitic stocks: *La Colorada gold-porphyry mine* in Sonora, Mexico.

These photos show the large, potentially huge, size and overall appearance of porphyry deposits. Many of these porphyry deposits are, or originally were, characterized at surface by extensive rusty-limonitic thumbprints (e.g., Casino in Figure 1 and Don Luis in Figure 4).

The porphyry deposits, above and as mentioned in the text that follows, are located by decimal-latitude and -longitude in Appendix B. Satellite imagery for these deposits are readily accessible in EarthExplorer, a United States Geological Survey website at <https://earthexplorer.usgs.gov>.



Figure 1. Looking north to Patton Hill at the Casino calkalkaline copper-gold-molybdenum porphyry deposit in central Yukon, Canada.

The deposit is related to a calkalkalic stock. 1971 photo, looking northwest, shows the rusty limonite thumbprint and large size common to porphyry deposits.



Figure 2. Aerial view of the Endako porphyry molybdenum mine in central British Columbia, Canada.

The deposit is hosted within a quartz-rich calcalkaline batholith. The overall length of the pits is about four kilometres. 2010 photo, looking southeast, is courtesy of Centerra Gold Inc., Vancouver, BC, Canada.



Figure 3. Aerial view of the Copper Mountain alkaline porphyry copper-gold mine in south-central British Columbia, Canada.

The deposit is hosted within a quartz-poor alkaline and dioritic batholith. Photo, taken in 2018, looks southeast along the axis of pits 1 and 3 merged with pit 2 on the left. Overall, the pits in the picture span about 2.8 km. 2015 photo courtesy of Peter Holbek, Vice President Exploration, Copper Mountain Mining Corporation, Vancouver, BC, Canada.



Figure 4. Don Luis tungsten-silver greisen-porphyry prospect in Sonora, Mexico.
The greisen represents cupolas related to underlying stocks. 2010 photo | Looking northwest to an old adit within a limonite-rich area characterized by greisen and abundant brain rock with unidirectional solidification texture.



Figure 5. The Creston pit at the La Colorada gold-silver porphyry mine in Sonora, Mexico. This pit, photographed in 2006 and looking east, is centred on a calcalkaline stock. The bottom of the pit, in and immediately surrounding the water, is a granodiorite stock. The walls of the pit are carbonaceous sandstone/quartzite. A major east-west fault passes through the end-centre of the picture, marked by a colour change. Gold-silver occurs in a) veins in the stock, b) veins in the easterly trending fault, and c) veins and disseminations in the carbonaceous sandstone/quartzite.

Be sure you understand from this section that porphyry deposits:

- ➔ can be subdivided into two major categories those a) hosted mainly within genetically related batholiths and b) hosted in or spatially related to granitic dykes and/or to apices and cupolas of granitic stocks,
- ➔ are large and commonly mined by open-pit methods, and
- ➔ are often initially marked by a prominent rusty-limonitic thumbprint.

HABITS OF MINERALIZATION AND ALTERATION

In this section you will:

- review the habits of alteration that are commonly related to veins and breccias,
- learn the characteristics, and significance, of quartz blobs and unidirectional solidification texture in brain rock,
- understand the characteristics and origin of gusano habit, and
- learn about describing multiple alteration events.

Common Alteration Habits in Porphyry Deposits

The habit of alteration is generally equivalent to texture in describing *how* alteration occurs; however, some habits can embrace variable textures. Because of this, the term *habit* is a more explicit term than *texture*. The habits most relevant to porphyry deposits are reviewed in the book *Porphyry and Epithermal Deposits: Mineralization, Alteration and Logging* (Godwin, 2020). Descriptions are repeated here but often in more detail. These habits characterize porphyry deposit mineralization, so field identification is important.

The most common habits (veins, selvages, envelopes, pervasive and disseminations) of mineral alteration in porphyry deposits are illustrated in Figure 6. Veins are fracture fillings. Mineralization that occurs at the wallrock margin of the vein, but is part of the vein, is called a selvedge. Altered wallrock outside of the vein is called an envelope; successive envelopes can occur. Broadly altered wallrock is said to be pervasively altered. Disseminated mineralization occurs as discrete, scattered grains; pyrite disseminations are a typical example. Disseminations can occur within veins, in envelopes and pervasive alteration. In the literature, there are different interpretations and names for some of these habits of occurrence. Specifically, it is not always clear that a selvedge is part of the vein as defined here, and an envelope is commonly called a 'halo', which is not used here because an envelope is not circular but planar.

Habits of alteration common in porphyry deposits are summarized in TABLE 2, which is keyed to Figures 6 to 16. A complete listing of habits with their three-capitalized-letter codes for describing them may be found in Godwin (2020).

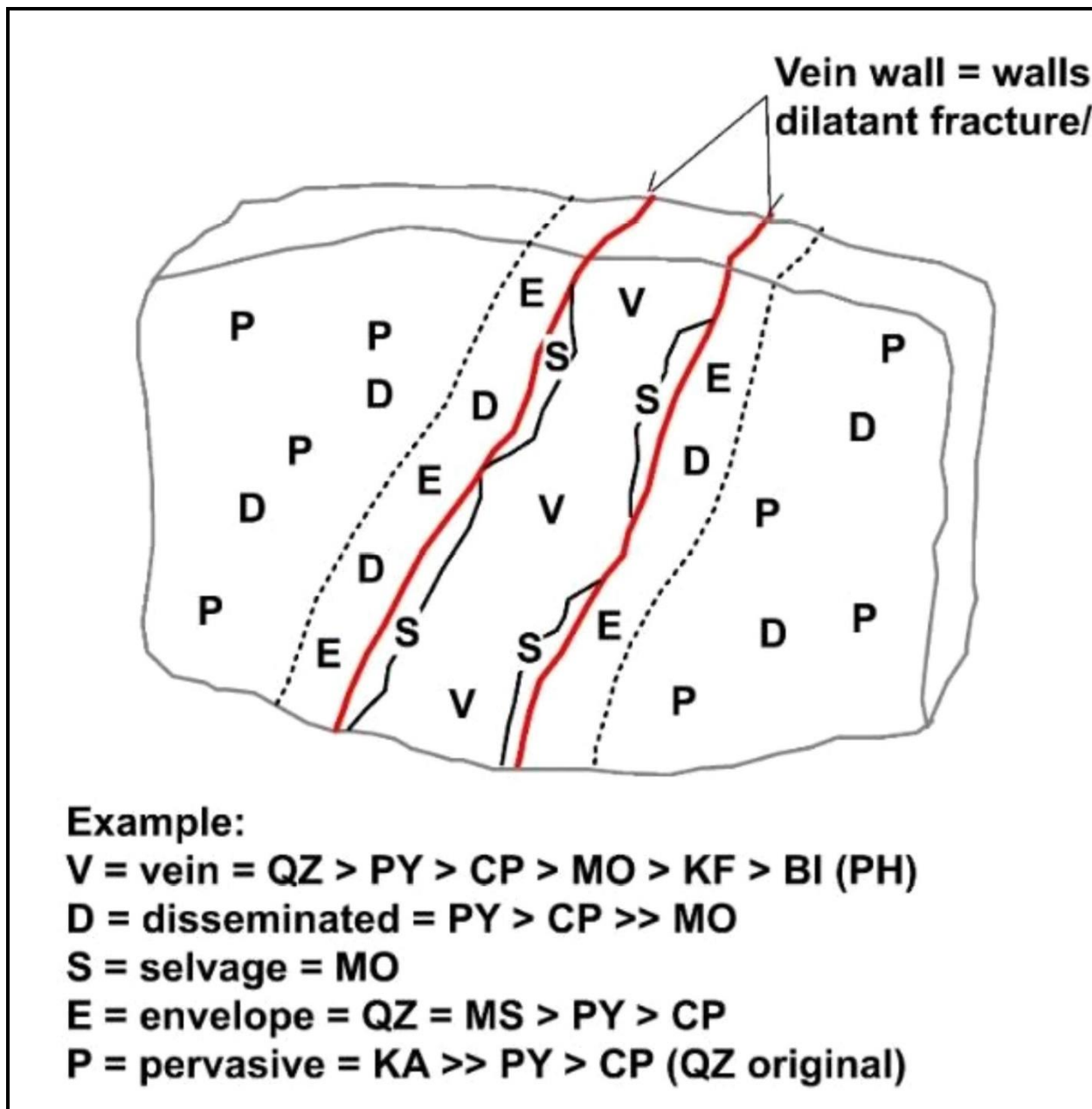


Figure 6. Spatial relationships among vein, selvedge, envelope, pervasive and disseminated habits of alteration.

Veins (V) are fracture fillings. The selvedge (S) is part of the vein but at the rock-fracture wall. The envelope (E) and pervasive habits (P) are altered host rock. Disseminations, of course, can also occur within veins, envelopes, and selvedges. Other abbreviations are: BI = biotite (or phlogopite: PH), CP = chalcopyrite, KA = kaolinite, KF = K-feldspar (orthoclase), MO = molybdenite, MS = muscovite/sericite, PY = pyrite and QZ = quartz, > = greater than and >> = much greater than. The figure is from Godwin (2020).

TABLE 2. *Habit of alteration.*

Habit of alteration/ code/figure(s)	Description of habit
Breccia	Breccia is a rock composed of breccia clasts that are broken fragments of rock or minerals that are cemented together by a breccia matrix that is markedly finer grained than the clasts. Breccia clast <i>rotation</i> and/or <i>inflation</i> is essential to the definition of a breccia.
Breccia clasts BRC Figure 7	Breccia clasts can be a) fresh rock, b) variably altered and mineralized during breccia formation, or c) previously altered and/or mineralized (e.g., quartz vein clasts or sulfide-mineralized breccia fragments). <i>Fragment supported</i> or <i>closed</i> describes breccia with a framework of touching fragments. This contrasts with <i>matrix-supported</i> or <i>open</i> , which describes breccia where the fragments do not form a touching framework. See insert <i>Definition of breccia</i> .
Breccia matrix BRM Figure 7	Breccia matrix consists of markedly finer grains than the fragments. It is variously altered and mineralized before, during and after breccia formation. Mineralization is often concentrated at fragment margins where wedge-shaped spaces open due to fragment rotation. Breccia matrix can display bedding formed by sorting from the passage of the hydrothermal fluids and gasses that accompanied the brecciation.
Disseminated DIS or D Figures 6 and 8	Disseminated refers to discrete and scattered secondary mineral grains dispersed throughout a rock or vein. Disseminated pyrite is common. Limonite boxwork shapes can sometimes identify the mineralogy of prior sulfides.
Envelope ENV or E Figures 6, 9 and 10	Envelope is the planar zone of altered wallrock flanking and outside a causative vein (cf. selvedge, which is part of the vein); several envelopes can exist beyond a vein. Border contacts of envelopes are usually sharp. Original textures and minerals within the envelope generally are destroyed—the term ‘halo’ is not appropriate because haloes are round.
Flooded FLD Figure 11	Flooded alteration occurs where a mineral (such as albite or quartz) or minerals (such as quartz–K-feldspar) extensively swamp original minerals and textures. It differs from pervasive alteration

	because the flooding alteration mineral(s) represents a massive material addition.
Gusano GUS Figure 12	Gusano (<i>worm</i> in Spanish; also called ovoidal and mottled texture [Noble et al., 2010]) habit consists of ovoid and irregularly mottled or patchy, worm-like bodies several millimetres to about three centimetres in diameter. This habit in epithermal deposits indicates a shallowly underlying porphyry deposit. See insert <i>Origin of gusano habit</i> .
Pervasive PER or P Figures 6 and 38	Pervasive alteration refers to wallrock beyond veins and envelopes that is altered throughout (versus disseminated, which describes discrete grains) by diffusion of hydrothermal fluids from veins. Pervasive alteration sometimes refers to alteration resulting from merging abundant envelope alteration to a uniform-looking altered rock. Flooded is a more appropriate description where there is a significant addition of alteration components.
Porphyritic POR Figure 13	Porphyritic describes an igneous rock with conspicuously larger crystals (phenocrysts) set in a finer grained to glassy matrix or groundmass. See also the insert <i>Definition of porphyry</i> .
Selvedge SEL or S Figures 6 and 14	Selvedge is the zone within but at the wallrock margin of the vein. There is no universal acceptance of this definition; however, adoption as proposed here can be of exploration significance (e.g., a selvedge could aid beneficiation, as in the case where molybdenite occurs in a selvedge might be beneficiated by simple crushing and screening).
Unidirectional solidification texture UST Figures 17 and 18	Unidirectional solidification texture is a habit (Shannon et al., 1982) that defines brain rock. It is also known as 'crenulate quartz layers' (White et al., 1981) and 'comb-quartz layers' (Kirkham and Sinclair, 1988; Sinclair, 2007). Multiple and contorted quartz bands exhibit quartz teeth that point in the same direction, either away from or toward the intrusive core (i.e., toward the causative intrusive core or the outer country-rock). The quartz bands are separated by aplite, greisen, or rarely, tourmalinite. This habit indicates hydrous late- or end-stage magmatic formation and a continuous supply of magmatic-hydrothermal fluid from subjacent magma (Sinclair, 2007). Some world-class porphyry deposits (e.g., Climax and Henderson molybdenum porphyry deposits in Colorado, United States, and Oyu Tolgoi copper-gold porphyry deposit in the south Gobi Desert of Mongolia) are associated with UST in brain rock. For this reason alone, it demands attention as

	an <i>index fossil</i> for major porphyry deposits. See also the insert <i>Explanations of UST textures in brain rock</i> .
Quartz blobs (quartzolite or silexite) and associated quartz breccia QZOT, SILX, BRQZ Figure 19	Quartz blobs (quartzolite or silexite) and quartz breccia can be 100 m or more across. They can be associated with UST in brain rock, and they resemble, and may be related to, massive, quartz-dominant pegmatite bodies. These massive quartz blobs are associated with some major porphyry deposits (e.g., the Ok Tedi mine in Papua New Guinea and the Mineral Park mine in Arizona, United States).
Vein, macrovein and microvein VEN or V, VMA and VMC Figures 6, 9 and 10	Vein, macrovein and microvein in porphyry deposits should be viewed as fracture fillings. Descriptions can vary. For example, veins can have parallel or unequal sides and/or be vuggy, ribboned, symmetrically zoned and brecciated. Crosscutting relationships, symmetrical zoning and variations in mineralogy can define the relative timing of mineralizing episodes. Size differences between macroveins, veins and microveins are commonly defined: macrovein = greater than 10 cm; vein = 1 mm to 10 cm; and microvein = less than 1 mm. All veins Detailed studies of veins within porphyry deposits commonly subdivide them into a, b, c and d types following Gustafason and Hunt (1975). Microscopic fluid inclusion studies can divide them into I, II, III and IV types (Nash, 1976).
Veins, sheeted VSH Figures 9 and 15	Veins, sheeted , describes numerous, densely spaced subparallel veins.
Vein stockwork VSK Figure 16	Vein stockwork describes abundant, crisscrossing veins over a large area. The density of the veins is too great to define them individually easily.
Weathering WET Figures 10 and 15	Weathering describes how soil and rocks are changed by surficial agents, causing mechanical and chemical changes and/or disintegration.

Breccia: Breccia Clasts and Breccia Matrix Habits

Essential characteristics of breccia, breccia clasts and breccia matrix are shown in TABLE 2 and Figure 7. (See also insert *Definitions of porphyry, breccia, breccia pipes and greisen.*)

Breccia is a rock composed of **breccia clasts** that are broken fragments of rock or minerals that are cemented together by a **breccia matrix** that is markedly finer grained than the clasts. The composition of the breccia matrix can be like, or different from, the composition of the breccia clasts. Breccia clast rotation and/or inflation is essential to the definition of a breccia.

Breccia clasts can be fresh rock, variably altered and mineralized during breccia formation, or previously altered and/or mineralized (e.g., quartz vein clasts or sulfide-mineralized breccia fragments). Mineralized vein or breccia fragments or clasts within a breccia indicate multiple mineralizing/brecciation episodes; multiple mineralizing episodes signal multiple opportunities for significant ore mineralization. *Fragment-supported* or *closed* describes breccia with a framework of touching fragments. *Matrix-supported* or *open* describes breccia where the fragments do not form a touching framework. In general, *matrix-supported* breccia indicates a higher energy of emplacement than *fragment-supported* breccia. A sliced surface of *fragment-supported* breccia will have about 50% matrix that might appear to be *matrix-supported* on a cut surface (imagine slicing a bowl of packed marbles). See insert *Definition of breccia*.

Breccia matrix consists of markedly finer grains (it can be rock flour) than the fragments. It is variously altered and mineralized before, during and after breccia formation. Mineralization is often concentrated at fragment margins where wedge-shaped spaces open due to fragment rotation. Thus, wedge-shaped sulfide- or limonite-rich wedges are often key indicators of breccia; these tend to be more abundant at the margins of breccia bodies. Breccia matrix can display bedding formed by sorting from the passage of the hydrothermal fluids and gasses that accompanied the brecciation. Bedding in breccia can also indicate the surface infill of craters formed by breccia intrusion.

Disseminated Habit

Disseminated habit (Figures 6 and 8) describes the scattered occurrence of a discrete mineral (or minerals) in a rock. Well known to all geologists is the common occurrence of disseminated pyrite. Figure 8 shows two examples of supergene-altered, disseminated sulfide mineral grains altered to limonite. The specimen in Figure 8a is also characterized by *shatter cleavage*, which is a significant marker for breccia bodies in porphyry deposits (see the section on breccia; Figures 20, 21 and 24; TABLE 5, and insert *Story about shatter cleavage, an index fossil*).

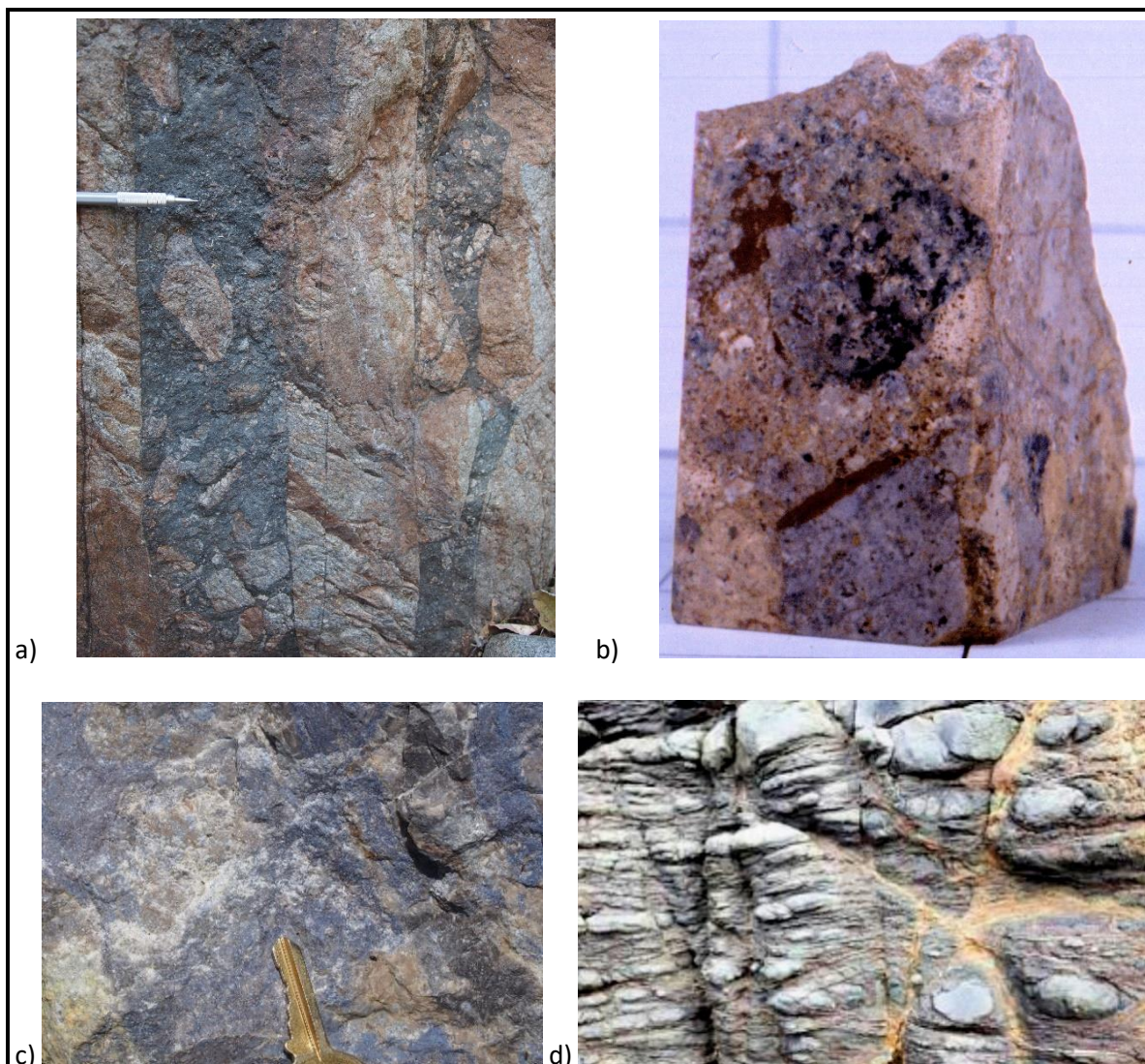


Figure 7. Breccia, breccia clasts, breccia matrix, and ‘pseudobreccia’ or ‘crackle breccia’.
a) Magmatic magnetite-apatite breccia is from the Inguaran porphyry prospect, central Michoacan, Mexico. b) Hydrothermal cobble breccia is from the Casino porphyry copper-gold-molybdenum deposit (Godwin, 1975; Bower et al., 1995), central Yukon, Canada. Breccia clasts are tourmalinized cobbles (black specks, indicating pre-brecciation mineralization). Hypogene sulfide mineralization is mainly in the breccia matrix. Prominent wedges of brown limonite occur at cobble boundaries because of spaces opened from fragment rotation. c) Hydrothermal breccia replaced with pyrophyllite (white) and dumortierite (blue). The specimen is from the Island Copper mine, northern Vancouver Island, British Columbia, Canada (Cargill et al., 1976 and Perrelló et al., 1995). d) Outcrop (location unknown, about 2 m across) illustrates a commonly called ‘pseudobreccia’ or ‘crackle breccia’. However, these terms should not be used because fragment rotation and/or inflation—essential to the definition of a breccia—does not occur.

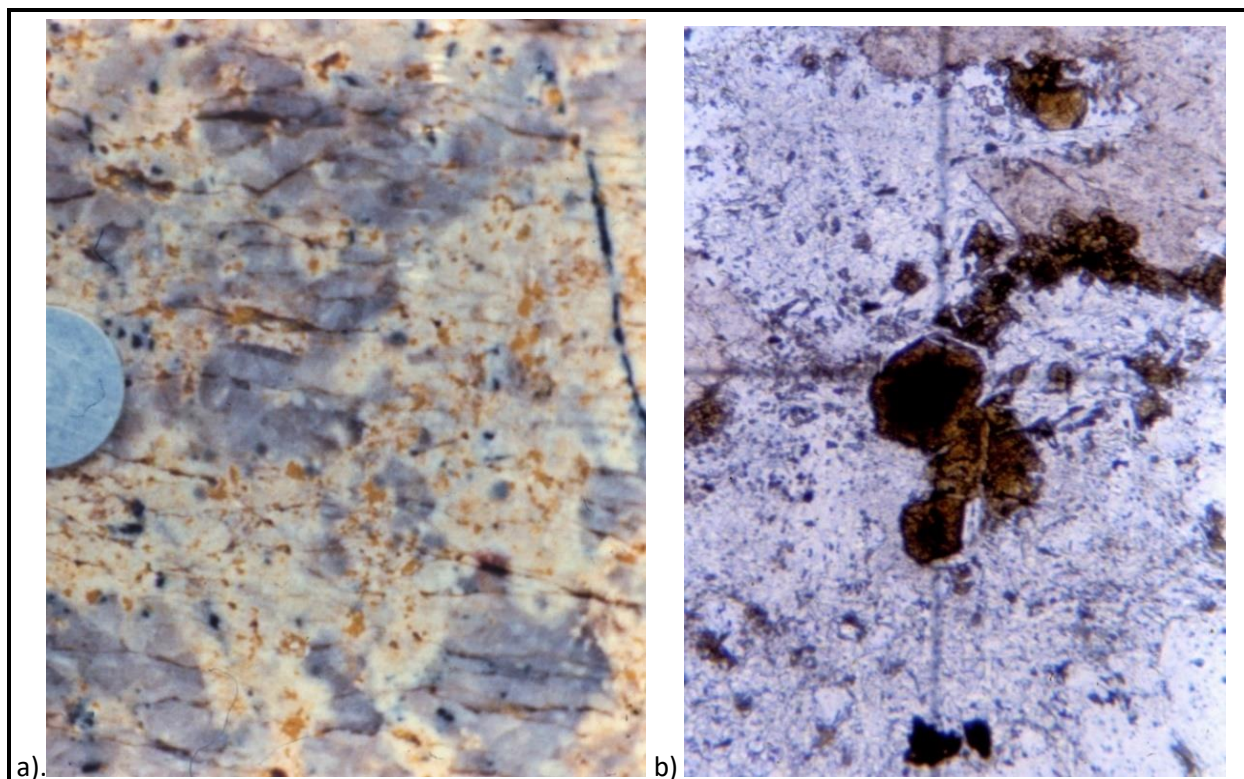


Figure 8. Disseminated habit.

Specimens are from the Casino deposit (Godwin, 1975; Bower et al., 1995), central Yukon, Canada. a) Disseminated limonite (brown spots) after sulfide in granitic rock with shatter cleavage (the disc is 5 mm in diameter). b) Thin section showing disseminated limonite (jarosite) boxwork. The pyritohedral boxwork shape identifies the original mineral as pyrite. The specimen is from a pyrite halo in phyllic alteration (originally quartz, sericite, and pyrite). Limonite grain in the centre of the thin section is 2 mm in diameter.

Envelope Habit

Envelope habit describes the zone of altered wallrock flanking and outside a vein (Figures 6, 9 and 10). Successive envelopes can exist but are not common. Original textures and minerals in the country-rock have often been destroyed. The term 'halo' is not appropriate because envelopes are planar, not circular. Note that selvedge, as defined here, refers to vein mineralization at the wallrock contact. Some definitions equate selvedge with envelope, negating the opportunity to uniquely describe both selvedges (within and at vein margins) and envelopes (outside but adjacent to veins).

Flooded Habit

Flooded habit describes rock that has been inundated with an alteration mineral such as quartz, K-feldspar, albite, or carbonate (Figure 11). The flooding commonly results from coalescence of envelopes developed around veins and microveins. The resulting product can look like massive rock.

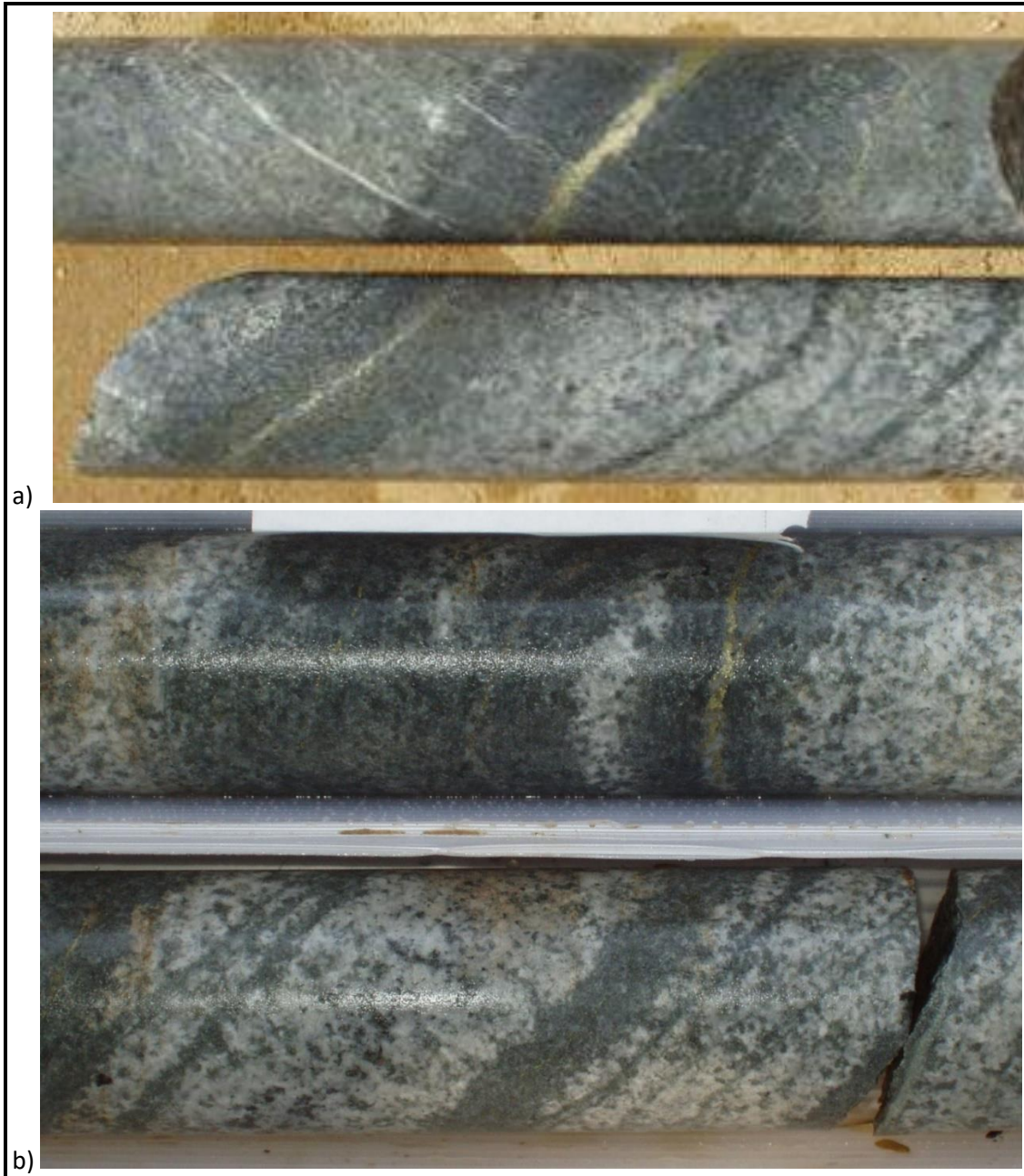


Figure 9. Drill core illustrating envelope habit.

Specimens about 4 cm in diameter are from the Inguaran porphyry prospect, Michoacan, Mexico. a) Veins of chalcopyrite greater than quartz with distinct sericite-quartz envelopes. b) Even where chalcopyrite-quartz veins are not apparent, envelopes of quartz-sericite flanking microveins/fractures are apparent. Splitting the rock along the microveins/fractures reveals traces of quartz and chalcopyrite on the fracture faces. Note that in a) and b), the sericite looks green but is not chlorite. The parallel veins with envelopes additionally can be described as sheeted veins (see Figure 15).

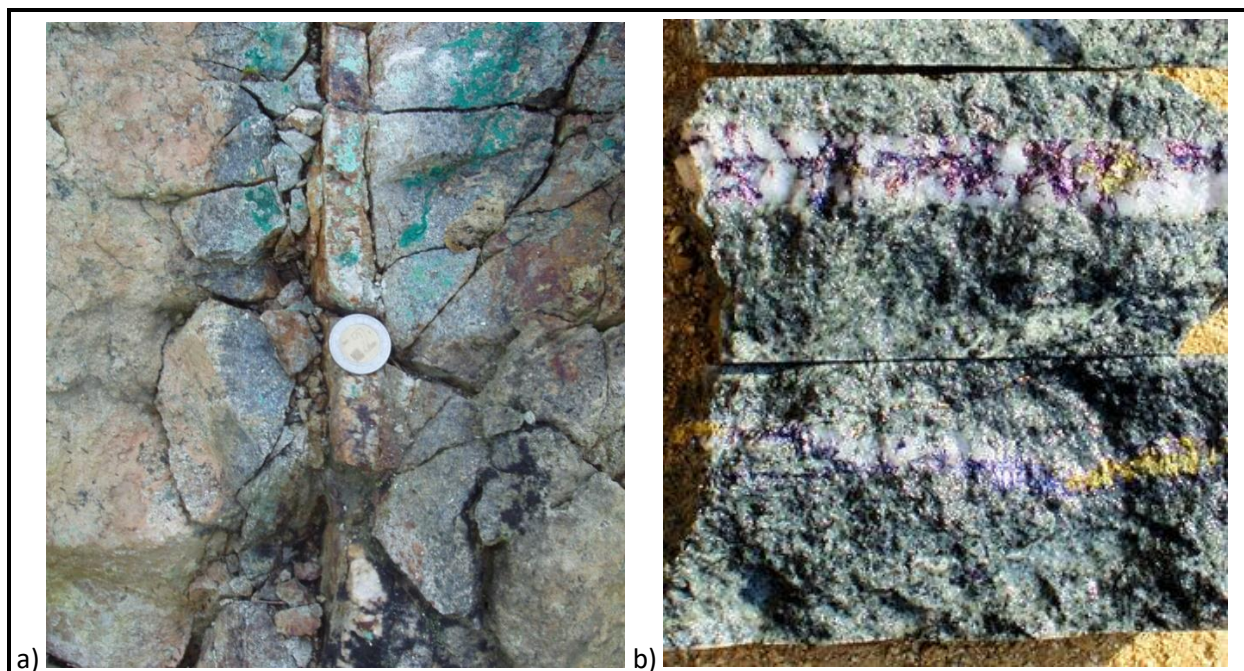


Figure 10. Veins and envelopes, locally with malachite from weathering.
 Photos are from the Inguaran porphyry prospect in Michoacan, Mexico. a) Quartz vein with a quartz-sericite envelope and secondary malachite from weathering, reflecting the copper sulfide within the vein. b) Quartz veins with more bornite than chalcopyrite and envelopes of more muscovite than quartz representing phyllic alteration (note that the envelope width almost exceeds that of the drill core; envelope width would be evident in longer sections of drill core).

Index Fossil Gusano Habit

Gusano habit (also called ovoidal and mottled texture [Noble et al., 2010]) consists of worm-like ('gusano' is a *worm* in Spanish), ovoid and irregularly mottled or patchy bodies. Generally, several millimetres to about three centimetres in diameter (Figure 12), they are up to 20 cm in maximum dimension. Gusano bodies are usually composed of intermixed pyrophyllite and alunite in a fine-grained quartz or chalcedony matrix. Boundaries of gusano-textured bodies are sharp against a matrix of lithocap rock in an epithermal environment. Gusano bodies imply the likely presence of an underlying porphyry deposit (i.e., in the order of 300 m to 500 m) that is enhanced by the presence of copper-bearing minerals (e.g., covellite). A theoretical origin of gusano habit is described in the insert *Origin of gusano habit*. Gusano habit in epithermal lithocaps is an *index fossil* for potential porphyry deposits at depth.

Origin of gusano habit: a theory.

Gusano habit forms from immiscible, fluid- and vapour-rich and silica-rich blebs (Noble et al., 2010). These blebs, deformed to variable ovoid shapes, are of magmatic origin and are derived from the outgassing of underlying magmas with porphyry deposit potential. The magmatic origin of the blebs is supported by the associated pyrophyllite that forms at magmatic temperatures.

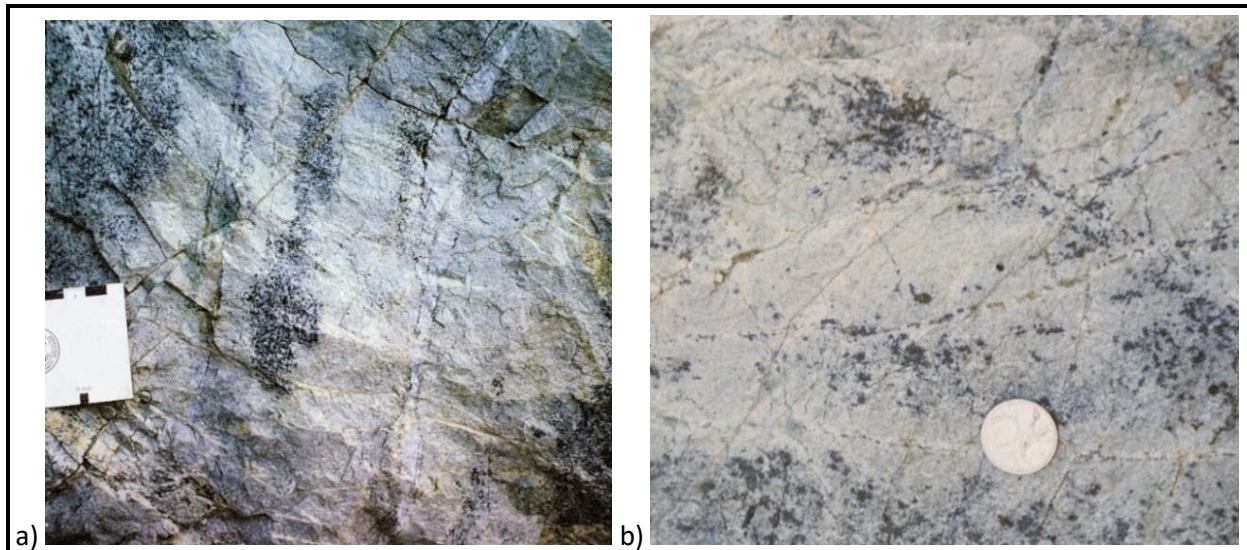


Figure 11. Flooded habit.

Flooded white albite alteration in a) and b) is from the Ajax alkaline porphyry deposit in south-central British Columbia, Canada. The albite alteration coalesces from envelopes around sulfide-bearing veins and microveins to form flooded, massive, white rock. K. Ross took photos in 1991 (Ross et al., 1995).

Porphyritic Habit

Porphyritic habit describes porphyries with conspicuous phenocrysts (larger crystals) set in a finer grained to glassy matrix or groundmass (Figure 13). Timing of intrusion for these rocks as stocks and dykes is essential and leads to pre-, syn- or post-ore mineralization classification. Some porphyritic rocks explode into breccia. They can also exude hydrothermal fluids leading to ore mineralization and alteration.

'**Productive porphyries**' can be identified by a) the abundance of hydrous, mineral phases (e.g., biotite is more hydrous than hornblende), b) the degree to which mineral components are late differentiates (e.g., abundant K-feldspar, albite, and biotite), and c) the presence of sulfides or other valuable minerals not typically found in igneous rocks. 'Productive porphyries' positively correlate with hydrothermal alteration (including ore minerals) and breccia formation. A common statement is that 'wet porphyries' are more important—especially if ore-mineral bearing—than 'dry porphyries' in the genesis of porphyry deposits.

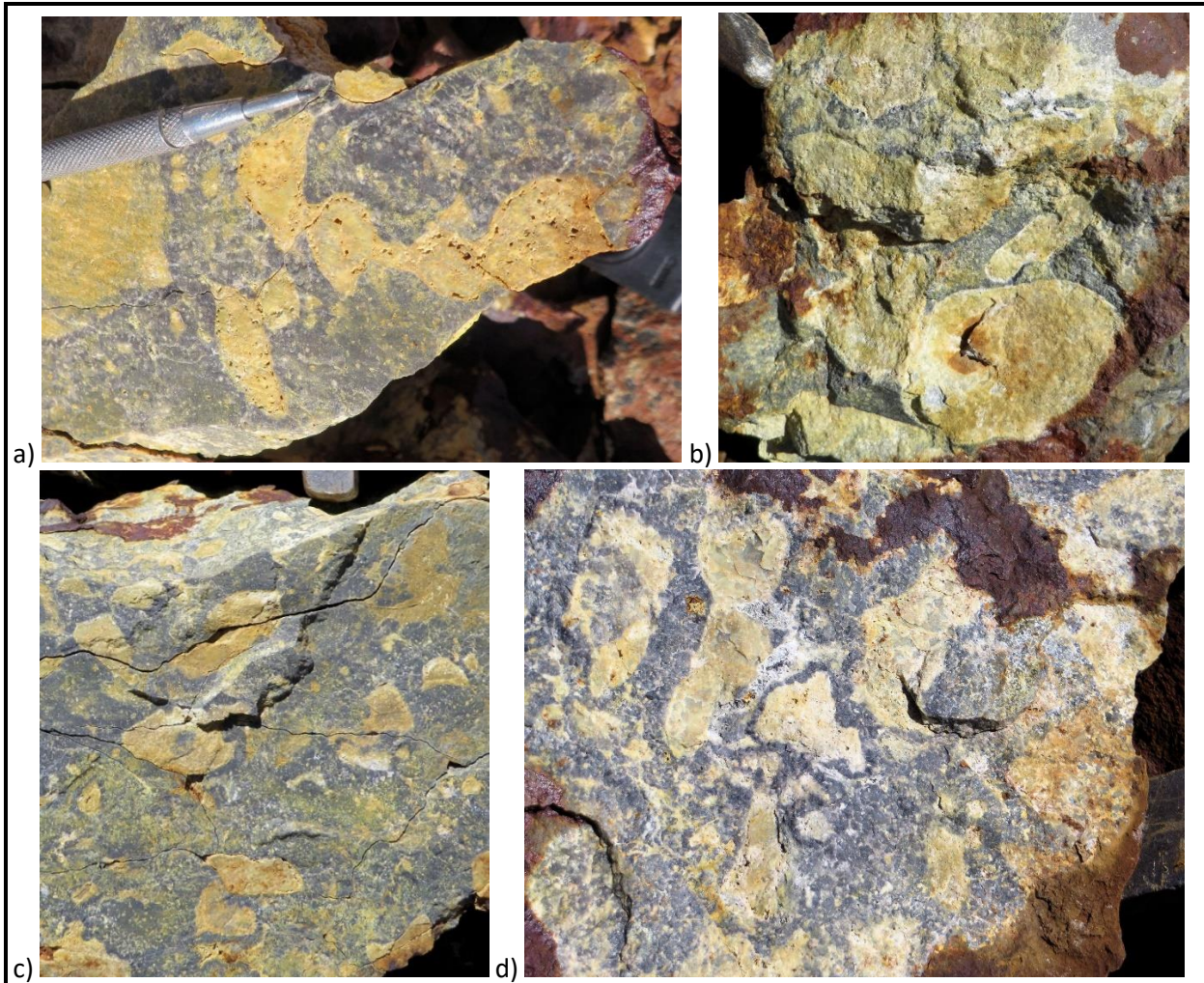
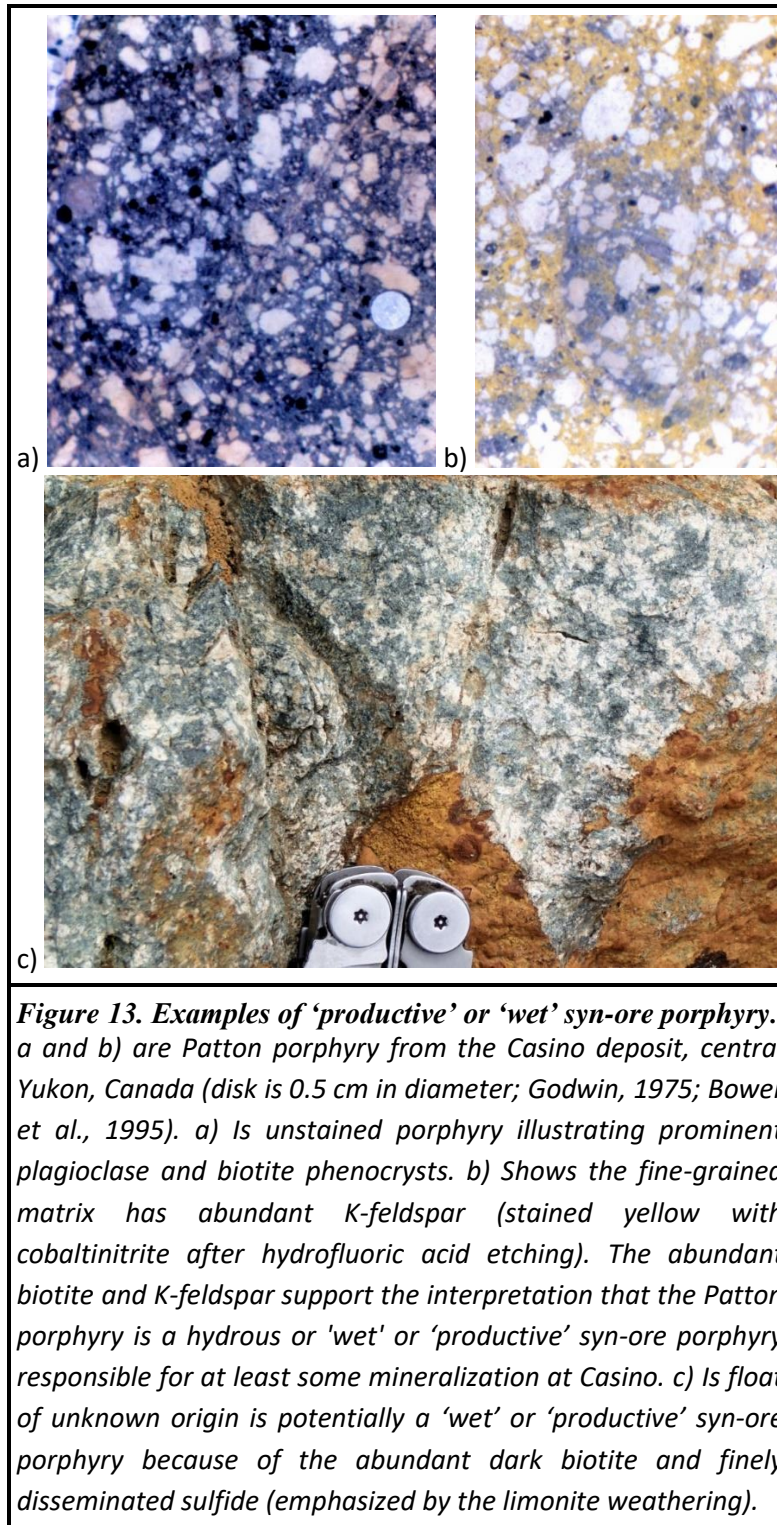


Figure 12. Gusano habit an index fossil for potential porphyry deposits at depth. Gusano habit is also known as ovoid and mottled texture. Ovoids consist mainly of pyrophyllite and alunite. Gusano habit in a high-sulfidation epithermal environment is an index fossil for potential underlying porphyry deposits. Scales in the photos are (a) magnet-scriber, (b and c) prospector's pick and d) ovoid in the centre is 3 cm across. John Bradford took the photos in 2015 at the Tanzilla epithermal-porphyry prospect, northwestern British Columbia, Canada.



Selvedge Habit

Selvedge is the zone at the wallrock margin of the vein but within the vein (Figures 6 and 14). Although not universally defined this way, adoption as defined here can be of exploration

significance. For example, molybdenite selvage can enhance beneficiation by simple, relatively cheap screening.



Figure 14. Selvage of quartz in contact with the wallrock, but within and the outer part of the vein.

Selvage of quartz is in contact with the wallrock but is the outside part of the vein. The example is from Goldfield, south-central Nevada, United States.

Sheeted Vein Habit

Sheeted veins are multiple, subparallel veins (Figures 9 and 15). Within a deposit, they can occur locally, or they can characterize the overall veining habit.



Figure 15. *Outcrop illustrating sheeted veins.*

Sheeted quartz-chalcopyrite veins (locally weathered to malachite) with muscovite-quartz (phyllic) envelopes are from the Inguaran porphyry prospect, central Michoacan, Mexico (see also Figure 9).

Stockwork Vein Habit

Stockwork vein habit describes large numbers of densely crisscrossing veins over a large area (Figure 16). The veins are too numerous to describe individually easily. Quartz-vein stockwork and carbonate-vein stockwork is common.

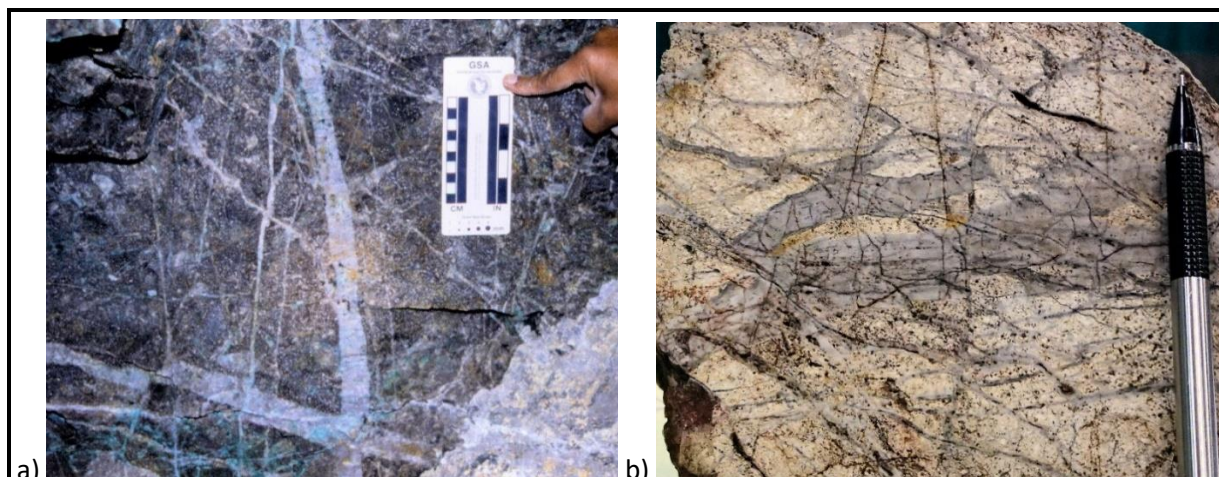


Figure 16. Stockwork quartz veins.

Stockwork is characterized by crisscrossing quartz veins. **a)** Stockwork quartz veins in wallrock adjacent to, but outside of, the Braden Pipe at El Teniente, central Chile. **b)** Stockwork quartz veins from the Caballo Blanco porphyry prospect, Veracruz, Mexico.

Index Fossils: Unidirectional Solidification Texture (UST) or Habit in Brain Rock, Quartz Blobs and Quartz Breccias

Unidirectional solidification texture (UST; Shannon et al., 1982; Kirwin, 2005) describes multiple contorted quartz layers in 'brain rock' (Figures 17 and 18) that forms in the apices or cupolas of highly differentiated and hydrous plutons. The teeth in each quartz layer points in the same direction. The texture is also known as 'crenulate quartz layers' (White et al., 1981) or 'comb-quartz layers' (Kirkham and Sinclair, 1988; Sinclair, 2007). Debatable origins of this texture are elaborated on in the insert *Explaining UST banding in brain rock*.

The quartz teeth point inward toward the core of the associated hydrous intrusion, according to Kirkham and Sinclair (1988) and Sinclair (2007). However, Figure 18 indicates that the teeth are pointing outward away from the core. Determining the direction is complicated by the complex convolutions of the UST quartz layers.

Aplite is most common between the quartz layers in brain rock. However, greisen (dominantly muscovite and quartz [Figures 17 and 18]), not previously noted in geological literature, occurs between the layers at the Don Luis greisen prospect in Sonora, Mexico. Tourmalinite between the quartz bands has been noted by Kirwin (2005).

UST in brain rock is commonly associated with molybdenum porphyry deposits. Other localities include the Glacier Gulch molybdenum deposit in British Columbia, Canada; the Logtung tungsten molybdenum porphyry deposit in south-central Yukon, Canada, and the Don Luis greisen-porphyry prospect in central Sonora, Mexico.

Brain rock is a potential index fossil for major porphyry deposits because it occurs in several world-class porphyry deposits. For example, brain rock occurs at the Climax and Henderson molybdenum porphyry

deposits in Colorado, United States, and the Oyu Tolgoi copper-gold porphyry deposit in the south Gobi Desert of Mongolia. The occurrence of this habit demands attention, if only because some world-class deposits are known to have these features.

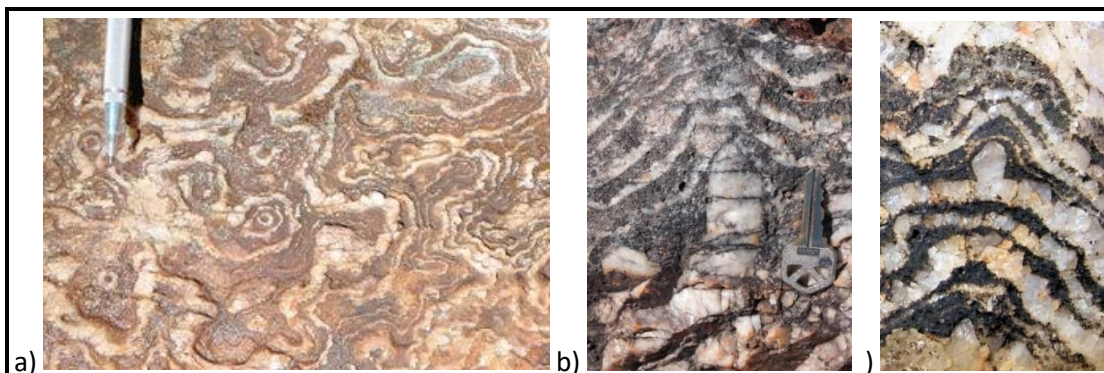


Figure 17. Unidirectional solidification banding in brain rock (*index fossil*).

Greisen in these photos separates the quartz layers and is locally weathered to black pyrolusite because the muscovite is rich in manganese. a) Shows typical brain-like multiple layering resulting in the name 'brain rock'. a) and b) emphasize the consistent pointing direction of the quartz teeth up in both photos. The large quartz tooth in the centre of the photo b) is 3 cm long, in c) it is 1 cm long. The draping of the layers around the central quartz tooth in b) and c) cannot have been formed by structural deformation, as suggested in some literature. Photos are of specimens from the Don Luis greisen prospect in Sonora, Mexico.

Story about brain rock with unidirectional solidification texture.

Brain rock with unidirectional solidification texture was identified some time ago at the Climax and Henderson molybdenum mines (White et al., 1981) in Colorado, United States. The company geologists at that time thought that brain rock with this texture was a critical, positive feature for ore-discovery. Consequently, believing it to be a major marker for mine discovery, they searched energetically, widely, and secretly for other deposits that hosted brain rock with unidirectional solidification texture. They clearly believed it to be a significant ore guide—an *index fossil* for porphyry deposits.

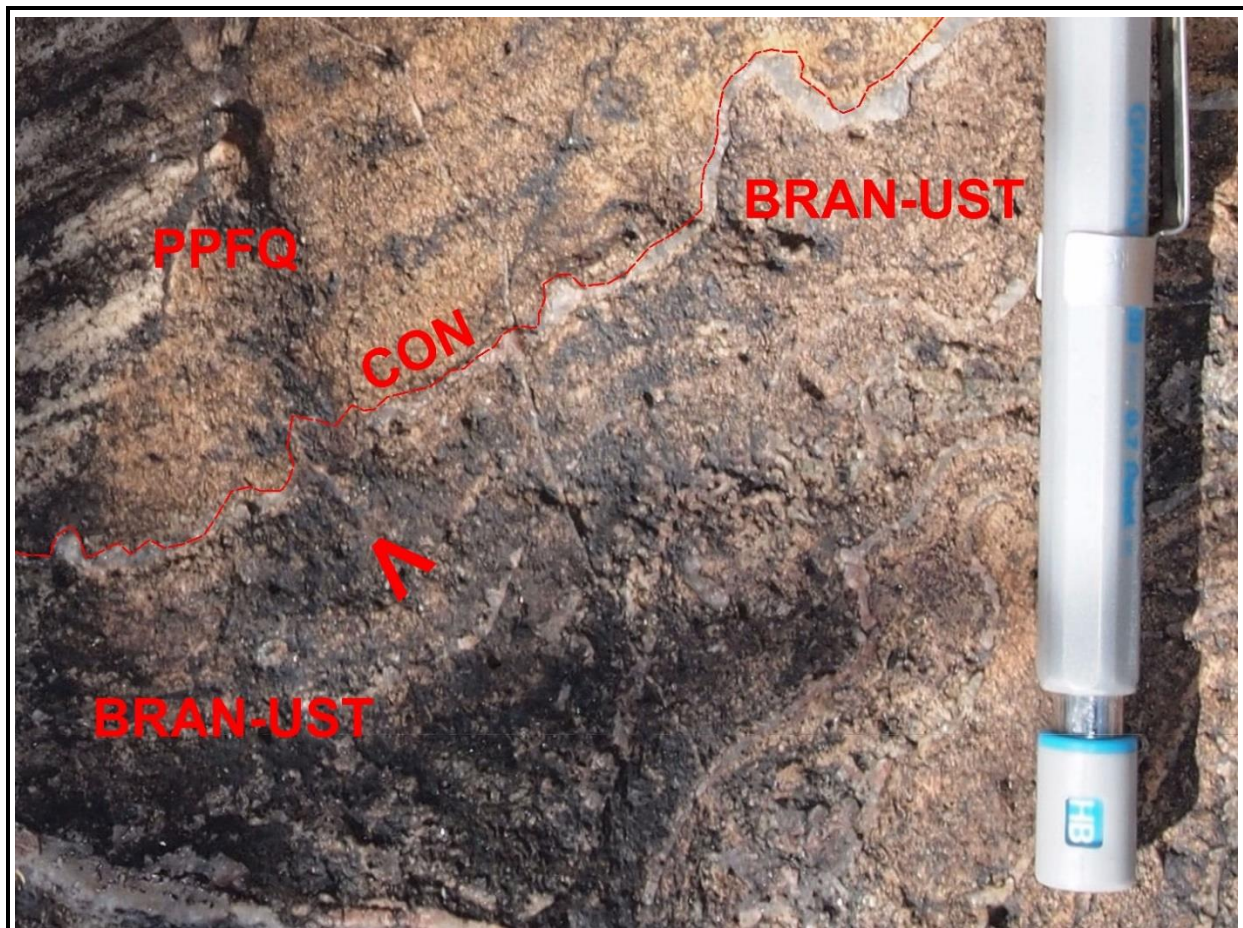


Figure 18. Brain rock with unidirectional solidification bands in contact with earlier, surrounding feldspar-quartz porphyry at the Don Luis greisen prospect in Sonora, Mexico. Contact (CON = red dashed line) of brain rock characterized by unidirectional solidification texture (BRAN-UST with the V in the quartz-tooth direction) with intruded feldspar-quartz porphyry host rock (PPFQ). Teeth in brain rock point toward the contact, away from the greisen centre based on the regional mapping. Both layering in the brain rock and the parallel layers in the porphyry host rock resemble 'diffusion bands', as in Liesegang rings.

Quartz blobs and associated quartz breccia (Figure 19), although rare, have been noted at some significant porphyry copper-molybdenum deposits (OK Tedi in Papua New Guinea [Bamford, 1972]; Mineral Park mine, Arizona, United States [Wilkinson et al., 1982]) and greisen porphyry deposits (Don Luis, Sonora, Mexico [Figure 19]). At Don Luis, the quartz blobs are also associated with UST in brain rock. The quartz blobs (quartzolite or silexite) resemble massive, quartz-dominant pegmatite bodies. These massive quartz bodies (Figure 19) are associated with calcalkaline stocks, quartz breccia, greisen deposits and some major porphyry deposits. Thus, brain rock, quartz breccia and quartz blobs are index fossils for porphyry deposits.

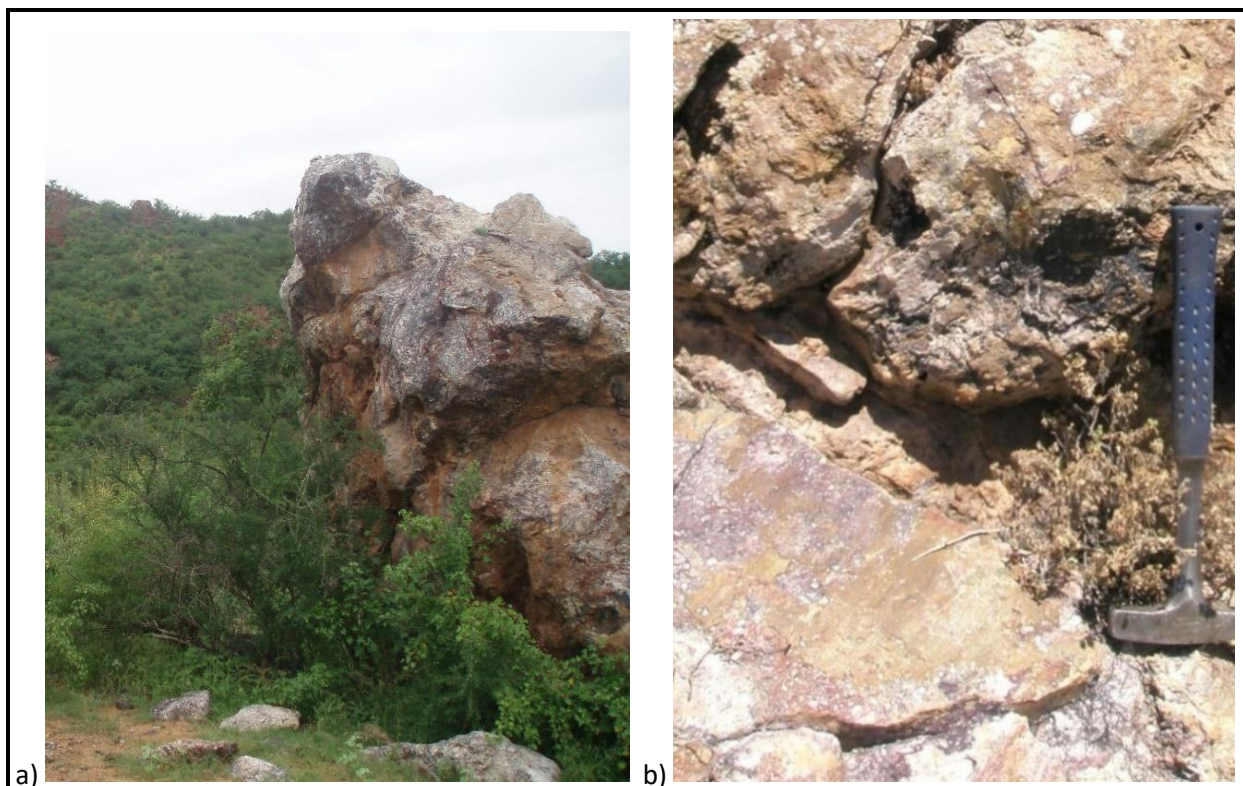


Figure 19. a) Massive magmatic quartz blob and b) associated quartz breccia at Don Luis greisen-porphyry prospect in Sonora, Mexico.

Quartz breccia and brain rock with unidirectional solidification texture occur at the margins of the quartz blob.

Explaining UST banding in brain rock.

The traditional interpretation for UST formation is based on the albite-quartz-orthoclase ternary diagram of Tuttle and Bowen (described in Carmichael et al., 1974 and Kirwin, 2005; cf. White et al., 1981 and Erdenebayar et al., 2014). Variations in water vapour pressure move the system back and forth from the cotectic (where aplite is precipitated) to the quartz field (where quartz only is precipitated). This scheme requires repeated back and forth pressure fluctuations from the quartz field to the exact point of the cotectic, which is postulated to have been caused by periodic rupture of the wallrock. Rare UST within aplite dykes at the Yerington porphyry deposit in Nevada are interpreted by Carter et al. (2021) as due to such rapid pressure changes causing the quartz to precipitate from fluids exsolved from an apatite crystal mush via 'first type' boiling (Candela, 1989). This interpretation does not address a) the cause of repeated pressure change, b) the consistent orientation quartz crystals in every layer and c) composition of intermediate layers that are not aplite (e.g., greisen and tourmalinite).

A brain rock contact with intruded feldspar-quartz porphyry is shown in Figure 18. Note that a) UST quartz teeth point toward the contact, away from the greisen centre (in the direction of the red 'V'), and b) parallel layers in the feldspar-quartz porphyry look like 'diffusion bands'. A possible interpretation is that the quartz teeth point in the flow direction of the hydrothermal fluid that forms them. This flow will be outward from crystallizing rock in the cupola, which, because the crystallizing rock is relatively

anhydrous, exudes hydrothermal solutions. Typically, this will be from the core of the cupola outward, but a cupola carapace solidifying inward might exude fluids inward.

Quartz crystals in unidirectional solidification layers might have formed by a diffusion mechanism. The multiple layers formed could be analogous to the formation of Liesegang rings. Diffusion of a silica-water hydrothermal fluid would result in the water component moving more rapidly than the silica component. Lagging silica transport causes an increase in silica concentration. Upon supersaturation of silica, quartz is precipitated. Crystals continue to grow in the direction of fluid flow forming unidirectional quartz teeth. Because silica is being precipitated, the water passing the band is silica poor and quartz is not precipitated immediately past the quartz crystal layer. As the fluid continues to advance, the silica again builds up until quartz is precipitated. This matches the way Liesegang rings form as suggested by William Ostwald, and summarized in the following quote from Nakouzi and Steinbock (2016):

"Specifically, the diffusion . . . increases the local ion concentrations beyond a threshold supersaturation value. As a result, microcrystals begin to nucleate and grow, creating a distinct precipitation band that eventually lowers the ion concentrations in its close vicinity. Accordingly, the precipitate does not grow homogeneously throughout the reaction medium; instead, the diffusion of reactant ions creates supersaturation conditions at a farther location, leading to the formation of another precipitation band. The precipitate then self-organizes into characteristic Liesegang bands that are rich in crystal aggregates and gaps which contain almost no crystals."

The fluid flow that makes the bands in brain rock is probably through a nonhomogeneous crystal mush, resulting in different path lengths to supersaturation. The unique individual quartz crystals and prominence of some (e.g., the larger tooth-like quartz crystals in Figures 17b and 17c) might be related to a) phase separation, where silica naturally breaks up into separate gobs that clump together because of different density from surrounding crystal mush, b) crystallization of silica gobs within a continuing flow of diffusing fluids and c) 'post nucleation', where relatively larger crystals grow where there is more permeability at the expense of the smaller crystals. A Liesegang-like method of origin of UST in brain rock appears to explain adequately a) bands composed uniquely of quartz, b) repeating, multiple quartz bands, c) common orientation of quartz-tooth crystals, d) locally enhanced growth of specific quartz teeth, e) non-structurally deformed brain-like contortions, and f) variable compositions of layers between the quartz bands. If the hydrothermal fluids that form UST are ore-fluids related economic mineralization might form.

Index Fossil: Shatter Cleavage Related to Breccia

Shatter cleavage, also described as 'shingle cleavage' and 'sheeting' by Silitoe and Sawkins (1971) and 'sheet fracturing' by Allen (1971), is illustrated in Figures 8, 20 and 21 (see also insert *Story on index fossil shatter cleavage*). Shatter cleavage has been identified at some significant porphyry deposits, including a) Casino (Godwin, 1973 and 1975; Figures 8 and 20) in central Yukon, Canada, b) El Teniente (Figure 21a) in central Chile, c) Sierra Gorda, in northern Chile, and d) Galore Creek (Figure 21b) in northern British Columbia, Canada. These associations with significant porphyry deposits indicate that shatter cleavage is an important habit—simultaneously an index fossil for breccia pipes and porphyry deposits. The origin of the closely spaced, generally sub-horizontal or sub-vertical fractures is controversial. However, since shatter cleavage is closely associated spatially with breccia pipes, the author has postulated that shatter

cleavage represents multiple extension fractures related to brisance (shattering capability) present during the highly explosive emplacement of breccias (Godwin, 1973, 1975, 1976).

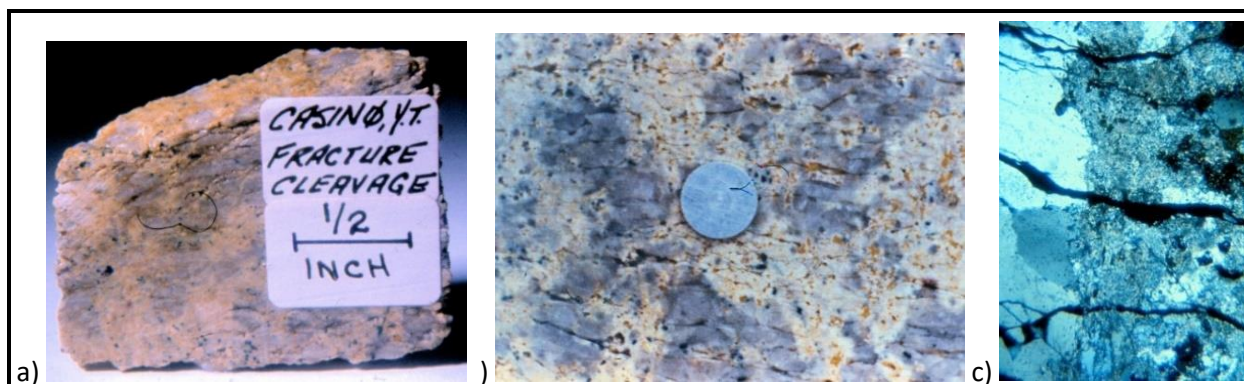


Figure 20. Index fossil shatter cleavage from the Casino porphyry copper-gold deposit in central Yukon, Canada.

Closely spaced, parallel fractures are apparent in **a)** drill core (1/2 in = 1.3 cm), **b)** detailed surface of drill core (disk diameter is 5 mm), and **c)** thin section (fracture spacing about 0.25 mm).

Story about shatter cleavage, an index fossil.

I first encountered shatter cleavage at the Galore Creek alkaline porphyry copper deposit in northern British Columbia, Canada, in 1963 (Figure 21b). One could readily pull a handful of horizontal, shingle-like sheets of rock from the outcrop. Later, in 1969, I recognized it at the Sierra Gorda porphyry copper deposit in central northern Chile, where it surrounded a breccia pipe. I learned then that shatter cleavage was well documented by Howell and Melloy (1960) at the surface around the Braden Pipe at the El Teniente porphyry copper mine in central Chile. In 1971, I also encountered shatter cleavage at Casino, central Yukon, Canada. As a result of these experiences, I formed the opinion that shatter cleavage resulted from multiple extension fractures caused by explosive waves related to the emplacement of breccia pipes (Godwin, 1973, 1975, 1976). As such, I consider shatter cleavage to be an index fossil for breccia pipes and associated porphyry deposits. Because, I like to say, although not always true, that 'I have never seen a breccia pipe that I did not want to drill!' shatter cleavage identification is important.

Other interpretations about the origin of shatter cleavage have been made, notably by Allen (1971; sheet fractures resulting from anhydrite formation in the Galore Creek porphyry, northern British Columbia, Canada), and Sillitoe and Sawkins (1971; vertical sheeting along margins of tourmaline breccia pipes in Chile). Onion-skin spall (Lovering, 1949) that occurs on some margins of quartzite pebbles in the Tintic Breccia in Utah, United States, might have a related origin.

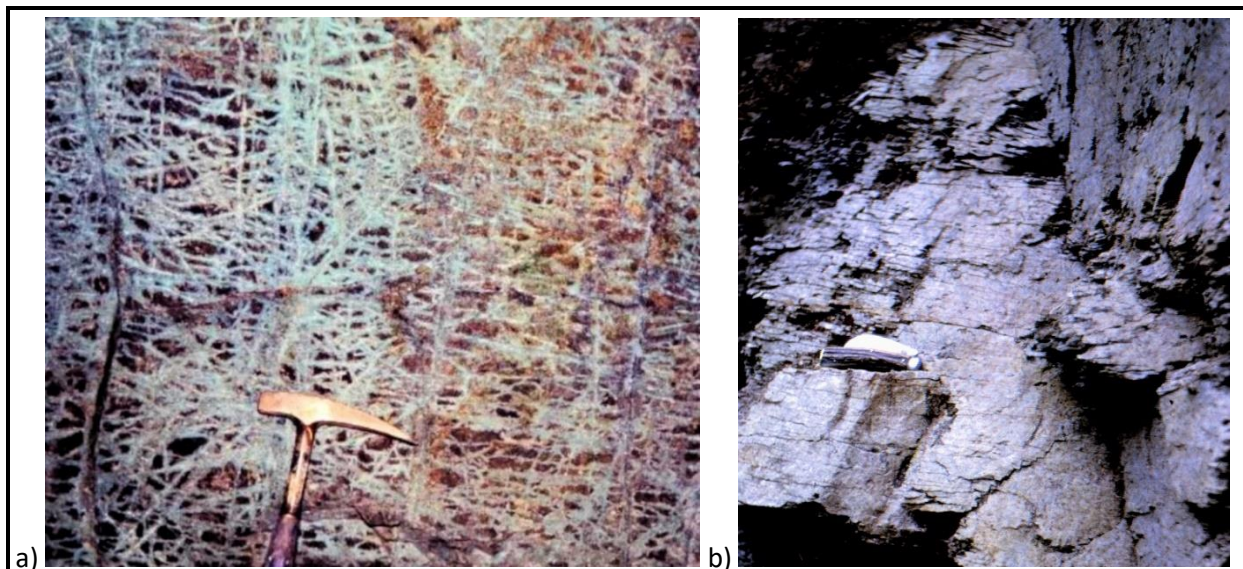


Figure 21. Shatter cleavage a) adjacent to the Braden pipe, El Teniente, central Chile, and b) at Galore Creek, British Columbia, Canada.

a) The shattering adjacent to the Braden Pipe breccia might have been facilitated by brittle ground preparation by hornfelsing that facilitated shatter cleavage development resulting from the explosive intrusion of the breccia. Howell and Melloy (1960) describe shatter cleavage at El Teniente only in surface outcrops. The copper deposit surrounding the pipe was likely facilitated by the fracturing and the iron-rich nature of the hornfelsed, mafic host rock. **b)** At the Galore Creek outcrop, handfals of the shatter cleavage could be pulled from the outcrop as though they were shingles. The cleavage is mainly sub-horizontal in both photos, but vertically oriented cleavage also appears in both (e.g., top-right in b).

Habits Occurring in Multiple Ways or Events

Multiple alteration ways or events with crosscutting relationships between habits (e.g., pyrite as veins and disseminations; veins running in different directions with crosscutting relationships as in Figure 22) require complex descriptions and might be important. The difficulty of describing these types of features consistently and in digital format emphasizes the need for, and the usefulness of, handwritten paper logs with the ability to sketch relationships on a graphic strip log (Godwin, 2020).



Figure 22. Example of two veins of probable different ages.

The bluer vein appears to be younger than the white veins because of the offset of the white vein by the fracture occupied by the blue vein and the different vein colours; however, this interpretation is debatable. The location is unknown.

Be sure you know from this section:

- ➔ common habits or textures of alteration and mineralization and how to name them,
- ➔ how to identify and describe multiple alteration events, and
- ➔ how to recognize particularly significant habits referred to as index fossils.

REGIONAL SETTING, GROUND PREPARATION AND INTERMINERAL HISTORY

In this section you will learn:

- ➔ **Two main features required for a porphyry deposit,**
- ➔ **regional settings for porphyry deposits,**
- ➔ **ground preparation for porphyry deposits, and**
- ➔ **intermineral characteristics of porphyry deposits.**

Main features related to porphyry deposits involve a) regional setting, b) ground preparation, and c) intermineral history. These, detailed below, are summarized in Figure 23 and TABLE 3.

Regional setting for porphyry deposits is most commonly an island arc or a continental margin. Consequently, common regional host rocks are andesite and associated volcano-sedimentary (Figure 23, label **1**). Granitic intrusion (**2a**) and volcanic and sedimentary units (**3**) are pre-porphyry deposit and not related directly to porphyry mineralization.

Ground preparation is mainly related to regional structures and processes that produce large volumes of densely fractured rock (Figure 23, labels **4** and **6**). Fractured rock a) facilitates emplacement of intermineral dykes, plugs and breccias that cause additional fracturing and b) provides permeability and porosity for infiltration by and deposition from hydrothermal fluids. Ground preparation fracturing is mainly related to a) brittle rock types, b) abyssal faults, c) intermineral intrusive forces, and d) alteration volume changes, detailed as follows.

- **Brittle rock types** fracture more readily. Andesite within unit **1** would fragment more than associated sedimentary units. Hornfels (**2b**) would shatter more easily than the original rock unit **1** (note the asymmetry of the fracturing in Figure 23 [**2b** and **6a**] where the hornfelsed country-rock is extensively fractured on the side adjacent to the pre-mineral intrusion).
- **Abyssal faults** provide ground preparation by (**4**) providing fractured pathways to intermineral intrusive rocks and breccias (**5**, **7** and **8**). Abyssal faults have surface fault lengths greater than 50 km (such as the orogen-parallel West Fissure in northern Chile, which is at least 170 km long) and can extend downward for 25–50 km to the mantle. Such deep, pre-mineralization fractures facilitate upward migration and evolution of magmas that form batholiths and stocks, some of which are related to porphyry deposits. In addition, abyssal fault-related dilatational structures facilitate the accommodation of high-level plutons. Long-lived lineaments provide prime real estate for porphyry deposits.
- **Intermineral intrusive forces** (**5**, **7** and **8**) also enhance shattering (**6a**), faulting (thrusts **6a** and normal **6c**) associated with ground preparation. Shallow thrust faulting at deeper depths (**6b**) occurs because the maximum stress is outward from pushing by the flanks of the stock. Steep normal faulting (**6c**) occurs near the surface because the maximum stress from the stock is upward. Radial and concentric fracture patterns can also provide vectors toward stock apices.
- **Alteration volume changes** during ground preparation by hydrothermal fluids from intermineral intrusive rocks and breccias can also enhance permeability.

Fracture density will often increase and provide vectors to the core of porphyry deposits. Standard methods of evaluating fracturing include a) identification of lineaments and fracture density mapped from ground observation and/or air photo, satellite and light detection and ranging (LiDAR), and b) location of irregular topography (high topo-variance) and circular and radial structures at various scales. At a property scale, fracture density—as measured in outcrop, trenches, drill core and remote imagery—is an integral part of an alteration study.

Intermineral rocks are ubiquitous in porphyry deposits. They include intrusive stocks (Figure 23, label 5), porphyry dykes and plugs (7) and breccias (8) provide a) carapace fracturing related to intrusions, b) temperature gradients related to granitic, porphyritic and breccia rock formation, and c) magmatic-hydrothermal fluids with chemical and pressure gradients related to mineralization and alteration. The hydrothermal fluids lead to cupola and porphyry deposit style alteration and mineralization. The magmatic, hydrothermal accumulation in the cupola (and vacuole if present [Norton and Cathles,1973]) will be a) at magmatic temperatures (in the order of 1,000°C), b) metal-chloride rich, and c) pass upward and outward to form porphyry mineralization at cooler temperatures (in the order of 250°C). Intermineral dykes and plugs (7) and breccia (8) enhance ground preparation, alteration, and mineralization. Additional intermineral features include peripheral lead-zinc veins and pyrometasomatic deposits. Key features related to Figure 23 are:

- **Intermineral porphyritic dykes and plugs (7).**
- **Hydrothermal breccias (8)** are always noteworthy if only because “I have seldom seen a hydrothermal breccia I did not want to drill!”.
- **Lead-zinc veins** (not in Figure 23) can occur in country rocks outside of porphyry deposits and be a key indicator of their presence (e.g., the Bomber and Helicopter veins of galena, sphalerite and barite occur outside the Casino porphyry deposit in central Yukon, Canada).
- **Pyrometasomatic deposits** (not in Figure 23) with copper-lead-zinc and skarn minerals can form when carbonate rocks occur in peripheral country rocks. They are cousins to porphyry deposits, can be economic in themselves, and their outward location is a vector toward potential porphyry deposits. Peripheral lead-zinc-silver and copper skarn deposits at the Bingham Canyon porphyry deposit in Colorado, United States, have produced significant tonnages of ore (Einaudi, 1982).

Definition of hornfels.

Hornfels is a volcanic or sedimentary rock that has been ‘baked’ and metamorphosed by contact with, or proximity to, an intrusive pluton. Hornfels (German for *hornstone* because it commonly looks like a horn) is usually purplish-grey-black and very fine-grained. Commonly it has a purplish lustre caused by very fine-grained, felt-textured hydrothermal biotite (usually only identifiable in thin section). The biotite indicates added potassium if the original rock may have been andesite. When hit with a hammer, hornfels is hard to break but brittle, and it often rings like a bell when struck with a prospector’s pick. The brittleness of hornfels is a classic example of ground preparation because it facilitates fracturing when stressed by subsequent faulting and/or intrusion of plutons, dykes and breccias.

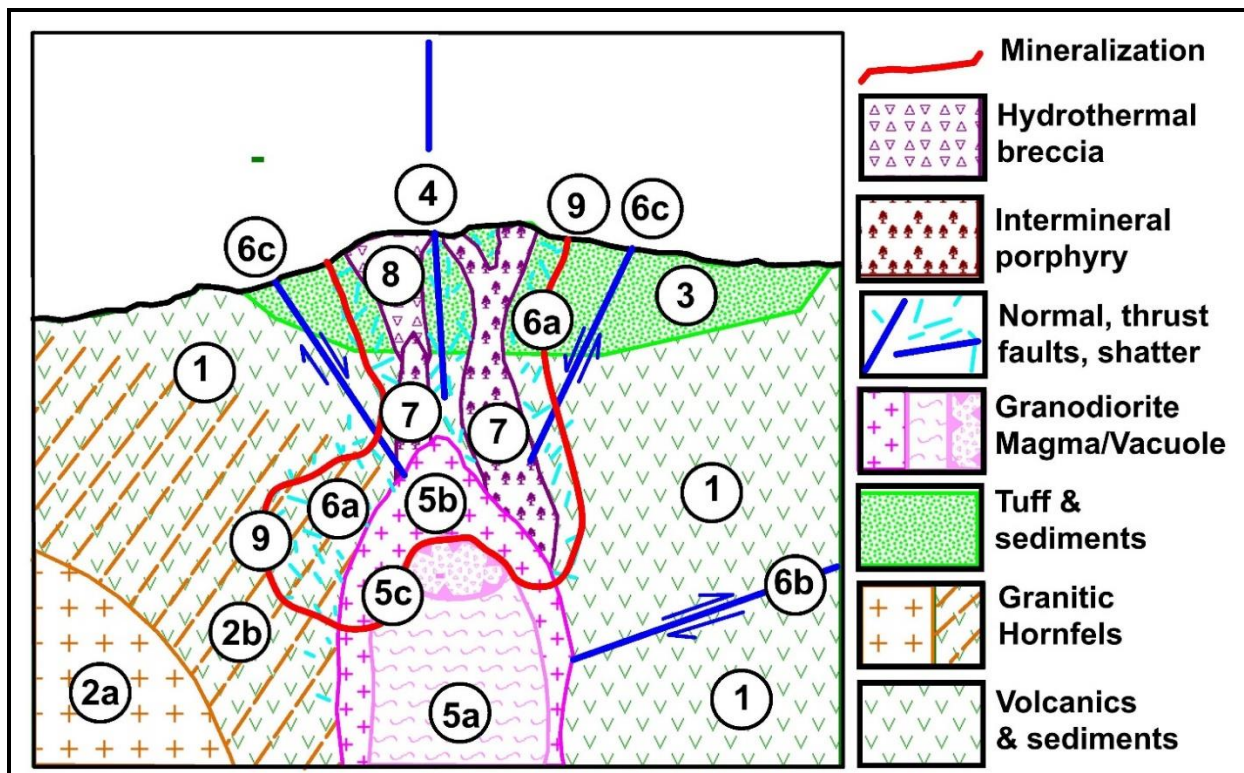


Figure 23. The regional setting, ground preparation and intrusion and intermineral history of porphyry mineralization.

This model applies to porphyry deposits in an island arc or continental margin setting. Key features, in approximate order of formation, are **1** = regional setting of volcanic and sedimentary country-rock; **2** = regional setting of intrusion of pre-mineralization, often batholithic, granitic rock (**2a**) with hornfelsing (**2b**) of surrounding country-rock; **3** = regional setting of younger volcanic and sedimentary rocks; **4** = ground preparation by an abyssal faults that become potential guides for mineralizing intrusions; **5** = intermineral intrusion of an apical stock as a magma (**5a**), as a granodioritic carapace (**5b**), and a potential hydrous vacuole (**5c**); **6** = ground preparation and intermineral fracturing which includes shattering above the stock that is more extensive within brittle hornfels (**6a**) and includes deep thrust faulting (**6b**) and shallow normal faulting (**6c**); **7** = intermineral intrusion of porphyritic rocks; and **8** = intermineral hydrothermal breccia formation. These features, detailed in TABLE 3, come from many sources, including Burnham (1979) and Norton and Cathles (1973).

TABLE 3. Features of regional setting, ground preparation and intrusion and intermineral history of porphyry mineralization in Figure 23.

Features, in approximate decreasing age, are cross-referenced to numbered features in Figure 23. An island arc or continental margin setting is typical.

Feature and Number in Figure 23	Explanation
1: Regional setting: volcanic and sedimentary rocks	Volcanic and sedimentary rocks are common basement country-rocks to porphyry deposits. The volcanic rocks are commonly andesitic in an island arc or continental margin setting.
2: Regional setting: pre-mineralization granitic intrusion (2a) and hornfelsing of intruded terrane (2b)	Early intrusion, commonly batholithic, can hornfels intruded rocks but is not responsible for porphyry mineralization. Brittle hornfelsed rock can shatter, enhancing the flow of hydrothermal solutions leading to porphyry-style mineralization.
3: Regional setting of younger volcanic and sedimentary rocks	Later volcanic and sedimentary rock units unconformably on units 1 and 2 .
4: Ground preparation: abyssal fault guide for plutons	Abyssal faults are potential guides to the intrusion of magmas related to porphyry deposits and are index fossils for multiple-aligned porphyry deposits.
5: Intermineral, mineralizing magma (5a), forms a solid apical stock (5b), sometimes above a vacuole (5c)	Intermineral hydrous stocks, often granodioritic in composition, can exude hydrothermal fluids that result in an altered cupola at the top of the stock. The magmatic, hydrothermal accumulation in the cupola (and vacuole if present) will be a) at magmatic temperatures (in the order of 1,000°C), b) metal-chloride rich, and c) pass upward and outward to form porphyry mineralization at cooler temperatures (in the order of 250°C).
6: Ground preparation and intermineral: fracturing and faulting is characterized by shattering (6a), thrust faults (6b) and normal faults (6c)	<i>Ground preparation</i> for mineralization is marked by intense fracturing (6a). Increased fracture density will generally increase toward the core of porphyry mineralization. Rock that is brittle—or made more brittle by hornfelsing from a pre-existing or the mineralizing plutons—tends to be more densely fractured. Note the asymmetry of the fracturing in Figure 23 where the hornfelsed country-rock is more fractured on the side adjacent to the pre-mineral intrusion.
7: Intermineral: the intrusion of porphyritic rocks	Intermineral porphyritic dykes and plugs (7) result from intrusion of hydrous magma and/or crystal mush derived from the underlying stock (5a). Fracturing that is caused by forceful intrusion, cooling-contraction, local and regional stresses facilitate the upward and outward flux of mineralizing

	hydrothermal fluids exuded from the porphyritic rocks and the underlying stock.
8: Intermineral: the upward explosion of breccia dykes and pipes	Hydrothermal breccias can form in many ways, but formation from an upward explosion of porphyritic bodies is illustrated. Breccias can be richly mineralized because they are permeable and porous. They can be formed and subsequently mineralized by hydrothermal fluids.
9: Intermineral: envelope of porphyry-style mineralization and alteration	Porphyry mineralization is concentrated a) above and in cupolas of stocks (5), b) in the highly fractured ground (6), c) in and around intermineral porphyry dykes and plugs (7), and d) in and around breccia bodies (8).
Intermineral (not on Figure 23): polymetallic macroveins	Lead-zinc veins occur in country rocks outside of many porphyry deposits and can be a crucial vector to potential porphyry deposits.
Intermineral (not on Figure 23): pyrometasomatic (skarn) deposits	Pyrometasomatic deposits with copper-lead-zinc and skarn minerals can form when carbonate country rocks occur peripherally to porphyry deposits. Their outward location can be used to vector toward porphyry deposits.

The need for geological field mapping of rock types, structures, and geometry as a basis for studies of porphyry deposits are emphasized by the feature in Figure 23 and TABLE 3. Regional and detailed mapping provides vectors pointing to the cores of porphyry deposits.

Be sure you know from this section:

- ➔ the regional settings for most porphyry deposits,
- ➔ the characteristics and importance of ground preparation,
- ➔ the role of intermineral intrusive bodies, and
- ➔ why field mapping is needed.

PLUTON ASSOCIATIONS

In this section you will learn:

- about the genetic relationship between ore, alteration zoning and spatially associated igneous rocks.

Hydrothermal alteration and ore and spatially associated igneous rocks in porphyry deposits have a clear and close genetic relationship. Specifically, the zonation of alteration and ore to a source from an intrusive rock is compelling (Moore et al., 1968). TABLE 4 generalizes igneous granitic rock associations (see inserts *Origin of S-, A- and I-type granitic rocks* and *Origin of alkaline plutons*) with different types of porphyry deposits. Volcanic country rocks intruded by granitic plutons are commonly mineralized and become part of the porphyry deposit. Where carbonate rocks occur close to ore mineralization, they can become valuable as pyrometasomatic deposits with skarn mineral assemblages rich in copper, lead, and zinc.

Origin of S-, A- and I-type granitic rocks.

The origins of S- or A-type and I-type granitic rocks have been defined by Chappell and White (1974, 1992). *S-type granitic rocks* (and probably the less well defined anorogenic *A-type*) are derived from anatectic melting of deeply buried, intracontinental, metamorphosed sedimentary rock. Consequently, associated ore deposits have lithophile elements (e.g., Be, Bi, Mo, Sn, W) and abundant quartz and lithium- and potassium-rich micas. Hornblende is absent, muscovite is common, and accessory monazite, instead of sphene, is common. *I-type granitic rocks* occur at convergent plate margins and are enriched in mantle signature elements (high Na and Ca); hornblende is common and accessory sphene, instead of monazite, is common. Abundant xenoliths and a range of granitic phases (e.g., diorite to monzonite) are common. The level and initial water content of porphyry deposit related magmas might result in the split between copper greater than molybdenum and molybdenum greater than copper porphyry deposits. Copper greater than molybdenum porphyry deposits is associated with shallower level magmas containing relatively less water. Molybdenum greater than copper porphyry deposits is related to deeper and relatively more hydrous magmas.

Origin of alkaline plutons

The origin of alkaline plutons is related to upwelling of upper mantle ultramafic peridotite below a continental (or island arc) rift zone, which results in a low degree of partial melting by decompression. This origin leads to an excess of alkaline metals (Na_2O and K_2O) over silica (SiO_2), resulting in rocks rich in albite, K-feldspar and feldspathoid (such as nepheline), but with little or no quartz. Other abundant components are barium, phosphorous and volatiles (H_2O , CO_2 , and F). Phosphorous and fluorine components are reflected in the common occurrence of fluorapatite in commonly associated magnetite-apatite magmatic dykes and breccias.

TABLE 4. Different types of porphyry deposits related to granitic associations.

S-, A- and I-type refer to the origin of granitic rocks in variable tectonic settings. A list of rock names and abbreviations that are pertinent to porphyry deposits are included in Appendix A and Godwin (2020). Abbreviation: PGE = platinum group element.

Porphyry deposit type / granitic type	Example(s)	Geochemistry of ore minerals	Tectonic origin¹	Rock types
Greisen and porphyry tin ± molybdenum <i>Quartz rich, calcalkaline</i>	Ardlethan Tin Mine, New South Wales, Australia	Lithophile	S- or A-type anatectic granitic rocks	Granite, ± rhyolite, ± greisen, ± rhyodacite
Porphyry tungsten ± molybdenum ± gold <i>Quartz rich, calcalkaline</i>	Dublin Gulch gold properties, Yukon, Canada Don Luis tungsten-silver-gold prospect, Sonora, Mexico	Lithophile	S-type anatectic granitic rocks	Granite, ± rhyolite, ± greisen
Porphyry molybdenum <i>Quartz rich, calcalkaline</i>	Endako Molybdenum Mine, British Columbia, Canada Climax – Henderson, Colorado Mines, United States	Transition(?): lithophile to chalcophile	Transition(?): S-type anatectic to I-type subduction	Granite, quartz monzonite

<p>Porphyry copper-molybdenum, ± silver, ± gold <i>Quartz rich, calcalkaline</i></p>	<p>Island Copper Mine, British Columbia, Canada</p> <p>Bingham Canyon Mine, Utah, United States</p> <p>Valley Copper Mine, British Columbia, Canada</p> <p>Casino Copper-Gold Mine, Yukon, Canada</p>	<p>Chalcophile</p>	<p>I-type continental margin subduction</p>	<p>Granite, granodiorite, ± quartz monzonite, ± quartz diorite</p>
<p>Porphyry copper-gold ± PGE <i>Quartz poor, alkaline</i></p>	<p>Afton Copper Mine, British Columbia, Canada</p> <p>Mount Polley Mine, British Columbia, Canada</p> <p>Galore Creek deposit, British Columbia, Canada</p> <p>Copper Mountain Mine, British Columbia, Canada</p>	<p>Chalcophile</p>	<p>Rift(?) within an established continental (or island arc) crust</p>	<p>Monzodiorite, diorite, ± syenite</p>

Be sure you know from this section:

- ➔ the main differences between granitic rocks associated with different types of porphyry deposits.

GENERALIZED MORPHOLOGY AND DESCRIPTION OF HYDROTHERMAL BRECCIAS

In this section, you will learn:

- ➔ the generalized morphology of breccia pipes,
- ➔ the key features of breccia, and
- ➔ why the use of the term pseudobreccia is inappropriate.

Breccia pipes are masses of breccia with an irregular cylindrical shape that intrude and crosscut earlier rocks. Breccias are significant because they a) are formed from and become conduits for hydrothermal fluids causing alteration and ore mineralization, b) are common in porphyry deposits, c) can be significantly ore-mineralized, and d) are conduits to surrounding ore-mineralization. Sillitoe (1985) summarized many features of breccias. A morphological description of breccia is presented below. Genetic models are interpretative and challenging to define without a detailed understanding of morphology and field relationships. Commonly cited genetic models are not elaborated upon here but include:

- **Magmatic hydrothermal or carapace breccias** that are products of juvenile, hydrothermal fluids exsolved from magmas,
- **Phreatic breccias or hydrothermal eruption breccias** are caused by the expansion of steam and gas from circulating groundwater but driven by magmatic heat and
- **Phreatomagmatic breccias** are formed by the direct interaction of magma and external water.

The **generalized morphology of a breccia pipe in cross-section** is shown in Figure 24. Key features, numbered in this figure, are explained in detail in TABLE 5. See also the section below, on the significance and characteristics of magmatic dykes and magmatic breccias.

Breccia bodies are important because they are formed from, and become conduits for, hydrothermal fluids that can cause alteration and ore mineralization.

Breccias can be mapped and described based on clast or fragment and matrix a) lithology or composition, b) shapes, sizes, packing and sorting or bedding, c) degree of alteration and mineralization. Brecciation implies rock expansion, often greater than 30%.

Clast or fragment descriptions should include rock type, degree of hydrothermal alteration and, of course, mineralization. Look for fragments from varied types of wallrock, porphyritic rock, intrusive rock, vein rock and ore-mineralized rock, and prior breccia fragments. Indications of multiple events of brecciation, alteration and mineralization enhance the likelihood of ore grades. It is also helpful to describe fragments in a breccia as either open (matrix-supported) or closed (fragment-supported, where fragments touch each other). The open type implies a more energetic emplacement (maximum fragment size can be another measure of energy emplacement). Be aware that cutting a breccia does not necessarily show fragments touching because a closed spherical fragment breccia or conglomerate is about 50% matrix.

Matrix descriptions should include rock type (if discernable), alteration and mineralization. The composition of a matrix can sometimes be unmineralized comminuted rock flour.

A **general visual representation of breccia** is presented in Figures 7 and 25 to 27. As noted above, the inappropriately named 'pseudobreccia' or 'crackle breccia' in Figure 7d is better described as a 'crackle

zone of alteration' or an 'altered fracture zone', because there has been neither rotation nor inflation of fragments by a matrix.

Sedimentary conglomerate and volcanic breccia can be confused with hydrothermal breccia. An example of this is addressed in the insert *Story of conglomerate versus breccia at Casino, central Yukon, Canada*. A specimen of the outcrop at Casino that confused is in Figures 7b and 25.

Story of conglomerate versus breccia at Casino, central Yukon, Canada.

Cobble breccia at the Casino deposit (Figures 7b and 25), Yukon, Canada, was originally thought to be a conglomerate because the fragments were mainly rounded cobbles. Indications that the conglomerate was a hydrothermal breccia was apparent from the tourmalinized cobbles and the wedges of limonite after sulfide at cobble boundaries. Earlier recognition of this as a hydrothermal breccia would have led more quickly to the conclusion that Patton Hill (Figure 3), centred on the Casino deposit, marked the core of a porphyry deposit.

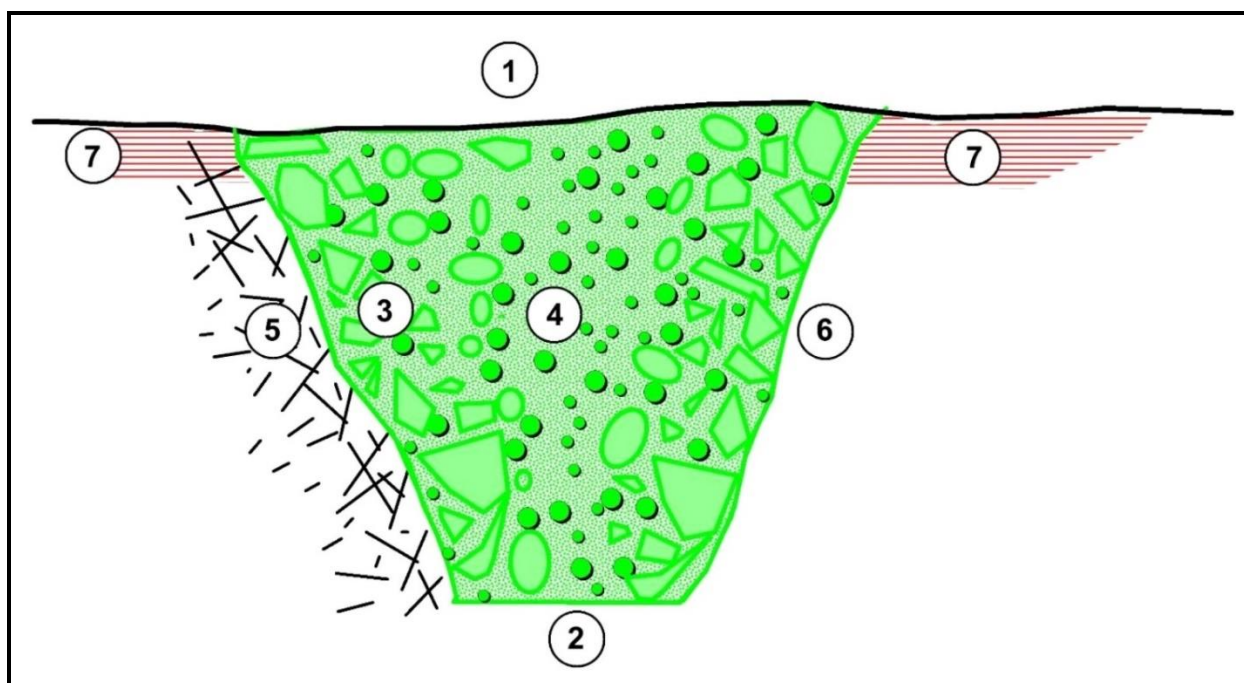


Figure 24. Generalized morphology of a breccia pipe in cross-section.

Diagram key: 1 = breccia can be blind (not open at the surface), 2 = an upward conical or pipe shape is common, 3 = marginal breccia material is angular, and fragment supported (closed), 4 = central breccia material increases in roundness and tends to be matrix-supported (open), 5 = crackle zones of fracturing, 6 = sharp contacts without crackle zones, 7 = shatter cleavage. See TABLE 5 for more thorough descriptions keyed to numbers 1 to 7.

TABLE 5. Explanation of numbered features in Figure 24 on the morphology of hydrothermal breccias.

Feature	Number in Figure 24	Explanation
Blind breccia	1 (but not on the figure)	Breccia can be blind and not open to the surface if the energy is insufficient to propagate it that far or if the breccia is due to collapse from magma withdrawal or dissolution.
Upward conical or pipe shape	2	Upward conical or pipe shape is common and is a result of upward expansion and erosion on intrusion.
Margins of breccia	3	Margins of breccia commonly are choked with angular, platy, closed or fragment-supported wallrock fragments (classification as breccia requires fragment rotation and matrix-inflation of fragments). Enhanced permeability occurs if the matrix is porous or sparse. High-grade sulfide can cement the matrix. Wedge- or cuneiform-shaped sulfides often occur between angular and rotated fragments. Thus, finding wedge-shaped sulfide (or limonite in capping) is a strong indication of a breccia. Previously ore-mineralized fragments indicate prior ore-mineralizing events; every event might contribute to the overall grade of mineralization.
Central portions of the breccia	4	Central portions of breccia pipes tend to have fragments of mixed composition and increasing sphericity and roundness. Open, or matrix-supported, fabric is more common, and the matrix tends to be increasingly finer-grained toward the centre, reducing permeability, and sometimes resulting in less significant ore mineralization. The matrix can consist of unmineralized comminuted rock flour; however, it is commonly mineralized. Previously ore-mineralized fragments indicate prior ore-mineralizing events; every event might contribute to the overall grade of mineralization. Breccia bodies sometimes display bedding originating from gas streaming through the pipe or crater infill at the top of a pipe.
Crackle zones of fracturing	5	Crackle zones of fracturing tend to decrease in intensity outward; when altered, these can look like breccia and are commonly inappropriately called 'pseudobreccia' or 'crackle breccia'. These terms are inaccurate because fragment rotation and fragment separation by matrix inflation—which defines breccia—are not present!

Sharp contacts	6	Sharp contacts without crackle zones can occur between breccia and country-rock; this can result from erosion of the walls by through-going breccia emplacement.
Shatter cleavage	7	Shatter cleavage (see Figures 8a, 20, 21 and 24) is uncommon and local. It is fascinating as an index fossil for breccia body proximity. It appears to be related to the brisance associated with hydrothermal breccia emplacement and occurs as thinly spaced cleavage that usually is sub horizontal, vertical, or parallel to breccia wall contacts. Shatter cleavage is associated with breccia bodies in some porphyry deposits (see insert <i>Story on index fossil shatter cleavage</i>). Some example occurrences are a) the El Teniente Mine in Chile, b) the Sierra Gorda Mine in Chile, c) the Galore Creek deposit in northern British Columbia, Canada, d) the Glacier Gulch deposit in central British Columbia, Canada, and e) the Casino deposit in central Yukon, Canada.

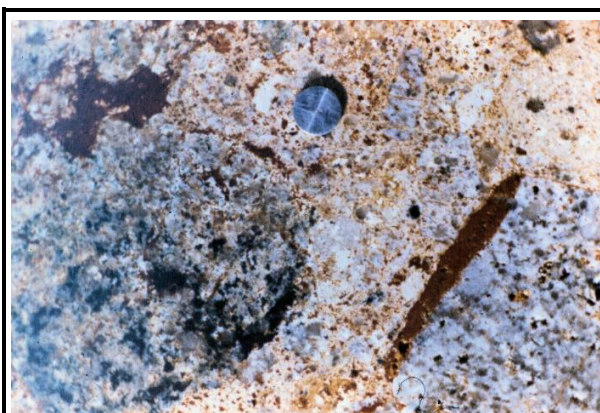


Figure 25. Hydrothermal cobble breccia from the Casino deposit in the Yukon, Canada.
The Casino breccia has tourmalinized cobbles at the left side of the photo (indicating mineralizing events before brecciation) and wedges of limonite in the lower right of the photo after sulfide mineralization at cobble boundaries (wedge-shaped limonite after sulfides reflects fragment rotation).

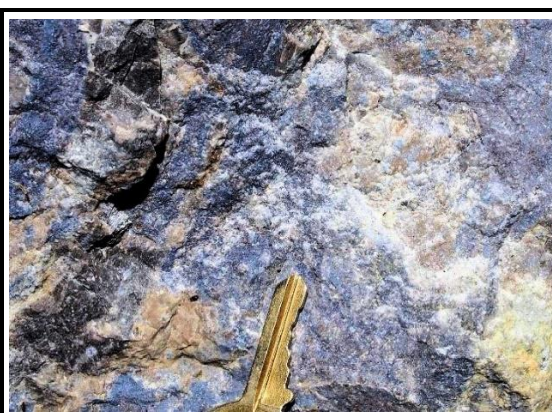


Figure 26. Hydrothermal breccia from Island Copper porphyry deposit, northern Vancouver Island, British Columbia, Canada.
Breccia is altered with pervasive pyrophyllite (white) and dumortierite (blue) The alteration obliterates fragment outlines. This breccia was formed from an upward explosion and alteration related to a porphyritic dyke, as indicated in Figures 23 and 28 (BRPP).



Figure 27. Hydrothermal breccia from the Granisle porphyry deposit, central British Columbia, Canada.

The breccia is crosscut with late and barren calcite veins.

Be sure you know from this section:

- the critical features of breccias,
- why shatter cleavage is an index fossil for breccia bodies,
- how to describe breccias, and
- why the terms 'pseudobreccia and crackle breccia are inappropriate.

ORIGINS OF HYDROTHERMAL BRECCIA AND RELATIONSHIPS WITH PORPHYRITIC ROCKS

In this section, you will learn about:

- ➔ the hydrothermal formation of breccias, and
- ➔ the relationship between porphyritic rocks and breccias.

Hydrothermal breccias, commonly associated with porphyry deposits, are formed from the pressure-cooker-like-explosion of hydrothermal fluids from hydrous (volatile-rich) magmas. An explosion of hydrothermal fluids results in fracturing and fragmentation of wall rocks and the grinding, transportation, alteration, and ore-mineralization of rock fragments. The hydrothermal fluids also can result in ore mineralization in rocks surrounding the breccia. One cannot overemphasize the importance of breccia in the porphyry deposit environment.

Explosion causing the brecciation can be the result of:

- **An ascending volatile-rich magma** experiencing a decrease in pressure as it rises.
- **Exothermic phenocryst growth in a porphyritic rock** resulting in a temperature increase.
- **Faulting from the surface to deep volatile-rich pockets or vacuoles** that changes the confining pressure. And
- **Crack propagation.**

The following paragraphs detail these mechanisms.

Ascending volatile-rich magma, often forming dykes or stocks, vesiculates upon reduction in pressure. The expansion from volatile-vesiculation can cause an explosive release of energy leading to brecciation. One would expect the brecciation to be at the margins and in the upper parts of the intrusion, where volatile release is more likely. The formation of breccia from porphyritic rocks is demonstrated in the cross-section in Figure 28 (after Cargill et al., 1976, and Perrelló et al., 1995) of the now-closed Island Copper mine on northern Vancouver Island, British Columbia, Canada. The intrusion of the rhyodacite dyke intrusion was accompanied by marginal (**BRHT**) and upward (**BRPP** [Figure 26]) brecciation.

Exothermic phenocryst growth in porphyritic rocks can increase pressure (see insert *Discussion on Disequilibrium Porphyry and Breccia Formation*). Figure 29 is a disequilibrium model where temperature increase from crystal growth causes pressure increase. Either a) breccia forms, or b) porphyritic rock forms. Breccia forms if the pressure exceeds the lithostatic pressure, the magma-crystal mush's surface tension and the surrounding rock's tensile strength. This mechanism of breccia formation could also be related to the brecciation at Island Copper in Figure 28.

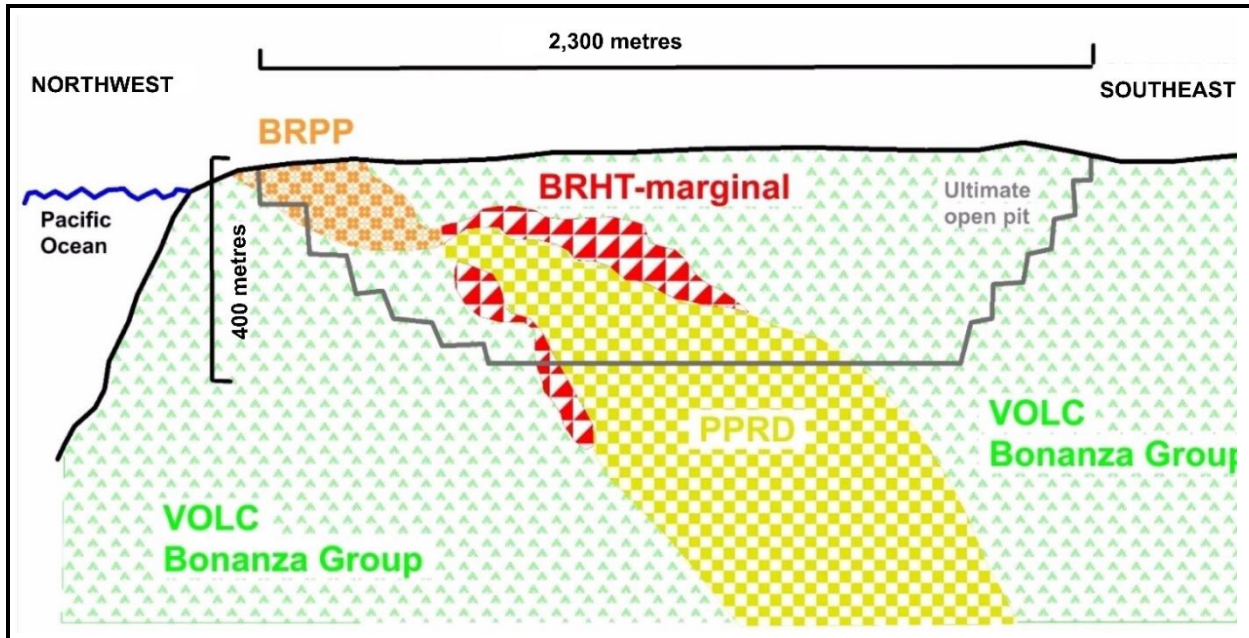


Figure 28. Marginal hydrothermal breccia at the Island Copper Mine, northern Vancouver Island, British Columbia, Canada.

Cross-section of Island Copper Mine (after Cargill et al., 1976, and Perrelló et al., 1995), showing marginal and upward explosion of a porphyry dyke. Explosion, related to the intrusion of the rhyodacite dyke (**PPRD**), resulted in marginal and upward brecciation. Zoning of mineralization and alteration, generated from the dyke, is centred on and around the dyke. Abbreviations are **BRHT** = marginal hydrothermal breccia, **BRPP** = pyrophyllite (plus blue dumortierite) breccia (Figure 26), **PPRD** = rhyodacite porphyry dyke and **VOLC** = volcanic.

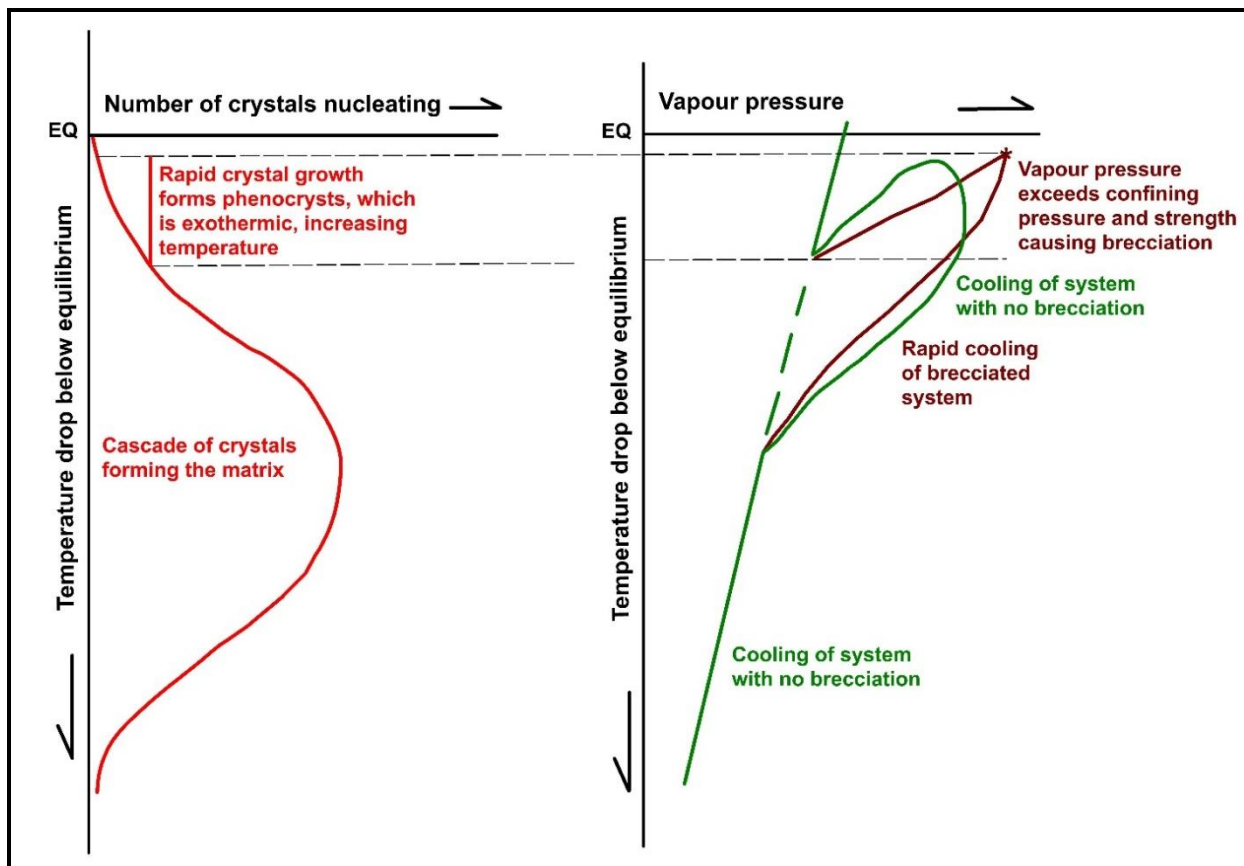


Figure 29. Relationships between porphyritic rocks and breccia bodies.

EQ = equilibrium temperature. Sudden and rapid crystal growth, marked by the vertical red line, occurs in the unstable system below the equilibrium temperature and is exothermic. The rapid increase in temperature during the rapid and exothermic crystal growth to phenocrysts (vertical red line) leads to increased vapour pressure. If the resulting pressure exceeds the lithostatic-plus-tensile strength of the surroundings (purple curve), the rocks rupture, breccia is formed, and the system cools rapidly.

Discussion on Disequilibrium Porphyry and Breccia Formation

Methods of phenocryst formation in porphyritic rocks are debated. Most geologists assume that growth occurs in conditions of equilibrium. A compelling alternative to the equilibrium assumption is provided by Figure 29. This figure describes non-equilibrium crystallization analogous to a supersaturated salt solution cooled below equilibrium. Crystals generally do not form until it has cooled below the equilibrium temperature. However, when a few seed crystals form, they can rapidly overgrow to become phenocrysts. Crystallization is exothermic, and rapid crystal growth causes a sudden increase in temperature and pressure. The magma will vesiculate if the increased pressure exceeds the lithostatic plus tensile strength of confining rocks. The work expansion from vesiculation causes pressure-cooker-type explosion and brecciation followed by rapid cooling. The rapidly grown phenocrysts are in a crystal mush that cools to the fine-grained matrix of a porphyritic rock. Formation of porphyritic rock from such a supersaturated, super-cooled and unstable magma might be related to cooling and pressure drop during upward intrusion of a dyke. Thus, many features in Figure 29 relate well to the close association of porphyritic rocks and

breccias (Figures 23 and 28). A porphyritic rock without breccia is formed if the exploding pressure is not attained.

Faults can tap from the surface large pockets or vacuoles of immiscible and volatile-rich magmas or crystal mushes at depth. Faulting can abruptly lower the pressure in the pockets or vacuoles from lithostatic to hydrostatic (see insert Brecciation from Abrupt Pressure Drop at Yellowstone Park, Wyoming, United States). Instant pressure reduction results in vesiculation that release enormous amounts of energy leading to emplacement and brecciation.

Brecciation from Abrupt Pressure Drop at Yellowstone Park, Wyoming, United States

Explosion by an abrupt pressure drop leading to breccia formation is typical. This mechanism formed the hydrothermal explosion craters, up to 1,000 m in diameter, at Yellowstone Park, Wyoming, United States. The sudden lowering of an ice-dammed lake triggered the formation of these craters. The sudden decrease in confining pressure caused by the lake level drop resulted in the explosion and brecciation of the underlying hot-water-saturated rock (Muffler et al., 1971). Of course, the decrease in pressure from the upward emplacement of intrusions or by faulting must be orders of magnitude greater.

Crack propagation of fractures is likely to occur at the leading edge of advancing magmas. The process is repetitive a) magma migrates upward in a fracture or crack, b) magma pressure propagates a crack, c) magma explodes by vesiculation of hydrothermal-volatiles, exerting additional pressures on the walls of the crack and causing additional crack propagation, rupturing and transport of material, and d) the process repeats itself.

Be sure you know from this section:

- ➔ the different mechanisms that can cause brecciation, and
- ➔ the relationships among breccia, porphyritic rocks, and porphyry deposits.

SIGNIFICANCE AND CHARACTERISTICS OF MAGMATIC DYKES AND MAGMATIC BRECCIAS

In this section you will learn:

- ➔ the difference between a dyke and a vein,
- ➔ the characteristics and magmatic formation of tourmalinite dykes and breccia, and
- ➔ the characteristics and magmatic formation of magnetite-apatite dykes and breccia.

Classification of magmatic dykes and magmatic breccia adopted here differentiates these features from veins and breccias of strictly hydrothermal origin (see inserts *Definitions: Distinguishing a dyke from a vein*, and *Opinion about the magmatic origin of tourmalinite breccia at Los Bronces, central-eastern Chile*). Seldom addressed in porphyry deposit literature are the distinctions between a magmatic and a hydrothermal origin. The lack of clarity might be because there is a gradation between hydrothermal breccia and magmatic breccia that depends on the ratio of the volatile component to magma or crystal mush component.

Dykes and breccias are emplaced by the energy released during the hydrothermal expansion of volatile components by vesiculation within these magmas or crystal mushes, which can also be rich in ore mineral components. (See inserts *Opinion on mechanisms of breccia emplacement*, and *Opinion on the magmatic origin of magnetite-apatite dykes and magnetite-apatite breccia*). The hydrous nature of these dykes and breccias results in them being more commonly ascribed to a hydrothermal origin. However, in the author's opinion, their origin is more appropriately described as magmatic—primarily because of dyke-like features and jigsaw inflation of rotated border fragments in breccia.

Ore metals associated with magnetite-apatite and tourmalinite dykes and breccias is a positive indication that ore deposits will be close by—indeed, these types of dykes and breccias can themselves be ore deposits. Thus, they have positive exploration significance, mainly because a magma or crystal mush source can be potentially large enough to produce a 'world class' ore deposit!

The following sections discuss the dominantly magmatic features mentioned for:

1. Tourmalinite dykes or dykelets and breccia (Figures 30 to 33).
2. Magnetite-apatite dykes and breccia (Figures 34 and 35; often associated with diorite-alkaline-type porphyry deposits).

Tourmalinite Dykes and Breccia

Tourmalinite dykes and breccia are associated with granitic batholiths or stocks (see insert *Definition of tourmalinite*) and are commonly associated with granodiorite. The magmatic origin is speculative, as explained in the inserts *Opinion about the magmatic origin of tourmalinite breccia at Los Bronces, central-eastern Chile*, and *Story of tourmalinite balls at Syenite Mountain, west-central Yukon, Canada*.

Fragments are variably digested. Toward the centre of tourmalinite dykes they commonly appear more corroded than fragments at dyke borders, where they sometimes have a sharp, jigsaw fit at wallrock contacts. Fragments fade out toward the centre of 0.5 m wide tourmalinite dykes at Sierra Gorda in

northern Chile, probably due to digestion aided by the high fluorine content indicated by the tourmaline. Some of the tourmalinites at Sierra Gorda (Figure 32) are uraniferous, reflecting a concentration of elements incompatible with common granitic minerals. Black, popcorn-like, tourmalinite gravel in the desert pavement at Sierra Gorda indicates underlying tourmalinites.

Definition of tourmalinite.

Tourmalinite is a rock that consists primarily of tourmaline and quartz. The tourmaline and quartz are generally very fine-grained to aphanitic. A magmatic origin is supported by a) breccia fragments inflated by tourmalinite matrix (Figure 31a) and b) tourmalinite brain rock with UST texture (Kirwin, 2005). Tourmalinite, described as veins, is more magmatic than hydrothermal—although the tourmalinite magma is undoubtedly rich in volatiles. See *Opinion about the magmatic origin of tourmalinite breccia at Los Bronces, central-eastern Chile*, and *Story of tourmalinite balls at Syenite Mountain, west-central Yukon, Canada*, below.

Opinion about the magmatic origin of tourmalinite breccia at Los Bronces, central-eastern Chile.

Tourmalinite breccia is actively mined at Los Bronces in central-eastern Chile, near the border with Argentina. A magmatic origin is supported by a) fragments in breccias near contacts are inflated by tourmalinite and can be put together with a jigsaw fit, and b) copper sulfides occur as rounded blebs concentrated in the quartz-tourmaline matrix. Matrix inflation is a magmatic injection feature and not one of sequential hydrothermal deposition. Sulfide blebs could have originated from immiscible sulfide segregations within a quartz-tourmaline magma.

Story of tourmalinite balls at Syenite Mountain, west-central Yukon, Canada.

Tourmalinite balls or orbicules up to 1 m in diameter occur in a small granite stock-like body (and talus float) at the apex of Syenite Mountain in west-central Yukon, Canada. Quartz-poor syenite envelopes the granite body. The tourmalinite balls are composed dominantly of large tourmaline crystals radiating from their centres upon being split open. Sulfide blebs up to 3 mm in diameter commonly occur near the cores of the balls. The balls appear to be solidified, immiscible, hydrous, late-stage melts. Support for an immiscible-magma origin includes a) their circular form, which is the shape that an immiscible bleb would take, b) occurrence at the apex of the small granite body, which reflects the lower specific gravity of the tourmalinite that would allow them to diapirically rise to the top of a late-stage granite magma, and c) association of elements incompatible with granitic silicates, such as, fluorine and boron in tourmaline, and sulfur in sulfides. Similar tourmalinite balls or orbicules occur in the Seagull batholith in south-central Yukon, Canada, and in apices of tin granites in western Tasmania, Australia (Hong et al., 2017). Thus, it is easy to imagine vast accumulations of this tourmalinite magma, as illustrated in Figure 30. The huge Braden breccia pipe (about 1,000 m in diameter at the surface) at the El Teniente mine in central Chile, the largest underground porphyry copper mine in the world, supports the sizeable potential of such a tourmalinite magma. The matrix of the Braden breccia has abundant tourmaline (Figures 31 and 32). The energy required to generate this pipe is phenomenal.

The tourmalinite origin model in Figure 30 provides a model related to the generation of the Braden breccia pipe at El Teniente in central Chile, which is the largest underground porphyry copper mine in the world. The main copper mineralization occurs adjacent to the Braden tourmaline breccia pipe, which is about 1 km in diameter at the surface. The matrix of this breccia has abundant tourmaline (Figures 31 and

32). The energy required to generate this pipe is phenomenal. The following, with reference to Figure 30, is a logical way of generating this breccia pipe.

1. Differentiation of granitic magma leads to an immiscible fluorine-water-rich crystal-liquid vacuole or bubble.
2. The buoyant bubble accumulates at the apex of the granitic intrusion.
3. The vacuole is enriched in components incompatible with minerals in the granitic rock (e.g., water, silica, sodium, boron, fluorine, sulfur, copper, and uranium).
4. The immiscible crystal-liquid mush is joined to the surface by a normal fault or faults (because of the maximum upward stress exerted by the pluton).
5. The faulting causes a change in pressure from lithostatic to hydrostatic in the tourmalinite magma.
6. The change in pressure results in vesiculation causing a pressure-cooker-like explosion resulting in brecciation.
7. Breccia intrusion is guided by the causative fault(s).
8. Mineralization is related to the composition of tourmalinite magma and associated hydrothermal fluids.

The magmatic origin of tourmalinite, albeit hydrous, produces tourmalinite breccia (Figures 30 to 33) and tabular dykes or dykelets (e.g., tourmalinites in Figure 31 are dykelets [magmatic] and not veins [hydrothermal], as commonly called). My model for magmatic tourmalinite (tourmaline-quartz) dykes and breccia is in Figure 30.

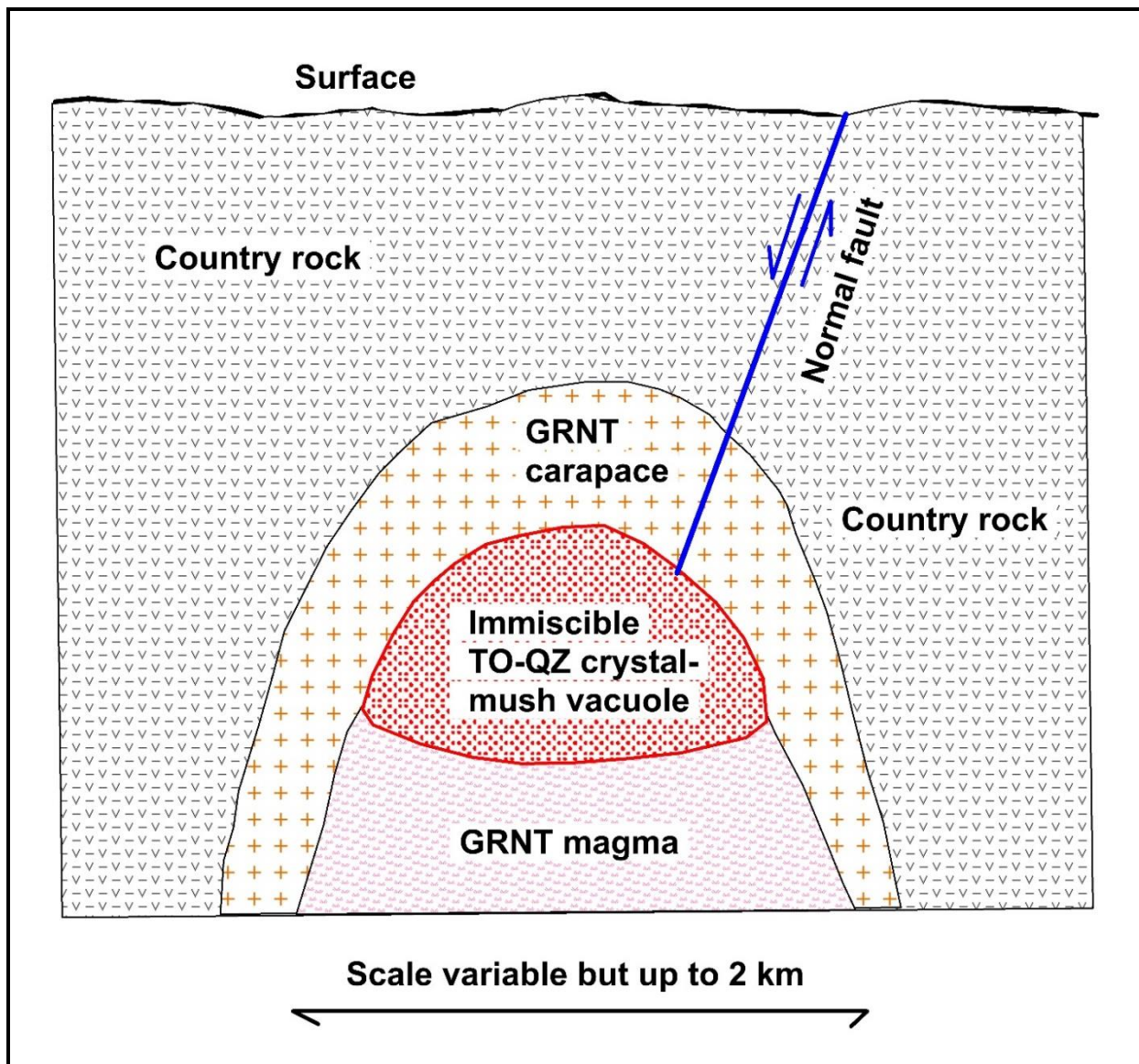


Figure 30. Model for magmatic tourmalinite (tourmaline- quartz) dykes and breccia.

An immiscible bubble or vacuole forms at the apex of a magma and consists of a crystal mush of tourmaline, quartz plus sulfides and/or their components. These vacuoles can be huge, as indicated in this figure, and can erupt with enormous energy release due to a change in pressure from lithostatic to hydrostatic (upon being tapped by a fault or faults) to form dykes and large breccia bodies. Increasing temperature due to heating of magma so that the vapour pressure exceeds lithostatic pressure, surface tension of the magma and tensile strength of the rock might also cause rupture and brecciation. Abbreviations: **GRNT** = granitic rock, **QZ** = quartz, **TO** = tourmaline, and **TO-QZ** = tourmalinite.



Figure 31. Magmatic tourmalinite (quartz-tourmaline) dykelets.
a) Tourmalinite magmatic breccia dykelet from near St. John's, Newfoundland and Labrador, Canada. **b)** Dykelets with white, albitic envelopes from the Inguaran mine area, Michoacan, Mexico; the albitic envelopes and locally associated quartz veins emphasize the close hydrothermal association.

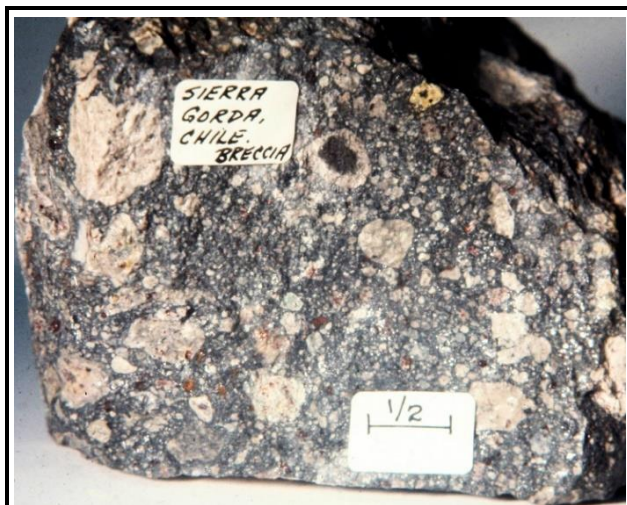


Figure 32. *Tourmalinite breccia from the main breccia pipe at Sierra Gorda, northern Chile. Fragments are rounded suggesting digestion by the fluorine-rich tourmalinite matrix. The scale tag shows 0.5 inches (1.25 cm).*

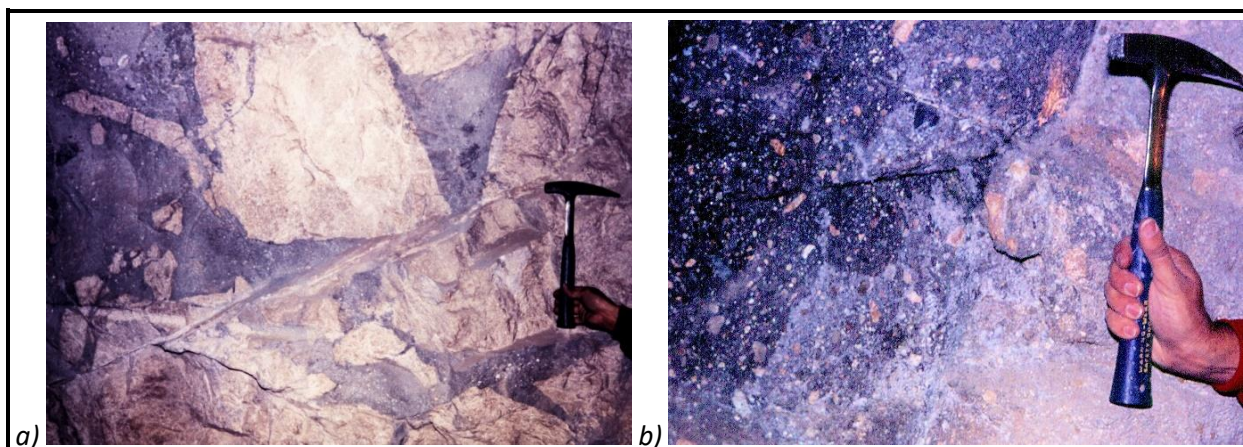


Figure 33. *Tourmalinite (quartz-tourmaline) breccia in the Braden breccia pipe at the El Teniente underground porphyry copper mine in central Chile.*

Both photos are from the central part of the Braden breccia pipe. a) is dominated by fragments, and b) is dominated by the dark matrix of tourmalinite (tourmaline and quartz). The Braden breccia pipe, although not considered economic, grades up to 0.5% copper. The breccia locally has a bedded appearance, presumably from gas streaming during emplacement. The hydrothermal fluids associated with the emplacement of the breccia are likely a major source for the copper mineralization at the El Teniente porphyry copper mine, which surrounds the pipe and is the largest underground porphyry copper mine in the world. The cupriferous margin at the outer contact of the pipe is shown in Figure 16a.

Opinion on the mechanism of breccia emplacement.

Tapping of a vacuole or bubble of volatile-rich magmas by normal faults is the most likely means for emplacement of the magmatic tourmalinite and magnetite-apatite models in Figures 30 and 34, respectively. Vesiculation in volatile-rich magma caused by an abrupt change from lithostatic to hydrostatic pressure releases prodigious amounts of energy. The vacuole or bubble occurrence follows the model proposed by Norton and Cathles (1973).

Opinion on the magmatic origin of magnetite–apatite dykes and magnetite–apatite breccia.

The magmatic classification of magnetite-apatite dykes and breccias (also called 'Kiruna-type') is preferred here but is speculative. The Kiruna mine, in northern Sweden, is the largest and most modern underground iron ore mine in the world. The orebody (about 4 km long, 80 to 120 m thick and up to 2 km deep) has reserves of 2,500 million tonnes with 30 to 70 wt.% iron with 0.05 to 5 wt.% phosphorous. Kiruna ore is Paleoproterozoic titanium-poor magnetite with minor apatite. Pervasive sodium and potassium metasomatism surround the deposit. Theories of origin are varied because textural evidence is inconclusive. However, recent high-precision dating (Westhues et al., 2016) supports the magmatic origin for Kiruna, which is the model adopted here. (Westhues et al., 2016, provide an excellent overview of the historical and varied interpretations for Kiruna-type deposits' genesis.) High contents of rare earth elements (REE) with a dominance of light REE have led some to suggest a connection to the iron oxide–copper-gold (IOCG) class of deposits, such as the Olympic Dam mine in southern Australia (the fourth-largest copper [plus uranium, silver, gold and REE] deposit in the world).

Definitions: Distinguishing a dyke from a vein.

A dyke is a variably thick sheet of magmatic rock intruded as magma or crystal mush into fractures or cracks in host rock. A dykelet is a small dyke, up to a few centimetres in width. (Not addressed here are sedimentary dykes.)

A vein is a variably thick sheet of minerals precipitated from hydrothermal solutions passing through and filling fractures/cracks in host rock.

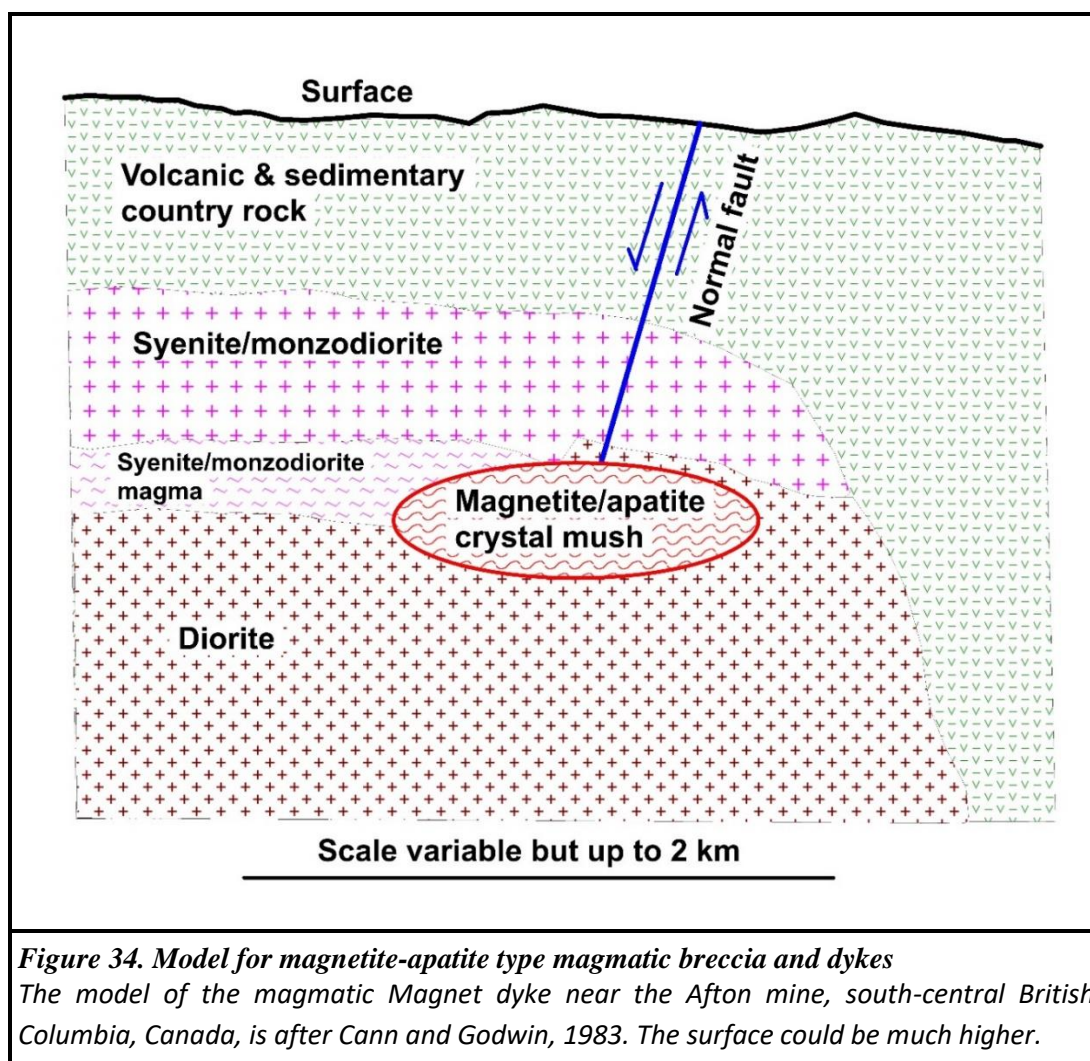
Dykes are magmatic in origin, and veins are hydrothermal. Controversy occurs where magmas are markedly hydrous, where the term magmatic-hydrothermal can be applied. I prefer to stick to a magmatic classification for tourmalinite (quartz-tourmaline) and magnetite-apatite dykes and breccia. These originate from molten or crystal mush magmas that inflate and fill by intrusion and not by sequential deposition from hydrothermal fluids.

Magnetite-Apatite Dykes and Breccias

Low-titanium magnetite-apatite dykes and breccias are closely related to batholiths associated with the diorite-alkaline type of porphyry deposit, although they also occur with calcalkaline plutons (Badham and Morton, 1976). Figure 34 is a model, modified from the Cann and Godwin (1983), of the origin for the Magnet dyke, which is adjacent to the Afton porphyry copper mine in the Iron Mask batholith in south-central British Columbia, Canada. Near the end of diorite formation, a magma or crystal mush of low-titanium-magnetite and apatite formed a vacuole. Faults tapped the vacuole, and dykes and breccias were intruded. Faulting changed the pressure in the vacuole from lithostatic to hydrostatic resulting in vesiculation-energy for emplacement. The dioritic magma is a likely source for the magnetite-apatite magma or mush. The diorite is iron-rich, as indicated by local areas of up to 80% disseminated, high-

titanium magnetite in the diorite. Spinifex-like amphibole quench texture at the contact margin of the dyke also supports a magmatic origin for the Magnet dyke. Minor magnetite-apatite breccia within the Afton mine contains minor pre-ore copper mineralization.

These types of magmatic dykes and breccias consist mainly of low-titanium magnetite with minor (up to 10%) apatite (Figure 35). They are commonly associated with albite and K-feldspar alteration, indicating a highly differentiated source. The trick to identifying this type of dyke or breccia is to look for white to pink apatite, which can occur deceptively as tiny pale specks do not look like apatite. The apatite is fluorine rich. Philpotts (1967) noted that fluorine might lower the melting point of the magnetite, causing it to remain fluid at lower temperatures. The high melting point of magnetite (about 1500°C, which is too high to be a convenient magma) causes many to doubt the magmatic origin of these dykes; however, fluorine- or chlorine-rich magmas or crystal mushes might form at lower temperatures. Recent dating has supported a magmatic origin for the magnetite-apatite lodes at the Kiruna iron mine in northern Sweden (Westhues et al., 2016). Some consider magnetite-apatite lodes to be one end member of the iron-oxide–copper–gold type of deposits (e.g., Hitzman et al., 1992; see insert *Opinion on the magmatic origin of magnetite-apatite dykes and magnetite-apatite breccias*).



A magmatic origin supports the observation that these deposits can be world-class in size (e.g., Kiruna in northern Sweden and the Olympic Dam in southern Australia). Consequently, their occurrence should always demand careful attention (see insert *Opinion on the significance of magnetite-apatite dykes and breccia in alkaline porphyry deposits*).

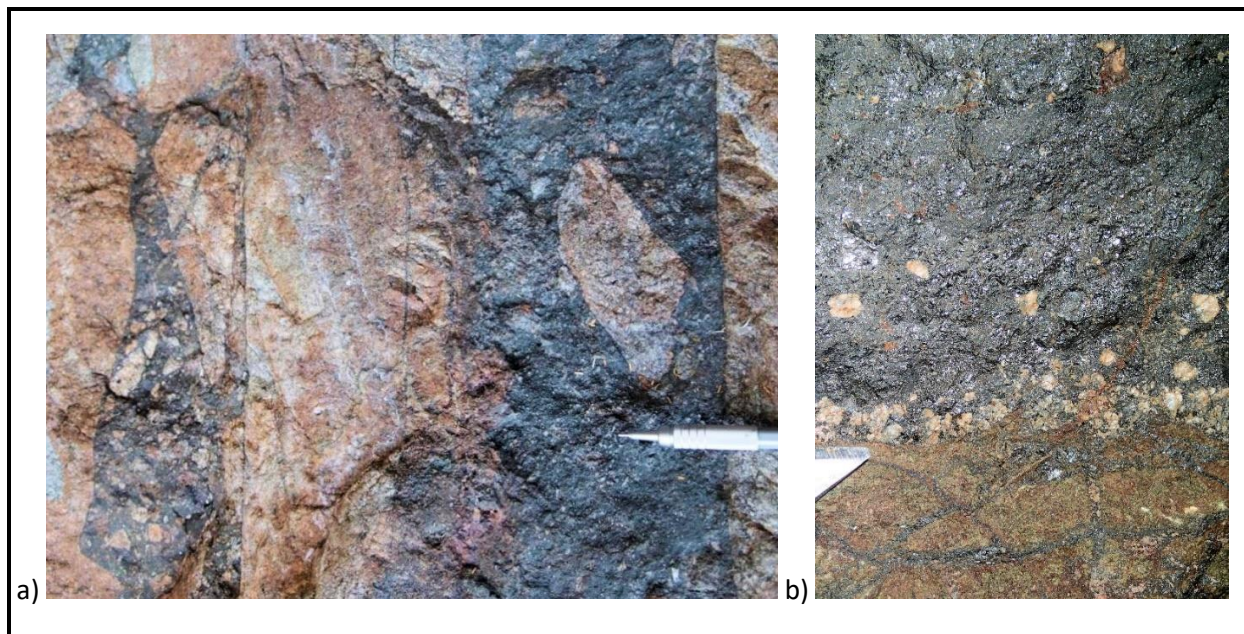


Figure 35. Magnetite-apatite magmatic breccia.

These magnetite-apatite magmatic breccias are from a) the Inguaran mine area, Michoacan, Mexico, and b) the Magnet Dyke adjacent to the Afton mine in British Columbia, Canada. In a) the inflation from the magnetite (magnetite \pm apatite) matrix requires intrusion of magma or crystal mush. The pink colour of the fragments indicates K-feldspar alteration. In b) the pale pink apatite is concentrated at the contact. The thin lines of magnetite in both examples are more appropriately called dykelets than veinlets because they are more magmatic than hydrothermal.

Opinion on the significance of magnetite-apatite dykes and breccia in alkaline porphyry deposits.

Magnetite-apatite dykes and breccia occur within and adjacent to (the Magnet Dyke), the Afton alkaline porphyry copper-gold mine near Kamloops, south-central British Columbia, Canada. The Afton mine was an open pit and abandoned when thought to be mined out. It is now an operating underground mine because deep drilling established that mineralization extended and is open to depth.

Conceptually, continuation at depth is more likely if the origin of a deposit is magmatic because it then is an integral, late-stage part of a substantial batholithic system—in the case of the Afton mine, the Iron Mask batholith. A significant clue to the end-stage magmatic origin of the Afton mine is the occurrence of diagnostically magmatic magnetite-apatite dykes. There is potential for large orebodies and justification for deep drilling when one can infer a magmatic signature to a deposit. Thus, magnetite-apatite dykes and breccia are index fossils for big and sometimes 'world class' orebodies!

Be sure you know from this section:

- the difference between a dyke and a vein,**
- the likely magmatic origin of tourmalinite and magnetite-apatite bodies, and**
- the size significance of a magmatic origin of deposits within batholithic bodies.**

CHEMISTRY AND PHASE RELATIONSHIPS AMONG HYPOGENE ALTERATION MINERALS

In this section you will learn:

→ fundamental chemistry and phase relationships related to hydrothermal alteration.

Hydrothermal fluids coursing through rock by upward and outward infiltration (advection) and diffusion, cause alteration by changing existing and adding additional minerals. One of the more relevant phase diagrams for a framework understanding of changing sequences in alteration minerals in porphyry deposits is in Figure 36 (where T = temperature in degrees centigrade and m_{KCl} and m_{HCl} are molar concentrations of potassium chloride and hydrogen chloride [hydrochloric acid], respectively). The stability of feldspars, micas and clays are controlled by hydrolysis (where K^+ , Na^+ , Ca^{2+} , Mg^{2+} and other cations are transferred to or from the mineral and solution, and H^+ ions enter the solid phase).

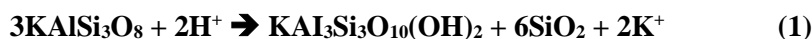
The cooling paths A, B and C (red, green, and blue lines in Figure 36) dictate likely alteration mineral sequences. All are decreasing temperature paths representing cooling from source magmatic temperatures. The cooling trends flatten because the alteration reactions are exothermic restricting abrupt temperature drop. Note that a) the higher temperature path A results in the formation of andalusite, b) the intermediate temperature path B results in pyrophyllite, and c) the more common, lower temperature path C results in kaolinite. Consequently, occurrences of andalusite (**AA**) and pyrophyllite (**PP**) indicates higher temperatures of alteration. For all paths, mineral stability depends on the $m_{\text{KCl}}/m_{\text{HCl}}$ ratio resulting from reactions in the infiltration-diffusion model (presented in the next section). Solutions beyond the left side of the diagram have a low potassium content resulting in the generation of low-potassium hydrous minerals, like chlorite, which are characteristic of propylitic alteration.

Path C is the one most observed in porphyry deposits. Equations 1 and 2 describe the chemical reactions at mineral boundaries in the figure.

Equation 1 is the reaction between K-feldspar and muscovite (or sericite).

In this equation there is:

- destruction of original K-feldspar (orthoclase, KAlSi_3O_8),
- formation of muscovite (or sericite, $\text{KAl}_3\text{Si}_3\text{O}_{10}(\text{OH})_2$), and quartz (SiO_2), and
- an increase of K^+ in solution, which, along with K^+ in the hydrothermal fluid, can be reprecipitated as secondary K-feldspar.

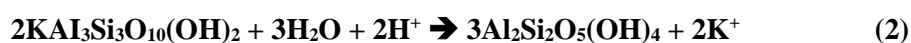


K-feldspar + hydrogen ion → muscovite + quartz + potassium ion

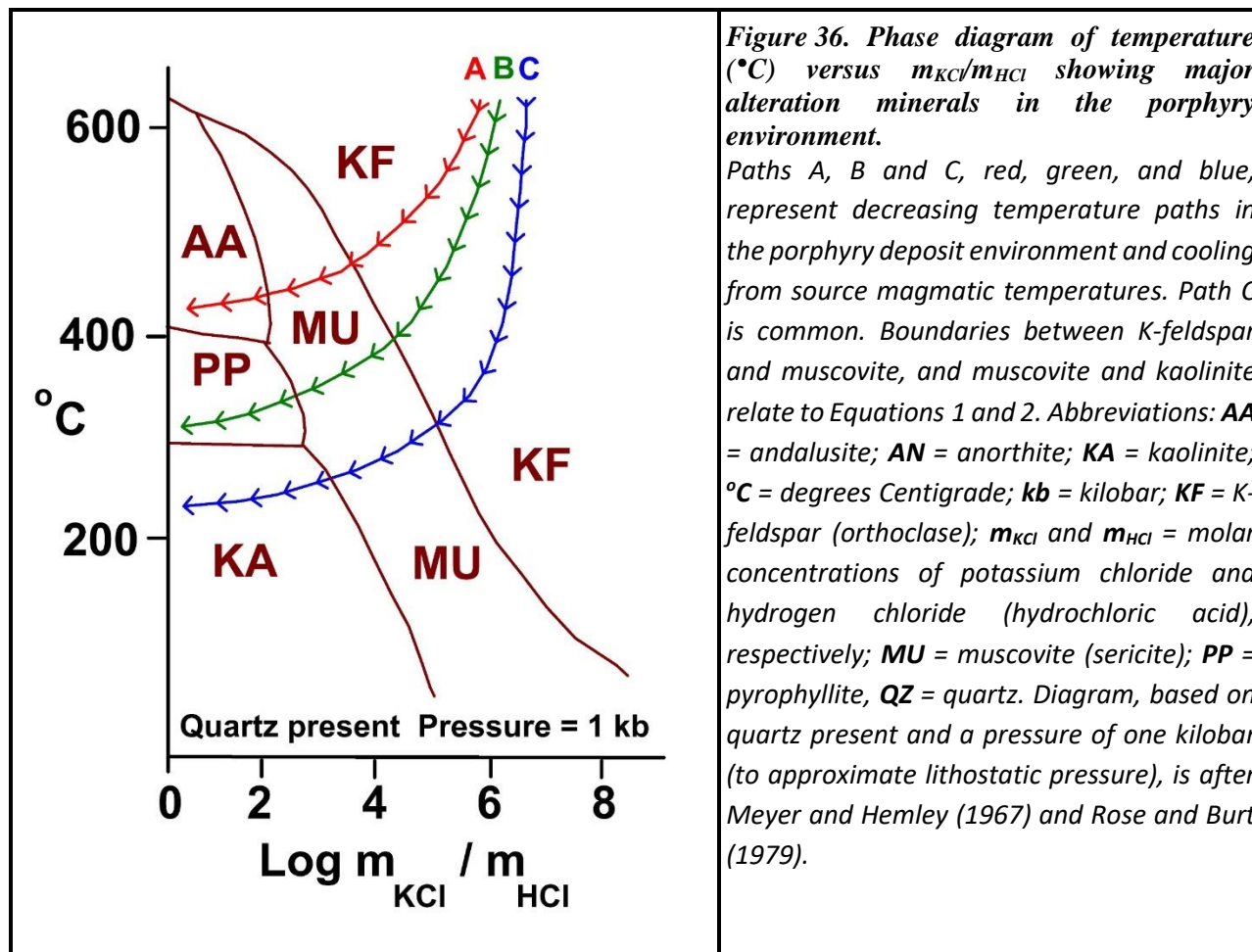
Equation 2 describes the reaction at the phase boundary between muscovite and kaolinite.

It explains:

- the development of kaolinite ($\text{Al}_2\text{Si}_2\text{O}_5(\text{OH})_4$) from muscovite (or sericite, $2\text{KAl}_3\text{Si}_3\text{O}_{10}(\text{OH})_2$).



muscovite + water + hydrogen ion → kaolinite + potassium ion



Plagioclase and amphibole sericitization, not addressed by Figure 36, results from alteration by potassium addition. Consumption of potassium by these minerals releases calcium and sodium to the hydrothermal fluid, which flows outward to the peripheral propylitic zone.

In the peripheral propylitic zone, the hydrothermal fluid—potassium-poor because the potassium has been consumed in the core—causes hydrolysis of mainly mafic minerals to chlorite (e.g., hornblende with 0.2% hydrogen to chlorite with 2.0% hydrogen). A decrease in hydrogen ions and acidity in this zone causes precipitation of calcium and sodium mobilized from the core. The calcium forms carbonates and epidote, and the sodium forms albite. Characteristic minerals in the propylitic zone are consequently chlorite, carbonate, epidote, and albite.

Be sure you know from this section:

- how a simple phase diagram relates mineralogy to alteration facies,
- the chemical relationships among K-feldspar, muscovite, and kaolinite,
- what minerals to expect from different high-temperature alteration paths, and
- why specific minerals characterize the peripheral propylitic zone.

INFILTRATION-DIFFUSION MODEL FOR ALL SCALES OF HYPOGENE ALTERATION ZONING

In this section you will learn about:

- ➔ the similarity of alteration zoning in hand samples and at a deposit-scale,
- ➔ zoning related to diffusion and infiltration (advection) in hydrothermal fluid flow, and
- ➔ how alteration relates to the phase diagram in the previous section.

Analogous zonation at a hand specimen scale of centimeters and a deposit scale of hundreds of meters might seem surprising. Hand specimens can zone outward from a vein, as in the left part of Figure 37, from a vein with quartz, K-feldspar, and biotite (phlogopite), to successively a) an envelope of quartz with K-feldspar and biotite (phlogopite), b) and envelope of quartz plus muscovite (sericite) and sometimes c) pervasive kaolinite (not shown in the figure). The hand specimen zoning sequence is like the bulk, deposit-scale zonation, as shown in the centre of Figure 37, from a) potassic (occurrences of K-feldspar and biotite [phlogopite] near the core) through b) phyllic (dominated by quartz and muscovite (sericite), to c) kaolinite-rich intermediate argillic, and peripherally to d) propylitic.

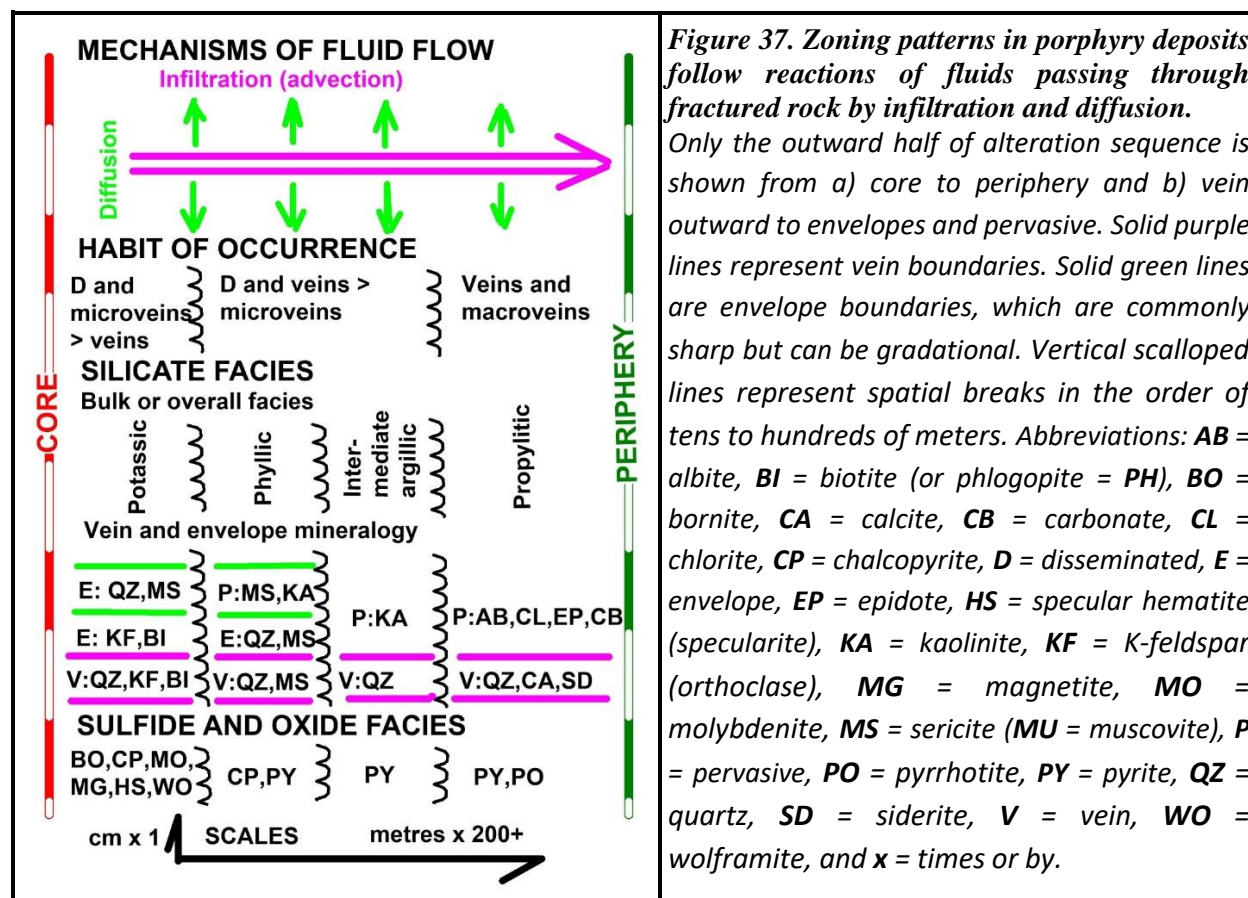
The similar zonation at totally different scales is mainly due to two contrasting mechanisms of hydrothermal fluid transport (top part of Figure 37): a) diffusion at the hand specimen scale, and b) infiltration (Korzinski, 1970), also known as advection, at a deposit scale. Diffusion involves hydrothermal fluids moving through solid rock perpendicular to veins, and infiltration is upward and outward flowing along fractures at a deposit scale. The changes in mineralogy by both mechanisms over distance, albeit at different scales (note scale at the bottom of Figure 36), reflect equivalent systematic change in the m_{KCl}/m_{HCl} ratio of the fluids as defined in Figure 36 along downward cooling paths A, B or C (the most common). The two main phase boundaries in this figure are defined by Equations 1 and 2.

The main conduits for heat and mass transfer are veins, but diffusion away from the veins is also significant. Consumption of potassium by generating new potassium bearing minerals reduces the m_{KCl}/m_{HCl} upon passage of the hydrothermal fluid. Together with decreasing temperature, sequentially stable silicate phases, along with quartz, are a) K-feldspar and biotite [phlogopite]), b) muscovite (sericite) and c) kaolinite. Potassium added during the sericitization of plagioclase and amphibole kicks out calcium and sodium. The calcium and sodium are transported outward to the peripheral chlorite-rich propylitic facies. Calcium and sodium are precipitated in minerals that include carbonates (commonly calcite), epidote, smectite (e.g., calcitic-montmorillonite), and albite. In the propylitic zone, the low m_{KCl}/m_{HCl} precludes the formation of potassium-rich minerals, but mafic minerals are hydrated to chlorite.

Changes in the habit of occurrence of mineralization, as in Figure 37, tend to zone from the core outward from a) disseminations and microveins more abundant than veins, through b) disseminations and veins more abundant than microveins, to c) macroveins commonly outside of porphyry-style mineralization. This zonation is variable and can reflect variations in fracturing related to intermineral intrusions. Within the intrusion, mineralization will tend to be tightly within microveins and disseminations. Borders of the intermineral intrusion tend to be more fractured, resulting in enhanced veining. Outward from the porphyry mineralization, major fractures can become mineralized to form macroveins.

Sulfide and oxide zoning occurs, as shown at the bottom of Figure 37. Core mineralization is commonly chalcopyrite- and bornite-rich and associated with minor pyrite and molybdenite. Magnetite or specularite (hematite), if present, signals potential gold content. Outwardly from the core, chalcopyrite becomes dominant, and pyrite increases. Best mineralization, commonly called an 'ore shell', spans the boundary between the potassic and phyllic phases. A relatively copper-barren pyrite-rich 'pyrite halo' occurs at the outer margin of the phyllic facies. Peripherally, in the propylitic facies, pyrrhotite sometimes occurs.

Viewing alteration in porphyry deposits as a three-dimensional chromatogram in which altering hydrothermal fluids change as they pass upward and outward through a large body of fractured rocks helps to relate the diffusion and infiltration zoning in Figure 37 to the phase diagram of Figure 36. Thus, Figure 37 is a qualitative representation of bulk zoning caused by infiltration and smaller-scale zonation by diffusion that generates envelopes and pervasive alteration. And mineral alteration sequences from veins to envelopes in hand specimens (formed mainly by diffusion) mimic bulk deposit-scale zonation patterns (primarily a result of infiltration or advection).



Crosscutting and superimposed relationships can identify different alteration events among different styles or facies of alteration, especially veins and envelopes. Reaction path lengths can vary as other veins of varying direction and shape are followed. Even if the path length differences are short and related to

the same mineralizing pulse, complex crosscutting relationships with little difference in time can form. Systems can, of course, become complex when formed from multiple pulses of hydrothermal mineralization. In addition, toward the end of their activity, hydrothermal systems tend to cool and collapse so that lower temperature assemblages are superimposed on earlier ones. For example, secondary biotite of potassic alteration can become chloritized, and sericite of phyllic alteration can be hydrated to illite. Similarly, late-stage calcite-zeolite veins are commonly superimposed on earlier ore-stage hypogene alteration (e.g., Figure 27).

Be sure you know from this section:

- ➔ **what the difference is between diffusion and infiltration,**
- ➔ **why alteration zoning in hand samples can mimic deposit-scale zoning, and**
- ➔ **how alteration relates to the phase diagram in the previous section.**

SUMMARY OF ALTERATION FACIES FOR HYPOGENE ZONING

In this section you will learn:

- mineralogy and identification of hydrothermal alteration facies in hydrothermal deposits, and
- the relevance of zoned hydrothermal alteration to ore discovery.

Classical facies of hypogene alteration zoning in porphyry deposits, from core to periphery, are:

1. Deep potassic (**DPT = 9**).
2. Potassic (**POT = 8**).
3. Advanced argillic (**AAR = 7**).
4. Phyllic (**PHY = 6**).
5. K-feldspar stable (**KFS = 5**).
6. Intermediate argillic (**IAR = 4**).
7. Smectitic (montmorillonitic; **SMC = 3**).
8. Propylitic (**PRP = 2**).
9. Zeolitic (**ZEL = 1**).
10. Fresh, unaltered, or original rock (**FRX = 0**).

Facies from top to bottom of TABLE 6 are in the order encountered from core to periphery of porphyry deposits as in Figure 37. This order also follows the progression of decreasing temperature and m_{KCl}/m_{HCl} (in part following Figure 36) from highest (9) down to unaltered or original (0). The 'ore shell' overlaps the contact between the potassic and the phyllic facies. The 'pyrite halo' occurs in the outer part of the phyllic facies. Mineral order in each section of TABLE 6 follows the order dictated by Figures 36 and 37.

Field identification of alteration facies depends primarily on identifying mineral associations, as generalized in the model in the previous section (Figure 37) and the more detailed models of porphyry deposits presented in the next few sections. TABLE 6 summarizes the distribution of alteration minerals in classic porphyry deposit zones or facies. Note that a) secondary biotite is generally phlogopite, and b) montmorillonite is more accurately smectite. Simple zap tests can aid in the identification of some minerals (Godwin, 2020). Definitive identification of some minerals requires thin and polished sections, X-ray diffraction (XRD), X-ray fluorescence (XRF) and short-wave infrared spectral analysis (SWIR). More detailed descriptions of these alteration zones or facies, models of their occurrence and identification tips follow in TABLE 6 and the text below.

Deep potassic facies (DPT = 9; TABLE 6) is characterized by high-temperature alteration minerals. Paths A and B in Figure 36 include the high-temperature minerals andalusite and pyrophyllite. Magnetite and specular hematite are common. These iron oxides indicate strong oxidation, and if gold is present in the hydrothermal solutions, it can be co-precipitated due to coupled oxidation-reduction.

TABLE 6. Mineral zoning of alteration facies from core to the periphery in calcalkaline (copper, molybdenum and gold), alkaline (copper and gold) and greisen (tin and tungsten and gold porphyry deposits).

Note that the more abundant minerals, in red (**H** = high) and green (**M** = medium) trend generally from top-left to bottom-right within the alteration silicates, carbonates and zeolites category. Calcalkaline deposit-related abundances are in normal font. Alkaline and greisen porphyry deposit-related abundances are italicized. Facies from top to bottom in the table (from core to periphery of porphyry deposits) are from highest (**9**) down to unaltered rock (**0**). Names and codes for the facies are: deep potassic (**9 = DPT**), potassic (**8 = POT**), advanced argillic (**7 = AAR**), phyllic (**6 = PHY**), K-feldspar stable (**5 = KFS**), intermediate argillic (**4 = IAR**), smectitic (**3 = SMC**), propylitic (**2 = PRP**), zeolitic (**1 = ZEL**) and fresh, unaltered or original rock (**0 = FRX**). The 'ore shell' overlaps the contact between the potassic and the phyllic facies. The 'pyrite halo' occurs in the outer part of the phyllic facies. Minerals in each section also follow the order dictated by Figures 36 and 37. Mineral abbreviations: **AA** = andalusite, **AB** = albite, **BI** = biotite, **BO** = bornite, **CA** = calcite, **CB** = carbonate, **CL** = chlorite, **CP** = chalcopyrite, **CT** = cassiterite, **CY** = clay, **EP** = epidote, **HS** = specular hematite, **KA** = kaolinite, **KF** = K-feldspar (orthoclase), **MG** = magnetite, **MM** = montmorillonite (smectite), **MO** = molybdenite, **MU** = muscovite, **MS** = muscovite-sericite, **PH** = phlogopite = secondary biotite = **BI**, **PO** = pyrrhotite, **PP** = pyrophyllite, **PY** = pyrite, **QZ** = quartz, **SM** = smectite and **ZE** = zeolite. Qualitative abundance abbreviations: **H** = high, **M** = medium, **L** = low, **T** = trace, **N** = none (absent), and **O** = original.

Mineral/ Facies	Alteration silicates, carbonates, and zeolites												Oxides and sulfides					
	QZ	AA	PP	KF	PH BI	MS MU	CY KA	SM MM	AB	CL ± EP	CB CA	ZE	MG HS	MO	BO	CP	PY ± PO	WO CT
DPT = 9	H	H	M	L	L	L	N	N	N	N	N	N	M	L	L	L	L	T
POT = 8 <i>Alkaline</i> <i>Greisen</i>	H L H	N N N	T N N	H H H	H M M	M L H	N N L	N N N	N H M	N M L	N T N	N N N	M M N	M T L	M M N	M M T	M L L	N N M
AAR = 7	H	N	T	N	N	M	H	N	N	N	N	N	N	T	T	L	L	N
PHY = 6 <i>Greisen</i>	H H	N N	N N	N M	N M	H H	N N	N N	N T	N L	N N	N N	N N	T T	L N	H N	H M	N T
KFS = 5	M	N	N	O	N	M	N	N	N	N	N	N	N	T	T	L	L	N
IAR = 4	O	N	N	N	N	T	H	N	N	N	N	N	N	N	N	N	N	N
MON = 3	O	N	N	N	N	N	L	H	N	L	L	N	N	N	N	N	N	N
PRP = 2 <i>Alkaline</i> <i>Greisen</i>	T T T	N N N	N N N	N N N	N N N	N N N	T N N	T T T	M M M	H H H	H H H	L L L	N T N	N N N	N N N	N N N	L L L	N N N
ZEL = 1	O	N	N	N	N	N	T	T	T	T	M	H	N	N	N	N	N	N
FRX = 0	O	N	N	O	N	N	N	N	N	T	T	N	O	N	N	N	T	N

Potassic-alkaline facies (POT = 8; TABLE 6) is illustrated in Figure 38a. It commonly consists of secondary, salmon-pink K-feldspar (see K-feldspar stain zap test in Godwin, 2020) and secondary biotite (phlogopite) in veins and envelopes. Magnetite and specular hematite are common and can be diagnostic. Muscovite (called sericite when fine-grained) is not as abundant as in phyllic alteration. This facies commonly includes relatively more bornite than chalcopyrite and only minor pyrite. Molybdenite is common. The outer part of the potassic facies zone is typically part of the 'ore shell'. The challenge in identifying potassic facies is to distinguish it from the original rock; thus, the habit of occurrence is critical and regional knowledge is sometimes required. Potassic alteration is characterized by a) K-feldspar and phlogopite-biotite in veins or envelopes, b) pseudomorphic phlogopite after hornblende (identified by barrel shapes, easily identified in thin section, that when scratched with a needle fluff to soft, brownish, flexible plates), c) overgrowths of phlogopite on biotite, and d) felted or shredded textures of phlogopite (common in the matrix of breccia). Specular hematite and magnetite can indicate gold due to coupled oxidation-reduction.

Potassic-alkaline facies (POT = 8; TABLE 6) mimics calcalkaline porphyry deposit alteration, but a) lacks abundant secondary quartz, b) commonly has albite in envelopes and as flooding. Albite, like K-feldspar, can be pink; K-feldspar staining (see zap test in Godwin, 2020) helps to identify the difference.

Advanced argillic facies (AAR = 7; TABLE 6) consists of abundant muscovite (sericite), quartz and kaolinite. Pyrophyllite, if present, requires XRD or SWIR to identify it from muscovite (sericite). Pyrite and secondary quartz are abundant. Quartz stockwork is common. Large amounts of quartz distinguish advanced argillic facies (**AAR = 7**) from the quartz-poor intermediate argillic facies (**IAR = 4**).

Phyllic facies (PHY = 6; TABLE 6) is illustrated in Figure 38a. It is characteristically pale white or pale green and consists of muscovite (sericite), quartz, and pyrite. In the wallrock, muscovite is generally finer-grained and replaces feldspars in the groundmass or occurs in envelopes around fractures. Textures of the original rock are commonly destroyed by alteration, leading to incorrect changes of primary rock names. Mafic minerals are sericitized, and originally iron-rich minerals are commonly sulfidized to produce disseminated pyrite. The muscovite (sericite) is commonly a pale green and is often incorrectly identified as chlorite. However, the shades of green for sericite (pale and bright) and chlorite (dark) are distinct. Note that abundant quartz and pyrite indicates phyllic alteration. In contrast, abundant calcite and darker greens from chlorite and epidote would signify propylitic facies. Muscovite (sericite) commonly occurs with kaolinite. Muscovite (sericite), compared to kaolinite, is a) not tacky to the tongue, b) is not argillaceous in odour, and c) has a silky sheen in bright light under magnification. Illite (which sometimes has a distinctive rainbow sheen) can be present, especially in retrograde alteration. Distinctions among kaolinite, sericite and illite (and their relative amounts) require the aid of thin sections, XRD and SWIR. Commonly, the 'pyrite halo' is at the outer part, and the 'ore shell' spans the inner and core side of the phyllic facies. The 'pyrite halo' is marked by abundant pyrite, high pyrite to chalcopyrite ratios and high chargeability anomalies in induced polarization (IP) geophysical surveys. (An IP geophysical survey to a facetious geologist is an 'iron pyrite' survey.) The 'ore shell' is marked by high chalcopyrite to pyrite ratios and IP chargeability anomalies that are less intense than those of the 'pyrite halo'.

K-feldspar-stable phyllic facies (KFS = 5; TABLE 6) is characterized by the alteration of plagioclase to sericite or paragonite, and quartz. Mafic minerals are sericitized, and the contained iron is commonly sulfidized to pyrite disseminations at the site of the original mafic mineral. Original K-feldspar, however, is fresh and hard (Mohs hardness is 6). Although not commonly mapped, this facies occurs at the Endako

molybdenum mine in British Columbia, Canada (Drummond and Kimura, 1969). The intensity of alteration can be indexed on relative hardness of plagioclase determined by scratching with a needle mounted in a mechanical pencil. If the plagioclase has a Mohs hardness of 6, it is unaltered; if it has a medium hardness it is partly altered; if it is soft, it is highly altered.

Intermediate argillic facies (IAR = 4; TABLE 6) is characterized by kaolinite alteration of feldspars. Original biotite can be retained, but generally, the entire rock is bleached white, tacky to the tongue and argillaceous in odour. Secondary quartz is notably rare. Pyrite is not abundant. The distinction of argillic alteration from supergene alteration can be difficult. Location at the ground surface is suspect, especially in residually weathered, supergene-altered terrain. Laboratory study of stable isotopes (oxygen and deuterium) can distinguish supergene from hypogene argillic alteration.

Smectite facies (SMC = 3; TABLE 6), illustrated in Figure 38b, is characterized by waxy, olive-green smectite (e.g., montmorillonite) clay. Cores of zoned calcic plagioclase may be preferentially altered to smectite. Some smectitic clays swell on the addition of water and can be associated with calcite; therefore, when tested with dilute hydrochloric acid, they tend to swell and fizz slightly (check for bubbling with a hand lens and by listening with a closely held ear). Drill core altered to smectitic facies is commonly soft and has a pock-marked, rough surface where drill fluid swells the clay and washes it away. Smectite-rich core from sedimentary rocks has been known to expand such that measured recoveries are markedly greater than 100%. Smectite alteration is extremely tacky to the tongue and has a strong clay odour. SWIR and XRD are useful for the identification of smectite.

Propylitic greisen and propylitic calcalkaline facies (PRP = 2; TABLE 6) are typically marked by alteration of iron- and magnesium-bearing minerals (biotite or amphibole) and feldspars to drab green rock. Common minerals are chlorite, carbonates (especially calcite), epidote, chlorite, albite, and pyrite. Chlorite pseudomorphs after barrel-shaped hornblende crystals are common; when scratched with a needle, the chlorite pseudomorphs will be soft and dark green. This alteration results from hydrolysis by lower temperature hydrothermal fluids depleted in potassium (low $m_{\text{KCl}}/m_{\text{HCl}}$, beyond the lower-left edge of Figure 36). Calcium and sodium, added to the hydrothermal fluid from alteration of plagioclase and mafic minerals in the deposit's core, are transported to the outer propylitic zone.

Propylitic-alkaline inner-zone facies (PRP = 2; TABLE 6) is equivalent to propylitic facies above but is marked by red hematite dusting of feldspars, distinguishing it from the propylitic-alkaline outer-zone facies, which is not hematized.

Propylitic-alkaline outer-zone facies (PRP = 2; TABLE 6) is equivalent to propylitic-alkaline inner-zone facies above but is without the red hematite dusting of feldspars that marks the propylitic inner-zone facies.

Zeolitic facies (ZEL = 1; TABLE 6) commonly occurs in microveins and veins, and vesicles. The pink zeolite, heulandite, is common in porphyry deposits in the Highland Valley, British Columbia, Canada. Zeolites usually occur with calcite. This alteration also commonly represents a late-stage collapse of a cooling hydrothermal system superimposed on earlier facies.

Fresh rock (FRX = 0; TABLE 6) is not always easy to identify because some altered rock can be deceptive. A knowledge of regionally occurring rock types helps in recognition of original rock types.

Overprint of a high-temperature alteration system by a late-stage hydrothermal collapse and meteoric water results in muscovite in high-temperature facies being changed to pale green mixtures of muscovite, illite and kaolinite. Superposition of zeolite and propylitic facies, described above, also occurs. Most of these overprints will occur at shallower levels in the original deposit.

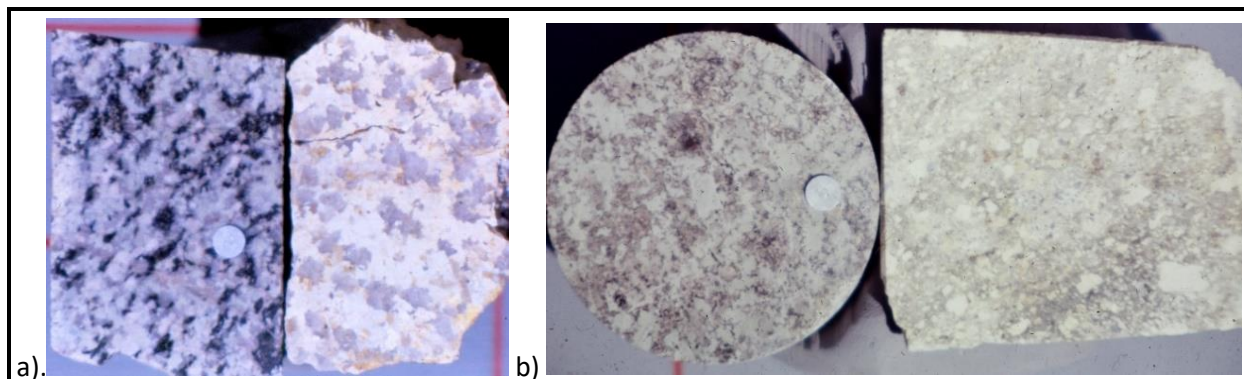


Figure 38. Examples in drillcore of pervasive a) potassic and phyllic and b) smectitic hydrothermal alteration.

a-left side) Potassic alteration marked by pervasive biotite (phlogopite) replacement of original hornblende, and pale green sericitization of feldspar. **a-right side)** Phyllic alteration characterized by pale green pervasive alteration of all feldspars, but intact original quartz (grey in the specimen). **b)** Smectite facies dominated by drab green smectite (montmorillonite). Photographs are of samples from the Casino deposit in central Yukon, Canada.

Be sure you know from this section:

- ➔ how to identify and describe alteration facies,
- ➔ where the 'ore shell' and the 'pyrite halo' occur within the alteration zones, and
- ➔ applicable shorthand codes to facilitate description of alteration facies.

MODELS FOR QUARTZ-BEARING, CALCALKALINE PORPHYRY DEPOSITS RELATED TO GRANITIC BATHOLITHS

In this section you will learn about:

- the Valley Copper mine in the Guichon Creek batholith,
- a speculative end-stage magmatic model for batholith-related porphyry deposits, and
- why batholith-related deposits can be world class.

A classic example of a quartz-bearing, calcalkaline porphyry deposit related to a granitic batholith (cf. plutonic type of Sutherland Brown, 1976a) is found at the Valley Copper porphyry mine (Figure 39) in the Highland Valley of south-central British Columbia, Canada. This mine is located near the centre of the Late Triassic Guichon Creek batholith, which is zoned progressively and concentrically from the mafic periphery to the felsic core. Valley Copper is a world-class porphyry copper deposit.

The Valley Copper porphyry deposit, has been tied by D'Angelo et al. (2017), based on lithogeochemistry and textural observations, to specific, late-productive magmatic intrusive pulses about eight million years later than the Guichon Creek batholith. However, Valley Copper and other porphyry deposits in the core of the batholith are readily envisioned as having formed from a late and end-stage hydrous, magmatic accumulation of the large, inwardly differentiating Guichon Creek batholith, despite the apparently younger age. The core-end of this progressive differentiation would have been a hydrous and siliceous magma that was a late-differentiate rich in potassium and sodium associated with a concentration of ore elements including copper, molybdenum, and sulfur—none of which fit easily into the pre-core rock silicates. This concentration mechanism is similar to the formation of some pegmatite and greisen related to S-type granites, with the distinction that Valley Copper occurs within the I-type granitic Guichon Creek batholith (granitic classification as I-, S-, and A-types was coined by Chappell and White [1974; 1992]; see insert *Origin of S-, A- and I-type granitic rocks*). Because of this, the author asserts that the Valley Copper deposit could also be called an I-type greisen porphyry deposit, characterized by later core granitic phases with higher concentrations of hydrous biotite, muscovite, K-feldspar and albitic plagioclase. It is within these late, core-phase granitic rocks that ore mineralization is found at Valley Copper.

How many tonnes of copper could be derived from the differentiation of the magma during the formation of the Guichon Creek batholith? The original magma forming the batholith was probably rich in copper given that a) there are many copper showings in the mafic border granitic phases of the batholith, b) the geometric mean copper concentration in the border phase of the batholith is about 60 ppm (McMillan, 1976) and c) the Craigmont copper pyrometasomatic-skarn deposit is adjacent to the southern contact of the batholith and was apparently generated from the batholith. Thus, the copper concentration in the original magma could easily have been more than 100 ppm copper. Suppose, as a conservative estimate, 5 ppm (5×10^{-6}) of copper was excluded from rocks as they crystallized, and that this copper became concentrated in the central hydrous magmatic phase. How many tonnes of copper would result? Based on gravity and magnetic surveys (Ager et al., 1972), the shape of the Guichon Creek batholith is downward-conical, but oval in plan view (about 20 km wide east-west [$r = 10$ km], 40 km long north-south [$R = 20$ km], with an average conical downward depth of about 6 km [$h = 6$ km]). The volume of an ovoid cone is $1/3 \times \pi \times r \times R \times h$. Tonnage is volume in cubic metres times specific gravity (2.5, which is low, but convenient for estimation). If the amount of excluded copper during crystallization is 5×10^{-6} (5 ppm) then

the tonnage of copper potentially accumulated is $1/3 \times \pi \times 10 \text{ km} \times 20 \text{ km} \times 6 \text{ km} \times 2.5 \text{ t/m}^3 \times 10^9 \text{ m}^3/\text{km}^3 \times 5 \times 10^{-6} \text{ Cu}$, or about 15 million tonnes of copper. A total of about 8 million tonnes of copper in all known Highland Valley porphyry copper deposits was identified by Sutherland Brown and Cathro (1976). Because the amount of copper excluded is speculative, and some deposit tonnage must have been lost in the erosion of the upper part of the batholith (which could double the source volume and add to the total copper excluded anyway), it is difficult to know if additional reserves are likely; however, the calculation does show that a batholithic-magmatic source for the copper is feasible. The 5 ppm in exclusions is conservative, so there is, in the author's opinion, a lot more copper to be found in the central part of the Guichon Creek batholith! Some of this potential is emphasized by the following new interpretation of a magmatic origin for the Alwyn copper porphyry deposit, which is in the core of the batholith close to the Valley Copper mine.

The Alwyn copper porphyry mine, now closed, is only 2 km west of Valley Copper (Figure 39). It has features that support the end-stage magmatic explanation of the Valley Copper deposit. A surface outcrop at Alwyn (Figure 40) is cut by what looks like a quartz-muscovite-sulfide dyke, which would traditionally be interpreted as a vein. What is the difference? Simply, a dyke is intruded into a fracture as a magma or crystal mush, and a vein is deposited in a fracture from hydrothermal solutions. If an end-stage magma at a certain point of cooling consisted of a hydrous, metal-rich, crystal mush of quartz and muscovite, it could be intruded into fractures as dykes. The surrounding rocks at the temperature of stability of the muscovite would have been brittle; therefore, the core magma could have consisted of a muscovite-quartz-copper-sulfur mush, and if this was structurally tapped it could form quartz-muscovite-copper sulfide dykes. Thus, it seems possible that the surface showing in Figure 40 at the Alwyn copper deposit is a dyke. If this is the case, the exploration potential related to such an interpretation is profound. One would look for the potentially huge magma source related to the mineralized dyke, presumably at depth (since magmas tend to rise diapirically) and/or laterally. In fact, the source, if magmatic, might be spatially and genetically related to the core magma that formed the Valley Copper deposit, which is only 2 km away.

The near proximity of the Valley Copper deposit to the Alwyn copper deposit is shown in Figure 39 and the dyke-like form of the quartz-muscovite-sulfide surface showing is illustrated in Figures 40 and 41. Note that the outcrop in these figures has no obvious quartz veins. The contact in Figure 41a is sharp and without marked envelope or pervasive alteration. Alwyn ore found in float commonly consists of massive quartz and muscovite with no obvious veining, although local quartz veining can be found; this is not surprising given that the muscovite-quartz-sulfide end-stage mush was undoubtedly silica rich and hydrous.

Viewing batholith-type porphyry deposits as end-stage magmas enhances their potential for 'world class' size and grade, as is the case for the Valley Copper porphyry deposit in the Guichon Creek batholith, because the copper source is the batholith—and it is huge! Furthermore, the magmatic, I-type greisen interpretation enhances the speculation that major ore potential remains in the core area of the Guichon Creek batholith.



Figure 39. View of the Valley Copper mine from near the Alwyn mine, in the Highland Valley of south-central British Columbia, Canada.

Valley Copper mine in the foreground is about 2 km east of the Alwyn deposit. Both deposits are in the core of the Guichon Creek batholith. Although the Valley Copper deposit is 2 km distant could they have a common hydrous magmatic source?



Figure 40. Alwyn dyke(?) overview.

This outcrop, stained green with sharp contact on the left, would normally be described as a vein; however, if it is from an injection of muscovite-quartz-sulfide magma or mush it is more appropriately described as a quartz-muscovite-sulfide magmatic dyke. The dyke(?) parallels prominent jointing (a weak structural direction[?]) in the surrounding granitic host rock, which was apparently brittle at the time of dyke(?) emplacement.



Figure 41. Alwyn dyke(?) contact and mineralized float.

a) A close-up photo of the sharp vertical left contact in Figure 40 and at the centre of the pen. Relatively fresh granite is granite on the left side of the pen and the quartz-muscovite-copper sulfide Alwyn dyke(?) on the right. There is no obvious envelope alteration. **b)** A specimen from float consisting of massive quartz-muscovite-sulfide that might be magmatic but is normally called phyllic alteration related to veining.

Be sure you know from this section that:

- ➔ the model for batholith-related deposits is speculative, and
- ➔ the batholith-related model can be associated with world-class deposits.

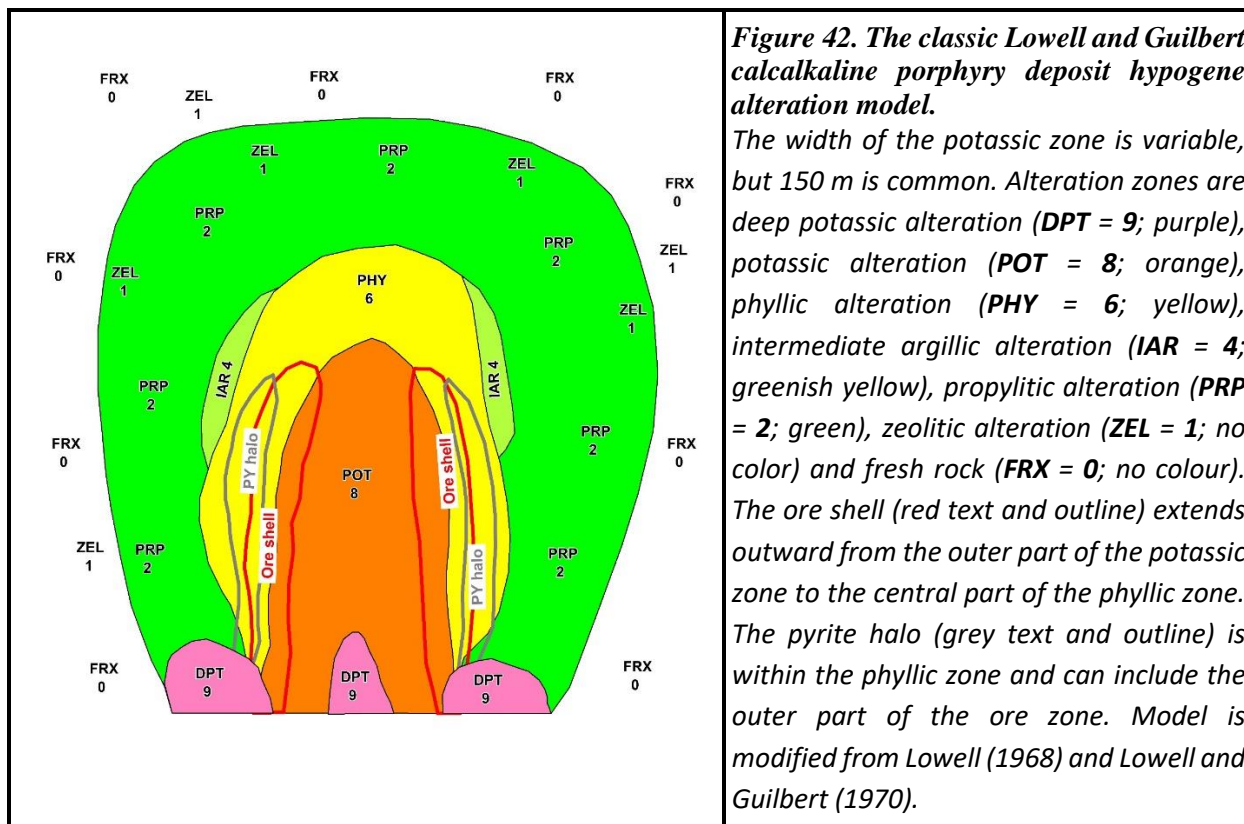
CLASSIC HYPOGENE ALTERATION MODELS FOR QUARTZ-BEARING, CALCALKALINE BATHOLITH- OR STOCK-RELATED COPPER-MOLYBDENUM PORPHYRY DEPOSITS

In this section you will learn about two hypogene porphyry deposit alteration models:

- ➔ the classic Lowell and Guilbert model showing hypogene alteration zoning that provides vectors to the ore shell and the pyrite halo, and
- ➔ a model, based largely on Chilean deposits, that defines alteration zoning, ore location and links underlying porphyry deposits to overlying epithermal deposits.

Copper-molybdenum deposits occur in quartz-bearing, calcalkaline granitic plutons. Alteration results from hydrothermal fluids with three obvious potential fluid sources: a) residual water from batholith-scale crystallization of magmas; b) exsolved fluids from crystallization of smaller magmatic bodies such as dykes (especially porphyry dykes), breccia and apices of stocks (cupolas) and c) groundwater heated and convected by proximity to hot intrusive rocks.

The classic Lowell and Guilbert model (1970) in Figure 42 is an anchor for the study of alteration in porphyry deposits. The phyllic zone (**PHY 6**) is commonly about 100 m wide and the potassic zone (**POT 7**) is about 150 m thick. Peripheral propylitic alteration can be extensive. Originally this model did not include the central deep potassic zone (**DPT 9**). The ore shell, outlined in red in Figure 42, spans the central part of the phyllic zone and the outer part of the potassic zone; however, ore mineralization can be more extensive than shown and occur more broadly within and above the central potassic zone (cf. Figure 43) and the deep potassic zone. The pyrite halo (horizontal lines in Figure 42) is near the outer part of the phyllic zone. Late-stage minerals, which include illite, chlorite, zeolite, and carbonate alteration, are commonly superimposed on the major alteration facies shown when the hydrothermal system collapses after the main mineralizing events. Lowell and Guilbert (1970) also noted additional zoning related to the habit of mineralization where the a) core mineralization is dominantly disseminated, b) ore shell and pyrite halo are mainly veins and microveins plus disseminations, and c) the peripheral propylitic zones are characterized by veins and macroveins (see Figure 37).



A newer model for porphyry deposits, presented in Figure 43, is modified from Sillitoe (1973) and Gustafson and Hunt (1975). This model, developed largely from studies of Andean porphyry deposits, shows the depth relationship between the epithermal deposit 'tops' and porphyry deposit 'bottoms'. Most alteration is a result of upward and outward flow of magmatic hydrothermal fluids through fractured rocks in and above a cupola (Figure 23). Groundwater is involved only peripherally and near surface. Sulfur from the magma is in the form of sulfur dioxide (SO_2), but upon cooling to about 400°C , the SO_2 converts to H_2S and H_2SO_4 , which produces sulfides (especially pyrite) associated with the sericite that is dominant in the phyllic zone and extends upward into the advanced argillic zone. Propylitic alteration represents hydrous alteration from potassium-poor, lower temperature fluids. Late-stage illite, zeolite and carbonate alterations are commonly superimposed on the central alteration facies and fresh rock when the thermal system collapses. Contact metamorphic skarn assemblages can occur where carbonate rocks are in contact with the mineralizing pluton.

Based largely on stable isotope data, the ore shell and pyrite halo in Figure 42 were thought to occur at the interface of central upward- and outward-flowing magmatic hydrothermal fluids and peripheral groundwater convecting in response to the heat of the causative intrusion; consequently, the ore shell in this early classic model was not expected to extend over the top of the potassic core. The stable isotope data, however, was likely based on supergene-altered samples with a groundwater component; thus, the role of groundwater probably is not as significant as previously thought and the model with a cupola geometry in Figure 43 is likely geometrically more accurate.

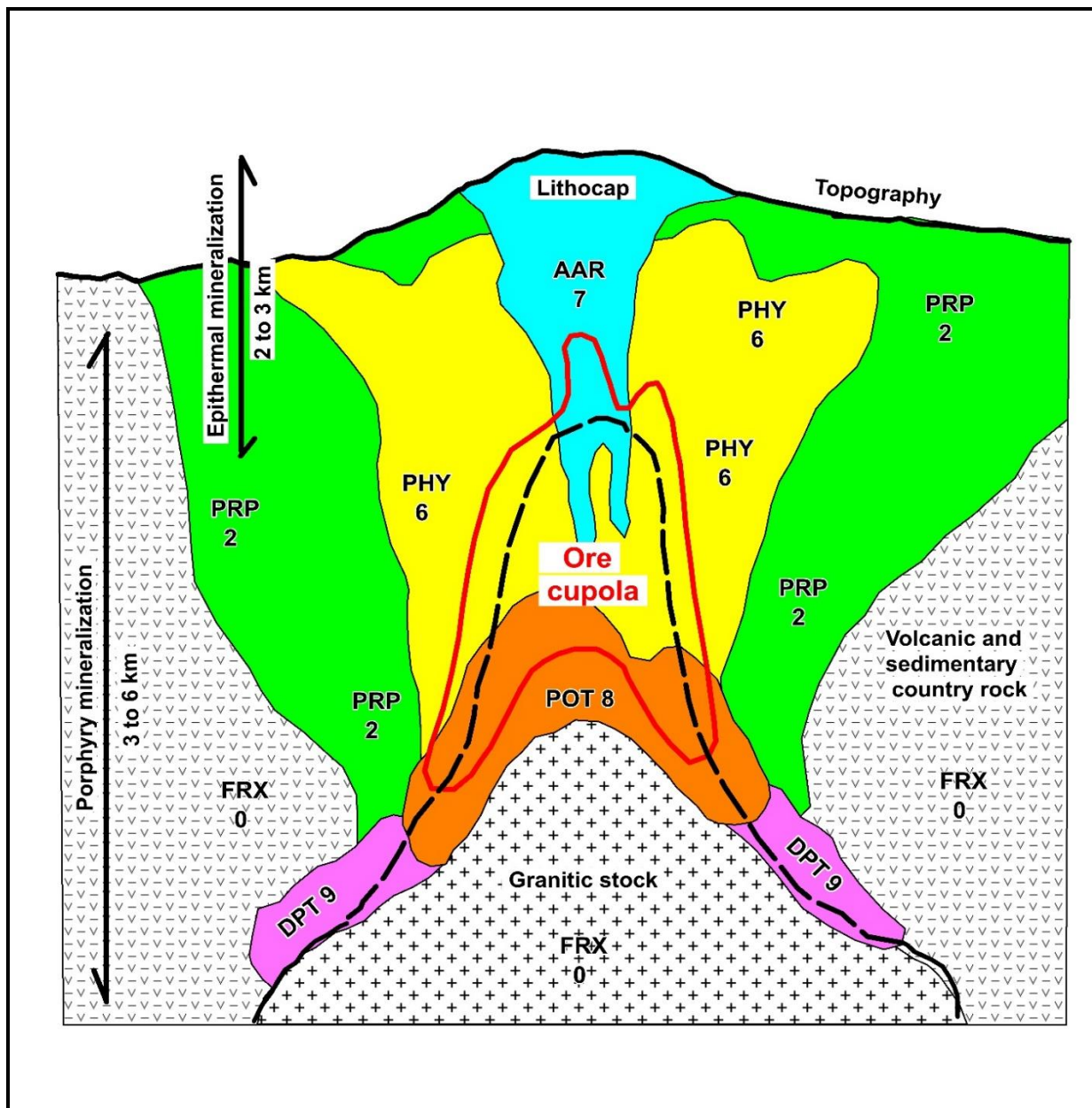


Figure 43. Andean epithermal top and porphyry bottom model.

In the Andean model, porphyry deposit bottoms are topped by epithermal deposits that are generated above productive intrusive stocks. The surface expression of the epithermal deposits is marked by a lithocap. The cupola-like ore zone is outlined in red. The contact of the granitic stock is outlined by black—solid where sharp and dashed where alteration obscured. Alteration zones are deep potassic alteration (DPT = 9; purple), advanced argillic alteration (AAR = 7; blue), potassic alteration (POT = 8; orange), phyllic alteration (PHY = 6; yellow), propylitic alteration (PRP = 2; green) and fresh rock (FRX = 0; no colour). Model is modified from Sillitoe (1973) and Gustafson and Hunt (1975).

Be sure you know from this section the two models for porphyry deposits:

- the classic Lowell and Gilbert model, and**
- the Andean epithermal top and porphyry bottom model.**

MODEL FOR QUARTZ-POOR, ALKALINE-DIORITE BATHOLITH-RELATED PORPHYRY DEPOSITS

In this section you will learn about:

→ a model for quartz-poor, alkaline-diorite porphyry deposits.

A model for alkaline-diorite porphyry copper-gold deposits is in Figure 44. The model is simplified from Wilson et al. (2003), with modification based on deposits in the Afton porphyry deposit area of south-central British Columbia, Canada. The main features added are the a) locally copper-mineralized picrite emplaced along fault zones, b) breccia or dyke bodies of magmatic magnetite-apatite, and c) concentration of alteration spanning a contact of different rock types commonly associated with alkaline porphyry deposits.

Quartz poor alkaline porphyry deposits (Figure 44) occur within dioritic batholiths commonly near marginal, more potassium rich granitic rocks such as monzodiorite, monzonite and syenite. Although the genetic relationship to alkalic porphyry deposits is not clear, close spatial associations and copper mineralization exists with a) magnetite-apatite breccias and dykes, and b) picrite, which is a coarse-grained ultramafic rock consisting of olivine and pyroxene (e.g., augite) with small amounts of plagioclase.

Magmatic magnetite-apatite dykes and breccia commonly occur within or close to porphyry deposits in space and time; they can be mineralized or nonmineralized. The concentration of mineralization spanning a major fault contact implies that this structure is a potential guide to late magmatic phases and fluids.

Picrite intrusion is a) generally later than, but locally penecontemporaneous with, porphyry mineralization, b) associated with major faults that can also be associated with the porphyry deposits, and c) derived from primitive mantle that might represent the underlying copper source for alkalic porphyry deposits (TABLE 4). Magnetite-apatite lodes can be pre-, post-, or syn-porphyry deposit ore mineralization; they can be copper rich or barren.

Ore mineralization occurs mainly within a central core of potassic alteration (Figure 44: **POT = 8**, which is red [inner zone] and orange [outer zone]) consisting of albite, K-feldspar, biotite, chlorite, vein quartz, bornite, chalcopyrite and minor pyrite; the inner potassic zone commonly hosts more bornite than chalcopyrite, which distinguishes it from the outer potassic zone where chalcopyrite is dominant. Propylitic alteration (**PRP = 2**; dark and pale green) tightly surrounds the potassic core without a marked phyllic zone, and consists of albite, chlorite, epidote, actinolite, chlorite, carbonate, and pyrite; however, a) the inner propylitic zone (dark green) commonly has red-hematite dusting of feldspars, which distinguishes it from b) the outer propylitic zone (pale green). Contact metamorphic skarn assemblages can occur where carbonate rocks are in contact with mineralization.

Alteration zones are commonly smaller in plan view than in calcalkaline porphyry deposits; however, because the end-stage magmatic mineralization and alteration is pluton hosted, the size and depth potential of these types of deposits reach world class (see inset *Comment on quartz-poor, alkaline-diorite granitic batholith- and stock-related porphyry deposits*).

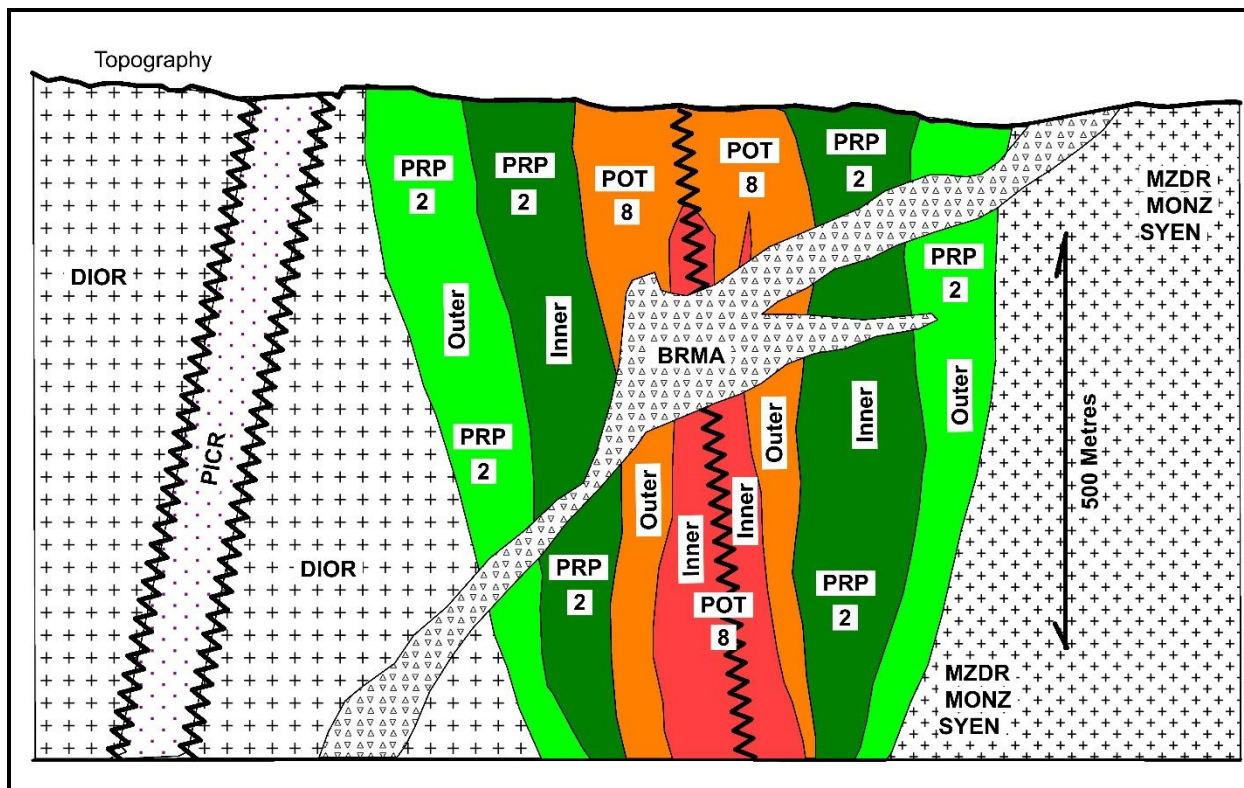


Figure 44. Alteration model for batholith-related, quartz-poor alkaline-diorite porphyry deposits. Quartz poor alkaline porphyry deposits occurs within dioritic (**DIOR**) batholiths commonly near a transition to marginal, more potassium rich granitic rocks (**MZDR** = monzodiorite, **MONZ** = monzonite, **SYEN** = syenite). Ore mineralization is within the central potassic core alteration (**POT = 8 inner**, red-orange, and **POT = 8 outer**, orange). Propylitic alteration (**PRP = 2 inner**, dark green and **PRP = 2 outer**, pale green) tightly surrounds the potassic core without a marked phyllic zone. Commonly spatially related are a) pre- post- or syn-ore mineralization by magmatic magnetite–apatite breccia or dykes (**BRMA**—shown post ore in the figure), and b) picrite (**PICR**, fault bounded grey stipple). Contact metamorphic skarn assemblages can occur where carbonate rocks are in contact with mineralization. Abbreviations: **BRMA** = magnetite-apatite breccia or dyke; **DIOR** = diorite; **MONZ** = monzonite; **MZDR** = monzodiorite; **SYEN** = syenite; **PICR** = picrite, an ultramafic rock; **POT = 8 inner** = potassic alteration of albite, K-feldspar, biotite, chlorite, vein quartz, and bornite greater than chalcopyrite; **POT = 8 outer** = potassic alteration of albite, K-feldspar, biotite, chlorite, vein quartz, chalcopyrite greater than bornite and minor pyrite; **PRP = 2 inner** = propylitic alteration of albite, chlorite, epidote, actinolite, chlorite, carbonate, pyrite, and feldspars with a red-hematite dusting; **PRP = 2 outer** = propylitic alteration of albite, chlorite, epidote, actinolite, chlorite, carbonate, pyrite and feldspars without red-hematite dusting. Zig-zag black lines are faults. The model is modified from Wilson et al. (2003).

Comment on quartz-poor, alkaline-diorite granitic batholith- and stock-related porphyry deposits

Recently recognized depth potential of alkaline porphyry deposits is, in my opinion, related to end-stage, magmatic, hydrous, alkaline, and metalliferous concentrations associated with large igneous bodies (e.g., the Afton porphyry copper deposit is within the Iron Mask batholith in south-central British Columbia, Canada). If the source is the size of a batholith (huge), and if there is a mechanism for concentration, then world-class deposits can be formed.

Be sure you know from this section:

- the differences and similarities between the calcalkaline and alkaline-diorite models,
- the likely significance in the alkaline-diorite model of associated picrite and magnetite-apatite dykes or breccias, and
- why the batholith-related models might be significant with respect to world-class deposits.

MODEL FOR QUARTZ- AND MUSCOVITE-RICH STOCK- AND CUPOLA-RELATED GREISEN PORPHYRY DEPOSITS

In this section you will learn about:

- a model for greisen porphyry deposits, and
- a specific greisen porphyry deposit in Sonora, Mexico.

A model for greisen porphyry deposits, related to highly evolved plutons, is in Figure 45. These are dominantly tin and tungsten deposits, but can be associated with copper, silver, gold, and potentially, uranium and rare earths. The model is somewhat speculative, but in part is after Elliott (1995) and Taylor (1979) with modification based on the Don Luis greisen porphyry tungsten prospect in central Sonora, Mexico (Figures 4 and 46). Geology of this class is generalized because these deposits are variable; however, the cupola aspect and potential porphyry deposit size are important. Greisen zones (Figures 45 and 46) and greisen veins are commonly zoned with ore mineral concentrations at intermediate elevations near the contact of the pluton with country-rock. Commonly associated kaolinite (China clay) is supergene in origin.

Don Luis greisen-porphyry prospect (Figures 4, 46 and 47) in central Sonora, Mexico, has three greisen porphyry zones (West, Central and East), each about 1 km in diameter. The greisen hosts tungsten, silver, and gold mineralization. A geological map of the West Zone is in Figure 46. The greisen-cupola is characterized by a) greisen (yellow), b) brain rock with unidirectional solidification texture (red stars; Figures 17 and 18), and c) outcrops of solid quartz (quartzolite or silexite) and quartz breccia (Figure 19). Muscovite from the greisen was dated by uranium-lead in zircon at 67.7 ± 0.7 Ma (J.K. Mortensen [Pacific Centre for Isotopic and Geochemical Research, The University of British Columbia, Canada] personal communication, 2011), which is Late Cretaceous. Muscovite in the greisen is rich in manganese and, as a result, weathered and supergene altered rocks have abundant, black pyrolusite (Figure 47a).

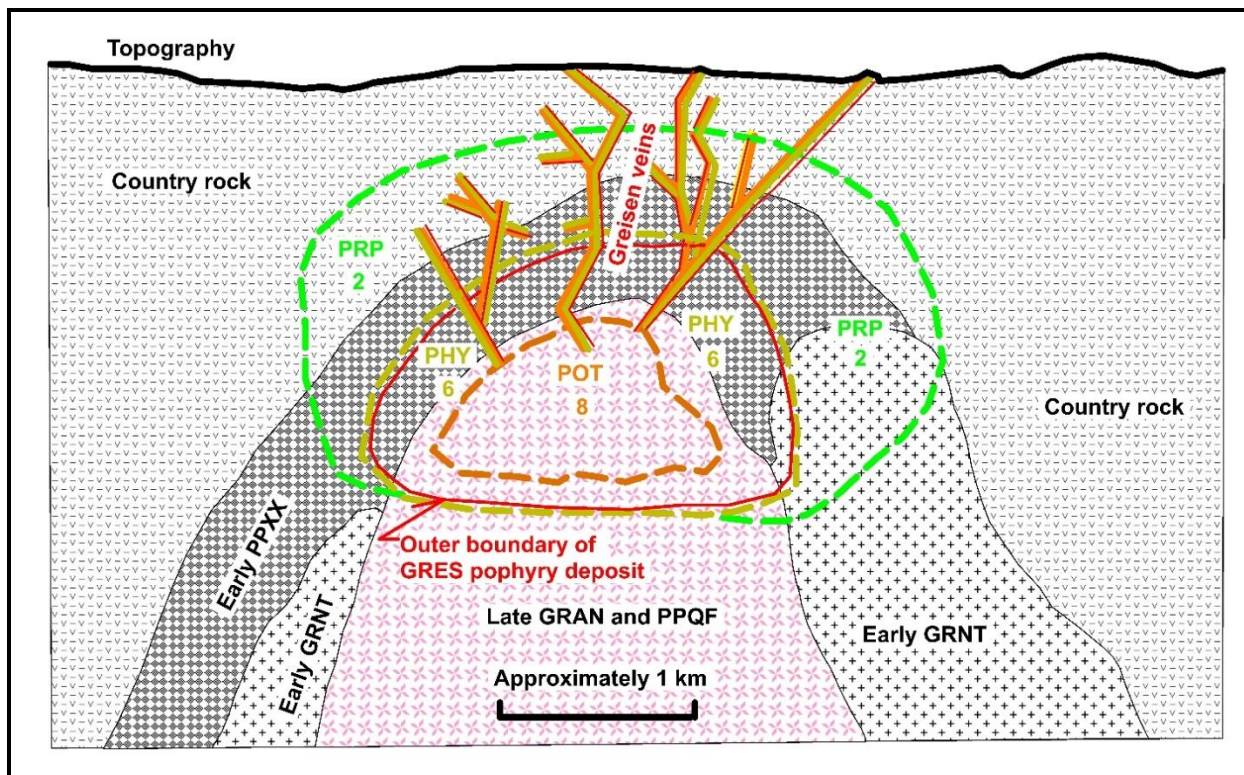


Figure 45. Alteration model for greisen porphyry deposits.

Potassic (**POT = 8**) alteration generally outlines a greisen-porphyry body but can include pegmatitic phases. Silicate minerals are quartz, muscovite, $\pm K$ -feldspar, \pm biotite, \pm albite, \pm tourmaline, \pm fluorite, \pm topaz, \pm beryl, \pm lepidolite. Ore minerals are wolframite, cassiterite, \pm molybdenite, \pm scheelite, \pm native gold and \pm native silver. Phyllic (**PHY = 6**) alteration is dominantly quartz, muscovite, \pm pyrite, \pm sulfosalts, \pm stannite. Propylitic (**PRP = 2**) alteration consists of chlorite, epidote, \pm albite, \pm pyrite, \pm quartz. Abbreviations: **Early GRNT** = granitic intrusion prior to greisen formation. **Early PPXX** = porphyry intrusion prior to greisen formation. **Late GRAN and PPQF** = late-stage granite and/or quartz porphyry with a greisen cupola. Note that the early and late granitic and porphyritic phases comprise a composite stock. **The Outer boundary of GRES porphyry deposit**, marked by a red line, indicates the outer boundary of greisen porphyry deposits. **Greisen veins**, however, are potentially significant and can extend into the **Country-rock**, which are of variable rock types. The model is speculative but follows Elliott (1995) and Taylor (1979).

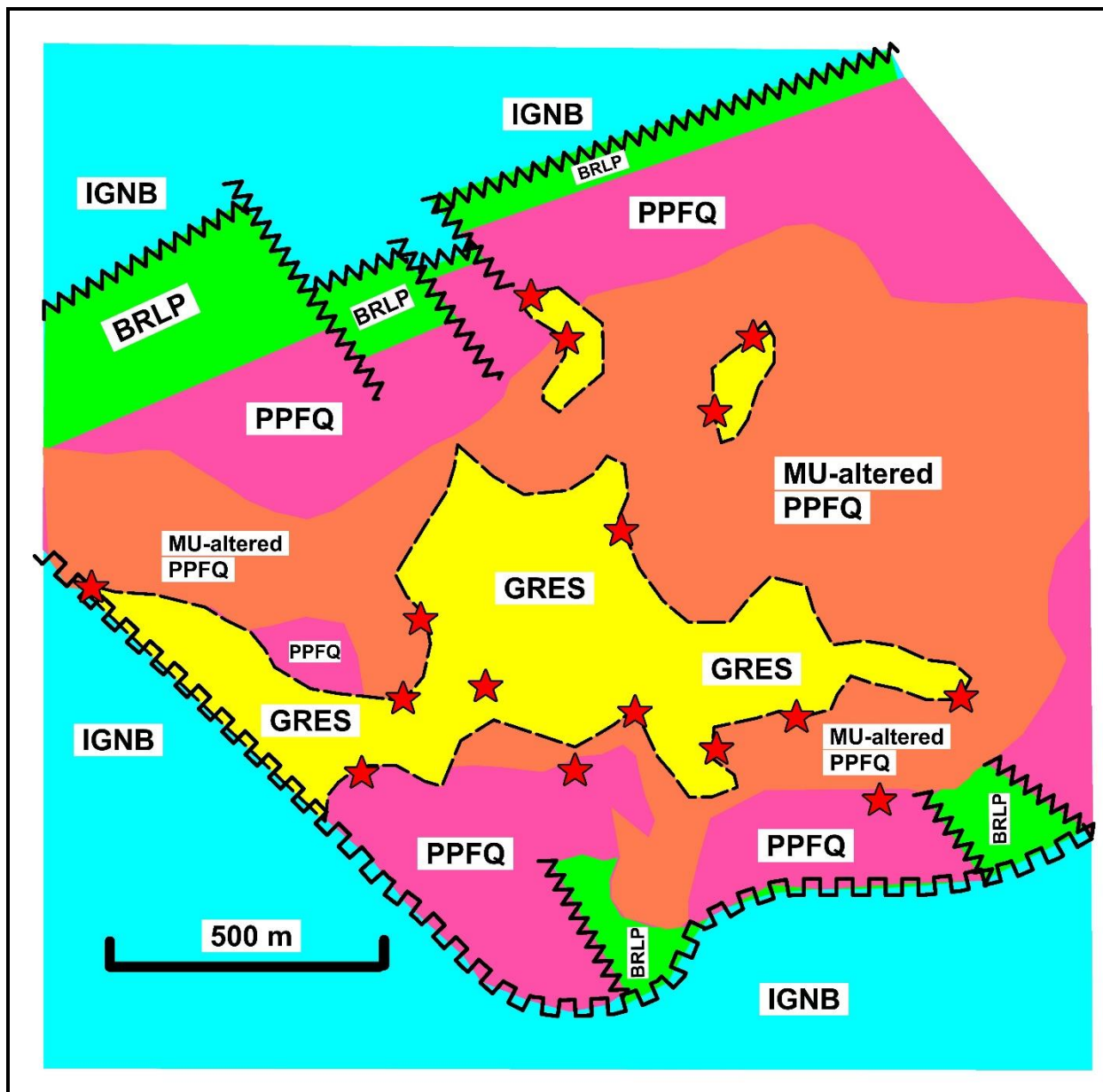


Figure 46. *Geology of the West Zone of the Don Luis tungsten-silver greisen-porphyry deposit in Sonora, Mexico.*

The West Zone is one of three equivalent sized zones on this property. Late Cretaceous units in decreasing age are: **BRLP** = marginal lapilli breccia with a porphyritic matrix, **PPFQ** = Felspar-quartz porphyry, **MU-altered PPFQ** = muscovite altered feldspar-quartz porphyry, and **GRES** = greisen (67.7 ± 0.7 Ma; Figure 47). Red stars mark locations of brain rock with unidirectional solidification texture (Figures 17 and 18). U-zag lines mark a mid-Tertiary (35 to 30 Ma) regional unconformity. **IGNB** is post-unconformity Tertiary ignimbrite. V-zag lines are late faults.



Figure 47. Surface-weathered greisen and fresh greisen in drill core.

Greisen specimens are from the Don Luis tungsten-silver greisen deposit in Sonora, Mexico. a) This weathered surface specimen is dark from a pyrolusite coating because the muscovite is manganese rich. b) Drill core, which is about 6 cm wide, demonstrates that the rock is mainly muscovite with lesser quartz.

Be sure you know from this section about:

→ the stock and cupola-related greisen porphyry deposit type.

COMMENTS ON GOLD-SILVER PORPHYRY DEPOSITS

In this section you will learn about:

→ **the probable category of gold-silver porphyry deposits.**

The model of gold-silver porphyry deposits discussed here is not well established; therefore, a detailed model is not presented. Regardless, the possibility of such deposits is significant, so an exploration geologist needs to keep the possibility of such a model in their evaluation repertoire.

The La Colorada gold deposit (Figure 5) in Sonora, Mexico, is a gold porphyry deposit, in the author's opinion, although it is described as an epithermal deposit. The gold-silver porphyry deposit classification is based mainly on the occurrence in the open pit area of the La Colorada gold mine, where two granodiorite stocks are cut by gold-bearing quartz veins with K-feldspar–biotite envelopes. In addition, fluid inclusions in the quartz veins have high salinity (daughter crystals of sylvanite and halite), as is characteristic of porphyry deposits. Most of the gold-silver mineralization is concentrated in veins and in fault zones, but it also occurs in the impure quartzite host surrounding the intrusions. Although the overall characteristics resemble Carlin-type deposits, the porphyry deposit characteristics of mineralization in the two mineralizing stocks are clear; consequently, the author suggests that La Colorada is a gold-silver porphyry deposit. In addition, it might be a good representation of the style of mineralization found below Carlin-type mineralization.

Be sure you know from this section that:

→ **gold-silver porphyry deposits might provide unique exploration opportunities.**

APPLICATION OF HYPOGENE ALTERATION STUDIES IN PORPHYRY DEPOSITS

In this section you will learn about:

- ➔ **using classic models to locate ore, and**
- ➔ **the identification of, and relationship of, 'pyrite halos' to 'ore shells' and alteration facies.**

Vectors toward likely ore locations are provided by the types and geometries of hypogene alteration. The following points illustrate some applications of field alteration studies:

- The classic discovery using a zoned alteration model was by Lowell (1968) when, from mapping the geometry of mainly phyllic alteration (it was markedly white in core and this was visually apparent without detailed studies), he located the Kalamazoo orebody as a faulted offset from the San Manuel porphyry deposit in Arizona, United States.
- Pyrite halos within the phyllic zone can often simply be identified by an abundance of pyrite or jarositic boxwork in capping. This pyrite halo is also commonly identified by induced polarization (IP) chargeability highs in geophysical surveys. Pyrite halos are within the phyllic zone but near to, or overlapping, the outside border of the ore shell. The ore shell is mainly within the phyllic zone but extends into the core potassic zone. Thus, identification of the location of pyrite concentrations, high IP chargeability anomalies, phyllic and potassic alteration provide vectors to ore shell location.
- Knowing that phyllic alteration zones are on the order of 100 m thick and potassic zones commonly are about 150 m thick, one can estimate appropriate drillhole depths to probe for potential ore. For example, given that one has a defined phyllic alteration zone, and the target is copper in the phyllic zone and molybdenite in the potassic core, one might want holes long enough to penetrate both zones. Assuming probing across true widths, hole lengths could be on the order of 450 m (100 m for the proximal phyllic zone, 250 m for the potassic core and another 100 m for the following phyllic zone). Such an exploratory hole, properly located, would do much to establish overall zoning and identify potential ore locations in the deposit being studied.

Be sure you know from this section:

- ➔ **the relationships between alteration zoning and ore location.**

SUPERGENE ALTERATION AND ENRICHMENT IN PORPHYRY DEPOSITS

In this section you will learn about:

- **supergene alteration and enrichment,**
- **chemical constraints on copper enrichment mineralogy,**
- **capping mineralogy and interpretation,**
- **copper enrichment mineralogy,**
- **single cycle supergene enrichment,**
- **multiple cycle supergene enrichment, and**
- **exotic copper deposits.**

Introduction

Supergene alteration refers to alteration from above (super = above; gene = origin), that is, from downward-weathering processes. Supergene processes modify original hypogene mineralization with new zoning patterns. Consequently, one must recognize this supergene alteration if one is to assess the copper resource potential of a) the original hypogene mineralization and b) underlying supergene copper enrichment. Original sulfides and silicates are altered by supergene events. Supergene clay can be difficult to distinguish from hypogene clay alteration. Spatial distribution of alteration can help to define the origin of clay in some cases (stable isotope data also can be helpful but is not readily applied in the field).

The following describes features of

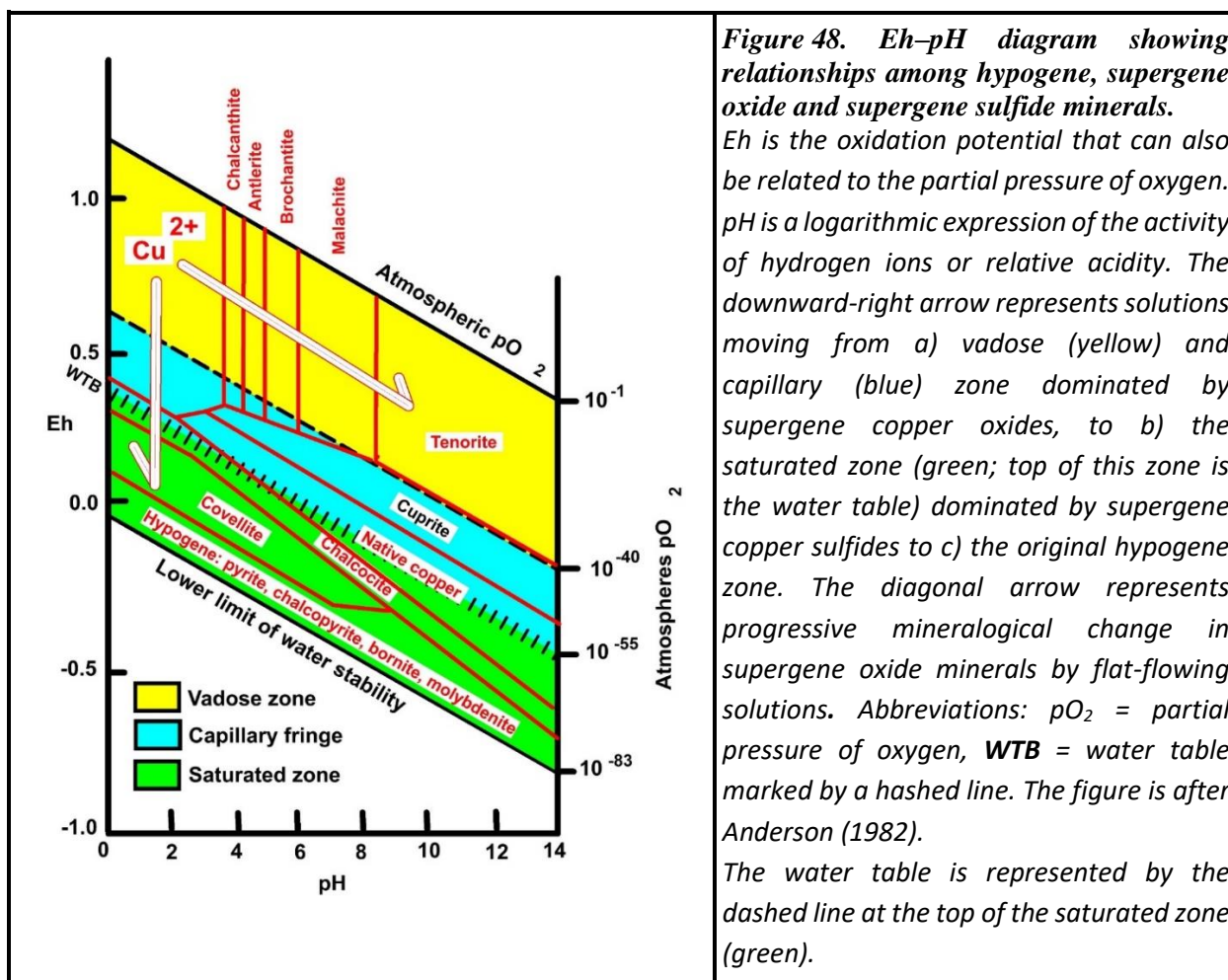
- Chemistry of supergene leaching and enrichment.
- Supergene silicate alteration.
- Supergene capping.
- Supergene copper enrichment.
- Supergene copper enrichment cycles.
- Exotic copper deposits.

Chemistry of Supergene Leaching and Enrichment

Supergene leaching and enrichment in porphyry copper deposits is related to downward percolation of water and chemical changes related to mineral-water interaction and to chemical changes related to a *water table*. The water table marks a switch from overlying oxidation in the *capping zone* to underlying reduction in the *enrichment zone*. If a water table at depth is fixed in position over a long period of time a *single cycle* capping and enrichment zone develops. A fixed position for the water table is, of course, a simplification of what can be complex variations in water table position due to modification of groundwater circulation by faulting, paleo-topographic and climatic events. Thus, *multiple cycle* supergene enrichment can develop. This emphasizes that a geomorphological understanding of landscape

development and climatic changes over time can be critical to the overall interpretation of the supergene processes involved in supergene leaching and enrichment.

Basic chemistry involved in supergene enrichment is shown in the Eh–pH diagram in Figure 48 (after Anderson, 1982). This diagram illustrates fields of copper mineral stability in terms of the activity of electrons (Eh, the oxidation potential related to the partial atmospheric pressure of oxygen [pO_2]) and hydrogen ions (pH, the logarithmic expression of the activity of hydrogen ions or relative acidity). The downward arrow represents solutions moving from a) markedly oxidized in the vadose zone (yellow; unsaturated hydraulic flow of ground water above the water table) to b) less oxidized in the capillary zone (blue; ground water movement by capillary action), to c) reduced in the saturated zone (green; all available spaces are filled with water), the upper contact of which marks the water table (**WTB** = hashed line). The vadose and capillary zones are dominated by copper oxides, and supergene sulfides are precipitated in the saturated zone. The downward-right arrow represents progressive mineralogical changes of copper oxide minerals by flat-flowing solutions in the vadose zone. Malachite and/or azurite are stable within most surface water in temperate zones with a pH of 6 to 7. Antlerite and brochantite are stable in dry desert conditions with surface pH of about 4 to 6. Chalcantinite ('once tasted, never forgotten!') reflects the most acid conditions, around pH 4; consequently, it is a common secondary mineral formed directly on the surface of copper sulfides.



A single stage of leaching and enrichment related to a specific water table position results in the following sequence down the vertical arrow.

1. Oxidation of hypogene sulfides (pyrite, chalcopyrite and bornite) results in sulfuric acid generation and downward movement of the copper generated from the oxidation of copper sulphides.
2. Downwardly percolated mobilized copper is reprecipitated as supergene sulfide copper minerals where chemical conditions change to a reducing environment below the water table in the saturated zone (green). These supergene sulfides are deposited mainly as chalcocite and covellite and commonly replace pre-existing hypogene sulfides like pyrite, chalcopyrite and bornite (see insert on *Micron-thick coatings of chalcocite on pyrite*).
3. Near the water table boundary (**WTB** marked by hashed line at the top of the green saturated zone) native copper and chalcocite can be at equilibrium and often form with fluctuations in the water table level.

Micron-thick coatings of chalcocite on pyrite.

Micron-thick coatings of chalcocite are a common beneficiation problem because in froth flotation the mineral grain looks like a copper sulfide (chalcocite), but the copper concentrate is diluted by the encrusted pyrite. On the other hand, chalcocite replacement of copper sulfides like chalcopyrite or bornite does not cause copper concentrate dilution. The habit of chalcocite is so important that in the companion guide [Godwin, 2020; cf. Figure 50] and Appendix B, codes for chalcocite, which facilitate recording economically significant features, are as follows: **CC** = chalcocite only, **C!** = chalcocite on pyrite—be aware(!) and **C\$** = chalcocite coating replacement on copper sulfide—valuable(\$).

Supergene Silicate Alteration

Supergene silicate alteration is commonly marked by alteration of feldspars to clay (mainly kaolinite) while original quartz remains intact—unless acid conditions are extreme, in which case only quartz might remain. Abundant hypogene quartz in veins or in flooding can encapsulate original, hypogene oxide or sulfide minerals so they are not altered. A good example of this is the useful exercise of breaking open surficial quartz vein outcrops or float to look for remnant pyrite, chalcopyrite and molybdenite (or its alteration to ferrimolybdite) within the quartz.

Supergene Capping

Supergene capping is the surface and near-surface remnants of leached hypogene sulfide or supergene enrichment mineralization, characterized by autogenetic (in place) gossan and limonite (often with a boxwork and colour fingerprint reflecting original hypogene sulfide). *Autogenetic gossan* (Figure 49) is formed from in-place mineralization, distinct from epigenetic (later than underlying rock), *transported or exotic gossan* (see insert *Definitions of autogenetic gossan and epigenetic, transported, or exotic gossan*). The copper mobilized from the capping is generally deposited in an underlying supergene copper enrichment zone but can be transported laterally and deposited as exotic copper deposits.

Interpreting the capping of hypogene mineralization for porphyry deposits with less than 10 volume percent sulfide (mainly pyrite, chalcopyrite, bornite, molybdenite and chalcocite or covellite) is straightforward (cf. Sutopo, 2005). Supergene processes generate acid conditions, based largely on sulfide mineralogy and host rock buffering ability. In the description that follows, a relatively acid-neutral granitic

host is assumed. The key to acid generation often relates to the amount of pyrite present, or the ratio of pyrite to chalcopyrite. The more pyrite, or the higher the pyrite to chalcopyrite ratio is, the more sulfuric acid is generated. Blanchard (1968) describes boxwork details for many minerals, but pyrite is common and the only one that is a cinch to identify because of its cubic or pyritohedral outlines (Figure 49b). Thus, the former presence and amount of pyrite often can be judged, and its abundance can be an effective way to field map the location of the pyrite halo. Some idea of the reactivity of the host rock and acidity of the supergene alteration can be estimated from the limonite mobility with respect to the boxwork. Increased acidity, and/or decreasing reactivity of the gangue host rock, following Blanchard (1968), goes from boxwork a) empty of limonite, b) with outer edges haloed by limonite, c) with outer edges internally rimmed by limonite, and d) filled with limonite. Highly acid environments convert sulfides to a sulfate-limonite (jarosite). Weakly acid environments convert sulfides to the limonite-hydroxide goethite. The corollary of this is that copper is mobile in highly acidic environments, immobile in weakly acidic environments and variably mobile in between environments; that mobility can be estimated by the ratio of jarosite to goethite.

Jarosite is honey yellow, goethite is chocolate brown and earthy hematite is earthy red; the ratios of these minerals can be estimated by the colour of the powdered limonite. Thus, if we know the copper content of the capping, we can estimate the original hypogene grades based on limonite mineralogy. This was the basis of the empirically derived 'Keneco credit card' methodology of capping interpretation that was held secret in the exploration game by the United States-based Kennecott Exploration Company for many years. But the secret is out and detailed in Anderson (1982); TABLE 7, after Anderson (1982), can be used to reconstruct hypogene grade from jarosite-goethite capping. The basics of limonite interpretation follow:

- **All jarosite** indicates the supergene environment was so acid (pyrite boxwork is likely to be found, e.g., Figure 49) that all copper, if present, could have been mobilized. Thus, all one knows is that the hypogene grade is greater than or equal to the copper content in the jarosite capping.
- **All goethite** indicates the supergene environment was neutral in acidity (pyrite boxwork is not likely to be found) so that all copper, if present, would not be mobilized; the hypogene grade is equal to the copper content in the goethite capping.
- **A mixture of jarosite and goethite** indicates that copper, if present, would be partially mobilized; the hypogene grade can be reconstructed with TABLE 7.
- **A mixture of jarosite and earthy hematite** (see section on Multiple Enrichment Cycles) indicates that there was a pre-existing enrichment blanket and a copper rich blanket enriched by multiple supergene leaching might exist below at depth—generally good news!

Definitions of autogenetic gossan and epigenetic, transported, or exotic gossan.

Gossan is composed mainly of limonite with variable copper mineral content. The main iron component of gossan can be transported various distances to precipitate as limonite with variable copper content. As a result, the main types of gossans are **autogenetic** or **epigenetic**, as described below.

Autogenetic gossan (Figure 49) forms where iron is relatively immobile and resulting limonite fills, rims or halos boxwork after pre-existing sulfide at the site of the mineralized zone (copper is variably mobile depending on overall acidity from sulfide dissolution and from the neutralizing properties of the host rock).

Epigenetic gossan, transported gossan or exotic gossan forms in extremely acid environments where iron is mobile and moves large distances—often well beyond the source mineralization—before it is precipitated as limonite on older underlying rock. Copper, generally more mobile than iron in an acid environment, can precipitate beyond the iron gossan as a gossanous cement in gravels to form an *exotic copper deposit*. The Exotica copper mine is a valuable exotic copper deposit (see section on Exotic Copper Deposits), adjacent to and below the Chuquicamata porphyry copper mine in central-northern Chile).

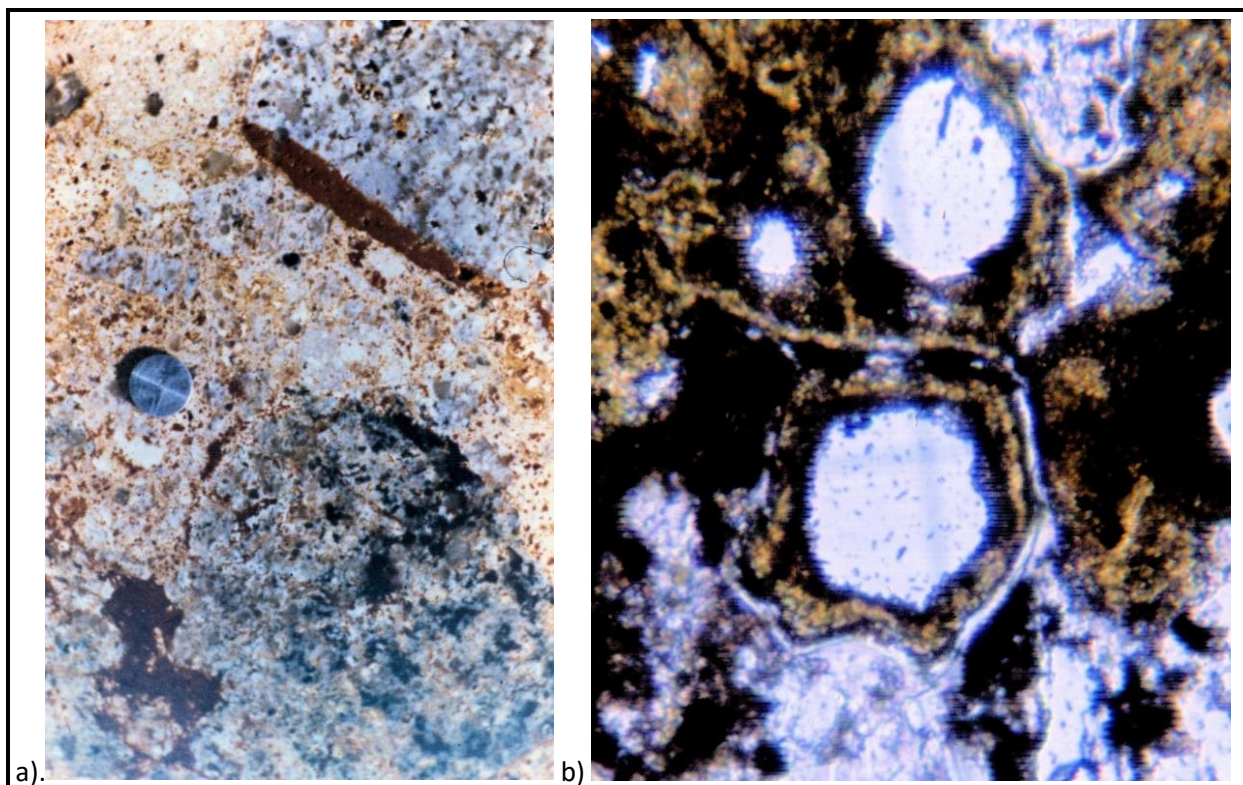


Figure 49. Autogenetic limonite in capping in a) hydrothermal breccia, and b) in thin section from phyllic alteration in a pyrite halo.

a) The wedge shape of the limonite indicates sulfide borders to rotated fragments in hydrothermal breccia. b) The pyritohedral boxwork shapes (about 3 mm in diameter) in the thin section are diagnostic of pyrite and are lined with yellow jarosite, indicating an acid environment, which one would expect given alteration of pyrite (the jarosite centres of the pyrite boxwork were probably removed during thin-section preparation). Both examples are from the Casino deposit, central Yukon, Canada.

TABLE 7. Calculation of minimum hypogene grade from jarosite and goethite percentages in capping generated by a single enrichment cycle.

The table is based on empirical observation that the percentage of goethite equals the percentage of residual copper in capping. Percentages of goethite and jarosite total 100%. Note that if the material is 100% goethite, the grade is equal to the analysis of the capping and if 100% jarosite, the grade is the same as, or undeterminably better than the analysis. This TABLE is after Anderson (1982). Abbreviations: GO = goethite and JA = jarosite.

Measured copper in capping (ppm)	Calculated original copper grade (ppm) based on capping limonite composition (jarosite + goethite)				
	100% JA 0% GO	75% JA 25% GO	50% JA 50% GO	25% JA 75% GO	0% JA 100% GO
2,000	$\geq 2,000$	8,000	4,000	2,670	2,000
1,000	$\geq 1,000$	4,000	2,000	1,330	1,000
500	≥ 500	2,000	1,000	670	500
250	≥ 250	1,000	500	330	250
0	≥ 0	0	0	0	0

Interpretation of autogenetic capping in the field can be carried out using the following process as a guide. At each sample site in the capping, preferably on a grid (say, every 50 m along lines 100 m apart), take about five representative, lemon-sized hand specimens near grid centres and submit them for geochemical analysis of, at least, copper and molybdenum. On these specimens, and/or on field outcrops at the site of sampling, use a 5 cm (2 in.) iron nail to scratch the limonite to a powder (the oxidized surface alteration on the limonite does not represent the colour of the underlying limonite minerals). Rub the powder on your thumb, and/or smear it on a white notebook page and estimate the overall colour and limonite mineral percentages. (You can make up your own triangular diagram with powdered jarosite, goethite and earthy hematite smudged in the three corners of a piece of white felt paper, with a few volume percentages smudged in between.) For jarosite-goethite mixtures, reconstruct the grade from assay results and by referring to TABLE 7. For hematite and jarosite mixtures, the reconstruction is more complicated, but one can refer to nomograms in Anderson (1982) for grade reconstruction based on hematite percentages and assay results. The most interesting possibility when finding earthy hematite in limonite capping is that there is a chance of finding a super-enriched, multi-cyclic chalcocite blanket at depth.

Watch carefully for canary yellow ferrimolybdate, encapsulated hypogene minerals (e.g., pyrite, chalcopyrite and molybdenite) in quartz veins or silica-flooded rock, and check molybdenum content in your analyses. Molybdenum is relatively immobile and can be used in a limited way to reconstruct core grades if you know or can estimate possible copper-molybdenum ratios (see insert *Story of grade reconstruction from capping limonite*).

The nail acid zap test (Godwin, 2020) can be used in the field to check for indications of significant copper. This is an obvious test to do, if black neotocite (cupriferous wad) or other secondary copper minerals (e.g.,

chalcantite) is noted. If malachite and/or azurite are present, the nail test will work, but note that the environment is not likely to be acid enough to substantially leach copper, so your copper assay will closely reflect original grade if it is a hypogene grade or a supergene oxide grade.

Story of grade reconstruction from capping limonite.

The Casino porphyry copper-gold-molybdenum deposit in central Yukon, Canada, has a supergene capping and a copper enrichment zone because the area escaped glaciation. In 1970, while I was visiting the property with the view of studying the deposit for a doctoral thesis, the principal geologist was showing an ex-Kennecott Exploration Corporation geologist around. The idea was that this ex-Kennecott geologist, who was in possession of a 'Kennco credit card' (held secret at that time by Kennecott!), could come up with some tonnage and grade estimates for the deposit based on a capping interpretation. We were reviewing some of the early core that was drilled in some of the better anomalies of the time and I was struck by the fact that this expert was always asking about the copper-molybdenum ratio in drill intersections.

Instructions on how to collect the samples to be sent to him for evaluation were to take about five lemon-sized samples at every 400 foot station along the established grid lines, which was done.

The following year, I mapped the deposit as part of my doctoral thesis. The limonite in the capping, as far as I could tell, was all jarosite. The interpretation from the ex-Kennecott specialist was in, and although I do not remember the figures, his estimates were not particularly exciting and positive. After figuring out the gist of the Kennecott interpretation method on my own, I could not understand how the expert had come up with his estimate. If the limonite in the capping was all jarosite, as I suspected, there was no way the hypogene grades could have been reconstructed from jarosite-goethite systematics (TABLE 7). We will never know for sure; however, I suspect he used the copper-molybdenum ratios in the hypogene zone of the discovery holes, and he then reconstructed the grade from the molybdenum grades in the sample suite collected. The result was low, probably because the molybdenum grades in the discovery holes (located in the deposit core) decreased away from the core, and were not, therefore representative of the deposit overall. In addition, it is known that there can be some leaching of molybdenum from surface rocks.

Supergene Copper Enrichment

Supergene copper enrichment zone underlies the capping and is commonly subdivided into an upper supergene oxide zone and an underlying supergene sulfide zone with common mineralogy as illustrated in Figures 50 and 51. Interrelationships are summarized in Figures 52 and 53, which are generalized cross-section models of supergene alteration of hypogene mineralization in porphyry deposits. Minerals of main interest, from the top and vertically downward, are:

- Supergene oxide (Figures 50 to 53): chalcantite, antlerite, brochantite, chrysocolla, native copper, and malachite and/or azurite.
- Supergene sulfide (Figures 51 to 53): covellite, chalcocite, and chalcocite coatings on copper sulfides and pyrite. And
- Hypogene (Figures 52 and 53): pyrite, chalcopyrite, bornite, and molybdenite (not shown).

The supergene oxide zone, shown in Figures 50-53, is developed by the destruction of the supergene sulfide enrichment blanket following a drop in the water table and continued leaching. Some of the copper oxides formed are soluble, chalcantite being common. Chalcantite in trace and nonvisible

amounts can be detected by its ‘once tasted, never forgotten!’ character because it makes one spit to get rid of the sharp, bitter taste. In addition, on chip boards with rock fragments glued with water-soluble white glue, the glue will turn blue-green—even where there is only trace and essentially invisible amounts of chalcantite—facilitating quick identification of the supergene oxide zone. Identification of supergene oxide can be important because the copper oxides will be lost during sulfide flotation beneficiation. Some oxide copper deposits can be economic, as indicated in the insert: *Story about oxide-copper recovery at Mina Quetena, Atacama Desert, northern Chile.*

Story about oxide-copper recovery at Mina Quetena, Atacama Desert, northern Chile.

Mina Quetena is a supergene oxide deposit that occurs in the dry Atacama Desert in northern Chile, a few kilometres northwest of the world-class Chuquicamata porphyry copper mine. Mina Quetena is a type-locality for many of the soluble minerals found in desert environments that include antlerite, atacamite, brochantite and chalcantite. Because these minerals are all water soluble, the operation at the old mine site in the 1960s consisted of a) irrigation of the old open pit—glory hole with agricultural-type water sprinklers, b) recovery of leachate water from the deeper parts of the old mine workings, c) pumping of the collected copper-rich leachate water over scrap tin (left over from the making of tin cans) in concrete vats, and d) production of native copper sludge that was sun dried for sale (called cement copper—formed by the reduction of copper in solution coupled with oxidation of the iron scrap). Extraction of copper is now commonly based on solvent extraction, electrowinning (SXEW) methods.

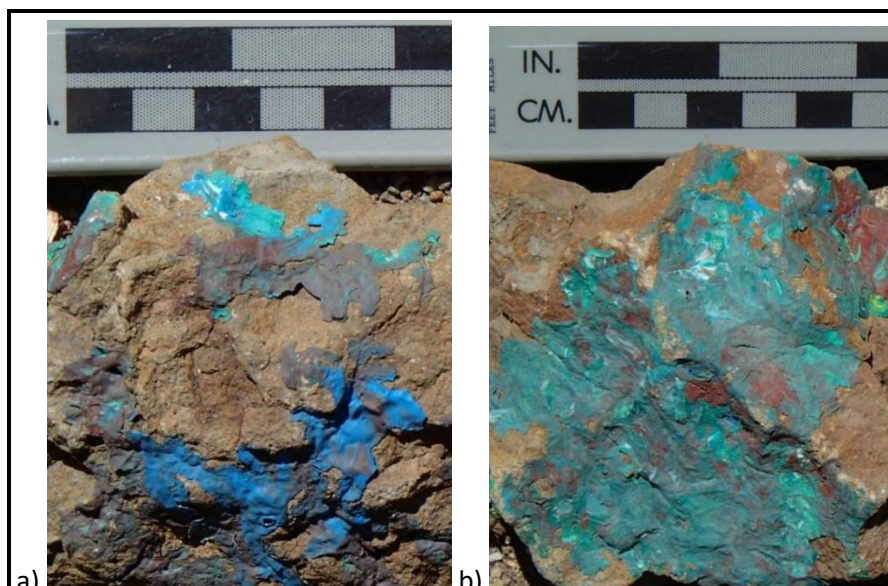
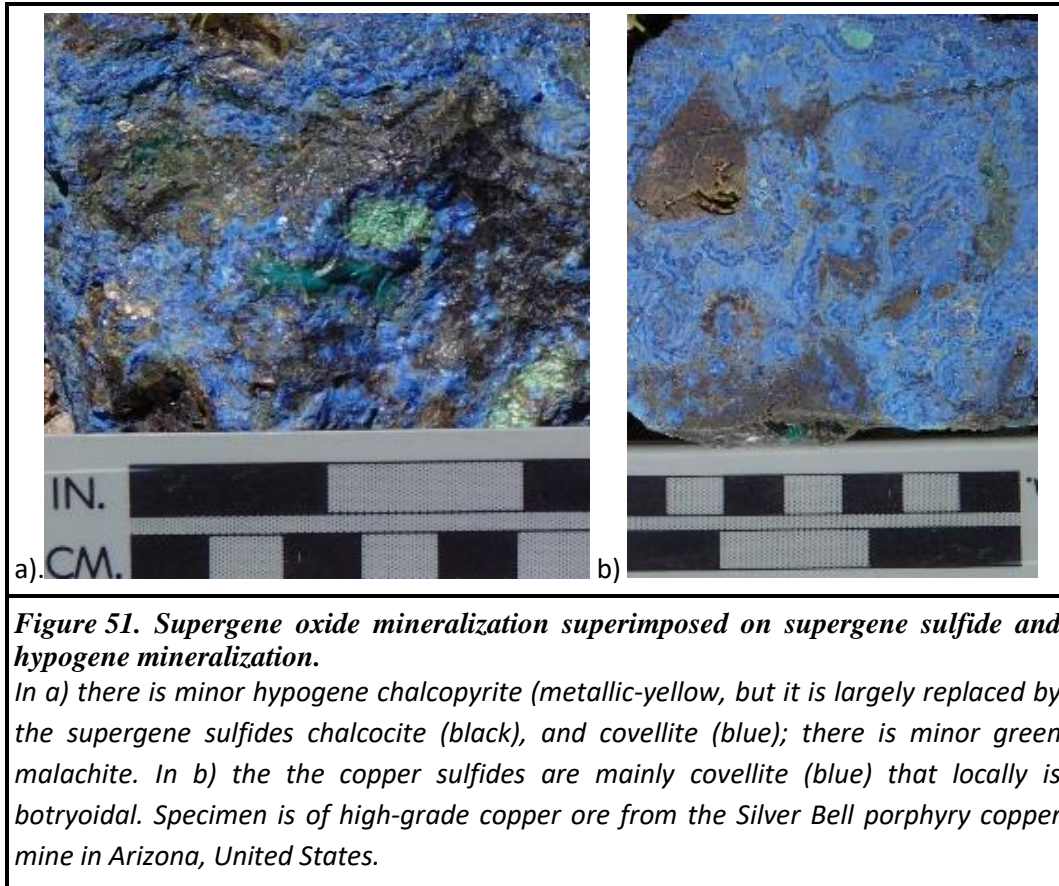


Figure 50. Supergene oxide mineralization with superimposed capping. Minerals are azurite (blue in a), malachite (green in a and b), earthy hematite after chalcocite (reddish brown in b) and limonite (goethite and jarosite; tan in a and b). Source of specimens is unknown.



A generalized model for supergene alteration from porphyry copper hypogene mineralization is in Figure 52 (after Anderson, 1982). Variation in the mineralogy of the original hypogene mineralization results in differences in potential acid generation and available copper. This is reflected in subsequent generations in the depths and mineralogy of the capping and enrichment zones.

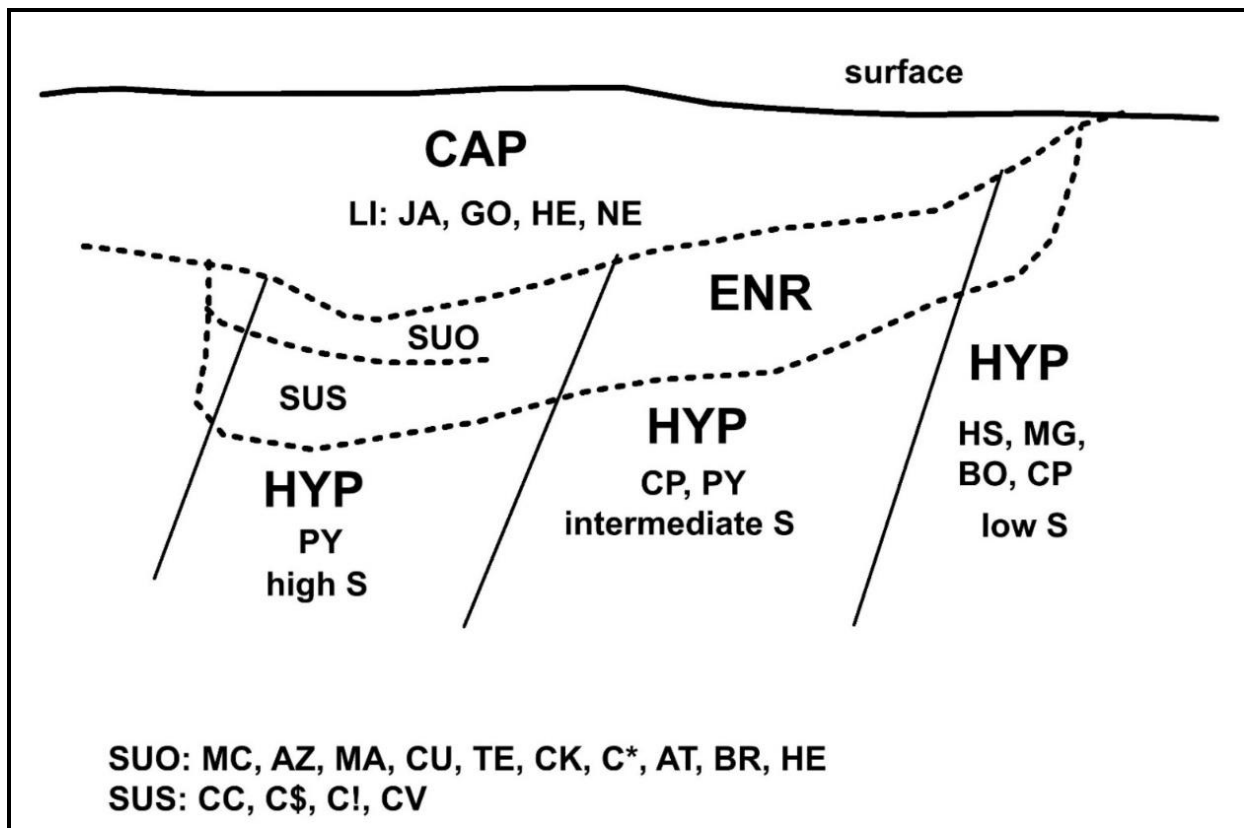


Figure 52. General model for supergene alteration of hypogene mineralization in porphyry deposits. CAP = capping, where: GO = goethite, HE = hematite, earthy, JA = jarosite, LI = limonite and NE = neotocite. ENR = enriched zone. SUO = supergene oxide zone within the enriched zone, where: AT = atacamite, AZ = azurite, BR = brochantite, CK = chrysocolla, CU = cuprite, C* = native copper, MA = malachite and azurite, MC = malachite and TE = tenorite. SUS = supergene sulfide zone within the enriched zone, where: CC = chalcocite, CV = covellite, C\$ = chalcocite replacing copper sulfide, and C! = chalcocite coatings replacing pyrite. HYP = original hypogene zone, where BO = bornite, CP = chalcopyrite, HS = hematite, specular (specularite), MG = magnetite, and PY = pyrite (molybdenite is not shown but would generally concentrate in the low S zone). S = total original sulfur available in hypogene sulfides. Model is after Anderson (1982).

Influence of faulting and variable hypogene mineralization on supergene alteration is apparent in the cross-section (Figure 53) of the El Abra porphyry copper deposit in Chile (modified from Dean et al., 1996). The deposit shows overall similarities to the generalized profile in Figure 52. However, the influence of faulting, which modifies the groundwater table and affects downward water percolation, is clear. Enrichment is also dependent on ratios of pyrite to copper-bearing hypogene sulfide, which is a measure of potential acid generation. The relative reactivity of the host rock can also be significant.

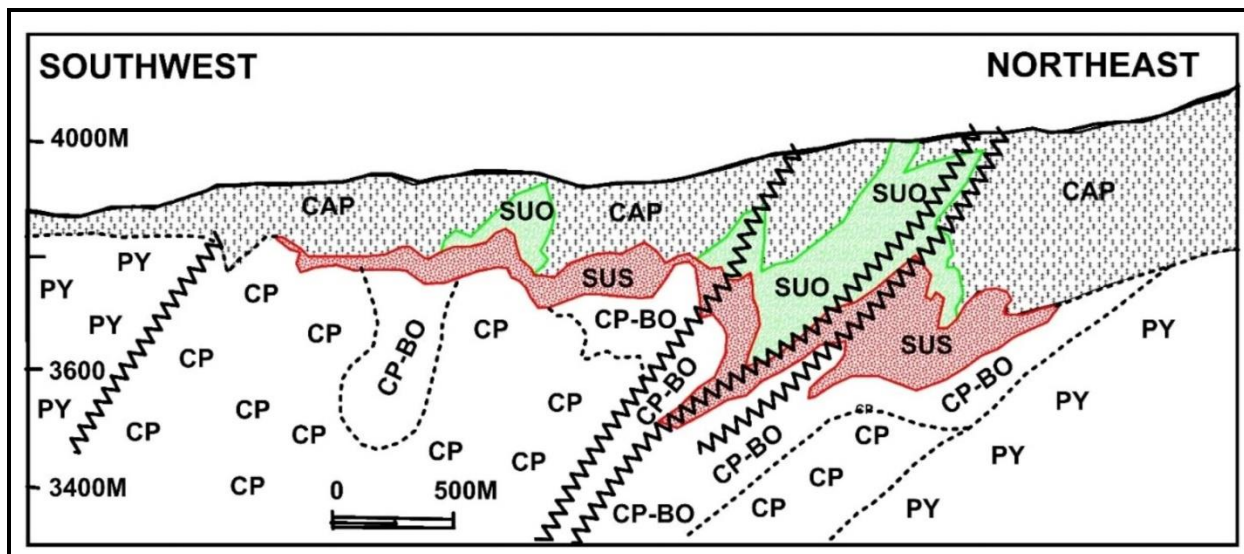


Figure 53. Cross section of the El Abra porphyry copper deposit, Chile, showing influence of faulting and hypogene mineralization on enrichment zones.

Abbreviations: CAP = capping (grey pattern), SUO = supergene oxide (green; chalcocite locally occurs) and SUS = supergene sulfide (red). Minerals in the hypogene are BO = bornite, CP = chalcopyrite and PY = pyrite. Black, zig-zag lines are faults. Black, dashed lines are mineral-type contacts in the hypogene. Model is generalized from Dean et al. (1996).

Supergene Copper Enrichment Cycles

Supergene sulfide zones form below the water table where conditions are reducing. If the water table drops, the supergene sulfide will be destroyed by oxidation, from the top down, to form supergene oxide, which when totally leached to capping will be marked by earthy hematite and jarosite (Figures 54 and 55).

Enrichment of supergene copper in the porphyry copper environment can be:

1. Single cycle copper enrichment (Figures 52, 53, and 54-left and centre), and
2. Two cycle copper enrichment (Figure 54-right)

Single and two cycle copper enrichment cycles in the porphyry copper environment is generalized in Figure 54-right (after Anderson, 1982). Mineralization in Figure 54 follows the chemical constraints for likely minerals defined in Figure 48. Generalized variations for minerals in the hypogene are shown from the centre of the porphyry deposits outward from porphyry deposit centre as: core, ore shell, pyrite halo and propylitic outer zone. Limonite variations in the capping are the result of variable acid-generating capability related mainly to pyrite abundance and to the pyrite to chalcopyrite ratios in the hypogene. Sulfides expected in the hypogene include pyrite, chalcopyrite, bornite and molybdenite. Extent of supergene enrichment is related to total available copper leached from what becomes the overlying capping. Columns from left to right show downward erosion of the topographic surface with the concomitant lowering of the water table. The models in Figure 54 are simplifications of what, of course, can be complex variations in water table position, modification of water table by faulting, tectonic uplift and tilting, paleo-topographic and paleo-climatic events. This also emphasizes that a geomorphological understanding of landscape development over time related to tectonics and climatic conditions can be

critical to understanding and interpreting supergene processes involved in enrichment. At a deposit mapping scale, however, an exploration geologist commonly will initially be faced with exposures of capping.

Single cycle copper enrichment, shown in Figures 54-left and 54-centre, results from a single drop in the water table (**WT1**). Copper originally in porphyry copper hypogene mineralization (**HYP**, no colour) is oxidized and leached to capping (**CAP**, yellow) and deposited in the reduced environment below the water table in the supergene sulfide zone (**SUS**, green). Minerals common to capping are jarosite (**JA**), goethite (**GO**), malachite and/or azurite (**MA**) and ferimolybdate (**FM**). Minerals in the supergene sulfide zone include chalcocite (**CC**, **C₂S**, **C₁**), covellite (**CV**) and native copper (**C***). In the central column a lowering of this water table (for example, to level of **WT2**—a position that is variable but representing a drop from level **WT1**)—results in the oxidation of the top of the supergene sulfide zone to form a supergene oxide zone (**SUO**, blue). Minerals in the supergene oxide zone include chalcantite (**CH**), atacamite (**AT**) and brochantite (**BR**), but cuprite (**CU**) and native copper (**C***) are common as well, as indicated in Figure 48 (blue area of diagram).

Two cycle copper enrichment is shown in the column on the right in Figure 54, a model generalized from Anderson (1982). Extensive erosion of the surface and marked drop to a stable water table to **WT3** results in a second underlying supergene sulfide zone (**SUS**). Capping derived directly from hypogene mineralization has the same mineralogy as in single cycle capping. However, limonite mineralogy of capping derived from supergene enriched zones are prominently marked, as in Figure 55, by earthy-red hematite (**HE**) and jarosite (**JA**). This second-cycle enrichment is super-enriched because the copper from the previously enriched zone has been leached and added to the second supergene enrichment zone.

Enrichment occur at Toquepala in Peru (Figure 55 from Figure 12.15 in Anderson [1982]; reprinting has been approved by the University of Arizona Press). All capping and ore zones in the photo formed in response to acid leaching and/or deposition of copper related to water table positions. The first major enrichment cycle leached copper from hypogene sulfides (now the 'Jarosite capping at the top of the pit) and deposited it as chalcocite in the earthy-red hematite-jarosite zone labeled 'Hematite capping'; the water table at that time was between the upper 'Jarosite capping' and the underlying 'Hematite capping'. The small, isolated patches of 'Hematite capping' mark a second cycle that likely represents chalcocite enrichment, now leached to hematite-jarosite, during pauses in water table descent. The major third cycle formed the enrichment zone labeled 'Chalcocite ore' at the bottom-left of the photo; the top of this zone was the level of the water table when it formed. The amount of copper in the lower blanket or zone marked 'Chalcocite ore' is 'high-grade' due to the sum of copper in the hypogene mineralization at the site of the blanket plus the copper mobilized from all the overlying leached cappings. The water table movements are related, in part, to uplift that includes tilting—as indicated by the inclination in the top surface of the upper 'Hematite capping'. If the top edge of the open pit were a surface being evaluated in initial exploration, note that a) the 'Jarosite capping' could provide information on potential grades of underlying hypogene mineralization, and b) the 'Hematite capping' would indicate that supergene sulfide enrichment had occurred and that a potentially high-grade copper enrichment blanket or zone could exist at depth.

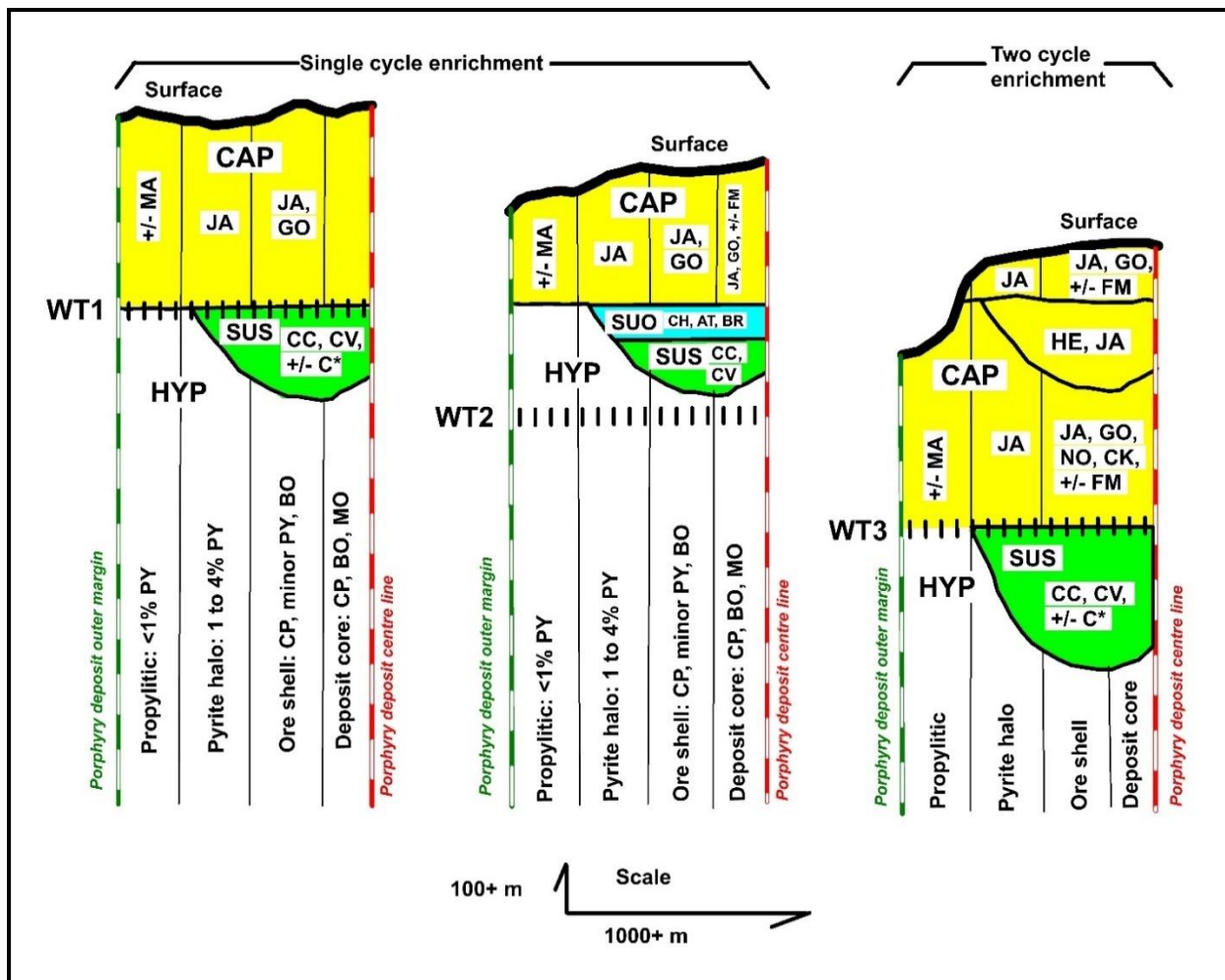


Figure 54. Single and two cycle supergene copper enrichment from hypogene porphyry.

Only half of hypogene alteration zones (**HYP**, no colour), from the core outward (thin solid lines) is shown. Limonite in supergene capping (**CAP**, yellow) varies due to varying acid-generating capability related to pyrite abundance and pyrite to chalcopyrite ratio. Columns (left to right) show downward erosion of the topographic surface and concomitant lowering of the water table. In the left column a fixed position of the water table (**WT1**) results in the development of a supergene sulfide zone (**SUS**, green). In the central column a lowering of this water table (for example, to level of **WT2**) results in the oxidation of the the supergene sulfide zone to form a supergene oxide zone (**SUO**, blue). Two cycle enrichment in the right column shows erosion of the surface and marked drop to a water table at **WT3** forms the supergene sulfide zone (**SUS**, green); this second-cycle enrichment is super-enriched by addition of copper from the previously enriched zone, now part of a cap marked by earthy-red hematite with jarosite. Abbreviations: **CAP** = capping; **HYP** = hypogene; **SUO** = supergene oxide; **SUS** = supergene sulfide; **WT1**, **WT2** and **WT3** = water table times 1, 2 and 3 (vertical hashed line); **AT** = atacamite; **BO** = bornite; **BR** = brochantite; **CC** = chalcocite; **CH** = chalcantinite; **CK** = chrysocolla; **CP** = chalcopyrite; **CU** = cuprite; **CV** = covellite; **C*** = native copper; **FM** = ferrimolybdite; **GO** = goethite; **JA** = jarosite; **MA** = malachite and/or azurite; **MO** = molybdenite; **NO** = neotocite; **PY** = pyrite.

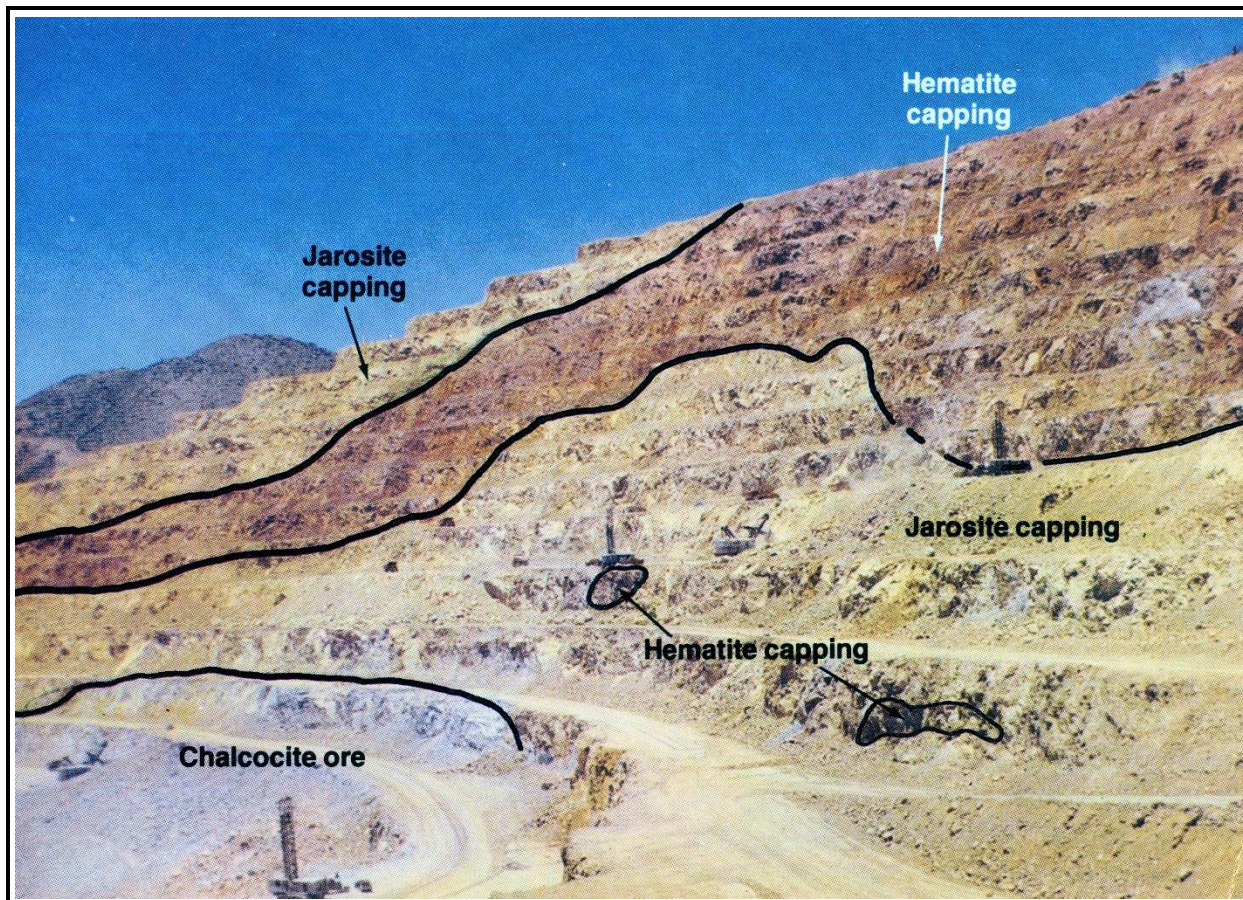


Figure 55. Supergene capping and ore zones at the Toquepala porphyry deposit, southern Peru. All capping and ore zones in the photo formed in response to acid leaching and/or deposition of copper related to water table positions. The first major enrichment cycle leached copper from hypogene sulfides (now the 'Jarosite capping at the top of the pit) and deposited it as chalcocite in the zone labeled 'Hematite capping'; the water table at that time was between the upper 'Jarosite capping' and the underlying 'Hematite capping'. The small, isolated patches of 'Hematite capping' mark a second cycle that likely represents enrichment during pauses in water table descent. A final major cycle formed the enrichment zone labeled 'Chalcocite ore' at the bottom-left of the photo; the top of this zone was the level of the water table when it formed. The amount of copper in the lower blanket marked 'Chalcocite ore' is "high-grade' due to the sum of copper in the hypogene mineralization at the site of the blanket plus all the copper mobilized from all the overlying leached capping. Photo was taken from figure 12.15 in Anderson (1982); reprinting has been approved by the University of Arizona Press.

Exotic Copper Deposits

Exotic deposits, like Exotica (Figure 56) and El Tesoro in the Atacama Desert of northern Chile, form in gravels (often fanglomerates) that have been cemented with soluble copper minerals. These exotic deposits are supergene copper oxide deposits, but were not formed from the destruction of overlying, and pre-existing, hypogene or supergene sulfide mineralization. These deposits were formed from acidic

and cupriferous solutions derived from a distant up-paleo-drainage source. For example, the source of the copper in the Exotica deposit (Figure 56) is near, but topographically down drainage from, the Chuquicamata porphyry copper mine, which is the most likely source of the copper. Interestingly, the source of the exotic copper at El Tesoro has yet to be discovered.

Copper mineralization is commonly chrysocolla. However, copper oxide minerals: chalcantite, antlerite, brochantite, tenorite, malachite, and azurite) are common as defined in the vadose zone of Figure 48 (yellow).

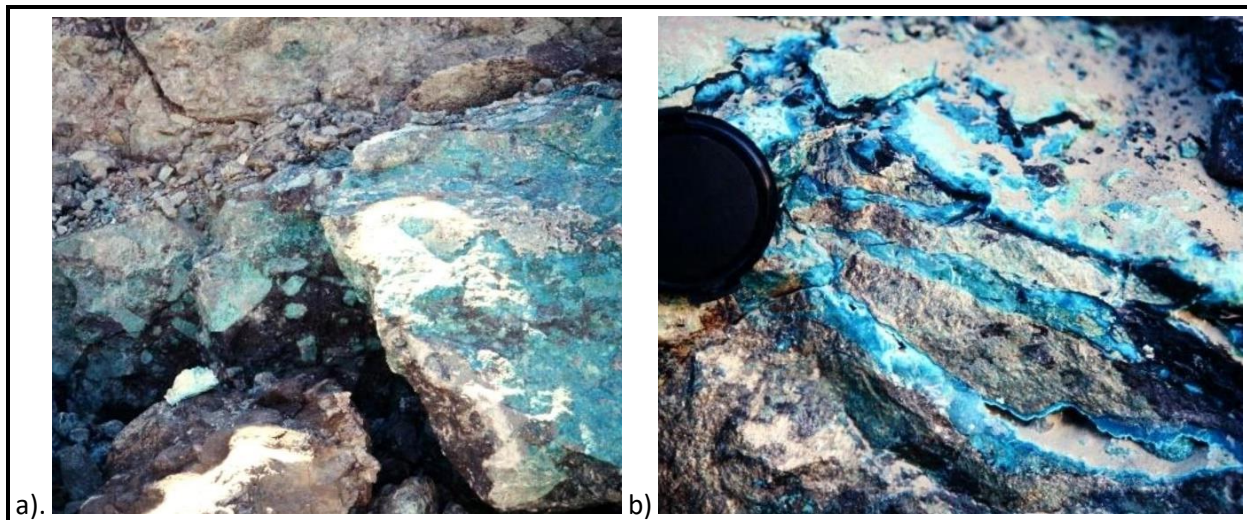


Figure 56. Exotic copper mineralization.

Copper, mainly blue green chrysocolla, cements fanglomerate. Photos are from outcrops (width of a is 4 m and the lens cap diameter in b is 5 cm) in the Exotica open pit mine, near the Chuquicamata porphyry copper deposit, northern Chile.

Know from this section about:

- ➔ supergene alteration and enrichment,
- ➔ chemical constraints on mineralogy and the role of the water table,
- ➔ capping mineralogy and interpretation,
- ➔ models of single cycle enrichment,
- ➔ multiple supergene enrichment cycles, and
- ➔ exotic copper deposits.

SUMMARY AND CONCLUSIONS ON PORPHYRY DEPOSITS

In this section you will review how:

- porphyry deposits can be grouped,
- hypogene alteration is described,
- supergene alteration is interpreted, and
- alteration studies can be guides to ore locations.

General Summary

This guide, in conjunction with the companion book *Porphyry and Epithermal Deposits: Mineralization, Alteration and Logging* (Godwin, 2020), provides a practical framework for understanding, describing, mapping, and interpreting the geology and alteration of porphyry deposits. Key characteristics of relevant features and generalized models are emphasized. In addition, genetic concepts are introduced to provide some logic to the origin of, and relationships among, relevant features. Together, these two books provide the background necessary to a) complete field mapping, b) evaluate preliminary exploration data, c) define vectors to ore zones and d) understand and evaluate detailed descriptions of deposits made by others. With respect to field observations, it is unfortunately difficult to observe something if you a) are not specifically looking for it, b) do not know what you are looking for and/or c) do not know why you are looking for it. That is why the models presented here are powerful; they define features that will direct your attention and observations in the field so that you will look for and identify relevant features quickly. Most aspects of the geology of porphyry deposits and the systematics of hypogene and supergene alteration in porphyry deposits described in this guide are summarized below.

Geology Summary

Division of porphyry deposits in this guide is based on related pluton morphology, and on the type of causative igneous pluton and related ore-metal mineralization. Related pluton morphology is either large-scale batholithic or smaller stocks, cupolas and/or dykes—either confined to the intrusive rocks or extending into surrounding rocks, often volcanic or batholithic. Causative igneous plutons are calcalkaline, alkaline and, as is generally the case in greisen porphyry deposits, S- or A-type granitic rocks. Related ore mineralization is most commonly copper, copper-gold-silver, copper-molybdenum, molybdenum, tungsten, or gold-silver.

Porphyritic rocks are central to most porphyry deposits, as the name of this deposit type suggests. Porphyritic rocks can be related to ground preparation fracturing, exsolving mineralizing hydrothermal fluids and generation of hydrothermal breccia.

Hydrothermal breccia is also a key to porphyry deposits. Breccia can be formed from hydrothermal pressures built up from temperature increases due to phenocryst development in porphyritic rocks. They also can form from tapping or explosion of immiscible hydrous magma or crystal mush concentrations of tourmalinite and magnetite-apatite in vacuoles within crystallizing plutons.

Hydrothermal Alteration Summary

Classic hydrothermal alteration zoning in porphyry deposits has been generalized with a T versus mKCl/mHCl plot, and a diffusion and infiltration model. Alteration facies have been identified with predictable habits of occurrence and mineral assemblages. Ore mineralization occurs in specific locations within these models of alteration facies distribution—and therein lies the ore-vector importance of these models.

Distinct models for different types of porphyry deposits have been described. These models are based mainly on hypogene mineralization. This hypogene mineralization can, of course, be modified by later supergene alteration.

Supergene Alteration and Enrichment Summary

Supergene alteration and enrichment results mainly from surface-water–generating sulfuric acid from sulfides. The generated acid leaches the hypogene or supergene sulfide mineralization, leaving behind thumbprint limonite. Topography, permeability, and fluctuations in the water table are important factors in supergene enrichment, where copper can form high-grade enrichment blankets of ore. Common supergene divisions in porphyry deposits are surface weathering, capping, and enrichment. Enrichment can commonly be divided into supergene oxide and supergene sulfide zones. Capping interpretation from different colours of limonite species can aid in interpreting the history of leaching and enrichment, and the potential value and characteristics of underlying supergene enrichment and hypogene mineralization.

Conclusions Regarding Porphyry Deposit Models

The framework simplification of the geology and alteration of porphyry deposits presented in this guide, in conjunction with the book *Porphyry and Epithermal Deposits: Mineralization, Alteration and Logging* (Godwin, 2020), does not address many important reviews and details that are published in the extensive literature noted at the beginning of this guide; however, it should provide focus and a framework for understanding research, field examinations, and exploration and development related to porphyry deposits.

Some geology/alteration models presented are revised from historical ones. Some new models, or modifications to existing models, are speculative and reflect biases arrived at from the author's fieldwork. Some of these will stimulate interest, application, and debate. For example, the batholithic differentiation model, and the emphasis on tourmalinite and magnetite-apatite magmatic dykes and breccia, are most certainly controversial.

Keep in mind features that are labelled *index fossils*. They are clues to important features and are not familiar to many geologists. Four major index fossils that have been introduced for porphyry deposits are:

- abyssal faults, which are index fossils for multiple and aligned porphyry deposits,
- shatter cleavage, which is an index fossil for breccia bodies,
- unidirectional solidification texture [**UST**] in brain rock, and quartz blobs, which indicate potentially hydrous-rich and metalliferous intrusive rocks, and
- gusano habit or texture in epithermal lithocaps, which can signal potential porphyry deposits at depth.

You now might attempt the challenge of answering the true-false questions in Appendix C. I hope that you enjoyed this guide, or at least found it useful. May it help you find the big one!

Know from this section that:

- ➔ **this guide is only a start to, and framework for, continuing and fascinating study,**
- ➔ **there are key structural and igneous associations with porphyry deposits,**
- ➔ **there are systematic ways of describing mineralization habits,**
- ➔ **there are index fossils of key significance to porphyry deposits,**
- ➔ **facies of hypogene alteration are effective vectors to ore locations, and**
- ➔ **there are ways of interpreting and judging the significance of supergene alteration.**

REFERENCES

- Ager, C.A., W.J. McMillan, and T.J. Ulrych, 1972: Gravity, Magnetism and Geology of the Guichon Creek Batholith. British Columbia Department of Mines and Petroleum Resources, Bulletin 62, 17p., maps.
- Anderson, J.A., 1982: Characteristics of Leached Capping and Techniques of Appraisal. *In* S.R. Titley, *ed.*, *Advances in geology of the porphyry copper deposits, southwestern North America*. Tucson: University of Arizona Press, p. 275-295.
- Badham, J.P.N. and R.D. Morton, 1976: Magnetite-Apatite Intrusions and Calc-Alkaline Magmatism, Camsell River, N.W.T. *Canadian Journal of Earth Sciences*, Vol. 13, No. 2, p. 348-354.
- Bamford, R.W., 1972. The Mount Fubilan (OK Tedi) Porphyry Copper Deposit, Territory of Papua and New Guinea; *Economic Geology*, Vol. 67, p. 1019-1033.
- Bean, R.E. and S.R. Titley, 1981: Porphyry Copper Deposits, Part II, Hydrothermal Alteration and Mineralization, *In* Brian J. Skinner, *ed.*, *Economic Geology Anniversary Volume 1905 – 1980*, p. 235-269.
- Blanchard, Roland, 1968: Interpretation of Leached Outcrops. Bulletin 66, Mackay School of Mines, University of Nevada, 196p.
- Blanchet, P.H. and C.I. Godwin, 1972: Geology System for Computer and Manual Analysis of Geologic Data from Porphyry and Other Deposits. *Economic Geology*, Vol. 67, p. 796-813.
- Bryant, D.G., 1968: Intrusive Breccias Associated with Ore, Warren (Bisbee) Mining district, Arizona. *Economic Geology*, Vol. 63, p. 1-12.
- Bryner, Leonid, 1968: Proposed Terminology for Hydrothermal Breccias and Conglomerates. *Economic Geology*, Vol. 63, p. 692.
- Burnham, C.W., 1979: Magma and Hydrothermal Fluids at the Magmatic Stage. *In* Barnes, H.L., *ed.*, *Geochemistry of Hydrothermal Ore Deposits*, 2nd edition: Miley Interscience, New York, p. 71-136.
- Burnham, C. Wayne, 1979. Magmas and Hydrothermal Fluids. *In* *Geochemistry of Hydrothermal Ore Deposits*, Second Edition, *ed.* Hubert Lloyd Barnes, p. 173-235.
- Butler, B.S., and H.S. Gale, 1912: Alunite—A Newly Discovered Deposit near Marysvale, Utah. U.S. Geological Survey Bulletin 511, 64p.
- Candela, P. A., 1989: Felsic magmas, volatiles, and metallogenesis. *In* *Ore Deposition Associated with Magmas*. *Reviews in Economic Geology*, eds. J.A. Whitney and Naldrett, A. J., p. 223–233.
- Candela, Philip A., and Philip M. Piccoli, 2005: Magmatic Processes in the Development of Porphyry-Type Ore Systems; *in* Mark D. Hannington (ed.), *Economic Geology, One Hundredth Anniversary Volume, 1905-2005*; p.25-38.

- Cann, R.M. and C.I. Godwin, 1983: Genesis of Magmatic Magnetite-Apatite Lodes, Iron Mask Batholith, South-Central British Columbia (921). In British Columbia Geological Survey, Geological Field work 1982, p. 268-284.
- Cargill, D.G., J. Lamb, M.J. Young and E.S. Rugg, 1976: Island Copper. *In* Porphyry Deposits of the Canadian Cordillera, Canadian Institute of Mining and Metallurgy, Special Volume 15, ed. A. Sutherland Brown, p. 206-218.
- Carmichael, I.S.E., F.J. Turner, and J. Verhoogen, 1974: *Igneous Petrology*; McGraw Hill, 739p.
- Carter, L.C., Williamson, B.J., Tapster, S.R., Costa, C., Grime, G.W., and Rollinson, G.K., 2021: Crystal mush dykes as conduits for mineralising fluids in the Yerington porphyry copper district, Nevada; *Commun Earth Environ* v. 2, no. 59. <https://doi.org/10.1038/s43247-021-00128-4>.
- Cerny, Petr, Philip L. Blevin, Michel Cuney, and David London, 2005: Granite-Related Ore Deposits. *In* Mark D. Hannington, ed., *Economic Geology, One Hundredth Anniversary Volume, 1905-2005*; p.337-370.
- Chappell, B.J. and White, A.J.R., 1974: Two Contrasting Granite Types. *Pacific Geology*, Vol. 8, p.173-174.
- Chappell, B.W. and A.J.R. White, 1992: I-and S-Type Granites in the Lachlan Fold Belt. *Transactions of the Royal Society of Edinburgh, Earth Sciences*, Vol. 83, p. 1-26.
- Chiaradia, M. (2020): Gold endowments of porphyry deposits controlled by precipitation efficiency; *Nature Communications*, v. 11, Article number 248. <https://www.nature.com/articles/s41467-019-14113-1.pdf> <https://doi.org/10.1038/s41467-019-14113-1>
- Cox, D.P. (1986): Descriptive model of porphyry copper; in *Mineral Deposit Models*, US Geological Survey, Bulletin 1693, p. 76–79.
- D'Angelo, Michael, Miguel Alfaro, Peter Hollings, Kevin Byrne, Stephen Piercey, and Robert A. Creaser, 2017: Petrogenesis and Magmatic Evolution of the Guichon Creek Batholith: Highland Valley Porphyry Cu + (Mo) District, South-Central British Columbia. *Economic Geology*, Vol. 112, p. 1857-1888.
- Dean, D.A., R.E. Graichen, L.E. Barrett, and W.D. Burton, 1996: El Abra Porphyry Copper Deposit. *In* S.M. Green, and E. Struhsacker, eds., *Geology and Ore Deposits of the American Cordillera: Geological Society of Nevada Field Trip Guidebook Compendium*, 1995, p. 457–464.
- Dilles, John H. and Francisco Camus, eds., 2001: *Economic Geology, A Special Issue Devoted to Porphyry Copper Deposits of Northern Chile*, Vol. 96, No. 2, p. 233-420.
- Drummond, A.D., and E.T. Kimura, 1969: Hydrothermal Alteration at Endako—A Comparison to Experimental Studies. *Canadian Institute of Mining, Bulletin*, Vol. 62, p. 709-714.
- Einaudi, Marco T., 1982: Description of Skarns Associated with Porphyry Copper Plutons, Southwestern North America. *In* Spencer R. Titley (ed.), *Advances in Geology of the Porphyry Copper Deposits, Southwestern North America*, p. 139-209.

- Elliott, James F., Robert J. Kamilli, William R. Miller, and K. Eric Livo, 1995: Vein and Greisen Sn and W Deposits. United States Geological Survey. Pfr. 95-0831, Chapter 9, p. 62-69.
- Erdenebayar, Jamsran, Takeyuki Ogata, Akiri Imai, and Jargalan Sereenen, 2014: Textural and Chemical Evolution of Unidirectional Solidification Textures in Highly Differentiated Granitic Rocks at Kharaatyagaan, Central Mongolia. *Resource Geology*, Vol. 64, pp. 283-300.
- Esmailiy, Dariush, Saeid Zakizadeh, Fatemeh Sepidbar, Ali Kanaanian, and Shojaaddin Niroomand, 2016: The Shaytor Apatite-Magnetite Deposit in the Kashmar-Kerman Tectonic Zone (Central Iran): A Kiruna-Type Iron Deposit. *Open Journal of Geology*, Vol. 6, pp. 895-910.
- Godwin, Colin I., 1973: Shock Brecciation, an Unrecognized Mechanism for Breccia Formation in the Porphyry Environment? *Proceedings of the Geological Association of Canada*, Vol. 21, p. 9-12.
- Godwin, Colin Inglis, 1975: Geology of Casino Porphyry Copper-Molybdenum Deposit, Dawson Range, Y.T. Unpublished PhD Thesis, University of British Columbia, 245p.
- Godwin, Colin I., 1976. Casino. *In* *Porphyry Deposits of the Canadian Cordillera*, Canadian Institute of Mining and Metallurgy, Special Volume 15, A. Sutherland Brown, *ed.*, p. 344-354.
- Godwin, Colin I., 2020. *Porphyry and Epithermal Deposits: Mineralization, Alteration and Logging*. Vancouver, BC, Canada: Mineral Deposit Research Unit, The University of British Columbia, and the Mineral Deposits Division, Geological Association of Canada, 254 p.
- Gustafson, L.B., and J.B. Hunt, 1975: The Porphyry Copper Deposit at El Salvador, Chile. *Economic Geology*, Vol. 70, p. 857-912.
- Halley, Scott and Tosdal, Richard M., 2015: Footprints: Hydrothermal Alteration and Geochemical Dispersion Around Porphyry Copper Deposits. *SEG Newsletter*, January.
- Hedenquist, J.W., and J.B. Lowenstern, 1994: The Role of Magmas in the Formation of Hydrothermal Ore Deposits. *Nature*, Vol. 370, p. 519-527.
- Hedenquist, Jeffrey W., Michael Harris, and Francisco Camus (*eds.*), 2012: *Geology and Genesis of Major Copper Deposits and Districts of the World, a Tribute to Richard H. Sillitoe*. Special Publication Number 16, Society of Economic Geologists, Inc., 618p.
- Hitzman, M.W., N. Oreskes, and M.T. Einaudi, 1992. Geological Characteristics and Tectonic Setting of Proterozoic Iron-Oxide (Cu-U-Au-REE) Deposits. *Precambrian Research*, Vol. 58, p. 241-287.
- Hollister, Victor F., 1978: *Geology of the Porphyry Copper Deposits of the Western Hemisphere*. Society of Mining Engineers of The American Institute of Mining, Metallurgical, and Petroleum Engineers, Inc., 219p.
- Howell, F.H., and J.S. Malloy, 1960: *Geology of the Braden orebody, Chile, South America*. *Economic Geology*, Vol. 55, p. 863-905.

- Kirkham, R.V., and K.P.E. Dunne, 2000: World Distribution of Porphyry, Porphyry-Associated Skarn, and Bulk-Tonnage Epithermal Deposits and Occurrences. Geological Survey of Canada, Open File 3792a, 26p.
- Kirkham, R.V., and W.D. Sinclair, 1988. Comb Quartz Layers in Felsic Intrusions and their Relationship to the Origin of Porphyry Deposits. *In* R.P. Taylor and D.F. Strong (eds.), Recent Advances in the Geology of Granite-Related Mineral Deposits; The Canadian Institute of Mining and Metallurgy, Special Volume 39, p. 50-71.
- Kirwin, D.J. (2005): Unidirectional solidification textures associated with intrusion-related Mongolian mineral deposits; in R. Seltmann, O. Gerel and D.J. Kirwin (eds.), Geodynamics and Metallogeny of Mongolia with a Special Emphasis on Copper and Gold Deposits; SEG-IAGOD Field Trip, 14–16 August 2005, 8th Biennial SGA Meeting, IAGOD Guidebook Series 11: CERCAMS/NHM London, p. 63–84.
- Korzinski, D.S., 1970: Theory of Metasomatic Zoning. Oxford.
- Locke, Augustus, 1926: The Formation of Certain Ore Bodies by Mineralization Stopping. *Economic Geology*, Vol. 21, p. 488-508.
- Lovering, T.S., 1949: Rock Alteration as a Guide to Ore—East Tintic District, Utah. Monograph 1, *Economic Geology*, 64p.
- Lowell, J.D., 1968: Geology of the Kalamazoo orebody, San Manuel District, Arizona. *Economic Geology*, Vol. 63, p. 645-654.
- Lowell, J.D. and J.M. Guilbert, 1970: Lateral and Vertical Alteration-Mineralization Zoning in Porphyry Copper Deposits. *Economic Geology*, Vol. 65, p. 373-408.
- McMillan, W.J., 1976. Geology and Genesis of the Highland Valley Ore Deposits and the Guichon Creek Batholith. *In* Porphyry Deposits of the Canadian Cordillera, Canadian Institute of Mining and Metallurgy, Special Volume 15, ed. A. Sutherland Brown, p. 85-104.
- Meyer, C. and J.J. Hemley, 1967: Wallrock Alteration. *In*: Geochemistry of Hydrothermal Deposits, Ed. Hubert L. Barnes, p.166-235.
- Moore, W.J., M.A. Lanphere, and J.D. Obradovich, 1968: Chronology of Intrusion, Volcanism, and Ore Deposition at Bingham, Utah. *Economic Geology*, Vol. 63, p. 612-621.
- Nakouzi, Elias, and Oliver Steinbock, 2016: Self-Organization in Precipitation Reactions Far from the Equilibrium; *Science Advances*, Vol. 2, e10601144.
- Nash, J. Thomas, 1976: Fluid-Inclusion Petrology—Data from Porphyry Copper Deposits and Applications to Exploration. United States Geological Survey Professional Paper 907-D, D16p.
- Noble, Donald C., César E. Vidale, Miguel Miranda, Walter Amaya A., and John K. McCormack, 2010: Ovoidal- and Mottled-Textured Rock and Associated Silica Veinlets and Their Formation by High-Temperature Outgassing of Subjacent Magmas. *In* Great Basin Evolution and Metallogeny, Volume II, Roger Steininger and Bill Pennell, ed., p. 795 – 811.

- Norton, Denis L., and Lawrence M. Cathles, 1973: Breccia Pipes, Products of Exsolved Vapor from Magmas. *Economic Geology*, Vol. 68, p. 540-546.
- Perrelló, J.A., J.A. Fleming, K.P. O'Kane, P.D. Burt, G.A. Clark, M.D. Himes and A.T. Reeves, 1995: Porphyry Copper-Gold-Molybdenum Deposits in the Island Copper Cluster, Northern Vancouver Island, British Columbia. *In* *Porphyry Deposits of the Northwestern Cordillera of North America*, T.G. Schroeter, *ed.*, p. 214-238.
- Philpotts, A.R., 1967: Origin of Certain Iron-Titanium Oxide and Apatite Rocks. *Economic Geology*, Vol. 62, p. 303-315.
- Reid, Mark H., 1997: Hydrothermal Alteration and its Relationship to Ore Fluid Composition. *In*: *Geochemistry of Hydrothermal Ore Deposits*, Third Edition. Hubert L. Barnes, *ed.*, p. 303-365.
- Rose, Arthur W., and Donald M. Burt, 1979. Hydrothermal Alteration. *In* *Geochemistry of Hydrothermal Ore Deposits*, Second Edition, Hubert Lloyd Barnes, *ed.*, p. 173-235.
- Ross, K.V., C.I. Godwin, L. Bond, and K.M. Dawson. 1995: Geology, Alteration and Mineralization of the Ajax East and Ajax West Copper-Gold Alkalic Porphyry Deposits, Southern Iron Mask Batholith, Kamloops, British Columbia. *In* *Porphyry Deposits of the Northwestern Cordillera of North America*, T.G. Schroeter, *ed.*; Special Volume 46; Canadian Institute of Mining, Metallurgy and Petroleum, p. 565-608.
- Schroeter, T.G., *ed.*, 1995: *Porphyry Deposits of the Northwestern Cordillera of North America*. Canadian Institute of Mining, Metallurgy and Petroleum, Special Volume 46, 888p.
- Seedorff, Eric, John. H. Dilles, John M. Proffett, Jr., Marco T. Einaudi, Lukas Zurcher, William J.A. Stavast, David A. Johnson, and Mark D. Barton, 2005: Porphyry Deposits: Characteristics and Origin of Hypogene Features. *In* Mark D. Hannington, *ed.*, *Economic Geology*, One Hundredth Anniversary Volume, 1905-2005; p.351-298.
- Shannon, J.R., B.M. Walker, R.B. Carten, and E.P. Geraghty, 1982: Unidirectional Solidification Textures and their Significance in Determining Relative Ages of Intrusions at the Henderson Mine, Colorado; *Geology*, Vol. 19, p. 293-297.
- Sharman, E.R., J.R. Lang and J.B. Chapman, editors 2021: *Porphyry deposits of the Northwestern Cordillera of North America: a 25-year update*; Canadian Institute of Mining, Metallurgy and Petroleum, Special Volume 57.
- Sillitoe, R.H., 1973: The Tops and Bottoms of Porphyry Deposits. *Economic Geology*, Vol. 68, p. 700-815.
- Sillitoe, R.H., 1985: Ore-related breccias in volcanoplutonic arcs. *Economic Geology*, Vol. 80, p. 1467-1514.
- Sillitoe, R.H., 1997: Characteristics and controls of the largest porphyry copper-gold and epithermal gold deposits in the circum-Pacific region. *Australian Journal of Earth Sciences*, Vol. 44, p. 373-388.
- Sillitoe, R.H., 1999: Styles of High-Sulphidation Gold, Silver and Copper Mineralisation in Porphyry and Epithermal Environments. *Pacrim '99*.

- Sinclair, W.D., 1996: Vein-Stockwork Tin, Tungsten. *In* Geology of Canadian Mineral Deposit Types. O.R. Eckstrand, W.D. Sinclair, and R.I. Thorpe, *eds.*, Geological Survey of Canada, Geology of Canada, No. 8, p. 409-420.
- Sinclair, W.D., 2007: Porphyry Deposits. *In* Goodfellow, W.D., *ed.*, Mineral Deposits of Canada: A Synthesis of Major Deposit-Types, District Metallogeny, the Evolution of Geological Provinces, and Exploration Methods. Geological Association of Canada, Mineral Deposits Division, Special Publication No. 5, p. 223-243.
- Singer, Donald A, V.I. Berger, and B.C. Moring, 2008: Porphyry Copper Deposits of the World: Database and Grade and Tonnage Models, 2008. U.S. Geological Survey, Open-File Report 2008-1155, version 1.0.
- Sutherland Brown, A. (*ed.*), 1976: Porphyry Deposits of the Canadian Cordillera. Canadian Institute of Mining and Metallurgy, Special Volume 15, 510p.
- Sutherland Brown, A., 1976a. Morphology and Classification. *In* Porphyry Deposits of the Canadian Cordillera, Canadian Institute of Mining and Metallurgy, Special Volume 15, A. Sutherland Brown, *ed.*, p. 44-51.
- Sutherland Brown, A. and R.J. Cathro, 1976: A Perspective of Porphyry Deposits. The Canadian Institute of Mining and Metallurgy, Special Volume 15, p. 7-16.
- Sutopo, Bronto, 2005: Geological and Geochemical Appraisals of Leached Capping Above Andean Porphyry Deposits. Internet publication by Centre of Excellence in Ore Deposits, University of Tasmania, Australia, 24p.
- Taylor, Roger G., 1979: Geology of Tin Deposits. *Developments in Economic Geology* 11, Elsevier Scientific Publishing Company, 543p.
- Thompson, A.J.B, and J.F.H. Thompson, 2015, *eds.*, Atlas of Alteration; a Field and Petrographic Guide to Hydrothermal Alteration Minerals. *Mineral Deposit Division Series Editor: K.P.E. Dunne.*
- Titley, S.R., and R.E. Bean, 1981: Porphyry Copper Deposits, Part I, Geologic Setting, Petrology, and Tectogenesis. *In* Brian J. Skinner, *ed.*, Economic Geology Anniversary Volume 1905 – 1980, p. 214-234.
- Titley, Spencer R., 1982: Advances in Geology of the Porphyry Copper Deposits, Southwestern North America. The University of Arizona Press, 560p.
- White, W.H., A.A. Bookstrom, R.J. Kamilli, M.W. Ganster, R.P. Smith, D.E. Ranta, and R.C. Steininger, 1981: Character and Origin of Climax-Type Molybdenum Deposits. *In* Brian J. Skinner, *ed.*, Economic Geology Anniversary Volume 1905 – 1980, p. 270-316.
- Wilkinson, William H. Jr., Luis A. Vega and Spencer R. Titley, 1982: Geology and Ore Deposits at Mineral Park, Mohave County, Arizona. *In* Spencer R. Titley, *ed.*, Advances in Geology of the Porphyry Copper Deposits, Southwestern North America. The University of Arizona Press, 560p.

Wilson, A.J., D.R. Cooke and B.L. Harper, 2003: The Ridgeway Gold-Copper Deposit; a High-Grade Alkalic Porphyry Deposit in the Lachlan Fold Belt, New South Wales, Australia. *Economic Geology*, Vol. 98, p. 1637-1666.

ACKNOWLEDGMENTS

I thank first all my inspiring geology professors and fellow students while studying undergraduate and graduate geology at The University of British Columbia. During my career, I have had the opportunity of working with many excellent field geologists who shared their wisdom generously. While teaching at The University of British Columbia I had insightful interaction with many professors. At the same time, graduate students involved me in stimulating and instructive collaborative field and laboratory studies on a great variety of deposit types. I have also worked closely and obtained much practical experience with junior and major mining companies keen to discover and develop mineral prospects. All of this was exciting and developed my keen interest in a practical and generalist approach to describing mineral deposits. I try here to pass on my accumulation of ideas over these years of experience to new exploration geologists, many of whom will be more comfortable with modern techniques than with the historical field approach championed here. I hope that this background methodology will aid field work leading to ore deposit discovery.

Many people have improved the text for this **Guide**. Chris Baldys, George Gorzynski, Ray Lett, Katja Freitag, and Carl Verley are especially thanked for their early corrections and insightful comments.

Most photos used in this book are mine. Photographs from the Ajax porphyry mine, BC, Canada, were obtained from Kika Ross of Panterra Consultants Ltd. John Bradford provided photos of gusano habit or texture from the Tanzilla prospect, BC, Canada. Two photos of supergene enrichment were copied from Anderson, 1982, and are reproduced with permission.

APPENDIX A: SUMMARY OF COMMON CODES, LOGGING TECHNIQUES AND DIAMOND DRILL LOGGING FORMATS USED IN DESCRIBING PORPHYRY DEPOSITS

Introduction

The following codes and logging formats applicable to porphyry deposits are modified from Godwin (2020) and based on Blanchet and Godwin's procedures (1972). The methodology was developed and applied to the early logging of drill holes at the Casino Porphyry, central Yukon, Canada. Since then, the logging approach presented here has been modified and applied to many porphyry deposits of many different kinds. Godwin (2020) details procedures and formats for logging drill chips from rotary air blast or reverse circulation drilling.

Codes that Facilitate Descriptions in Mapping and Logging of Porphyry Deposits

Four-Letter Rock Codes

4-letter rock names common to porphyry deposits are in TABLE A1. A complete listing of codes, applicable to most types of deposits, is available in Godwin (2020).

TABLE A1: Rock names (4-letters capitalized).

Codes are after Godwin (2020) and Blanchet and Godwin (1972).

ADAM = QZMZ = adamellite = quartz monzonite. **ANDS** = andesite. **ANOR** = anorthosite. **APLT** = aplite. **ARGL** = argillite. **BASL** = basalt. **BRAN** = brain rock with **UST** texture. **BRXX, BRFL, BRVL, BRTO, BRMA** = breccia, ~fault, ~volcanic, ~tourmalinite, ~ magnetite-apatite. **CARB** = carbonate. **CHER** = chert. **DACT** = dacite. **DIAB** = diabase. **DIOR** = diorite. **DOLM** = dolomite. **DYKE = DKXX, DKMA, DKQP, DKTO**= dyke, ~magnetite-apatite, ~quartz porphyry, ~tourmalinite. **FELS** = felsite. **GABR** = gabbro. **GNES** = gneiss. **GOSN = GOXX, GOEX, GOIN, GOTR, GOSX** = gossan, ~exotic, ~indigenous, ~transported, ~after massive sulfide. **GRAN** = granite. **GRNT = GRXX, GRFL, GRIN, GRMF, GRUM** = granitic, ~felsic, ~intermediate, ~mafic, ~ultramafic. **GRES** = greisen. **GREY** = greywacke. **GRDR** = granodiorite. **HORN** = hornfels. **MTVL** = metavolcanic. **PORP = PPXX, PPDR, PPFL, PPQZ, PPFQ, PPQF, PPMU** = porphyry, ~diorite, ~feldspar, ~quartz, ~feldspar>quartz, ~quartz>feldspar, ~muscovite. **QZIT** = quartzite. **QZDR** = quartz diorite. **QZMZ = ADAM** = quartz monzonite = adamellite. **RHYL** = rhyolite. **RYDC** = rhyodacite. **SCHS** = schist. **SEDM** = sedimentary. **SHAL** = shale. **SILX = QZLT** = silexite = quartzolite. **SKAR** = skarn. **SYEN** = syenite. **TONL** = tonalite. **UNKN** = unknown rock. **VOLC = VLXX, VLAK, VLBM, VLFL, VLIN, VLMF, VLMS, VLTS** = volcanic, ~alkalic, ~bimodal, ~felsic, ~intermediate, ~mafic, ~marine-sediment, ~terrestrial-sediment. **VLCL** = volcanoclastic.

Three- and One-Letter or One-Number Codes

1- and 3-letter comment code-names are in TABLE A2. It is a partial list of codes commonly used in descriptions of porphyry deposits. A more complete listing of these codes, applicable to most types of deposits, is available in Godwin (2020).

TABLE A2: General descriptive terms (1-number or 1- and 3-letters capitalized).*Codes are after Godwin (2020) and Blanchet and Godwin (1972).*

ALT = alteration. **CAP** = capping. **D = DIS** = disseminated. **ENR** = enrichment. **E = ENV** = envelope. **GUS** = gusano texture. **HAB** = habit. **HYD** = hydrothermal. **HYP** = hypogene. **LCP** = lithocap. **P = PER** = pervasive. **PPD** = porphyry deposit. **UNC = U** = unconformity. **UST** = unidirectional solidification texture in brain rock. **V = VEN** = vein. **WTH** = weathered. **SUO** = supergene oxide. **SUS** = supergene sulfide. **0 = FRX** = fresh rock, unaltered. **1 = ZEL** = zeolitic. **2 = PRP** = propylitic (chlorite, epidote, albite and carbonate [calcite]). **3 = SMC** = smectite [e.g., montmorillonite], and/or chlorite, and/or zeolite). **4 = IAR** = intermediate argillic (kaolinite). **5 = KFS** = K-feldspar stable (quartz and sericitic with intact, original K-feldspar). **6 = PHY** = phyllic (quartz, muscovite-sericite and pyrite). **7 = AAR** = advanced argillic (quartz and kaolinite). **8 = POT** = potassic (K-feldspar, quartz, secondary biotite or phlogopite). **9 = DPT** = deep potassic (quartz, andalusite, pyrophyllite, magnetite, hematite).

Two Letter Mineral Codes

TABLE A3 is a partial list of 2-letter mineral code names common to porphyry deposits. A more complete listing of these codes, applicable to most types of deposits is available in Godwin (2020).

TABLE A3: Mineral names (2-letters capitalized).*Codes are after Godwin (2020) and Blanchet and Godwin (1972).*

AB = albite. **AL** = alunite. **AA** = andalusite. **AH** = anhydrite. **AK** = antlerite. **AT** = atacamite. **AP** = apatite. **AZ** = azurite (**MA** = malachite and azurite). **BA, BV** = barite, ~vein. **BI** = biotite. **BO** = bornite. **BR** = brochantite. **C*** = native copper. **CA, CV** = calcite, ~vein. **CT** = cassiterite. **CH** = chalcantite. **CC, CI, C\$** = chalcocite, ~on pyrite, ~on Cu-mineral. **CP** = chalcopyrite. **CL** = chlorite. **CK** = chrysoc[k]olla. **CY** = clay. **CV** = covellite. **CU** = cuprite. **DK** = dickite. **DG** = digenite. **DU** = dumortierite. **EP** = epidote. **FL** = feldspar. **FD** = feldspathoid. **FM** = ferrimolybdenite. **G*** = native gold/electrum. **GL** = galena. **HE, HS** = hematite-earthy, ~specular. **HB** = hornblende. **IL** = illite. **JA** = jarosite. **KA** = kaolinite. **KF** = K-feldspar (orthoclase). **LI** = limonite. **MC** = malachite (**MA** = malachite and azurite). **MG** = magnetite. **MN** = manganite/alabandite. **MR** = marcasite. **MI** = mica. **MO** = molybdenite. **MM** = montmorillonite (smectite **SM**). **MU, MS, ML, MY** = muscovite, ~sericite, ~lepidolite (purple from Li), ~(yellow from F). **NE** = nepheline. **NO** = neotocite. **OQ** = opaques. **OX** = oxides. **PH** = phlogopite. **PL** = plagioclase. **PW** = powellite. **PY, PV, P#** = pyrite, ~vein, ~boxwork. **PE** = pyrolusite. **PP** = pyrophyllite. **PX** = pyroxene (commonly augite). **PO** = pyrrhotite. **QZ, QB, QH, QR, QS, QV** = quartz, ~brain (**UST**), ~hightemp (square-cristobalite), ~rutilated (blueish), ~smoky (often from radiation), ~vein. **SL, SV** = sphalerite, ~vein. **SM** = smectite (e.g., calcium **MM**). **SU** = sulfate. **SX** = sulfide. **TN** = tenorite. **TO** = tourmaline. **WD** = wad. **WO, WF, WH** = wolframite, ~ferberite, ~hubnerite. **ZE** = zeolite.

Logging Techniques for Describing Diamond Drillholes in Porphyry Deposits

Best practice for common procedures in diamond drill hole logging goes a long way to satisfying increasingly stringent quality-assessment (QA) and quality control (QC) requirements of regulatory agencies. Of course, the presented logging formats helps with this too. The following are some organizational hints for logging diamond drill hole core.

- **Drillhole names** are conveniently labeled: project, year, type and number of the hole (e.g., ING14DD012 or Prj/Yy/Tp/Num where: Prj = three letters for project name [ING]; Yy = last two numbers of the year 20[14]; Tp = type where DD = diamond drill hole, OC = outcrop, RC = reverse circulation, RB = reverse air blast, TR = trench and Num = number of the drillhole [012]). Note that this suggested convention is concise and convenient for digital sorting by project, year, type and number.
- **Core layout in core boxes** should mimic how one reads a letter: left to right, left to right, etc. Although obvious, I have seen junior drill helpers put the core in the box like a snake going from left to right and then right to the left. Check carefully, especially at the beginning of a program.
- **Drillhole deviations** as measured by downhole surveys, must be recorded separately from the drill logging forms presented here. If downhole survey data is lacking, hole deviations sometimes can be estimated. Vertical holes tend to deviate less than inclined holes. When plotting drill holes with geographical information systems (GIS), the deviation information is critical and facilitates accurate plots (e.g., cross-sections).
- **Build a core library** consisting of several core boxes that hold typical examples of various rock and alteration types. One can include field specimens as well as the core. These can be used for reference to help with consistent descriptions for yourself and other loggers/mappers during the current and subsequent programs. It is also compact and available for future detailed study, as required.
- **Compressed or skeletonized drillholes** are made by taking a representative sample of core from each assay interval and labelling and putting it in a separate core box. These are appropriate, especially for porphyry deposit logging, where assay intervals are constant. Because the compressed or skeletonized holes occupy only a few core boxes compared to the whole core, they help with quick review and are readily stored and transported for future study. In porphyry deposit logging, generally, look at the interval being described and pick out a core piece that looks to be characteristic of that interval. Use its properties to make entries in the log, sometimes with the aid of a binocular microscope, a needle to scratch, acid to detect carbonate and other field identification tools. One can then put the same specimen into a compressed log core box. Finally, insert a label (generally a driller's block notated with a carpenter's graphite pencil) in the original core box, noting specimen removal.
- **Core box photography** is a vital record. The core should be photographed and logged before it is split, but intervals to be assayed should be tagged with assay labels. After tagging, one can photograph core boxes stacked in order, four at a time, on an inclined board. Using daylight a handheld camera positioned at right angles from the centre of the assembled core boxes is usually adequate. The core should be unsplit, cleaned and wet, so textures become clearer. Include a scale and a colour format for more accurate future size and colour estimations. In addition to a standard record, some features can be recovered later if needed from the photos. Recoverable features include a) estimations of geology and alteration, b) core recovery and general nature of the core, and c) rock-quality designation. Both core recovery and rock-quality designation can be helpful in geotechnical assessments of rock stability in mining. Core recovery is the percentage of solid pieces of rock core. Rock-quality designation is a rough measure of the degree of jointing or fractures in the core, measured as a percentage of the drillcore in lengths of 10 cm or more (the 10 cm rule can be modified for core of different diameters).
- **Core sampling** is the most important corporate objective. Core is split or sawn in half. Sometimes it is necessary for the geologist to dictate how core is sampled by drawing lines along the centres of appropriately rotated core. The half-split of the core interval to be analyzed is bagged, along with the appropriate assay tag; a duplicate part remains in the core box. Books of assay tags,

available from assayers, are made of resistant paper, such as Tyvek®. Assay books have tags with a unique number sequence. Each tag has the same number on the book stub and two rip-off copies. For each tag: a) the assay stub is notated with drill hole number and from-to information, b) one rip-off tag is inserted in the sample split to be sent to the assay laboratory, and c) the remaining rip-off tag is affixed to the core box at the start of the assay interval sampled. The assay books with notated stubs must be retained for backup information and potential quality control (QC), and quality assurance (QA). Specimens removed for the core library, compressed logs or detailed study must be marked by pencilled notation on wooden drillers' block as removed. The removed specimen must be from the half-split core that stays in storage, not from the core sent for analysis. When metallurgical tests are likely to be required, it can be essential to protect samples and core from oxidation.

- **Logging formats in Figures A1 to A3** can also accommodate detailed descriptions of trenches or along surfaces of outcrops. Doing so provides compatible formats of all drill, trench or outcrop detail that facilitate digital display. For example, a surface trench or outcrop can be shown on a drill section as a sub-horizontal detail, along with underlying drill holes. Likewise, deflections in trench direction can be treated the same as drill hole deviations.
- **Describing geology, alteration and structure in core** is best done on the cleaned whole core before it is split. Structural angles, especially, are more easily measured (oriented core is sometimes required). Textures and rock types generally are best identified on whole core when it is wet. Alteration mineralogy is more easily recognized on the dry core. Typically, a series of boxes are laid out in order on the ground outside in daylight, but a logging table with good light is required for big projects. Measured core recovery and rock-quality designation must be made on the core before it is split and can often be done and recorded by an assistant. When beginning to log core, use flagging tape (several colours for different types of features) to mark a) zones: casing, overburden, lost core, supergene types, oxide, hypogene; b) rock type: major lithological contacts, significant textures; c) structures such as significant faults, bedding, axial plane cleavage and timing relationships, which can also be recorded on the graphic log; and d) mineralization and alteration: changes in percentages of individual minerals, broad changes in alteration style, significant habits or mode of occurrences. The core is then described systematically on the logging form. Detailed descriptions are commonly based on pieces of core picked out as representative of the interval being described. A hand lens, scratch needle tests, a hand magnet, 10% HCl acid and a binocular microscope can be helpful. Specimens can be put aside for the core library and additional detailed examination of specific gravity, thin sections, X-ray diffraction (XRD) element analyses and shortwave infrared (SWIR) mineral determinations. When logging in detail, the location of the original divisions marked by the flagging tape commonly needs to be moved. One can only achieve meaningful statistics relating geology and alteration to assay information if the logging descriptions match the assay intervals —if it is worth assaying, it is worth describing!
- **Permanently marking drillhole collar locations in the field** is essential so one can relocate them—sometimes years later. A common way is to put a box, approximately 10 cm deep and 30 cm square, over the hole. Fill this with concrete and scribe the whole number into the top of the cement slab while it is wet. Note that the labelling system for holes recommended here (Prj/Yy/Tp/Num) identifies the project, year drilled, type of drill hole and hole number for that project and year. This labelling method is usually sufficient, but additional information can be added as desired. One should plug the top of the to inhibit erosion that might displace the concrete marker slab. In some areas and instances, holes must be backfilled because of environmental concerns.

- **Core storage** is important, but expensive. Given the cost to obtain 1 m of core, it is evident that core must be available for later reference. Methods on how to construct core racks are available elsewhere. However, in Canada, porcupines eat wooden core boxes because they are attracted to the plywood glue; in Africa, termites eat wooden core boxes; plastic becomes brittle, particularly if exposed to the sun. Label boxes well with labels that will last. Thin aluminium labels that can be scribed with a ballpoint pen are commonly used.
- **Instrumental data that can be systematically collected** with handheld instruments and added to drill logs include magnetic susceptibility and conductivity of core; average spot scintillometer readings for U, Th and K; SWIR spectral analysis for minerals in the core; and handheld XRF element analyses. Ultraviolet scanning in short and long wavelengths is appropriate in some instances but be aware that without careful scrubbing of the core it is difficult because modern organic drill mud additives commonly fluoresce. This additional data can aid in the interpretation of geophysical, geological and alteration features.
- **Record of core recovery, rock-quality designator (RQD) and intervals assayed** can be done while organizing the core (by an assistant, if available) before logging. At the same time, tagged assay intervals should be established and recorded. A geologist's input will be required if this is not a systematic length, as is good practice for porphyry deposits. These are simple marking and measurement skills that relate to distance blocks inserted by the drillers. New assistants must be taught how to fill out this record. And the data must be systematically recorded with an ink pen as a separate record in a bound book with lined and prenumbered pages that cannot be removed (i.e., loose-leaf records are not acceptable). Errors in this record should be marked (crossed out, so the original is still readable) and the revisions rewritten (i.e., no erasing or whiteout). This book, and the books of notated assay stubs, are essential records for potential QC and QA examination. Headings in this record, modified as appropriate, should include Date, HoleName, FromToMetres, AssayTagNumber, MeasuredRecovery%, RockQualityDesignation% (RQD; if required), LabSentTo, DateSent and Remarks. This handwritten record is critical; relevant information from this record can be digitally entered as part of the total drill hole record (e.g., hole number, from-to, geology, recovery, RQD, assay tag numbers).

Formats for Describing Diamond Drillholes, Trenches, and Outcrops in Porphyry Deposits

Modification of logging formats (Figures A1 to A3) is necessary to capture features that are unique to specific porphyry deposits and different types of porphyry deposits. Changes should accommodate detailed descriptions of drill holes, trenches and along surfaces of outcrops. Doing so provides compatible formats of all drill, trench or outcrop detail that facilitate digital display. For example, a surface trench and outcrop can be shown on a drill section as a sub-horizontal detail, along with underlying drill holes. Note that deflections in trenches or outcrop can be treated the same as drill hole deviations.

All logging formats presented here have a common first page and simplified following pages The first page (Figures A1 and A2) has header information describing drill hole type, location, and the date drilled. Under the heading is the format for the description of the core. The following pages (Figures A1 and A3) are only for core description and duplicate only this part of the first page. Header details are described in TABLE A4. The log sheet has a logical and universal sequence that is, from left to right:

1. A graphic log to enable capture of features difficult to code (e.g., crosscutting structures), and especially if coloured, to facilitate visual interpretations,
2. General specification of what one is looking at in terms of 'zone' (e.g., capping, supergene oxide, supergene sulfide, hypogene),

3. From–to interval described,
4. Rock-type and its characteristics,
5. Structures superimposed on the rock type,
6. Alteration and mineralization superimposed on the rock type,
7. Optional interpretation of overall alteration/mineralization facies for interval, and
8. Written comments for important features not already captured (the codes in this appendix facilitate compact descriptions).

One is, therefore, going from noting what/where one is at, to what is the basic rock type, to what is superimposed upon the rock type, to comments. These descriptions should always be together. Because, for example, it is challenging to identify alteration features without knowing what is altered. (Rock type mineralogy must be known before one can determine superimposed alteration mineralogy).

Data entry can be done directly on a laptop or in paper forms like those presented here for subsequent data entry. One advantage of using direct computer entry into a program like Microsoft Excel (or Microsoft Access) is that entries can be controlled for consistency by making only agreed-upon codes allowable. Nevertheless, many prefer recording with an HB pencil on letter-sized paper, landscape orientation, carried in an open clipboard with either a leather pouch or a ledge glued to the clipboard for holding:

- A 0.7 mm HB mechanical pencil,
- A stick eraser,
- A hardness scratcher made by putting a fine needle in a 0.7 mm mechanical pencil,
- A pencil stud finder magnet, and
- Any other pertinent diagnostic tools.

On a paper format log, one can easily erase, and change entered information. More importantly, one can sketch on and colour a graphic log, which is especially valuable as an effective display that records a) structural and relative timing information or b) highlights geology, alteration and specific mineralization. The graphic log provides an instant strip-log for the hole that can aid in visualizing the geology.

General codes and formats for recording detailed data for porphyry deposits in drill cores, drill chips, trenches and outcrops are in TABLES A1 to A3. The example diamond drill log format in Figures A1 to A3 is generally applicable to calc-alkaline porphyry deposits. All headings are easily modified to describe better the specific deposit being studied. For computer/statistical analysis, one must consistently describe geological and alteration descriptions to match assay intervals, regardless of the logging method. Note that in mapping detail at a deposit scale, it is appropriate to map surface trenches and relevant outcrops in the same way as drill holes. For example, a surface trench or outcrop can be described as an approximately flat diamond drill hole. Survey information for all of these can be defined the same way. Detailed information from the surface trenches then becomes compatible with data from the diamond drill holes during computer-assisted analysis, such as the generation of cross-sections.

TABLE A4. Explanation of logging formats related to porphyry deposits.

Information is related to formats of Figures A1 to A3.

Entries in form	Explanation
Header information <i>Page 1 only. Basic information required in QA and QC control</i>	The header information at the top of page 1 is standard information for drill holes. It includes hole name, location and grid type, inclination, depth, who drilled and who logged the hole, whether or not the data has been entered into computer files, etc.
Hole ID <i>Embeds a lot of information and allows logical sorting</i>	Hole identification is ordered to facilitate sorting by project, year, type and number of the hole. E.g., GLD18DD005 describes the log in an organized way suitable for systematic sorting. The interpretation of this name is as follows a) the project in three letters [GLD for the Golden Project], b) the year in two numbers [18 for 2018], c) what is being described in two letters [DD for diamond drill hole, OC for outcrop, RB for reverse air blast; RC for reverse circulation; TR for trench, etc.], and c) the drill hole sequence in three numbers [005]. Alternating alphabetic symbols with numbers enhances readability.
Description titles <i>Logically from: graphic → zone → from-to → rock ± structure → alteration → notes</i>	Description titles on Page 1 below the header and at the top of each additional page are the same. These titles describe the two-line groups for the data to be entered in every form. Column entries enhance consistency in observation and facilitate subsequent computer statistical analysis. As an example, statistical correlations can be determined among a) visually estimated sericite (MS), b) visually estimated pyrite (PY), c) visually estimated chalcopyrite, and d) assayed copper percentages. All such factors can be also be plotted on strip logs and in three dimensions. These plots facilitate the discovery of alteration zoning, pyrite haloes and ore shells, to name a few possibilities.
Graphic ALT STR MIN ROC <i>Graphic Hand drawn/coloured</i>	The graphic log for sketching by hand is in the first two columns. Use can vary, but column 1 might be assigned alteration and structure, and the second column mineralization and rock type. Timing/crosscutting relationships are most easily captured graphically. Colouring of the graphic log (and or mineral columns) enhance visual interpretations.
Zone <i>Basically what one is looking at</i>	Zones are commonly CAP = cap; DIS = disseminated; HYP = hypogene; SUO = supergene oxide; SUS = supergene sulfide; SUL = sulfide; STK = stockwork and TRS = transition. Zones are modifiable as required.
From and To <i>Where you are at</i>	From–To description; note that this interval is commonly constant in porphyry/bulk mineable deposits (e.g., 1.5 or 2.0 m). Thus, in porphyry deposits the log form has a constant scale. However, a constant scale is not appropriate in logging all deposits. For example, variable From–To distances would be used for vein deposits where there might be long intervals of a constant rock with characteristic alteration and shorter intervals of significant alteration and veining where detailed information is needed. Always sample/assay intervals must have matching geological/alteration descriptions.
SamNo <i>Key to future assays</i>	Sample number of assay tags used for intervals assayed/analyzed; facilitates merging of analytical information later for statistical and geographical information system analysis/display of all assay and logged data.
Value <i>Can be added later if logs are used manually</i>	If desired, values of assays can be added to the logs after analysis. This can aid visual interpretations from original logs. This facilitates checking assay information against recorded mineralogy. For example, one would expect the copper assay to agree with the abundance of copper minerals (e.g., chalcopyrite = CP , bornite = BO , etc.).
Rock1 and % Rock2 and %	For every interval, two rock types can be entered. The percentages of each are recorded. For example, MONZ 80, DYKE 20 for an interval of 80% monzonite and 20% dyke. Additional rock complexities can be noted in comments and the graphic log.
Min1, Min2	Two qualifying minerals for the rock can be entered (e.g., biotite = BI ; hornblende = HB), where Min1 is generally in greater quantity or more important than Min2 .
Qual1, Qual2	Two qualifying textures or characteristics for the rock can be entered (e.g., FGR , MGR , CGR = fine, medium, coarse grained; SCV = shatter cleavage; UST = unidirectional solidification texture).
Struct1, Struct2 type Angle measured from 90° to core axis	Two structures— Struct1 , Struct2 —can be defined (e.g., B = bedding; F = fault; V = vein), plus the angle <i>perpendicular</i> to the core axis (e.g., V 42 , F 26 for a vein 42°, and a fault 26° to the core-axis perpendicular). Note that in a vertical hole, measuring angles with respect to the perpendicular of the core axis, is the same as a dip measured at surface.

<p>ALTERATION and MINERALIZATION GANGUE/ORE %</p> <p><i>Generally ordered logically from high to low intensities</i></p>	<p>Alteration and mineralization can be systematically recorded. Minerals (two-capitalized-letter codes) will change to correspond to specific projects. Common ones entered here as examples are: QZ = quartz; KF = K-feldspar; BI = secondary biotite; MS = muscovite sericitic; CY = clay; CB = carbonate; PP = pyrophyllite; CL = chlorite; EP = epidote; XX and YY = other minerals entered as two letters, or if unknown WW, XX, YY and ZZ; and LI = limonite; MO = molybdenite; BO = bornite; CP = chalcopryite; PY = pyrite; MG = magnetite; HS = hematite-specularite; LI = limonite; GO = goethite; JA = jarosite. Ore and gangue minerals should be organized from left to right, generally following mineralogy of decreasing facies.</p>
---	--

Conclusions

Advantages to using the codes and logging formats, as presented, are:

- Quick and precise, descriptive writing of observations'
- Enhanced consistency and detail of description among and within drill, trench, and outcrop data'
- Ease of digital entry of logged information and facility to generate readable computer output on maps and cross-sections.

Training to understand and use these codes and formats is an excellent way to ensure a high level of within- and between-geologist consistency and ability. Importantly, for any given project, note that the number of relevant codes is small. Consequently, the memory factor is not demanding for the relatively few codes required for any specific project—especially when most codes are logical and easily recallable.

Consistency is essential a) among mapping and logging geologists, b) within each project, and c) throughout the life of any given project. Written comments must be brief, readable and suitable for digital entry. The commonly used codes for porphyry deposits in TABLES A1 to A3 are tools for providing the useable, digitizable, and reliable data descriptions required for a) rapid recording of observations, b) readable display of geological/alteration observations and c) manual and computer/statistical analysis and d) rapid digital 3D development of geological and alteration models with vectors to ore zones. Application to porphyry deposits is emphasized here. However, studies of any kind of deposit will benefit from the approach presented. Logging descriptions must match assay intervals if one wants meaningful statistics relating geology, alteration, and assay information—if it is worth assaying, it is worth describing!

APPENDIX B: COORDINATES OF DEPOSITS MENTIONED IN THE TEXT

Deposits or Deposit Areas Mentioned in the Text

Mines or exploration areas, mentioned in the text are in TABLE B1. The coordinates provided generally are centred on mine workings. Locations provided by web-search commonly locate the mine plant buildings, rather than the deposit.

Satellite Images

Satellite images that allow visualization of these deposits/areas are readily available in Earth Explorer which is available from the United States Geological Survey at <https://earthexplorer.usgs.gov>. The extent, size, and number of open pits, common to porphyry deposits, are easily viewed. Drill hole locations can often be identified in areas under exploration and not developed into mines. Colour anomalies related to rock types and alteration, and regional structures are sometimes apparent on the images.

TABLE B1: Location of deposits mentioned in the text.			
Coordinates generally are centred on mine workings.			
DEPOSIT/AREA	COUNTRY/PROVINCE-STATE	LATITUDE- N	LONGITUDE- E
Ajax	Canada/British Columbia	50.6091	-120.3960
Ardlethan	Australia/New South Wales	-34.3301	146.8530
Afton	Canada/British Columbia	50.6607	-120.5130
Berg	Canada/British Columbia	53.8036	-127.4350
Bingham Copper	USA/Utah	40.5268	-112.1338
Butte (Berkley Pit)	USA/Montana	46.0166	-112.5099
Casino	Canada/Yukon	62.7378	-138.8281
Chuquicomata	Chile/El Loa	-22.2877	-68.9012
Climax/Henderson	USA/Colorado	39.3694	-106.1703
Copper Mountain	Canada/British Columbia	49.3295	-120.5179
Don Luis area	Mexico/Sonora	29.5351	-110.6391
El Teniente	Chile/Librador Gral Bernardo O'Higgins	-34.0776	-70.4341
El Tesoro	Chile/Antofagasta	-22.9751	-69.0617
Endako	Canada/British Columbia	54.0401	-125.1291
Exotica	Chile/El Loa	-22.3820	-68.9135
Galore Creek	Canada/British Columbia	57.1211	-131.4599
Glacier Gulch	Canada/British Columbia	54.8196	-127.2633

Inguaran area	Mexico/Michoacan	18.8703	-101.6799
Island Copper	Canada/British Columbia	50.6000	-127.4778
Kiruna	Sweden/Kiruna	67.8413	20.1805
La Colorada	Mexico/Sonora	28.8027	-110.5725
Logtung	Canada/British Columbia	60.0084	-131.6072
Los Bronces	Chile/Region Metropolitana de Santiago	-33.1493	-70.2852
Mineral Park	USA/Arizona	35.3622	-114.1480
Ok Tedi	Papua New Guinea	-5.2077	141.1400
Olympic Dam	Australia/South Australia	-30.4364	136.8590
Oyu Tolgoi	Mongolia/Khanbogd	43.0087	106.8461
Shator	Iran	unknown	unknown
Sierra Gorda	Chile/Antofagasta	-22.8519	-69.3380
Silver Bell	USA/Arizona	32.4036	-111.5249
Toquepala	Peru/Jorge Basadre	-17.2462	-70.6118

APPENDIX C. PROBLEM SET RELATED TO THE GEOLOGY AND ALTERATION OF PORPHYRY DEPOSITS

C1. General Questions on Alteration Mineralogy in Porphyry Deposits

Question GEN01 [11]: Potassic ore mineral alteration.

Potassic ore mineral alteration is most closely related to six of the following minerals (mark six true [T] and the rest false [F]).

1. Galena: ____
2. Pyrite: ____
3. Sphalerite: ____
4. Chalcopyrite: ____
5. Tetrahedrite: ____
6. Molybdenite: ____
7. Arsenopyrite: ____
8. Magnetite: ____
9. Hematite-specular: ____
10. Pyrrhotite: ____
11. Ferrimolybdate: ____

Question GEN02 [8]: Phyllic ore-mineral alteration.

Phyllic ore mineral alteration is closely related to two of the following minerals (mark two true [T] and the rest false [F]).

1. Galena: ____
2. Pyrite: ____
3. Sphalerite: ____
4. Chalcopyrite: ____
5. Tetrahedrite: ____
6. Molybdenite: ____
7. Arsenopyrite: ____
8. Pyrrhotite: ____

Question GEN03 [8]: Propylitic ore-mineral alteration.

Propylitic ore-mineral alteration is closely related to two of the following minerals (mark two true [T] and the rest false [F]).

1. Galena: ____
2. Pyrite: ____
3. Sphalerite: ____
4. Chalcopyrite: ____
5. Tetrahedrite: ____
6. Molybdenite: ____
7. Arsenopyrite: ____
8. Pyrrhotite: ____

Question GEN04 [11]: Potassic alteration.

Potassic alteration is closely related to four of the following minerals (mark four true [T] and the rest false [F]).

1. Quartz: ____
2. Muscovite-sericite: ____
3. Chlorite: ____
4. K-feldspar: ____
5. Epidote: ____
6. Actinolite: ____
7. Illite: ____
8. Albite: ____
9. Kaolinite: ____
10. Smectite (montmorillonite): ____
11. Calcite ____

Question GEN05 [11]: Phyllic mineral alteration.

Phyllic mineral alteration is closely related to two of the following minerals (mark two true [T] and the rest false [F]).

1. Quartz: ____
2. Muscovite-sericite: ____
3. Chlorite: ____
4. K-feldspar: ____
5. Epidote: ____
6. Actinolite: ____
7. Illite: ____
8. Albite: ____
9. Kaolinite: ____
10. Smectite (montmorillonite): ____
11. Calcite ____

Question GEN06 [11]: Advanced argillic mineral alteration.

Advanced argillic mineral alteration is closely related to two of the following minerals (mark two true [T] and the rest false [F]).

1. Quartz: ____
2. Muscovite-sericite: ____
3. Chlorite: ____
4. K-feldspar: ____
5. Epidote: ____
6. Actinolite: ____
7. Illite: ____
8. Albite: ____
9. Kaolinite: ____
10. Smectite (montmorillonite): ____
11. Calcite ____

Question GEN07 [11] Intermediate argillic mineral alteration.

Intermediate argillic mineral alteration is closely related to two of the following minerals (mark two true [T] and the rest false [F]).

1. Quartz: ___
2. Muscovite-sericite: ___
3. Chlorite: ___
4. K-feldspar: ___
5. Epidote: ___
6. Actinolite: ___
7. Illite: ___
8. Albite: ___
9. Kaolinite: ___
10. Smectite (montmorillonite): ___
11. Calcite ___

Question GEN08 [11]: Propylitic mineral alteration.

Propylitic mineral alteration is closely related to four of the following minerals (mark four true [T] and the rest false [F]).

1. Quartz: ___
2. Muscovite-sericite: ___
3. Chlorite: ___
4. K-feldspar: ___
5. Epidote: ___
6. Actinolite: ___
7. Illite: ___
8. Albite: ___
9. Kaolinite: ___
10. Smectite (montmorillonite): ___
11. Calcite ___

Question GEN09 [12]: Supergene capping alteration.

Supergene capping alteration is closely related to six of the following minerals (mark six true [T] and the rest false [F]).

1. Pyrite ___
2. Jarosite ___
3. Chalcopyrite ___
4. Limonite ___
5. Molybdenite ___
6. Ferrimolybdenite ___
7. Hematite-earthy ___
8. Goethite ___
9. Neotocite ___
10. Covellite ___
11. Malachite ___
12. Calcite ___

GEN10 [16]: Supergene oxide enrichment alteration.

Supergene oxide enrichment alteration is closely related to five of the following minerals (mark five true [T] and the rest false [F]).

1. Jarosite ___
2. Malachite ___
3. Chalcocite ___
4. Chalcopyrite ___
5. Covellite ___
6. Enargite ___
7. Cuprite ___
8. Copper-native ___
9. Azurite ___
10. Chalcanthite ___
11. Magnetite ___
12. Molybdenite ___
13. Neotocite ___
14. Pyrite ___
15. Secondary K-feldspar ___
16. Calcite ___

Question GEN11 [16]: Supergene sulfide enrichment alteration.

Supergene sulfide enrichment alteration is represented by three of the following minerals (mark four true [T] and the rest false [F]).

1. Jarosite ___
2. Malachite ___
3. Chalcocite ___
4. Chalcopyrite ___
5. Covellite ___
6. Enargite ___
7. Cuprite ___
8. Copper-native ___
9. Azurite ___
10. Chalcanthite ___
11. Magnetite ___
12. Molybdenite ___
13. Neotocite ___
14. Pyrite ___
15. Secondary K-feldspar ___
16. Calcite ___

C2. General Questions on Rocks and Mineralogy in Porphyry Deposits

Question GEN12 [14]: Rock descriptions.

Mark as true [T] or false [F] the following descriptions of the rock in Figure C1.

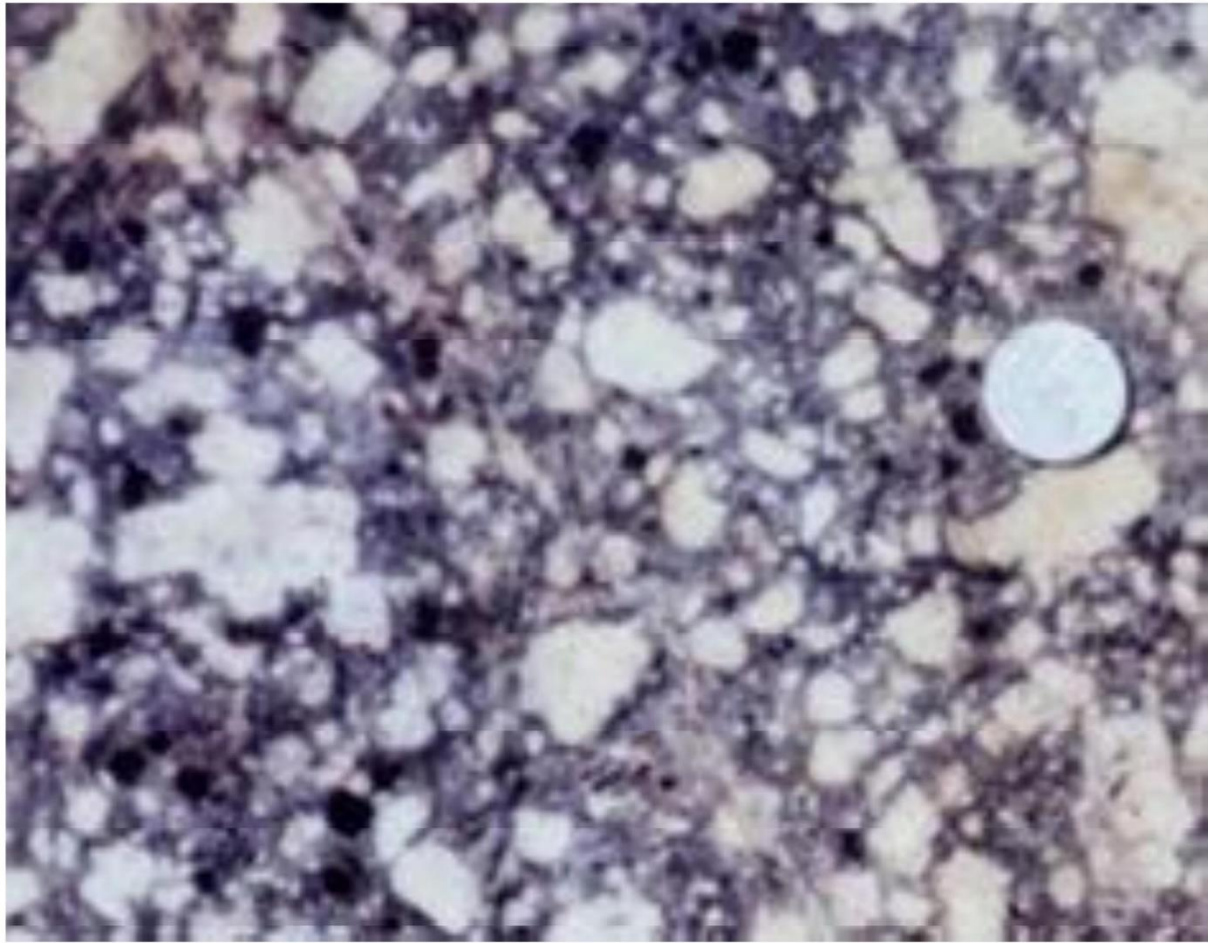


Figure C1. Rock with 3 mm diameter disk for scale.

1. The rock is an equigranular granite. ____
2. The rock is a breccia. ____
3. The rock is a porphyry. ____
4. The black biotite forms phenocrysts. ____
5. The presence of the black biotite is important. ____
6. The porphyry is "dead" with respect to being related to porphyry deposit mineralization. ____
7. The porphyry is "live" with respect to being related to porphyry deposit mineralization. ____
8. The rock has phenocrysts of feldspar and biotite. ____
9. A microvein cuts the specimen. ____
10. The matrix is fine-grained. ____
11. Because the matrix is grey it contains biotite. ____
12. The rock formed from a "wet" magma. ____
13. The rock formed from a "dry" magma. ____
14. You should map the distribution of this rock carefully? ____

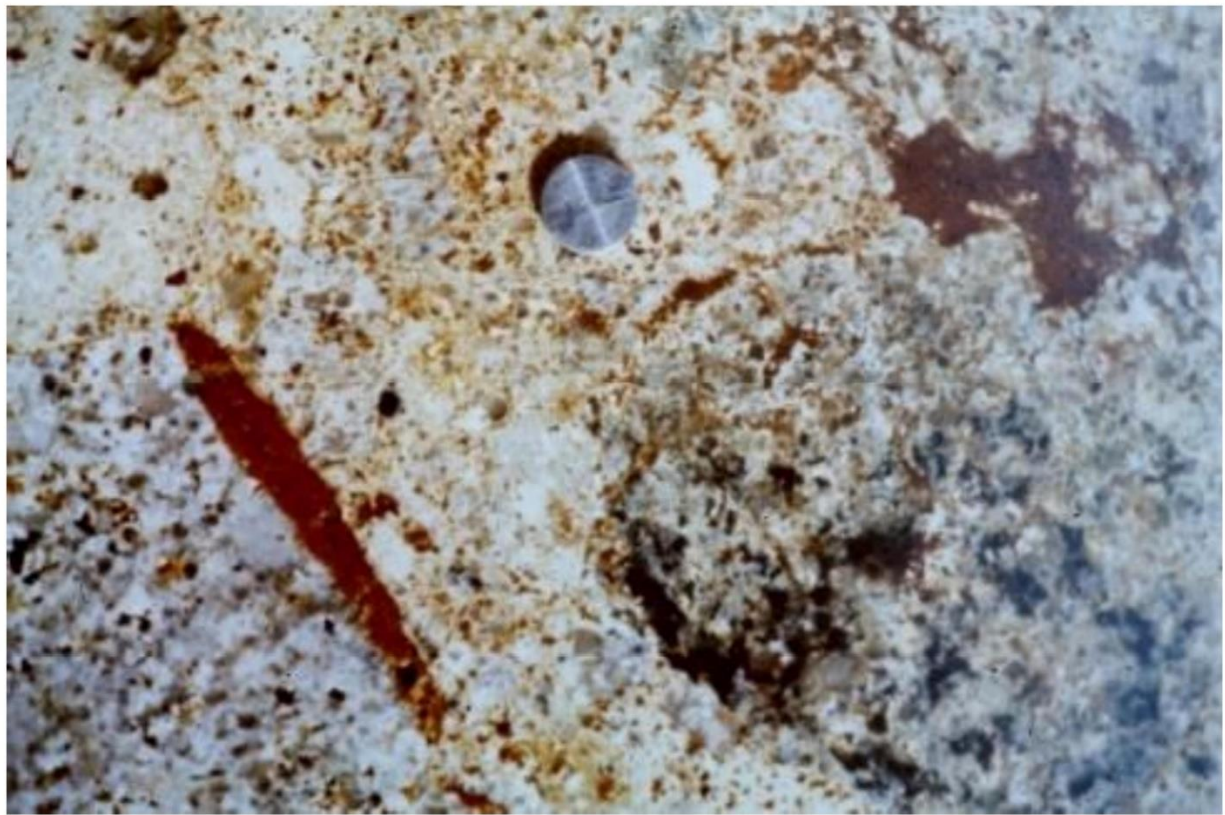
Question GEN13 [11]: Rock description.

Figure C2. Rock with 3 mm diameter disk for scale.

Mark as true [T] or false [F] the following descriptions of the rock in Figure C2.

1. The rock is a breccia. ____
2. The rock is a porphyry. ____
3. The blue-black mineral is tourmaline. ____
4. The presence of the black biotite is important. ____
5. The elongate 1.4 cm long wedge of brown mineral is after sulfide. ____
6. The 1.4 cm long wedge of brown mineral is after sulfide and indicates the rock is a breccia. ____
7. A microvein cuts the specimen. ____
8. The black mineral is neotocite. ____
9. The rock formed from a "wet" magma. ____
10. The rock formed from a "dry" magma. ____
11. The brown mineral is called limonite. ____

Question GEN14 [14]: Rock description.

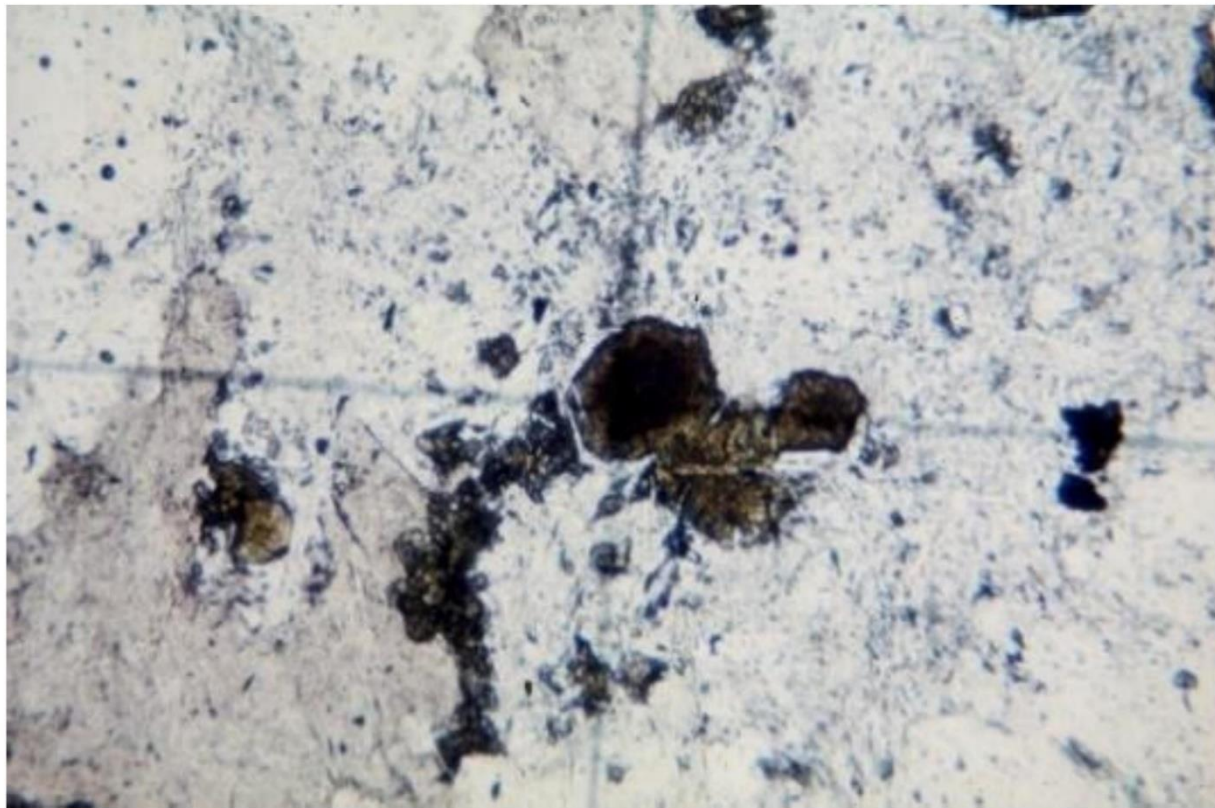


Figure C3. Rock thin section with 2 mm diameter central grain.

Mark as true [T] or false [F] the following descriptions of the rock in Figure C3

1. The specimen represents capping. ____
2. The specimen represents supergene. ____
3. The rock is a porphyry. ____
4. The rock is from the pyrite halo. ____
5. The rock is from the ore shell. ____
6. The alteration represents potassic facies. ____
7. The alteration represents phyllic facies. ____
8. The alteration represents intermediate argillic facies. ____
9. The alteration represents propylitic facies. ____
10. The central mineral is limonite. ____
11. The central mineral was chalcopyrite. ____
12. The central mineral was pyrite. ____
13. The boxwork in the centre represents a cube. ____
14. The boxwork in the centre represents a pyritohedron. ____

Question GEN15 [8]: Rock description.



Figure C4. Example of an important habit.
 Photo was taken by Bradford in 2015.

Mark as true [T] or false [F] the following descriptions of the rock in Figure C4

1. The rock is a breccia. ____
2. The rock is a porphyry. ____
3. The habit is gusano. ____
4. A microvein cuts the specimen. ____
5. The blobs likely contain pyrophyllite. ____
6. The blobs likely contain alunite. ____
7. The blobs likely contain quartz. ____
8. The habit is an *index fossil* for underlying porphyry deposits. ____

Question GEN16 [14]: Rock description.

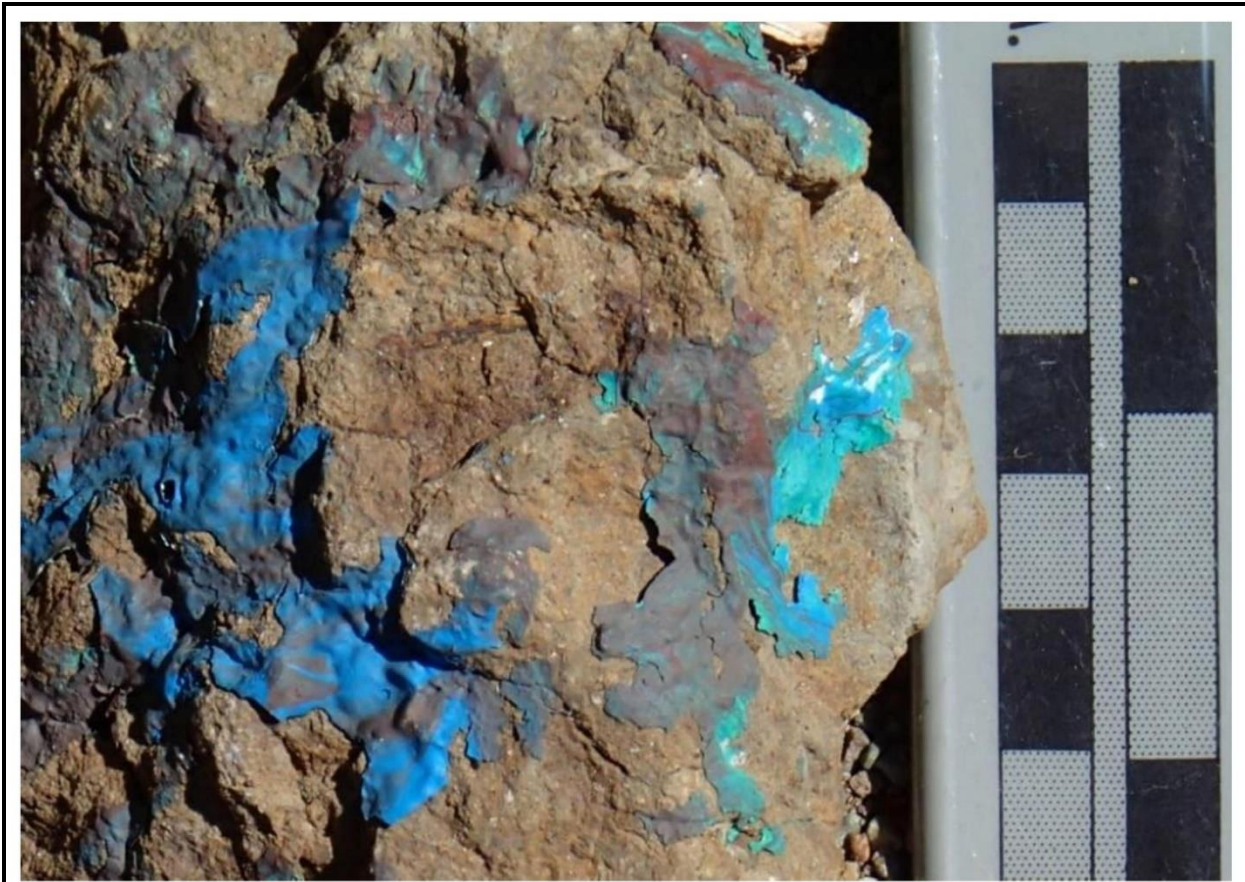


Figure C5. Altered rock.

Mark as true [T] or false [F] the following descriptions of the rock in Figure C5

1. The dark blue mineral is tourmaline. ___
2. The dark blue mineral is malachite. ___
3. The dark blue mineral is azurite. ___
4. The green mineral is azurite. ___
5. The green mineral is chalcantite. ___
6. The green mineral is malachite. ___
7. The green mineral is chalcantite. ___
8. The specimen represents capping. ___
9. The specimen represents supergene oxide. ___
10. The specimen represents supergene sulfide. ___
11. The brown mineral is called limonite. ___
12. The specimen contains chalcopyrite. ___
13. The specimen contains tetrahedrite. ___
14. The specimen contains chalcocite. ___

Question GEN17 [14]: Rock description.

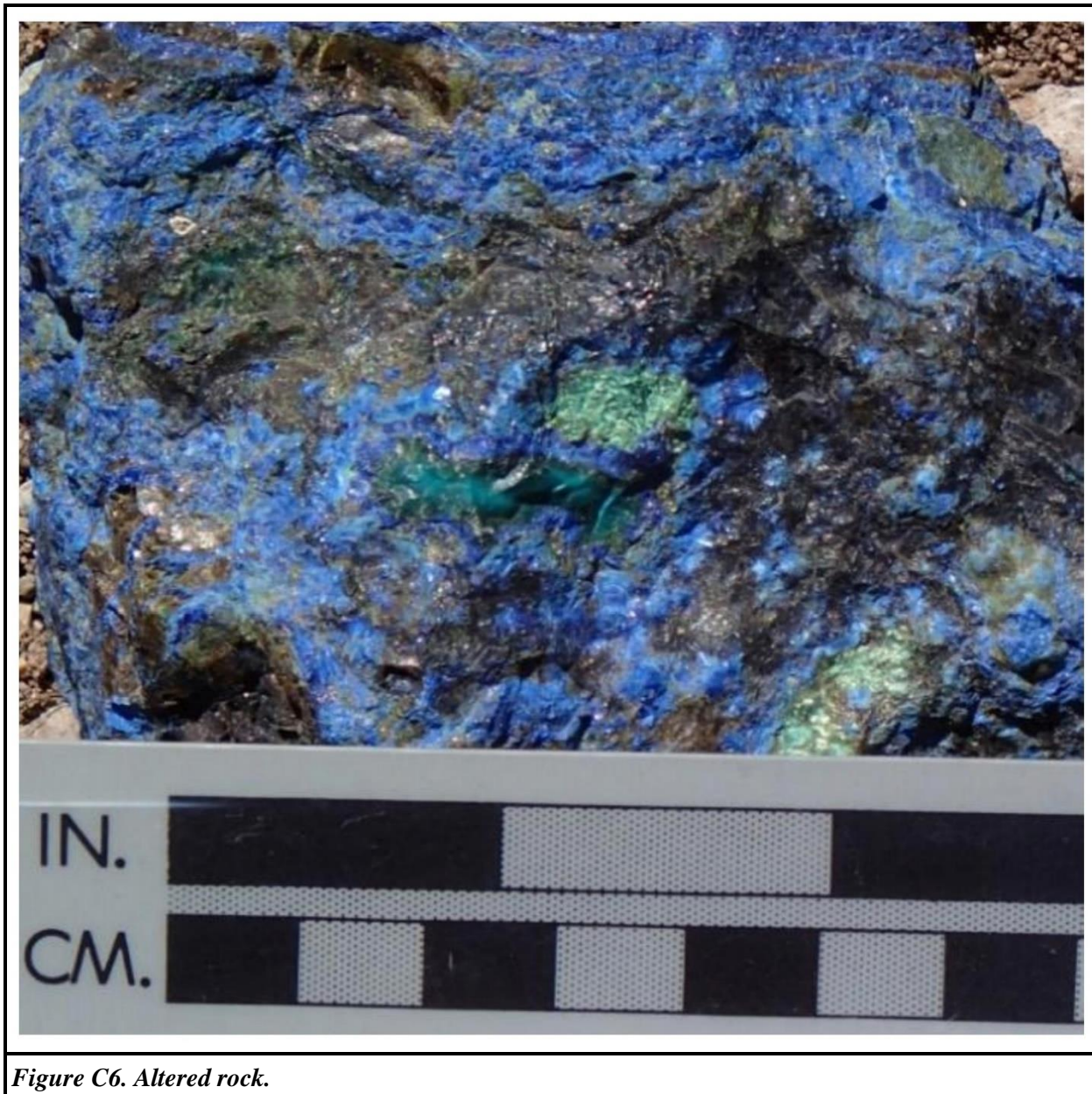


Figure C6. Altered rock.

Mark as true [T] or false [F] the following descriptions of the rock in Figure C6

1. The dark blue mineral is tourmaline. ___
2. The dark blue mineral is malachite. ___
3. The dark blue mineral is azurite. ___
4. The green mineral is azurite. ___
5. The green mineral is chalcantite. ___
6. The green mineral is malachite. ___
7. The green mineral is chalcantite. ___

8. The specimen represents capping. ___
9. The specimen represents supergene oxide. ___
10. The specimen represents supergene sulfide. ___
11. The brown mineral is called limonite. ___
12. The specimen contains chalcopyrite. ___
13. The specimen contains chalcopyrite. ___
14. The specimen contains chalcocite. ___

C3. PROBLEM SET FOR THE INTERPRETATION OF GEOLOGY AND HYPOGENE ALTERATION FROM MAPS

Island Copper porphyry deposit, Vancouver Island, British Columbia, Canada.

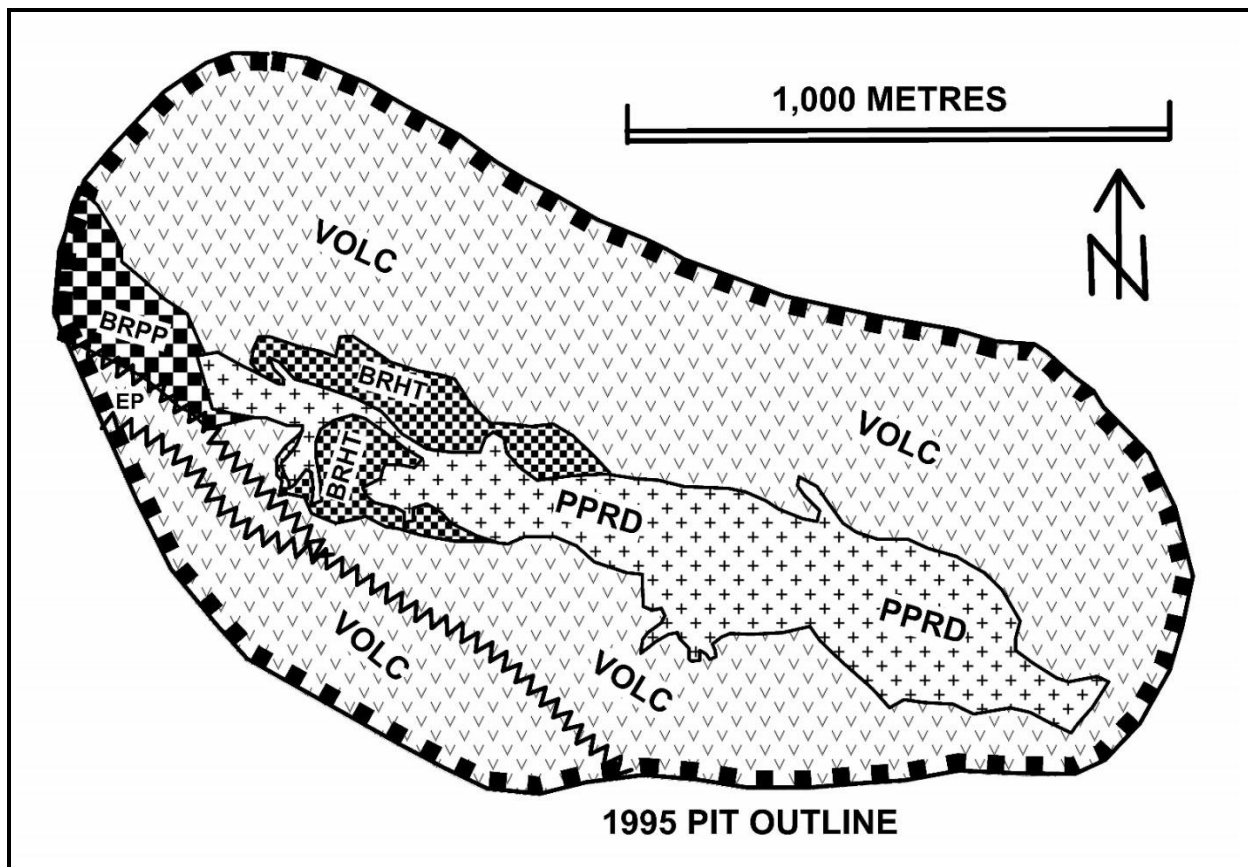


Figure C7. Geological map of the open pit for the Island Copper porphyry mine, Vancouver Island, British Columbia, Canada.

Zig-zag line = major faults. Downward V's (VOLC) = Bonanza Group volcanic rocks. Plus pattern (PPRD) = rhyodacite porphyries. Small squares pattern (BRHT) = marginal hydrothermal breccia. Large squares pattern (BRPP) = pyrophyllite ± dumortierite breccia. Map is simplified from figure 6 in Perelló et al. (1995).

Question ICU01 [4]: Rock descriptions.

Mark as true [T] or false [F] the following questions related to Figure C7

1. The rhyodacite porphyry was apparently intruded along a fault. ___
2. The rhyodacite porphyry likely exploded to breccia. ___
3. The breccia likely formed by faulting after intrusion of the rhyodacite porphyry. ___
4. The breccia could have resulted from formation of phenocrysts in the rhyodacite porphyry. ___

Question ICU02 [5]: Breccia description.

Mark as true [T] or false [F] related to the pyrophyllite breccia in Figure C7

1. The white pyrophyllite and blue dumortierite in the breccia implies ground water involvement. ___
2. The white pyrophyllite and blue dumortierite in the breccia implies low temperature formation. ___
3. The white pyrophyllite and blue dumortierite in the breccia implies high temperature formation. ___
4. The white pyrophyllite and blue dumortierite in the breccia implies intermediate temperature formation. ___
5. The white pyrophyllite and blue dumortierite indicates generation from the rhyodacite. ___

Question ICU03 [12]: Porphyry questions.

Mark as true [T] or false [F] the following questions related to Figure C7, given that the core of the deposits is a rhyodacite porphyry with 10 to 30% phenocrysts

1. Phenocrysts of chlorite are likely in the rhyodacite porphyry. ___
2. Phenocrysts of quartz are likely in the rhyodacite porphyry. ___
3. Phenocrysts of hornblende are likely in the rhyodacite porphyry. ___
4. Phenocrysts of apatite are likely in the rhyodacite porphyry. ___
5. Phenocrysts of biotite are likely in the rhyodacite porphyry. ___
6. Phenocrysts of feldspar are likely in the rhyodacite porphyry. ___
7. Biotite is likely to be in the matrix in the rhyodacite porphyry. ___
8. Calcite is likely to be in the matrix in the rhyodacite porphyry. ___
9. Quartz is likely to be in the matrix in the rhyodacite porphyry. ___
10. Feldspar is likely to be in the matrix in the rhyodacite porphyry. ___
11. Hornblende is likely to be in the matrix in the rhyodacite porphyry. ___
12. Chlorite is likely to be in the matrix in the rhyodacite porphyry. ___

Question ICU04 [4]: Volcanic rock questions.

Mark as true [T] or false [F] the following questions related to Figure C7 given that Bonanza Volcanic rocks are mafic.

1. Epidote reflects mainly alteration of calcic plagioclase. ___
2. The epidote might reflect regional metamorphism. ___
3. The iron content of the mafic volcanic rocks can contribute to the precipitation of copper in the mine. ___
4. The iron content of the mafic volcanic rocks can contribute to the precipitation of gold in the mine. ___

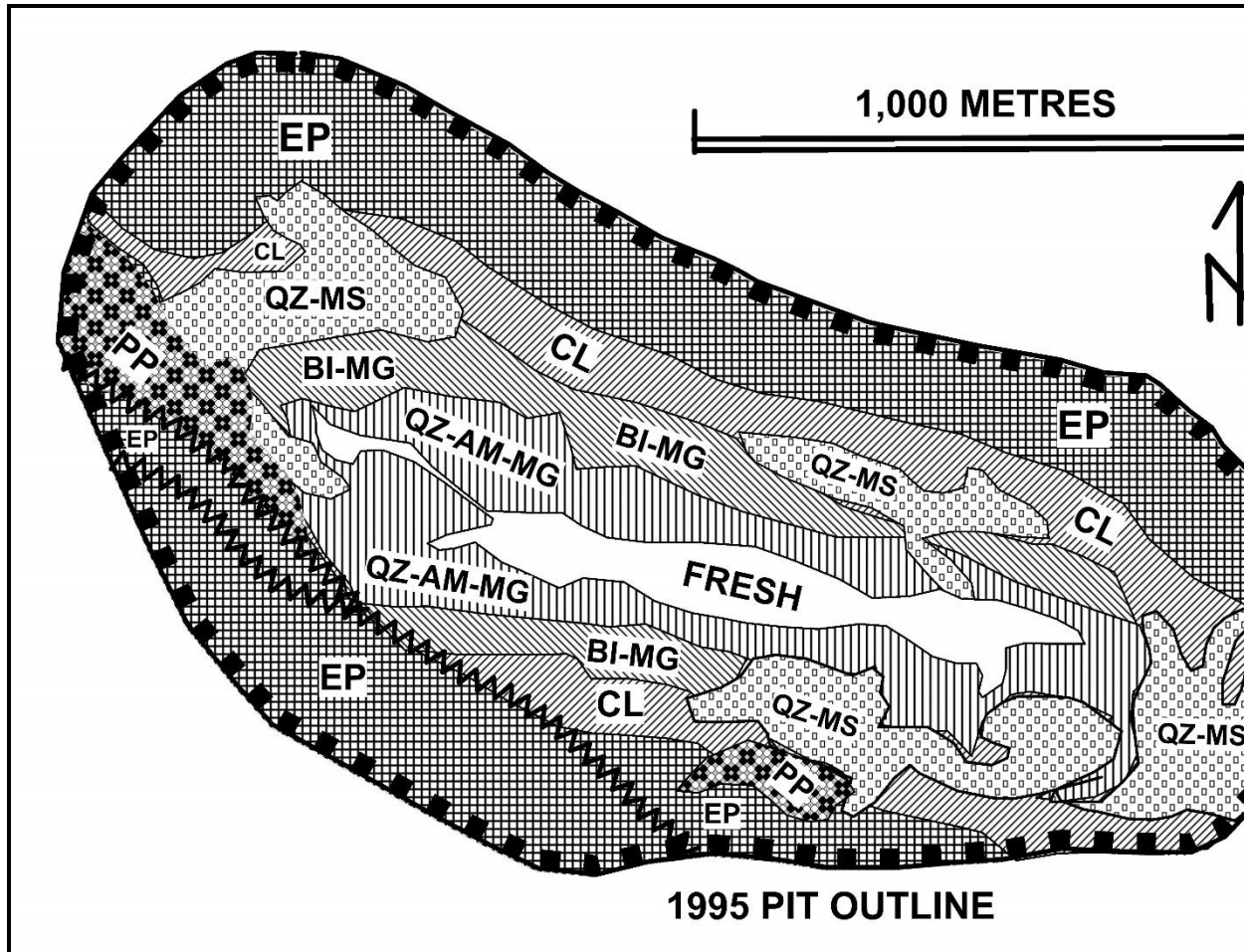


Figure C8. Alteration map for the Island Copper porphyry deposit, Vancouver Island, British Columbia, Canada.

Zig-zag lines mark major faults. Vertical square grid (EP) = epidote alteration. Down-left hash (CL) = chlorite ± magnetite alteration. Down-right hash (BI-MG) = biotite-magnetite alteration. Vertical hash (QZ-AM-MG) = quartz-amphibolite-magnetite alteration. Open-square pattern QZ-MS = quartz-sericite ± chlorite. Heavy square pattern PP = pyrophyllite ± dumortierite. Blank (FRESH) = relatively fresh core. Map is simplified from figure 12 in Perelló et al. (1995).

Question ICU05 [21].

Mark as true [T] or false [F] the following descriptions of the alteration in Figure C8

1. The pyrophyllite - dumortierite is best represented as potassic alteration. ___
2. The pyrophyllite - dumortierite is best represented as phyllic alteration. ___
3. The pyrophyllite - dumortierite is best represented as advanced argillic alteration. ___
4. The pyrophyllite - dumortierite is best represented as propylitic alteration. ___
5. The quartz-sericite ± chlorite is best represented as potassic alteration. ___
6. The quartz-sericite ± chlorite is best represented as phyllic alteration. ___
7. The quartz-sericite ± chlorite is best represented as advanced argillic alteration. ___
8. The quartz-sericite ± chlorite is best represented as propylitic alteration. ___

9. The biotite-magnetite is best represented as potassic alteration. ___
10. The biotite-magnetite is best represented as phyllic alteration. ___
11. The biotite-magnetite is best represented as advanced argillic alteration. ___
12. The biotite-magnetite is best represented as propylitic alteration. ___
13. The chlorite-magnetite is best represented as potassic alteration. ___
14. The chlorite-magnetite is best represented as phyllic alteration. ___
15. The chlorite-magnetite is best represented as advanced argillic alteration. ___
16. The chlorite-magnetite is best represented as propylitic alteration. ___
17. The epidote is best represented as potassic alteration. ___
18. The epidote is best represented as phyllic alteration. ___
19. The epidote is best represented as advanced argillic alteration. ___
20. The epidote is best represented as propylitic alteration. ___
21. The epidote is best represented as regional alteration. ___

Question ICU06 [2]: Gold associations.

Mark as true [T] or false [F] the following about gold occurrence in Figure C8

1. Gold is likely to be concentrated within the biotite - magnetite alteration. ___
2. Gold is likely to be concentrated within the quartz – sericite + chlorite alteration. ___

Question ICU07 [3]: Tonnage question.

Based on Figure C8 the tonnes mined in the open pit, which was mined to about 400 metre depth is roughly (use an approximate block 200 metres deep by 2,000 metres long by 1,200 metres wide). Mark as true (T) or false (F):

1. 120 million tonnes. ___ .
2. 1,200 million tonnes. ___ .
3. 12,000 million tonnes. ___ .

Berg porphyry deposit, central British Columbia, Canada.

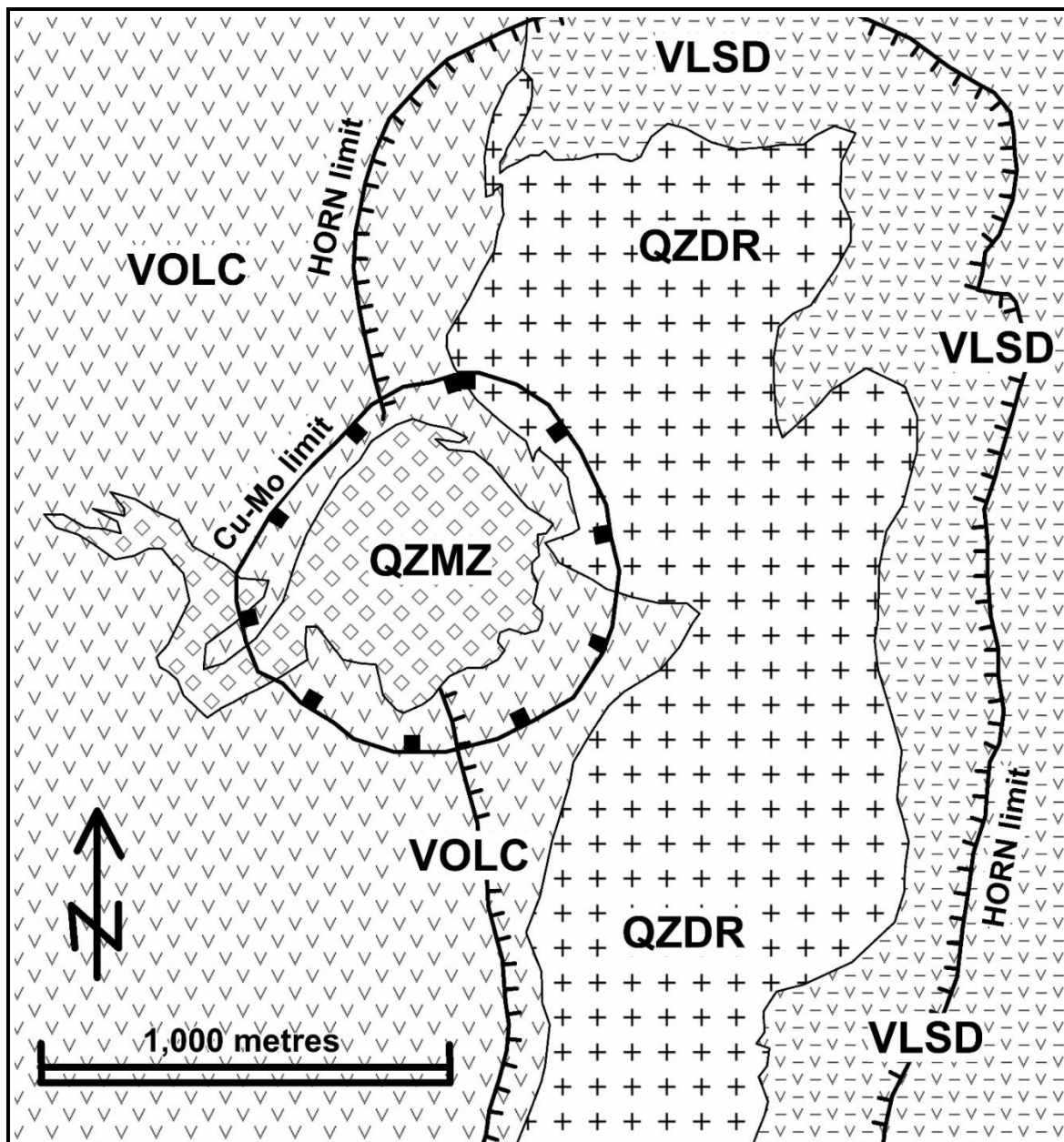


Figure C9. Geology map of the Berg porphyry deposit, central British Columbia, Canada.
 Downward V's (VOLC) = Telkwa Formation volcanic rocks in the Hazelton Group. Downward V's and dashes (VLSD) = Skeena Group volcanic and sedimentary rocks. Pluses (QZDR) = older quartz diorite. Diamonds (QZMZ) = younger Berg quartz monzonite. Hashed line (HORN limit) = approximate outer limit of biotite hornfels. Hammer-decorated line around the Berg quartz diorite (Cu-Mo limit) = approximate outer limit of copper-molybdenum zone. Map is simplified from Heberlein and Godwin (1984).

Question BER01 [7]: Significant regional geology.

Mark as true [T] or false [F] regarding the following statements related to Figure C9.

1. Hornfels is not likely to be important in concentration of "ore" mineralization. ____
2. The hornfels was developed from intrusion of the quartz diorite. ____
3. The hornfels was developed from intrusion of the Berg quartz monzonite stock. ____
4. Hornfels is likely to be important in concentration of "ore" mineralization. ____
5. The quartz diorite is responsible for the hornfels and pre-dates the Berg quartz monzonite stock. ____
6. The best "ore" mineralization is likely to occur at the northeast margin of the stock. ____
7. The best "ore" mineralization is likely to occur on the northwest side of the stock. ____

C4. PROBLEM SET FOR SUPERGENE ENRICHMENT IN PORPHYRY DEPOSITS

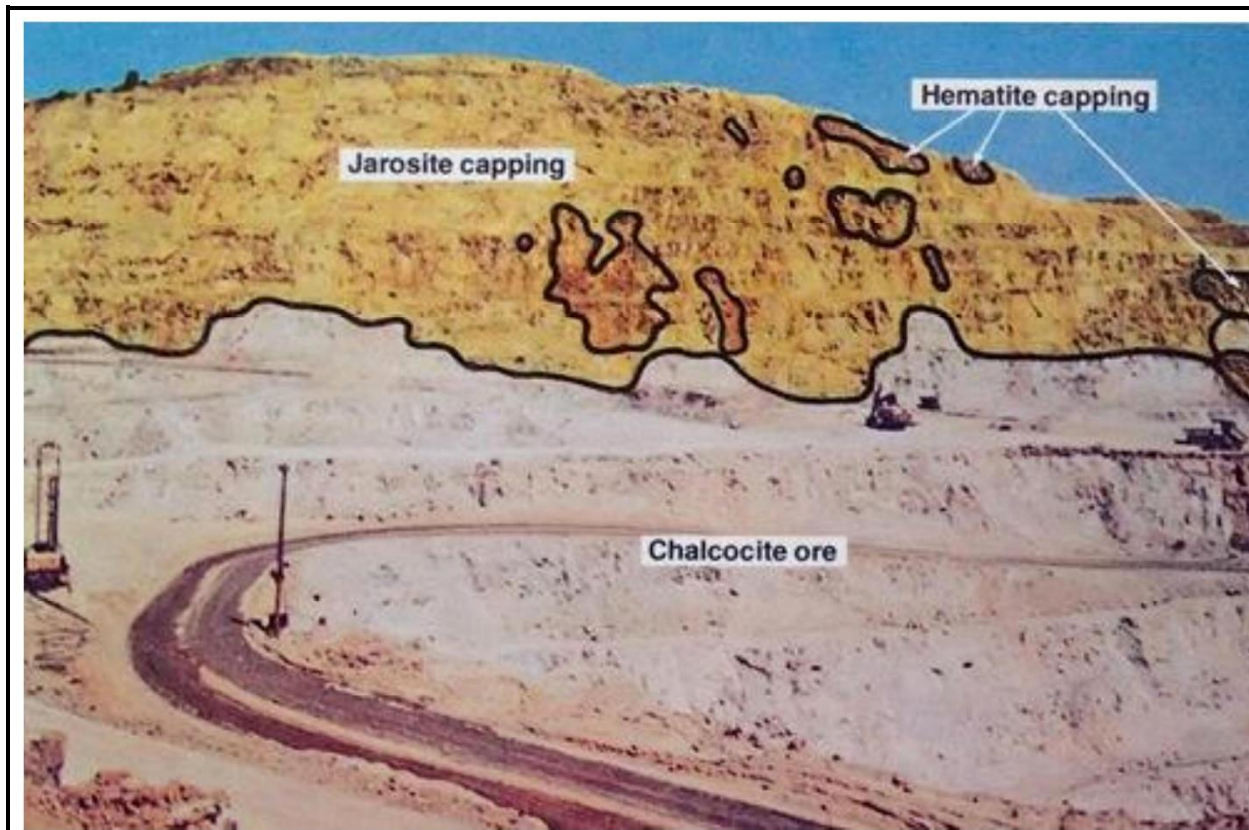


Figure C10. Supergene alteration at the Butte Porphyry Deposit (the richest hill on earth), Montana, USA.

Photo was taken from figure 12.17 in Anderson (1982); reprinting has been approved by The University of Arizona Press.

Question SUP01 [12]: Capping and enrichment questions.

Mark as true [T] or false [F] the following descriptions of the mapped units in the open pit in Figure C10.

1. The “jarosite capping” is only after hypogene mineralization. ____
2. The “jarosite capping” is only after hypogene and supergene enrichment mineralization. ____
3. The “jarosite capping” will have the same copper grade as the original hypogene mineralization. ____
4. The “jarosite capping” will have a lower copper grade than the original hypogene mineralization. ____
5. The “hematite capping” is only after hypogene mineralization. ____
6. The “hematite capping” is only after supergene enrichment mineralization. ____
7. The “chalcocite ore” represents supergene oxide mineralization. ____
8. The “chalcocite ore” represents supergene sulfide mineralization. ____
9. The “chalcocite ore” will have the same copper grade as the capping. ____
10. The “chalcocite ore” will have the same copper grade as the hypogene. ____
11. The “chalcocite ore” will have the better copper grade than the original hypogene mineralization. ____

12. The “chalcocite ore” will have the same copper grade as the original hypogene mineralization. ____

Question SUP02 [2]: Supergene cycles.

Mark as true [T] or false [F] the following descriptions of the supergene sequence represented in the open pit of Figure C10.

1. The supergene sequence represented is single cycle. ____
2. The supergene sequence represented is multiple cycle. ____

Mark Summary for Questions C1 to C4

Record and summarize your marks in TABLE C1.

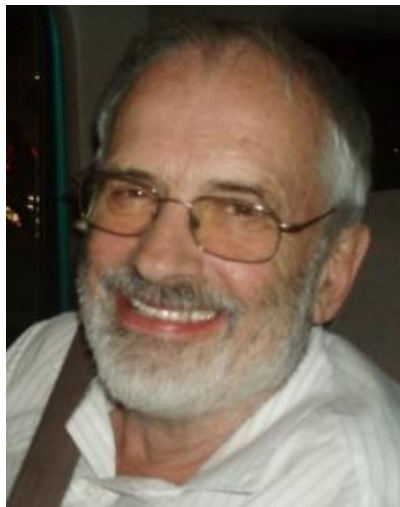
TABLE C1. Mark summary.		
TOPIC/QUESTION NUMBER	MAXIMUM	YOUR MARK
B1: General.		
GEN.01	11	
GEN.02	8	
GEN.03	8	
GEN.04	11	
GEN.05	11	
GEN.06	11	
GEN.07	11	
GEN.08	11	
GEN.09	12	
GEN.10	16	
GEN.11	16	
C1 Totals: General.	126	
C2: Porphyry Specimens.		
GEN.12	14	
GEN.13	11	
GEN.14	14	
GEN.15	08	
GEN.16	14	
GEN.17	14	
C2 Totals: Porphyry Specimens.	75	
C3: Porphyry Deposit Maps.		

ICU.01	4	
ICU.02	5	
ICU.03	12	
ICU.04	4	
ICU.05	21	
ICU.06	2	
ICU.07	3	
BER.01	7	
C3 Totals: Porphyry Deposit Maps.	58	
C4: Supergene Enrichment.		
SUP.01	12	
SUP.02	2	
C4 Totals: Supergene Enrichment.	14	
Totals: Section Totals C1 to C4.	273	

Your mark.

Calculate your percentage from: $[(\text{your total mark}) / 273] * 100 = (\text{your percentage correct})$.

Your mark = _____ %.



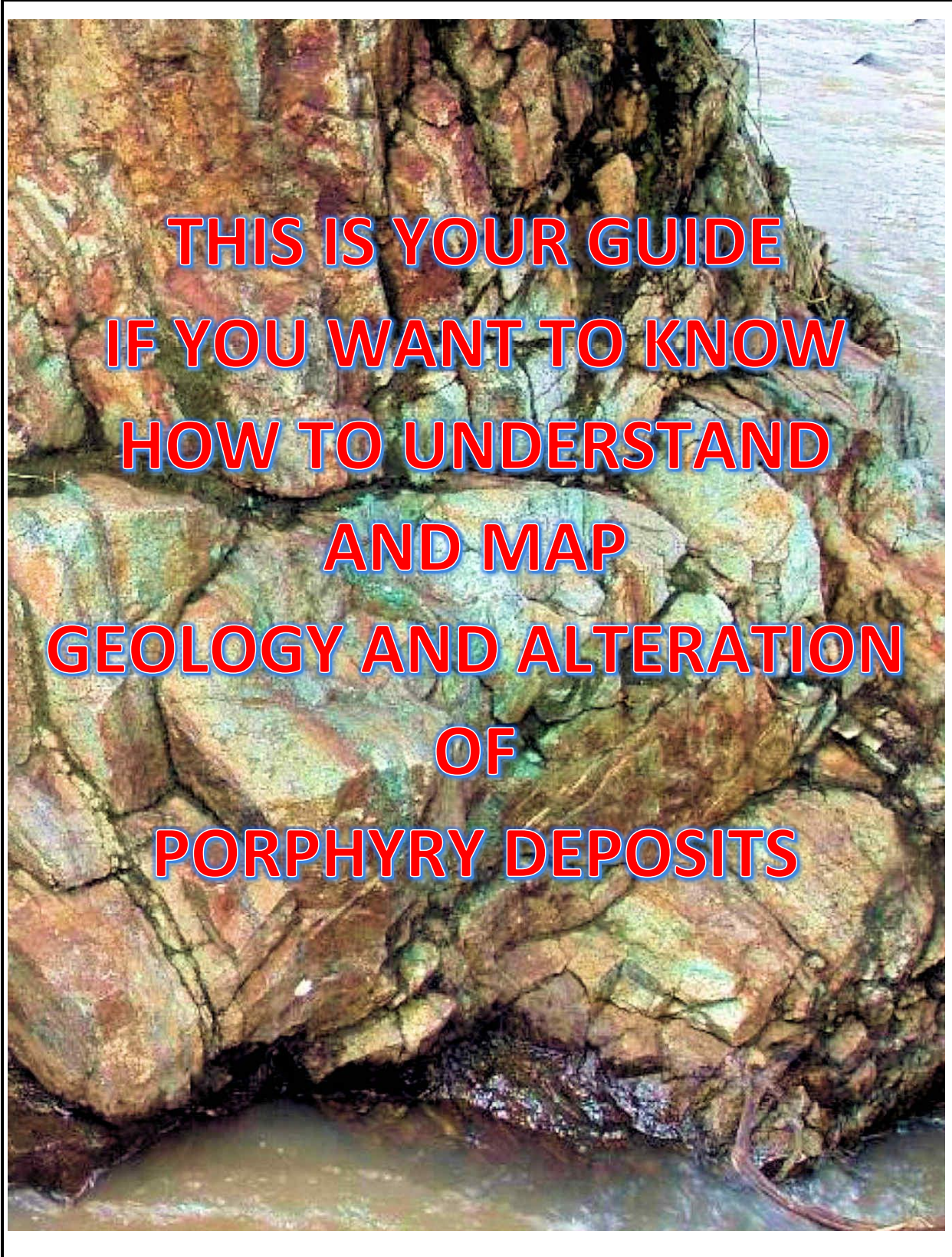
ABOUT THE AUTHOR

Dr Colin I. Godwin (BASc[UBC], PhD[UBC], PEng[BC], PGeo[BC]) taught exploration for, and the geology of, mineral deposits at The University of British Columbia (UBC) from 1975 to early retirement in December 1999. During part of that time, he was Director of Geological Engineering, and he is now a Professor Emeritus of the Department of Earth and Ocean Sciences. While at the university he collaborated with students specializing in field and laboratory studies of most types of deposits, including porphyry, skarn, epithermal, volcanogenic, and kimberlitic deposits. Interpretation of lead isotopes in galena, as related to mineral exploration, was an academic focus. Colin received the Duncan R. Derry Medal from the Mineral Deposits Division of the Geological Association of Canada in 1990.

Colin was a founding director of International Geosystems Ltd. in the early 1970's. At that time, he became involved in the development of the GEOLOG System while studying the Casino copper-gold-molybdenum porphyry deposit in the Yukon for his Doctorate. GEOLOG was one of the first computer-based schemes for the comprehensive capture and interpretation of data from exploration-development work, especially drill holes. He has worked on exploration programs in Australia, Canada, United States, Mexico, Central America, and South America.

He may be reached at: 2706—660 Nootka Way, Port Moody, BC, Canada V3H 0B7. Tel: (604)939-6507, cell: (778)989-6507. Email: cigodwin@gmail.com. Should copies of logging formats or answers to the questions be required, contact Colin Godwin.

Photo on the back cover is of an outcrop from the Inguaran porphyry prospect, Michoacan, Mexico. It illustrates sheeted veining.



**THIS IS YOUR GUIDE
IF YOU WANT TO KNOW
HOW TO UNDERSTAND
AND MAP
GEOLOGY AND ALTERATION
OF
PORPHYRY DEPOSITS**